Protein Interaction Studies on the Rotavirus Non-Structural Protein NSP1

Catherine Isabelle Thompson B.Sc. (Hons)

A thesis submitted for the degree of Doctor of Philosophy

of the University of Warwick

Department of Biological Sciences

University of Warwick

Coventry

United Kingdom

September 1999

Table of Contents

List of Figures

* Figures can be found on the page following that listed.

List of Tables

Acknowledgements

I would like to thank my supervisor Professor Malcolm McCrae for his help and guidance over the course of my Ph.D. studies. I would also like to thank the members of the Rotavirus laboratory for their advice over the past few years.

I would like to thank my family for their support. Thanks also go to my housemates and friends, especially Jackie, Sam, Graham, Mark, Nick, and Isa, and thanks to Andy for all his support and encouragement.

I would like to acknowledge Dr J. Cohen for providing me with the anti-NSP1 antiserum, and Dr J. Howes for providing the anti-VP6 antiserum.

This project was supported by a grant from the BBSRC.

Declaration

All the results presented in this thesis were obtained by the author unless otherwise stated, and no part has been previously presented in application for a degree. All sources of information and materials are indicated in the text.

Abbreviations

Å	Angstroms
aa	Amino acids
APS	Ammonium persulphate
ATP	Adenosine triphosphate
bp	Base pairs
BSA	Bovine serum albumin
BTV	Bluetongue virus
CAT	Chloramphenicol acetyltransferase
cDNA	Complementary DNA
CIP	Calf intestinal alkaline phosphatase
cpe	Cytopathic effect
dCTP	2'-deoxycytidine 5'-triphosphate
DMEM	Dulbecco's modification of Eagle's minimal essential medium
DMF	N,N-dimethylformamide
DMSO	Dimethylsulphoxide
DNA	Deoxyribonucleic acid
ds	Double-stranded
E. coli	*Escherichia coli*
EDTA	Ethylenediamine tetracetic acid
EM	Electron microscopy
ER	Endoplasmic reticulum
FCS	Foetal calf serum
GMEM	Glasgow modification of Eagle's minimum essential medium
HIV	Human immunodeficiency virus
HRR	Host range restriction
IAA	Isoamyl alcohol
Ig	Immunoglobulin
IP	Immunoprecipitation

Kb	Kilobase
KDa	Kilo Dalton
LB	Luria Bertani
mAb	Monoclonal antibody
MCS	Multiple cloning site
m.o.i.	Multiplicity of infection
mRNA	Messenger RNA
NLS	Nuclear localisation signal
NSP	Non-structural protein
NP40	Nonidet P40
OD	Optical density
ONPG	O-nitrophenyl β-D-galactopyranoside
ORF	Open reading frame
PBS	Phosphate buffered saline
PCR	Polymerase chain reaction
PEG	Polyethylene glycol
Pfu	Plaque forming unit
p.i.	Post-infection
RER	Rough endoplasmic reticulum
RIs	Replication intermediates
RNA	Ribonucleic acid
rpm	Revolutions per minute
S	Svedbergs
SAP	Shrimp alkaline phosphatase
SDS	Sodium dodecyl sulphate
SV40	Simian virus 40

T	Tumour
T	Triangulation number
TAE	Tris EDTA
TBE	Tris borate EDTA
TCA	Trichloroacetic acid
TE	Tris EDTA
TEMED	N,N,N'N'-tetramethylethylenediamine
Tris	Tris-(hydroxymethyl)-methylamine
ts	Temperature sensitive
UKtc	United Kingdom tissue-culture-adapted strain of bovine rotavirus
UAS	Upstream activating sequence
UTR	Untranslated region
VLP	Virus-like particle
VP	Viral protein
vRNA	Virion RNA
v/v	Volume for volume
w/v	Weight for volume
Xg	Times gravitation acceleration
X-Gal	5-bromo-4-chloro-3-indolyl-β-D-galactopyranoside

Standard abbreviations are used for SI units and amino acids.

Summary

Rotavirus encodes six structural and six non-structural proteins. In contrast to the structural proteins, the functional roles of the non-structural proteins are not well defined beyond a realisation that they must have a role in the viral replication cycle. A fuller understanding of the replication cycle must therefore rest on determining the specific roles played by the non-structural proteins.

Non-structural protein NSP1 shows high levels of sequence divergence. A generally well conserved cysteine-rich region at the amino-terminus may form a zinc finger structure. It has been shown to possess non-specific RNA-binding activity, and has been found associated with the smallest of three replication intermediates (RIs) found in infected cells, together with the viral proteins VP1, VP3 and NSP3. VP2 and VP6 are added sequentially to the pre-core RI to form the core RI and single-shelled RI respectively. The function of NSP1 in the replication cycle and the importance of its presence in early replication complexes has not been determined.

The intermolecular interactions that occur between the components of the RIs have not been defined. Protein-protein interactions between NSP1 and VP1, VP2, VP3, and NSP3, from the UKtc strain of bovine rotavirus, were investigated using a variety of approaches, the first of which was the yeast two-hybrid system. In this assay a self-interaction of NSP1 was not detected. Protein-protein interactions between NSP1 and VP1, VP2, VP3, and NSP3, were also not detected. Both the full-length protein and a truncated NSP1, consisting of only the amino terminal third of the protein, were tested. A direct self-interaction of NSP3 was shown and quantified. Radio-immunoprecipitation analysis of *in vitro* translated viral proteins using specific anti-NSP1 serum was also employed. However, it failed to detect direct protein-protein interactions between NSP1 and VP1, VP2, and VP3.

Immunoprecipitation of UKtc rotavirus-infected cell lysates with anti-NSP1 serum showed the co-precipitation of viral proteins VP1, VP2, VP3/VP4, VP6 and NSP3, with NSP1. It was proposed that NSP1 formed a previously unrecognised complex with these proteins. Immunoprecipitation of nuclease-treated infected cell lysates showed a reduction in the co-precipitation of VP2, VP3/VP4 and NSP3 with NSP1. No reduction in the co-precipitation of VP6 was seen. The association of the complex proteins may be mediated by RNA binding. Immunoprecipitation with an anti-VP6 monoclonal antibody reciprocally precipitated small amounts of NSP1, VP2, VP3/VP4, and NSP3, with VP6.

Introduction

1.1 Rotavirus as a pathogenic agent

1.1.1 Diarrhoeal disease

Diarrhoeal diseases are collectively one of the most prevalent infectious diseases and thus represent a serious threat to human health worldwide. The problem is particularly acute in developing countries where they constitute a major cause of mortality, especially among infants and young children (Guerrant *et al.*, 1990). It has been estimated that 744 million to one billion cases of diarrhoea, resulting in 4.6 million deaths, occur annually in children less than five years in developing countries (Snyder and Merson, 1982). More recently, the mortality rate was found to be lower than previously estimated at 3.3 million deaths annually (range 1.5 to 5.1 million) (Bern *et al.*, 1992), however the incidence of diarrhoea remained static. In the USA infectious gastroenteritis was found to be the second most common disease experience (Monto *et al.*, 1983), albeit the mortality rate was significantly lower than in less developed countries with an estimated average of 504 deaths per year in children under four years (Ho *et al.*, 1988).

1.1.2 The discovery of rotavirus

Until the early 1970's the causative agents of infectious diarrhoeal diseases remained elusive. A breakthrough came with the discovery in 1972 of the Norwalk virus, which was shown to be associated with viral gastroenteritis in older children and adults (Kapikian *et al.*, 1972). In 1973, Bishop *et al.* (Bishop *et al.*, 1973) visualized an agent by thin section electron microscopy (EM) of duodenal mucosa from infants with acute gastroenteritis. This 70 nm particle was subsequently identified by EM in the faeces of young children with gastroenteritis (Bishop *et al.*, 1974) (Flewett *et al.*, 1973) (Kapikian *et al.*, 1974) (Middleton *et al.*, 1974). Morphologically identical viruses were then detected in faecal extracts from both humans and animals in all species tested worldwide (reviewed in McNulty, 1978). It soon became clear that these viruses were the major etiologic agents of severe viral gastroenteritis (Kapikian and Chanock, 1996).

Several names were proposed for the virus and rotavirus, from the Latin 'rota' meaning wheel, was chosen as the virion resembles a wheel with short spokes and a

well-defined smooth outer rim when viewed by EM (Figure 1.1) (Flewett *et al.*, 1974). As the viruses differed both morphologically (Palmer *et al.*, 1977) and antigenically from *Orthoreoviruses* and *Orbiviruses* (Kapikian *et al.*, 1976) (Kalica *et al.*, 1977), it was suggested that they should be included as a new genus within the family *Reoviridae* (Davidson *et al.*, 1975). In 1978, the genus *Rotavirus* was officially recognised (Matthews, 1979).

1.1.3 The global significance of rotavirus infection

Rotaviruses are now known to be the single most important aetiologic agents of severe diarrhoeal disease in infants and young children worldwide (Kapikian and Chanock, 1996). In both developed and developing countries they account for the largest proportion of cases of severe diarrhoeal illness requiring hospitalisation (Figure 1.2). An Australian survey of children admitted to hospital with acute gastroenteritis over a year showed 50 % were infected with rotavirus, rising to a seasonal peak of 73 % during the winter months (Davidson *et al.*, 1975). It has been estimated that rotaviruses cause 3.1 million cases of diarrhoea, 65,000 to 70,000 hospitalisations and 125 deaths annually among infants and young children in the USA (Glass *et al.*, 1991) (Matson and Estes, 1990). The economic cost of rotavirus infection due to hospitalisation is considerable, indeed hospitalisation costs in the USA alone have been estimated at $664 million per annum (Matson and Estes, 1990).

In developing countries the mortality resulting from rotavirus infection is significantly higher. A study in Asia, Africa and Latin America estimated that rotavirus was responsible for 125 million cases of diarrhoea resulting in 870,000 deaths (Institute of Medicine, 1985). Thus, the development of an effective vaccine is highly desirable, to reduce both the mortality and the economic burden of healthcare resulting from rotavirus infection.

1.1.4 Overview of vaccination developments

By the age of five years the vast majority of children, whether living in rich or poor countries, will have been infected with rotavirus (Glass *et al.*, 1996). Improvements in food, water and hygiene have little impact on the control of rotavirus infection, and despite massive efforts to prevent diarrhoeal mortality with oral

Figure 1.1

Figure 1.1 Transmission electron micrograph of rotaviruses

Image reproduced from Murphy (1985). The characteristic wheel appearance of the virion, the inspiration for the name rotavirus (from the Latin 'rota' meaning wheel), can be clearly observed. Magnification X135,000.

Figure 1.2

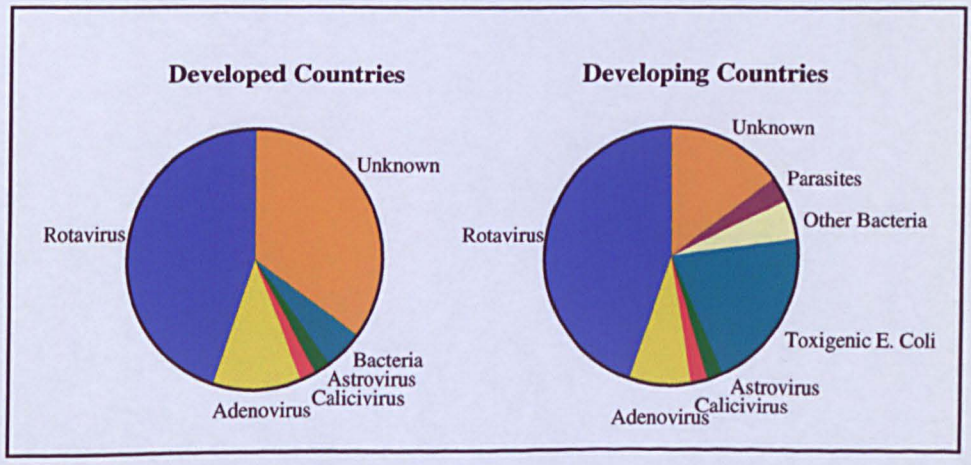

Figure 1.2 Diagram showing an estimate of the role of different etiological agents in severe diarrhoeal illness requiring hospitalization of infants and young children in developed countries and developing countries

Adapted from Kapikian and Chanock (1996).

rehydration therapy, diarrhoea still ranks as the first or second most common cause of death among children in developing countries (Bern *et al.*, 1992). Natural immunity to rotavirus infection was suggested by the decreased incidence of disease with increasing age (Bishop *et al.*, 1983). Thus, vaccination as a means of disease control has been extensively investigated.

The first rotavirus vaccine, a live vaccine prepared from bovine rotavirus, was effective in more than 80 % of cases in preventing clinically significant rotavirus diarrhoea (Vesikari *et al.*, 1984). The moderate success of this trial paved the way for the development and field testing of several candidate reassortant live rotavirus vaccines. In 1998 the rhesus-human reassortant tetravalent (RRV-TV) rotavirus vaccine was licensed for use in the USA. This is a multivalent vaccine, representing each of the four epidemiologically important VP7 serotypes. The reassortants contain the VP7 gene derived from the human rhesus rotavirus strain, and the remaining genes from the bovine strains. The vaccine was recommended to be given to all children in the USA along with other childhood vaccines and was licensed for use in Europe (Vesikari, 1999). However, recently the rotavirus vaccination programme has been halted due to the occurrence of a number of cases of intussusception, a blockage of the intestine, among recently vaccinated infants. Although a direct association between the cases of intussusception and the rotavirus vaccine has not been shown, it has been recommended by the Centers for Disease Control and Prevention (CDC) that use of the vaccine be suspended pending an evaluation of the vaccine programme.

In addition to the recent problems, the current vaccine only protects against the four main human serotypes. It does not give complete protection and in particular, the protective efficacy is lower in developing countries (Vesikari, 1999). Hence, a continued research effort is absolutely necessary. Research into alternatives using recombinant DNA technology to generate a non-live rotavirus vaccine has been performed. Several attempts have been made to produce β-galactosidase (β-gal):VP7 fusion proteins that will generate neutralising antibodies, with varying degrees of success (McCrae and McCorquodale, 1987) (Johnson and McCrae, 1989). Induction of rotavirus neutralising antibodies in guinea pigs and mice, following administration of VP4 protein expressed in a baculovirus system, has been demonstrated (Mackow *et al.*, 1989) (Mackow *et al.*, 1990). Low level anti-rotavirus and rotavirus neutralising antibodies were also raised in guinea pigs using baculovirus expressed VP7

(McGonigal *et al.*, 1992). Recombinant vaccinia (Andrew *et al.*, 1987) (Andrew *et al.*, 1990) and recombinant adenovirus (Both *et al.*, 1993) expressing hybrid VP7 were shown to raise serotype specific neutralising antibodies. Synthetic peptides (Streckert *et al.*, 1988) (Ijaz *et al.*, 1995), virus-like particles (Crawford *et al.*, 1994) (Connor *et al.*, 1996), and DNA based rotavirus vaccines (Herrmann *et al.*, 1996) (Chen *et al.*, 1997), have also been explored as potential methods of vaccination against rotavirus infection.

1.2 *Reoviridae* and other dsRNA viruses

Viruses with a dsRNA genome infect a wide variety of host species encompassing vertebrate and invertebrate animals, plants, protozoa and bacteria (Table 1.1). At present six virus families have been defined: *Birnaviridae*, *Cystoviridae*, *Hypoviridae*, *Partitiviridae*, *Reoviridae* and *Totiviridae* (Murphy, 1996). In the largest family, the *Reoviridae*, viruses of mammals, insects, fish, birds, plants, crustaceans and arachnids can be found. The members of the family *Reoviridae* share common features in their virion structure, genome and replication cycle. The near-spherical, non-enveloped virions are characteristically formed of a double or triple-layered protein shell with icosahedral symmetry. Structural data on the organisation of the capsid layers has lead to the proposal that the genera in the family *Reoviridae* can be divided into two distinct groups (Hill *et al.*, 1999). The turreted virus group, comprising *Orthoreoviruses*, *Aquareoviruses*, *Oryzaviruses*, and *Fijiviruses*, have an incomplete inner capsid layer penetrated by turret-like spikes at the icosahedral five-fold axes. *Cypoviruses*, which are unusual in only having a single capsid layer, also have the turret structure (Payne and Mertens, 1983). The smooth-core group of viruses, including *Orbiviruses*, *Rotaviruses*, *Phytoreoviruses*, and *Coltiviruses*, have channels at the five-fold axes rather than the turret-like spike structures, and a complete, spherical inner capsid layer (Roseto *et al.*, 1979) (Ludert *et al.*, 1976) (Roy, 1996). Recent work on the structure of the core protein shell of the *Orbiviruses* has shown that the core layer consists of 120 protein subunits arranged with T=2 icosahedral symmetry (Grimes *et al.*, 1998). This feature has been observed in other genera of the family *Reoviridae* (Lawton *et al.*, 1997b) and in several other families of dsRNA viruses such as L-A (*Totiviridae*) and ϕ6 (*Cystoviridae*) (Cheng *et al.*, 1994) (Butcher *et al.*, 1997), suggesting that this structure might be ubiquitous to

Table 1.1 The double-stranded RNA viruses

Family	Genus	Type species	Segment number	Host	Characteristic properties
Birnaviridae	*Aquabirnavirus* *Avibirnavirus* *Entomobirnavirus*	*Infectious pancreatic necrosis virus* *Infectious bursal disease virus* *Drosophilia X virus*	2	Fish Fowl Insect	2 genome segments (A,B). A encodes polyprotein, cleaved to structural proteins, and 5' genome linked protein VPg. B encodes polymerase.
Cystoviridae	*Cystovirus*	*Pseudomonas phage ϕ6*	3	Pseudomonads	Lipid envelope; polycistronic genome segments (S,M,L); *in vitro* assembly model
Hypoviridae	*Hypovirus* *Varicosavirus*	*Cryphonectria hypovirus 1-EP713* *Lettuce big-vein virus*	1 1	Fungi Plants	dsRNA transmitted by cytoplasmic exchange when hypae fuse; replication in intracellular vesicles; similar to potyviruses.
Partitiviridae	*Partitivirus* *Chrysovirus* *Alphacryptovirus* *Betacryptovirus*	*Gaeumannomyces graminis virus 019/6-A* *Penicillium chrysogenum virus* *White clover cryptic virus 1* *White clover cryptic virus 2*	2 3 2/3 2/3	Fungi Fungi Plants Plants	Encapsidated nucleic acid both genomic and satellite; genome divided between several different particle types; DI copies present.

Reoviridae	*Orthoreovirus*	*Mammalian orthoreovirus*	10	Vertebrates	Spherical virion; 2-3 protein shells with icosahedral symmetry; transcription of full-length mRNA from each genome segment within transcriptionally active particles; mRNA extruded from particle; replication in newly synthesised core particles in viral inclusion bodies in cytoplasm; virions are moderately resistant to heat, organic solvents, detergents and irradiation.; transmission by direct contact/ fecal-oral route (rotavirus/ reovirus) or arthropods (orbivirus/ coltivirus)
	Orbivirus	*Bluetongue virus*	10	Vertebrates	
	Rotavirus	*Rotavirus A*	11	Vertebrates	
	Coltivirus	*Colorado tick fever virus*	12	Vertebrates	
	Aquareovirus	*Aquareovirus A*	11	Vertebrates	
	Cypovirus	*Cypovirus 1*	10	Invertebrates	
	Fijivirus	*Fiji disease virus*	10	Plants	
	Phytoreovirus	*Wound tumour virus*	12	Plants	
	Oryzavirus	*Rice ragged stunt virus*	10	Plants	
	[*Seadornavirus*]	*Banna virus (BAV)*	12	Vertebrates	
	[*Entomovirus*]	*Hyposoter exiguae reovirus (HeRV)*	10	Invertebrates	
Totiviridae	*Totivirus*	*Saccharomyces cerevisiae virus L-A*	1	Fungi	Satellites of L-A, M1 etc., encode killer toxins
	Giardiavirus	*Giardia lamblia virus*		Protozoa	2 overlapping ORFs encode gag capsid protein and gag-pol polymerase protein by ribosomal frameshifting
	Leishmaniavirus	*Leishmania RNA virus 1-1*		Protozoa	

[Recently proposed genera of *Reoviridae*] (P.P.C. Mertens, pers. comm.)

Reference sources for Table 1.1

Fields Virology (1996), 3rd edn. Edited by B. N. Fields, D. M. Knipe, P. M. Howley, *et al.*. Philadelphia: Lippincott-Raven Publishers.
Encyclopedia of Virology (1994). Edited by R. G. Webster and A. Granoff. London: Academic Press.
The Australian National University ICTV database on *Reoviridae* (http://life.anu.edu.au/viruses/Ictv/fs_reovi.htm)
The *Reoviridae* home page at The Institute for Animal Health (http://www.iah.bbsrc.ac.uk/virus/Reoviridae/)
All the Virology on the WWW (http://www.virology.net/)

dsRNA viruses. Interestingly, at present this structure has only been found in viruses with a dsRNA genome, suggesting that this particular structural confirmation may be favourable for the unique replication cycle of these viruses, or possibly that all currently recognised dsRNA viruses have a common ancestor (Hill *et al.*, 1999).

The members of the family *Reoviridae* have dsRNA genomes consisting of 10-12 segments, in contrast with other dsRNA viruses that only have 1-3 segments (Table 1.1). All dsRNA viruses have an RNA-dependent RNA polymerase activity associated with the core of the virion, since cells do not have enzymes capable of transcribing dsRNA templates. The polymerase complex performs negative strand synthesis (replicase) and new positive strand synthesis (transcriptase) in a compartment shielded from the cytoplasm. In *Rotavirus*, the core protein VP1 has been identified as the RNA polymerase, although VP2 is also required for replicase activity (Patton *et al.*, 1997). Only double-layered particles (VP6 layer) have transcriptase activity. Similarly, in *Reovirus* the λ3 protein is the catalytic subunit of the transcriptase complex, but other core proteins are probably required for it to be fully functional (Starnes and Joklik, 1993). *Orbivirus* cores also exhibit an RNA-dependent RNA polymerase activity, and the VP1 protein of BTV is predicted to be the RNA polymerase (Roy *et al.*, 1988).

The members of the *Reoviridae* have a conservative transcription process that uses template dsRNA located within double-layered particles (Banerjee and Shatkin, 1970) (Patton, 1986-1987). However, in other dsRNA viruses, such as the *Birnaviridae*, and some members of the *Totiviridae* (*Aspergillus foetidus* slow virus) and the *Partitiviridae* (*Penicillium stoloniferum* slow virus), dsRNA transcription is semi-conservative (Wickner, 1996). The difference between conservative and semi-conservative transcription is whether the template (-) strand re-pairs with the parental (+) strand following displacement during the transcription reaction. The viruses of the *Reoviridae* family share a similar polymerase function in that the 5'-ends of the mRNA species are capped and methylated during transcription (Ramadevi *et al.*, 1998) (Mao and Joklik, 1991) (Pizarro *et al.*, 1991). The 5' cap is required for efficient elongation of mRNA transcripts (Spencer and Garcia, 1984). Virions of the family *Birnaviridae* contain two forms of the RNA polymerase VP1. It is found as a free polypeptide, and also as a genome-linked protein (VPg) attached to the 5' ends of both genome segments by a serine-5' GMP phosphodiester bond (Calvert *et al.*, 1991).

Transcription in viruses of the *Birnaviridae* is thought to proceed via an asymmetric, semiconservative, strand-displacement mechanism that is primed by VP1 (Dobos, 1995).

In the family *Reoviridae*, transcription of each segment occurs within transcriptionally active virion particles to produce a full-length mRNA copy, which is then exported into the cytoplasm of the infected cell. The turret-like spike structures found in *Cypoviruses* (Hill *et al.*, 1999) and *Orthoreoviruses* (White and Zweerink, 1976) form a channel through which the newly synthesised mRNA is extruded (Bartlett *et al.*, 1974). A transcription complex containing the RNA polymerase closely associated with the guanylyltransferase is thought to be localised at the five-fold axes (Dryden *et al.*, 1998). It has been suggested that this structure allows movement of both product and template RNAs during transcription in a so-called moving-template model (Joklik, 1983) (Shatkin and Kozak, 1983). *Rotaviruses* are also believed to have transcription complexes composed of the RNA polymerase and guanylyltransferase located at the five-fold axes (Prasad *et al.*, 1996), and in this case the viral mRNAs are thought to exit through the pores at the five fold axes (Lawton *et al.*, 1997a). It is thought that the RNA polymerase can reinitiate positive strand synthesis as transcriptase particles are able to carry out mRNA synthesis *in vitro* continuously over a period of hours (Cohen, 1977) (Spencer and Garcia, 1984). This implies that the same RNA polymerase can repeatedly transcribe at least one of the genome segments. Evidence that each of the genome segments of cytoplasmic polyhedrosis virus, a member of the *Reoviridae*, are held in a circular configuration suggests a model whereby the RNA polymerase could reinitiate transcription without releasing from the template (Yazaki *et al.*, 1986). A moving template model of transcription with the transcription complex anchored at the particle five-fold axes may be shared by other viruses in the family *Reoviridae* (Dryden *et al.*, 1998). Study of other dsRNA viruses has allowed comparisons to be drawn, for example the structure and function of the polymerase complex in $\phi 6$ is thought to bear similarities with that of members of the family *Reoviridae* (deHaas *et al.*, 1999). Further, the L-A virus of yeast (*Totiviridae*) is also thought to share a similar mechanism of transcription as the polymerase protein is constrained by its fusion to the capsid protein necessitating movement of the template (Wickner, 1996). Thus, it is

conceivable that this mechanism of transcription might be a common feature of dsRNA viruses.

Immunoelectron microscopy studies of bluetongue virus-infected cells have been used to examine the replication cycle of *Orbiviruses* (Eaton *et al.*, 1990). After infection the bluetongue virus (BTV) particle is uncoated and the core particles enter the cytoplasm. The mechanism by which the transcriptase particles of the dsRNA viruses are transported intact across the cell membrane and into the cytoplasm is poorly defined. Clearly these viruses must overcome the problem of transporting such a large structure across the membrane barrier. BTV particles are internalised by receptor-mediated endocytosis, and it is suggested that core particles then enter the cytoplasm by penetration of the endosomal membrane (Roy, 1996). Direct interaction of viral components with the cell membrane is expected to be one step in the process of reovirus entry (Nibert *et al.*, 1996). This might produce a breach or a pore in the membrane through which the transcriptase particle can enter. Both direct penetration and endocytosis have been proposed as mechanisms of entry for rotavirus (Section 1.5.2).

Following entry to the cytoplasm, the core particles of BTV bind to the cytoskeleton of the cell and initiate transcription of viral mRNA (Hyatt and Eaton, 1988). Viral inclusion bodies (VIBs), which contain newly synthesised viral mRNA, proteins, and particles at different stages of morphogenesis, are formed soon after the initiation of transcription and surround the core particle (Hyatt *et al.*, 1987) (Hyatt *et al.*, 1991) (Brookes *et al.*, 1993). The VIBs are also believed to be the assembly site of core particles (Hyatt and Eaton, 1988) (Brookes *et al.*, 1993). At present the site of mRNA synthesis of reovirus and rotavirus remains undetermined (Nibert *et al.*, 1996) (Estes, 1996). By analogy with BTV, transcription would be expected to occur in viroplasms similar to VIBs, however it has been suggested that primary transcriptase particles of reovirus may be free in the cytoplasm (Bodkin and Fields, 1989) (Borsa *et al.*, 1981). In rotavirus the viroplasm is thought to be the site of synthesis of double-layered particles containing RNA (Petrie *et al.*, 1984) (Richardson *et al.*, 1986), on the basis of the localization of the core protein VP2 and several non-structural proteins to the viroplasm, and the inner capsid protein VP6 to the periphery. Viral factories containing dsRNA, viral polypeptides and both complete and incomplete particles are also found in reovirus-infected cells (Nibert *et al.*, 1996).

A central question in the replication cycle of the segmented dsRNA viruses is the mechanism by which they accurately package one copy of each segment. Although a unique packaging model has been proposed for the phage ϕ6 (Mindich, 1999), the mechanism in members of the family *Reoviridae*, which have a greater number of segments, remains unknown. The genome of ϕ6 consists of three segments of polycistronic dsRNA of different lengths, identified as segments L, M and S (Mindich, 1999). Genome segment L encodes the four proteins that form the procapsid of the virus (P1, P2, P4 and P7). The packaging model requires a collapsed fully formed procapsid, which has binding sites on the outside for plus strands of segment S. Following packaging of S, the conformation of the procapsid changes, the binding sites for S disappear and those for segment M appear. Once M is packaged, these binding sites disappear and those for segment L appear. The change in the availability of the binding sites depends upon the amount of RNA inside the procapsid (Qiao *et al.*, 1997). The packaging signals on the RNA segments have been localised to the 5'-end, and include a sequence of about 200 nucleotides that is unique for each segment (Gottlieb *et al.*, 1994). The major structural protein P1 is probably the predominant determinant of packaging specificity, possibly in association with P4 and P7 (Mindich, 1999).

The synthesis of minus-strand RNA to complete the replication of the dsRNA genome always occurs in a procapsid structure shielded from the cell cytoplasm. Virus replicase particles have been well studied in the *Orthoreoviruses*. The earliest reovirus particles contain mRNAs in association with proteins σ3, μNS and σNS (Antczak and Joklik, 1992) (Gomatos *et al.*, 1981). The subsequent particle includes both inner and outer capsid proteins but lacks the non-structural proteins (Acs *et al.*, 1971) (Morgan and Zweerink, 1975). Minus-strand RNA synthesis occurs in this replicase particle (Morgan and Zweerink, 1975). The outer capsid shell is then completed to form the virion particle (Morgan and Zweerink, 1975) (Zweerink *et al.*, 1976). Replication of the rotavirus genome is also thought to occur in nascent core particles by analogy with the reovirus system (Helmberger-Jones and Patton, 1986). Three replication intermediates (RIs) have been identified (Gallegos and Patton, 1989), however it has not yet been possible to exactly characterise the rotavirus replicase particle. The structures of the rotavirus replicase intermediates are discussed in more depth in subsequent sections (Sections 1.5.4; 1.4.1.1/2; 1.6.7). Despite these

advances, much still remains unknown about the replication cycles and assembly processes in the viruses of the family *Reoviridae*.

1.3 Structure of the rotavirus particle and genome

1.3.1 Classification

Rotavirus is one of nine distinct genera which make up the family *Reoviridae*, as defined by the International Committee of Taxonomy of Viruses (ICTV), together with *Aquareovirus*, *Coltivirus*, *Cypovirus*, *Fijivirus*, *Orbivirus*, *Orthoreovirus*, *Oryzavirus*, and *Phytreovirus* (Murphy, 1996). Two new genera that have recently been proposed are *Seadornavirus* and *Entomoreovirus* (P.P.C. Mertens, pers. comm.). Rotaviruses have three major antigenic specificities: group, subgroup and serotype. The predominant group antigen is found on VP6, though group epitopes have been detected on all the structural proteins (Mattion *et al.*, 1994). Five groups (A to E) have been recognised, and a further two putative groups (F and G), which thus far have only been shown to infect avian species, have been described. Only groups A, B and C are associated with human disease. Group A rotaviruses are the most common cause of disease in infants and young children, and are the predominant group isolated and associated with disease to date. Group B viruses have been shown to cause epidemics of cholera-like illness in adults in China (Chen *et al.*, 1985) (Hung *et al.*, 1987). Group C rotaviruses only cause sporadic outbreaks of gastroenteritis in humans (von Bonsdorff and Svensson, 1988) (Bridger *et al.*, 1986) (Chen *et al.*, 1988). The subgroups, which are also determined by VP6 antigens, have only been clearly defined for Group A rotaviruses and fall into four categories: subgroup I, subgroup II, subgroup I + II, and non-I non-II (Hoshino *et al.*, 1987) (Svensson *et al.*, 1988). The focus of this thesis is the Group A rotaviruses which have been studied in more detail than any other group.

Group A rotaviruses have been classified into 14 serotypes on the basis of reciprocal neutralization assays with hyper-immune sera against the major neutralization antigen VP7 (G serotypes) (Kapikian and Chanock, 1996). Virus serotype has been identified by conventional assays including neutralization of cytopathic effect (cpe), reduction of virus yield in tube or plate cultures, and plaque or focus reduction (Kapikian and Chanock, 1996). A distinct VP7 serotype is recognised

by a reciprocal 20-fold or greater difference in serum antibody titre when a candidate serotype is tested against prototype viruses representing established serotypes (Hoshino *et al.*, 1984). A total of 14 VP7 (G) serotypes have been identified, comprising ten in humans and 13 in animals (Hoshino and Kapikian, 1994). A study of human isolates revealed that 95 % belonged to serotypes one to four (Beards *et al.*, 1989). Monoclonal antibodies to VP4 can also neutralize viral infectivity (Greenberg *et al.*, 1983), and eleven distinct serotypes (P types) have been distinguished (Hoshino and Kapikian, 1994). A binary classification system involving both G serotype (VP7) and P serotype (VP4) is now used (Hoshino and Kapikian, 1996).

1.3.2 Morphological structure of the virus particle

Examination of rotavirus by electron microscopy (EM) reveals three different types of particle each with its own distinctive morphological appearance. The infectious virion consists of three protein layers (triple-layered particle) enclosing the segmented double-stranded (ds) RNA genome, although this particle was historically known as double-shelled. The outer coat proteins of the triple-layered, intact virion are VP4 and VP7. Double-layered particles are transcriptionally active, but are not infectious and are equivalent to the cores of most other genera in the *Reoviridae*. Unlike the *Orthoreoviruses*, an infectious, transcriptionally active particle, or ISVP, is not found in *Rotavirus*. The double-layered particles lack the outer coat proteins, and have VP6 as surface protein. They are sometimes described as rough particles due to the projecting trimeric subunits of VP6 that are observed at their periphery (Estes, 1996). The single-layered core particle consists of VP1 and VP3, surrounded by an outer surface coat of 120 copies of VP2. These are equivalent to the subcores of other genera in the *Reoviridae* such as *Orbiviruses*. The VP2 shell surrounds a subcore consisting of VP1 and VP3, however the cores are the smallest particles that have been observed by EM (Estes, 1996).

Electron cryomicroscopy and image processing techniques have been used to resolve the three-dimensional structure of triple- and double-layered particles first to 40 Å resolution (Prasad *et al.*, 1988), and then subsequently to 26 Å resolution (Prasad *et al.*, 1990) (Prasad and Chiu, 1994). It is now established that the virion is approximately 75 nm in diameter, and that the two outer layers have T=13/(levo) icosahedral symmetry (Prasad *et al.*, 1988). The smooth outer layer that makes up the

majority of the outer capsid is composed of 780 molecules of the neutralization antigen VP7 arranged as trimers. From this smooth surface 60 spikes protrude to a length of approximately 120 Å from the outer capsid surface (Prasad *et al.*, 1990) (Yeager *et al.*, 1990). It was established that these surface spikes are composed of dimers of the haemagglutinin VP4 by the binding of two Fab fragments of a neutralizing monoclonal antibody against VP4 to the distal ends of the spikes (Prasad *et al.*, 1990). The VP4 spikes also extend inwards and interact with both VP7 and the inner capsid protein VP6. The inner capsid is composed of 780 molecules of VP6 arranged as 260 trimers in a T=13*l* icosahedral surface lattice (Prasad *et al.*, 1988) (Bican *et al.*, 1982). The VP6 layer is thought to interact with the inner VP2 shell. High affinity interactions between the structural proteins are suggested by their self-assembly into virus-like particles when co-expressed in insect cells (Crawford *et al.*, 1994) (Labbe *et al.*, 1991). Co-assembly of purified proteins of each layer onto preformed VP2 particles has also been demonstrated (Zeng *et al.*, 1994).

The inner VP2 capsid layer surrounds a sub-core consisting of the enzymes VP1 and VP3 and the dsRNA genome (Labbe *et al.*, 1991). Electron cryomicroscopy and image reconstruction studies of recombinant rotavirus-like particles have suggested that the VP2 layer is arranged as dimers of 120 quasi-equivalent molecules on an icosahedral lattice (Lawton *et al.*, 1997b). The majority of VP2 forms a smooth shell, however a small portion at the amino-terminus of the protein appears to extend inwards at the icosahedral five-fold axes where it is believed to interact with a transcription complex composed of VP1 and/or VP3 (Prasad *et al.*, 1996) (Lawton *et al.*, 1997b). The amino-terminus of VP2 has RNA-binding activity (Labbe *et al.*, 1994), and it is has been shown that the viral dsRNA interacts closely with VP2 and the enzyme complex at the five-fold axes (Prasad *et al.*, 1996). VP2 may have a role during transcription and viral morphogenesis as a scaffold for the proper assembly of the viral RNA, and VP1 and VP3 in the viral core (Labbe *et al.*, 1994) (Zeng *et al.*, 1998). Pores surrounding the five-fold axes of VP2 are large enough to allow mRNA to leave during transcription, although VP2 may also undergo conformational changes to facilitate this (Prasad *et al.*, 1996).

Complexes consisting of one copy of each of the minor structural proteins VP1 and VP3 are thought to be associated with the VP2 shell at the icosahedral five-fold axes (Prasad *et al.*, 1996). These two enzymes are involved in the transcription of the genome within the intact particle. VP1 is the viral RNA-dependent RNA

polymerase (Patton *et al.*, 1997) (Zeng *et al.*, 1996). VP3 has guanylyltransferase activity, and is responsible for capping of viral mRNAs (Patton and Chen, 1999) (Pizarro et al., 1991) (Liu et al., 1988). It has also been shown to have methyltransferase activity (Chen *et al.*, 1999), and thus is a multifunctional capping enzyme with similarities to capping enzymes of other members of the *Reoviridae*, such as VP4 of bluetongue virus (Ramadevi *et al.*, 1998). Other enzyme activities associated with transcription have not yet been attributed to particular proteins. The dsRNA genome is packed around the enzyme complex and interacts closely with the inner capsid layer (Prasad *et al.*, 1996). It is proposed that the organisation of the dsRNA allows movement of the RNA relative to the enzyme complex during transcription.

A distinctive feature of the virion structure is the presence of 132 large channels linking the outer surface with the inner core (Roseto *et al.*, 1979) (Ludert *et al.*, 1986). These comprise 120 channels along the six-fold axes, and 12 along the five-fold axes. The function of the channels is unknown at present, although they may be involved in importing the metabolites required for RNA transcription and export of nascent RNA transcripts for subsequent viral replication processes (Estes, 1996). Similar channels have been observed in the virion structure of the related *Orbiviruses* (Roy, 1996).

Recent X-ray crystallography studies on the particle structure of bluetongue virus (BTV), the prototype virus of the genus *Orbivirus*, have revealed similarities between the subcore of this virus and that of other members of the *Reoviridae* such as *Rotavirus* (Grimes *et al.*, 1998) (Gouet *et al.*, 1999) (Lawton *et al.*, 1997b). The structure of the BTV core particle has been determined to a high resolution (Grimes *et al.*, 1998). The core particle consists of an outer layer of 780 copies of the VP7(T13) protein arranged as trimers on an icosahedral lattice, equivalent to the VP6 layer in rotavirus (Prasad *et al.*, 1992) (Grimes *et al.*, 1997). This layer surrounds and interacts with a thin subcore of 120 copies of the VP3 (T2) protein (Grimes *et al.*, 1997) (Huismans *et al.*, 1987), which bears a striking resemblance to the structure of the VP2 layer of rotavirus (Lawton *et al*, 1997b). This arrangement of 120 subunits may prove to be a unique characteristic of dsRNA viruses (Grimes *et al*, 1998). VP3(T2) also binds RNA (Loudon and Roy, 1991), and can self-assemble into core particles (Moss and Nuttall, 1994). Pores at both the icosahedral five-fold and three-fold axes have been identified (Grimes *et al.*, 1998). Pores involved in substrate (NTP) entry to

the BTV core have also been identified in the VP3(T2) layer, by X-ray crstallography of transcriptionally active BTV particles (P.P.C. Mertens, pers. comm.) (Mertens *et al.*, 1999). These pores are situated at the base of the channels formed by the six membered rings of VP7(T13) trimers closest to the five-fold axes. The VP3(T2) exists as A form molecules (those adjacent to the five-fold axis) and B form (those positioned further out from the five-fold axis) (Grimes *et al.*, 1999), thereby forming decamers around each five-fold axis. The pores, which can be seen to contain an NTP molecule are situated between adjacent A and B forms. There is therefore a ring of five of these substrate entry pores around each five-fold axis.

Electron microscopy studies of the structure of cytoplasmic polyhedrosis virus, a member of the *Reoviridae*, suggested that the dsRNA genome was found in close association with proteins at the base of the spikes at the five-fold axes (Yazaki and Miura, 1980). Disruption of the virion released dsRNA attached to a part of the spike. During transcription the spike was observed to swell and dsRNA was seen with a protein particle, believed to be part of the spike, attached at various points along its length. The theory was thus suggested that the genomic dsRNA moves through the base of the spike containing the transcription complex, and the newly synthesised mRNA is released through the top.

It has been suggested that the proteins forming the transcription complex of BTV attach to the VP3(T2) layer at each of the icosahedral five-fold axes before the formation of the complete subcore (Grimes *et al.*, 1998). The model suggests that the amino-terminal 50 residues of the VP3(T2) subunit swing down to interact with the transcription complex, perhaps holding some of the enzyme components in the correct orientation, and thus suggesting an important function for this domain of VP3(T2) in RNA synthesis and virion morphogenesis (Gouet *et al*, 1999) (Grimes *et al*, 1998). This is similar to the structure proposed for the VP2 protein in rotavirus above. The dsRNA genome may then be laid down within the assembled protein shell leading to an ordered genome structure which may be a common feature of the *Reoviridae* (Prasad *et al.*, 1996) (Gouet *et al.*, 1999). The minor core proteins μ2 and λ3 (RNA-dependent RNA polymerase) of reovirus are also thought to form a similar transcription complex at the five-fold icosahedral axes of the inner capsid (Nibert *et al*, 1996). Many features of the subcores of viruses in different genera of the *Reoviridae*, such as *Rotavirus* and *Orbivirus*, appear to be conserved. Although there

is still much work to be done in this area it is speculated that further structural and functional similarities between the genera will be found (Gouet *et al*, 1999).

1.3.3 Physicochemical properties

The three different rotavirus particle types, double-shelled, single-shelled and core particles, possess differing biophysical and biological properties. Infectivity depends upon the presence of the outer capsid layer (Lopez *et al.*, 1986), and removal of this layer by treatment with calcium-chelating agents, such as EDTA and EGTA, results in a loss of infectivity (Estes *et al.*, 1979). Single-shelled particles have polymerase activity resulting from the loss of the outer capsid layer that activates the endogenous RNA-dependent RNA polymerase.

The particles possess different densities and sedimentation values, hence density gradient centrifugation can be used to separate them. The double-shelled particle has a density of 1.36 g/cm^3 in caesium chloride (CsCl) and a sedimentation value of 520 to 530 S in sucrose. The single-shelled particle has a density of 1.38 g/cm^3 in CsCl and sediments at 380 to 400 S (Tam *et al.*, 1976). Core particles have a density of 1.44 g/cm^3 in CsCl and a sedimentation value of 280 S (Bican *et al.*, 1982).

The mature virion is non-enveloped, a fact that is reflected by the general resistance of the particle and its infectivity to treatment with fluorocarbons, ether, chloroform and deoxycholate (Estes *et al.*, 1979) (Tam *et al.*, 1976) (Welch and Thompson, 1973). Virus infectivity is stable within the pH range 3 to 9, and virus samples can be stored at 4 °C for months (Estes *et al.*, 1979) (Palmer *et al.*, 1977). The physicochemical properties of rotaviruses are relatively consistent among viruses of both animal (bovine or simian) and human origin.

1.3.4 Rotavirus genome structure

Rotaviruses are the only known viruses of mammals or birds to have eleven double-stranded (ds) RNA segments, although viruses of other species with 11 dsRNA segements are known (Eley *et al.*, 1987). The segments range in size from 3302 bp to 667 bp. The nucleotide sequence for all eleven RNA segments has been elucidated for several strains, and general features have been described. The open reading frame (ORF) is surrounded by conserved non-coding regions of varying

length dependent upon the gene segment. Each RNA segment starts with a 5' guanylate and ends with a 3'-terminal cytidine. The dsRNA segments are base paired end to end and the positive sense strand has a conserved 5' cap sequence $m^7GpppG^{(m)}GPy$ (Imai *et al.*, 1983) (McCrae and McCorquodale, 1983). The rotaviruses share similar features, such as the 5' cap and the conserved sequence at the 5' and 3' ends of the RNA segments, with other viruses (e.g. reovirus, cytoplasmic polyhedrosis virus, and viruses of the genus *Orbivirus*) in the family *Reoviridae* (Furuichi *et al.*, 1975) (Kuchino *et al.*, 1982) (Mertens and Sanger, 1985), and in other virus families with segmented genomes such as the *Orthomyxoviridae*, *Arenaviridae* and *Bunyaviridae*. Short sequences of about eight nucleotides at the extreme 5' and 3' ends are conserved on all Group A rotavirus genome segments (Desselberger and McCrae, 1994). Among different virus strains there are high levels of segment specific conservation in the non-coding regions which are suggested to contain signals involved with genome transcription, RNA transport, replication and assembly.

The RNA segments are packaged within the virus core capsid. The proteins responsible for packaging are unknown and while VP1, VP2 and VP3 are obvious candidates, the non-structural proteins may also have a role. A strict limit on the number of segments packaged appears to operate such that only eleven segments are included in the virion. At present the upper limit on segment length is unknown (McIntyre *et al.*, 1987), although a rotavirus variant, brvA, has been described which encodes a novel dsRNA, gene A, which at 2693 bp is the largest rearranged segment reported for the rotaviruses. This rotavirus variant can package 6 % more RNA than the standard rotavirus (Hua and Patton, 1994). Gene A is a head-to-tail duplication of 1112 bp that originates from the gene 5 ORF (Hua and Patton, 1994). To date the only atypical genotypes described for Group A rotaviruses are rearrangements resulting from sequence duplications within a single genome segment. It has been suggested that this genome rearrangement arises during viral transcription when the RNA polymerase detaches from the template without releasing the nascent transcript, and then reinitiates transcription at an upstream site on the template (Gorziglia *et al.*, 1989) (Hundley *et al.*, 1987) (Matsui *et al.*, 1990). This mechanism supports the existence of a specific association between a single genome segment and a transcriptase complex in the transcriptionally active virus particle, possibly involving simultaneous contact of both ends of the genome segment during transcription. The isolation from *Cypoviruses* of an active replicase particle composed of a transcriptase

complex and a single genome segment also supports this mechanism of transcription (Wu and Sun, 1986).

A feature of the segmented genome that has proved invaluable in studying the molecular biology of the virus and in vaccine development, is reassortment of the RNA segments between strains and recovery of infectious virus (Glass *et al.*, 1994).

1.3.5 Gene-Protein coding assignments

The proteins encoded by the eleven RNA gene segments have now been fully ascribed (Figure 1.3). The coding assignment for each segment was determined by *in vitro* translation of mRNA or denatured dsRNA (Mason *et al.*, 1980) (McCrae and McCorquodale, 1982) and the analysis of rotavirus reassortants (Greenberg *et al.*, 1981) (Liu *et al.*, 1988) (Offit and Blavat, 1986). The general consensus is that 12 proteins are encoded, of which six are structural (Table 1.2). Early studies presented conflicting results as confusion arose due to the post-translational modification of the proteins.

Different rotavirus strains produce a varying order of RNA segments when they are resolved by electrophoresis. Hence, identification of cognate genes has been based on hybridization with gene-specific probes (Dyall-Smith *et al.*, 1983), reassortant analysis (Gombold *et al.*, 1985), sequence homology (Green *et al.*, 1987), or biochemical or immunological identification of the protein synthesized in a cell-free translation system programmed with mRNA specific to the gene.

1.4 Protein structure and function

1.4.1 Structural proteins

1.4.1.1 Inner core proteins VP1 and VP3

The product of genome segment one, VP1, is a minor component of the viral core. Early experiments demonstrated that temperature-sensitive mutants that mapped to genome segment one had RNA-negative phenotypes, suggesting an enzymatic role for VP1 (Gombold and Ramig, 1987). VP1 has been found to be a minor but consistent component of all rotavirus complexes that possess polymerase activity (Gallegos and Patton, 1989) (Zeng *et al.*, 1996). It contains regions of sequence

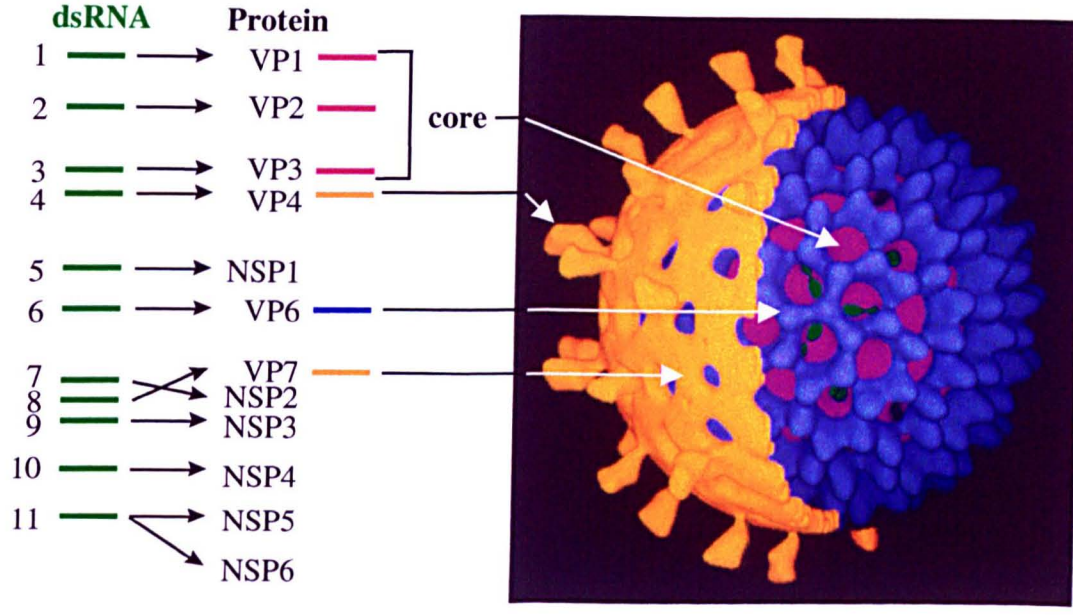

Figure 1.3 The rotavirus particle and gene-protein coding assignments

The eleven segments of dsRNA that comprise the rotavirus genome and the proteins encoded by each gene are shown for the UKtc strain of bovine rotavirus. The structural proteins which make up the triple-layered particle are indicated on a cryo-electron reconstruction of a rotavirus particle at 24 Å resolution (cryo-electron reconstruction courtesy of R. F. Ramig) (Prasad and Chiu 1994). The outer capsid is shown in yellow, the inner capsid in blue and the inner core in purple. The dsRNA segments are shown in green.

Figure adapted from Estes (1996).

Genome segment	Protein product	Molecular mass	Mature protein modified	Location in virus particles	Number of molecules per virion
1	VP1	125 kDa	-	Inner core	ND
2	VP2	94 kDa	-	Inner core	120
3	VP3	88 kDa	-	Inner core	ND
4	VP4 (VP5*+VP8*)	88 kDa	Cleaved	Outer capsid	120
5	NSP1	53 kDa	-	Nonstructural	
6	VP6	41 kDa	-	Inner capsid	780
7	NSP2	35 kDa	-	Nonstructural	
8	VP7	38 kDa	Cleaved signal sequence; glycosylated	Outer capsid	780
9	NSP3	34 kDa	-	Nonstructural	
10	NSP4	28 kDa	Glycosylated	Nonstructural	
11	NSP5	26 kDa	Phosphorylated; o-glycosylated	Nonstructural	
11	NSP6	12 kDa	-	Nonstructural	

Table 1.2 Properties of rotavirus proteins

Table reproduced and adapted from Estes (1996). The gene-protein coding assignments are for the UKtc strain of bovine rotavirus. Approximate molecular weights for the polypeptides were deduced by SDS-polyacrylamide gel electrophoresis. All gene segments are monocistronic with the exception of gene 11, which contains a second out of frame ORF known to be expressed during infection (Mattion *et al.* 1991). ND = not yet determined.

homology with consensus motifs of the putative RNA-dependent RNA polymerases of several other RNA viruses of eukaryotes, by comparison to the known poliovirus polymerase (Cohen *et al.*, 1989) (Fukuhara *et al.*, 1989) (Mitchell and Both, 1990b). The photoreactable nucleotide analogue [α-^{32}P] azido ATP was shown to cross-link exclusively with VP1 when transcriptionally active VP6 particles were exposed to light (Valenzuela *et al.*, 1991). The cross-linking blocked the activity of the transcriptase, demonstrating that VP1 is a nucleotide-binding protein and also implying it is the RNA polymerase. For the these reasons it is now generally accepted that VP1 is the RNA-dependent RNA polymerase.

Cis-acting signals, localised within the 26 3'-terminal nucleotides, of rotavirus mRNA are recognised by the replicase complex and used to promote replication (Chen *et al.*, 1994). The essential part of the signal is composed of seven nucleotides at the extreme 3' end of viral mRNA (Wentz *et al.*, 1996). VP1 specifically binds the 3' end of viral mRNA in the absence of any other proteins (Patton, 1996). This is further evidence for the function of VP1 as the polymerase. However, it is now known that VP1 alone is not sufficient for replicase activity, and VP2 is also required, though its exact function is still uncertain (Patton *et al.*, 1997).

The product of gene segment 3, VP3, is a basic protein that is a minor component of the virion core (Liu *et al.*, 1988). It is estimated that approximately one or fewer molecules of VP3 per dsRNA segment are present in the core. VP3 is found in early replication intermediates (RIs) in the viroplasm and is thought to associate with viral mRNA at early stages in the virus replication cycle (Gallegos and Patton, 1989). It is known to bind to proteins involved in RNA replication (Zeng *et al.*, 1998) and transcription (Sandino *et al.*, 1994).

VP3 is thought to be a guanylyltransferase, and thus to have a function in mRNA capping by transferring GMP to the phosphate end of nascent RNAs. Guanylyltransferases are evolutionary conserved enzymes and have features in common with other members of the nucleotidyltransferase superfamily, which includes among others ATP-dependent DNA ligases and RNA ligases (Cong and Shuman, 1993) (Shuman *et al.*, 1994) (Shuman and Schwer, 1995). VP3 is also known to have some sequence similarity with the RNA polymerases of the negative-strand RNA viruses (e.g. vesicular stomatitis virus, measles virus)

suggesting the protein is a component of the polymerase complex (Liu and Estes, 1989) (Mitchell and Both, 1990b).

Several studies have provided evidence for the role of VP3 as a guanylyltransferase. It has been shown that VP3 forms a reversible, covalent bond with GTP which is a characteristic of both eukaryotic and viral guanylyltransferases (Fukuhara *et al.*, 1989) (Liu *et al.*, 1992). When expressed in the baculovirus system it binds GTP in the absence of other viral proteins, suggesting that the GTP-binding activity is an intrinsic property of the protein (Liu *et al.*, 1992). VP3 is probably an essential component of the transcriptase complex rather than the replicase complex, and it has been shown that baculovirus-expressed core-like particles that lack VP3 have replicase activity (Zeng *et al.*, 1996). In particular, Pizarro *et al.* (1991) demonstrated that VP3 was the only viral core protein to have associated guanylyltransferase activity. An assay specific for guanylyltransferase activity which detects an intermediate of the reaction, a covalent GMP-enzyme complex made from GTP, was used (Cleveland *et al.*, 1986) (Shuman, 1982) and it was shown that only VP3 formed a complex with the nucleotide. The GMP-VP3 complex transfers GMP to the pyrophosphate group of GDP, resulting in the formation of a GpppG cap. In the related *Orbivirus* system, both guanylyltransferase and methyltransferase type I and type II activities have been found associated with one viral protein which is the minor core protein VP4 of bluetongue virus (Le Blois *et al.*, 1992) (Ramadevi *et al.*, 1998).

Recent evidence demonstrated that VP3 is an RNA-binding protein. Gel shift assays using open virion-derived cores and virus-specific RNA probes have shown that VP3 has a sequence-independent affinity for ssRNA, but not for dsRNA (Patton and Chen, 1999). The guanylyltransferase activity of VP3 was found to be non-specific and able to cap RNAs initiating with either a guanine or an adenine residue. Moreover, the results also indicated that VP3 has a preferential affinity for uncapped rather than capped ssRNA.

1.4.1.2 Core protein VP2

VP2 forms the inner core layer and constitutes 12 % of the virion protein (Kumar *et al.*, 1989). It encapsidates the genomic RNA and the minor structural proteins VP1 and VP3. It is found in the viroplasm during replication, which is the site of assembly of single-shelled particles and replication of dsRNA (Petrie *et al.*,

1982). VP2 is known to be essential for replicase activity (Mansell and Patton, 1990), and is also involved in transcriptase activity, although the exact domains of the protein involved in these diverse functions are unknown at present (Estes *et al.*, 1983). Temperature-sensitive mutants were used to demonstrate that VP2 is required for replicase activity and the simplest structures that were able to synthesize dsRNA were core-like particles (Mansell and Patton, 1990). More recently, experiments with baculovirus-expressed proteins have suggested that VP2 is a necessary component of complexes that synthesize rotavirus dsRNA (Zeng *et al.*, 1996), and that the minimal replicase complex is VP1 and VP2 (Patton *et al.*, 1997).

VP2 has been shown to have sequence-independent RNA binding activity in north-western blotting assays (Boyle and Holmes, 1986). Although it associated with both ssRNA and dsRNA, it has been shown to preferentially bind to ssRNA. Deletion analysis of recombinant baculovirus expressed VP2 localised the nucleic acid binding domain to the amino terminal region between aa 1 and 132 (Labbe *et al.*, 1994). Although the recombinant protein bound both double-stranded and single-stranded probes, it showed less affinity for dsRNA and DNA.

Several motifs were identified in the amino-terminal domain that could function in RNA-binding, albeit they were not strictly conserved in all strains. The motifs which may play a role in the RNA-binding function of VP2 were: (i) a predicted helix-turn-helix structure (aa 65 to 121); (ii) heptad repeats of lysine and glutamic acid residues (aa 53 to 81); (iii) a motif found in several proteins known to bind ss- and ds-RNA (aa 64 to 76) (Labbe *et al.*, 1994). As VP2 binds to ssRNA, it has been suggested that it plays a role in encapsidation of viral ssRNA (Patton, 1995). More recent studies have suggested that its primary role in replication is linked to its ability to bind the mRNA template for minus strand synthesis, because when the N-terminal RNA-binding domain is deleted VP2 does not co-operate with VP1 to generate replicase activity (Patton *et al.*, 1997).

VP2 can self-assemble into the core particle required for dsRNA synthesis, but other viral products, such as viral mRNA, are probably required for the core to condense into its mature form (Labbe *et al.*, 1991). It is possible that two leucine zippers present between aa 536 and 686 are involved in the oligomerization of VP2 into cores (Patton, 1995). Co-expression of baculovirus recombinant proteins for VP1, VP2 and VP3 leads to the assembly of core-like particles (Crawford *et al.*, 1994), suggesting that VP1 and VP3 have specific sites of interaction with VP2 (Chen *et al.*,

1994). Expression of VP2 lacking the N-terminal 92 aa showed that the truncated protein had lost the capacity to encapsidate VP1 alone, VP3 alone, or a VP1-VP3 complex (Zeng *et al.*, 1998). Results of far-western blotting experiments established the amino-terminal aa 1 to 25 of VP2 as necessary for binding VP1 (Zeng *et al.*, 1998). It has to-date not been possible to map the domain necessary for VP3 binding more precisely than the N-terminal 92 aa.

1.4.1.3 Intermediate capsid protein VP6

VP6 is the inner capsid protein and is a major structural component of the virion, making up 51 % of the total protein content (Liu *et al.*, 1988). It is the group antigen and also carries sub-group determinants. It has an important role in the virion structure, due to its interactions with both the outer capsid proteins VP4 and VP7, and with the core protein VP2 (Estes, 1996). VP6 spontaneously forms trimers which are extremely stable and contain several highly immunogenic, conserved epitopes (Estes *et al.*, 1987).

VP6 is necessary for transcriptase activity and its addition to core particles activates the particle-associated RNA-dependent RNA polymerase (transcriptase) and thus synthesis of viral mRNA. However, it is not known whether VP6 plays a structural or functional role in this process (Bican *et al.*, 1982) (Sandino *et al.*, 1986). Temperature-sensitive mutants were used to show that VP6 is not necessary for synthesis of dsRNA (replicase activity) (Mansell and Patton, 1990). Expression of rotavirus-like particles from baculovirus recombinants also demonstrated that VP6 is not an essential component of particles supporting replicase activity (Zeng *et al.*, 1996). Addition of VP6 to core particles activates transcription and suppresses replicase activity (Kohli *et al.*, 1993), suggesting VP6 plays a role in modulating the enzymatic activity of single- and double-layered particles.

1.4.1.4 Outer capsid proteins VP4 and VP7

Although it is only a minor component of the outer capsid, forming spikes on the surface of the rotavirus particle (Prasad *et al.*, 1990), VP4 is an important multifunctional protein. Proteolytic cleavage of VP4 to form VP5* and VP8* potentiates infectivity by enhancing penetration of the virus into cells, but not

adsorption (Fukuhara *et al.*, 1988). The trypsin cleavage sites are conserved in every VP4 sequence analysed to date (Estes, 1996).

VP4 is probably the cell attachment protein (Ruggeri and Greenberg, 1991). It has a putative fusion region (residues 384 to 401) that shares some homology with internal fusion sites in Semliki Forest and Sindbis virus proteins (Mackow *et al.*, 1988). As these regions have been implicated in cell fusion, it is hypothesised that the region might perform a similar function in VP4. This region is conserved among rotaviruses, suggesting is has an important function in the replication cycle (Estes, 1996).

VP4 was identified as the viral haemagglutinin on the basis of studies of reassortants produced following dual infection of a rotavirus with haemagglutination activity (RRV) and a rotavirus lacking this activity (bovine UK rotavirus) (Kalica *et al.*, 1983). It has been implicated as a virulence determinant in mice (Offit *et al.*, 1986). It has also been shown to induce neutralising antibodies, which can protect animals experimentally infected with rotavirus (Offit *et al.*, 1986).

VP7 forms the smooth external surface of the outer capsid and constitutes 30% of the virion protein (Kapikian and Chanock, 1996). It is the major neutralisation antigen (Sabara *et al.*, 1985) and is largely responsible for serotype specificity defined by neutralisation with hyper-immune antiserum (Matsui *et al.*, 1989). VP7 is a glycoprotein containing only N-linked high mannose oligosaccharides, which are acquired in the endoplasmic reticulum (ER) and processed by trimming (Ericson *et al.*, 1982) (Kabcenell and Atkinson, 1985). It contains between one and three potential sites for N-linked glycosylation. VP7 is co-translationally glycosylated as it is inserted into the membrane of the endoplasmic reticulum (ER). Insertion is directed by a cleavable signal sequence, proposed to involve two regions of hydrophobic amino acids (aa) at the amino terminus which are cleaved at an amino terminal residue, glutamine 51 (Stirzaker *et al.*, 1987) (Whitteld *et al.*, 1987). Regions in VP7 that mediate the retention of the protein in the ER have been identified (Stirzaker *et al.*, 1987), but the mechanism by which this occurs is unknown (Estes, 1996). It has been proposed that VP7 is responsible for attachment of virus to host cells, although VP4 is now thought likely to be the main viral attachment protein (Fukuhara *et al.*, 1988) (Sabara *et al.*, 1985).

1.4.2 Non-structural proteins

1.4.2.1 NSP1

The product of genome segment five, NSP1, is a 58 kDa non-structural protein, which has the lowest level of expression of all the viral proteins in the infected cell (Johnson and McCrae, 1989). Its exact function is still unknown, despite the fact that several properties of the protein have been described. The primary sequence of NSP1 is highly divergent (Xu *et al.*, 1994), with the exception of a cysteine-rich sequence at the amino-terminus which may form a zinc finger structure (Hua *et al.*, 1993). NSP1 has been shown to have an affinity for zinc (Brottier *et al.*, 1992). It has non-specific RNA-binding activity (Brottier *et al.*, 1992), and the RNA-binding site has been mapped to the amino-terminus of the protein (Hua *et al.*, 1994). NSP1 localises to the cytoplasm during viral infection and accumulates in association with the cytoskeletal matrix (Hua *et al.*, 1994) (Hua and Patton, 1994). It is a component of early replication intermediates and is thought to have a role in the viral replication cycle (Gallegos and Patton, 1989). Gene five from a non-defective mutant virus, p9Δ5, has a deletion in the coding sequence resulting in an NSP1 of only the amino-terminal 150 aa compared to the usual 490 aa, possibly indicating that only the amino-terminus of the protein is essential for gene function *in vitro* (Tian *et al.*, 1993). Non-defective rotavirus mutants carrying truncated NSP1 of about 40 aa and lacking the conserved amino-terminal cysteine-rich region have recently been identified (Taniguchi *et al.*, 1996), suggesting that this region of NSP1 may also not be necessary for virus replication *in vitro* (Taniguchi *et al.*, 1999). The properties and proposed functions of NSP1 are discussed in more detail in Section 1.6.

1.4.2.2 NSP2 and NSP3

NSP2 is encoded by genome segment seven in the UKtc strain of bovine rotavirus. It accumulates predominantly in the viroplasm in rotavirus-infected cells (Petrie *et al.*, 1984). Experiments with temperature-sensitive mutants have indicated that NSP2 is essential for the formation of viroplasms and also for genome replication (Ramig and Petrie, 1984) (Gombold *et al.*, 1985). NSP2 has intrinsic RNA-binding activity that is not dependent upon the presence of other viral proteins (Kattoura *et al.*, 1992). It has non-specific affinity for both ss and dsRNA. Kattoura *et al.* (1994)

proposed that the RNA-binding activity of NSP2 may be dependent upon its ability to form multimers in infected cells. Immunoprecipitation with specific monoclonal antibodies from UV-crosslinked rotavirus-infected cells demonstrated that NSP2 interacted directly with all eleven dsRNA rotavirus genomic segments and with partially double-stranded RNA (Aponte *et al.*, 1996). However, as NSP2 has previously been shown to have non-specific RNA-binding activity, it was suggested that it co-localised with the RNA segments in infected cells. NSP2 has been shown to interact with the viral polymerase VP1 (Kattoura *et al.*, 1994). Evidence has also been presented to suggest NSP2 is associated with an enzyme complex exhibiting replicase activity in rotavirus-infected cells (Aponte *et al.*, 1996). The current view on the role of NSP2 is that it is involved in RNA replication and may have a role in the assembly of an efficient replicase complex.

NSP3 is a slightly acidic protein found distributed in a filamentous manner in the cytoplasm, possibly in association with the cytoskeleton (Mattion *et al.*, 1992). The secondary structure is predicted to be predominantly alpha-helical. Several heptad repeats of hydrophobic amino acids are found in the carboxy half of the protein, while a basic region, which is a candidate for a functional domain, is found in the amino half (Mattion *et al.*, 1992). NSP3 forms homo-oligomers *in vivo* and deletion mutagenesis has implicated the carboxy terminus in oligomerisation (Mattion *et al.*, 1992).

NSP3 has ssRNA and dsRNA binding activity and both monomeric and multimeric forms of NSP3 bind to rotavirus mRNA (Mattion *et al.*, 1992) (Poncet *et al.*, 1993). NSP3 binds the conserved consensus sequence AUGUGACC found at the 3'-end of all rotavirus mRNAs (Poncet *et al.*, 1994). *In vitro* the minimal RNA sequence required for binding is GACC. NSP3 was also shown to bind to the 3'-end of viral mRNA in infected cells (Poncet *et al.*, 1996). The RNA-binding domain is believed to lie between aa 4 and 149 at the amino terminus of the protein (Piron *et al.*, 1999). This amino-terminal region also contains a consensus sequence found in ssRNA-binding proteins of both *Orbiviruses* (NS2) and *Orthoreoviruses* (σ NS). It is pertinent to note that the binding site of NSP3 overlaps with the 3'-terminal seven nucleotides which form part of the *cis*-acting signal that functions as the promoter for minus-strand RNA synthesis during genome replication (Wentz *et al.*, 1996). This

suggests that NSP3 may be associated with RNA replication, perhaps by mediating transport of mRNA templates to the viroplasm for replication. NSP3 has sequence-specific RNA-binding activity and thus could play a role in discriminating between viral and cellular RNA. However, it is unlikely to be involved in selection of the 11 individual mRNA segments as it recognises a consensus sequence common to the 3'-end of the positive-strand of all segments. More recently, it has been suggested that by binding to the 3'-end of viral mRNAs, NSP3 protects them from degradation (Piron *et al.*, 1999). NSP3 has also been shown to interact with the cellular protein eukaryotic initiation factor 4GI (eIF-4GI) (Piron *et al.*, 1998), and the binding domain for eIF-4GI has been mapped to the last 107 aa of the carboxy-terminus of NSP3 (Piron *et al.*, 1999). It has thus been suggested that NSP3 has a role in ensuring efficient translation of viral mRNA.

1.4.2.3 NSP4

NSP4 is a transmembrane glycoprotein found in the ER (Ericson *et al.*, 1982) (Kabcenell and Atkinson, 1985). It has three hydrophobic amino-terminal regions, which are maintained in the ER membrane, and a hydrophilic carboxy terminus that extends into the cytoplasm (Chan *et al.*, 1988). NSP4 may have a role in viral morphogenesis, and it is thought that the cytoplasmic domain acts as a receptor for subviral (double-layered) particles and mediates their budding into the lumen of the ER (Ericson *et al.*, 1983). It may also have a function in the acquisition of the outer capsid protein layer (Au *et al.*, 1989) (Meyer *et al.*, 1989). Evidence to support this role for NSP4 includes the localisation of the VP6 binding site on NSP4 to the cytoplasmic domain between aa 161 and 175 (Au *et al.*, 1993) (Taylor *et al.*, 1992) (Taylor *et al.*, 1993). In addition, double-layered particles have been observed to bind to ER membranes containing only NSP4 (Au *et al.*, 1989) (Meyer *et al.*, 1989). NSP4 also has membrane destabilization activity and glycosylated NSP4 may have a role in the removal of the transient envelope from budding particles during viral morphogenesis (Tian *et al.*, 1996).

NSP4 is known to be cytotoxic (Tian *et al.*, 1994) and may function as a viral enterotoxin in rotavirus-induced diarrhoea by causing calcium-dependent chloride secretion across the mammalian small intestinal mucosa (Ball *et al.*, 1996). It has been shown to induce diarrhoea when injected intraperitoneally into young mice.

Preliminary data showed structural changes between aa 131 and 140 in NSP4 when virulent and attenuated strains were compared, which suggested that this region may be important for the protein function (Zhang *et al.*, 1998).

1.4.2.4 NSP5 and NSP6

The primary product of genome segment eleven is the 26 kDa non-structural protein NSP5, which is normally found in the phosphorylated 28 kDa form. However, it is now known that a second out-of-phase ORF (OP-ORF) in genome segment eleven, beginning at base 80, encodes a 12 kDa protein that is expressed in rotavirus-infected cells (Mattion *et al.*, 1991). This protein, NSP6, accumulates in viroplasms and may function as part of a complex, but is, as yet, largely uncharacterised.

The role of NSP5 in the virus replication cycle is still unclear. It is a phosphoprotein that exists in several different phosphorylated forms, the major isoforms being 26, 28 and 35 kDa, which are formed by phosphorylation of different serine residues (Blackhall *et al.*, 1997). There is also evidence to suggest that NSP5 has protein kinase activity (Poncet *et al.*, 1997) (Blackhall *et al.*, 1997), though this is not detected until all the major phosphorylated forms of NSP5 are present in the cell (Blackhall *et al.*, 1998). NSP5 is found in the viroplasm in rotavirus-infected cells, but phosphorylation is not required for its localization there (Blackhall *et al.*, 1998).

NSP5 forms homo-dimers (González *et al.*, 1998), and is known to interact with NSP2 (Poncet *et al.*, 1997). Interaction with NSP2 appears to up-regulate NSP5 phosphorylation (Afrikanova *et al.*, 1998). Both proteins co-localise in the viroplasm and it has been suggested that NSP5 may have a role in forming the structure of the viroplasm, and this may be mediated by its interaction with NSP2 (Fabbretti *et al.*, 1999).

1.5 Rotavirus replication cycle

1.5.1 Overview

Rotavirus has a lytic replication cycle, which takes place in the cytoplasm of infected cells. Although the natural cell tropism for rotavirus is the differentiated enterocyte in the small intestine, it has been mainly studied in continuous cell cultures derived from monkey kidneys, due to the difficulty in culturing intestinal cell lines (Estes, 1996). Rotavirus has a rapid replication cycle in these cells with a maximum yield of virus after 10-12 hours (McCrae and Faulkner-Valle, 1981). Viral infectivity is activated by proteolytic cleavage of VP4. Once the virus gains entry to the cell, the replication cycle proceeds solely in the cytoplasm. Viral mRNA transcripts are synthesised asymmetrically from the minus dsRNA template and are used both to produce proteins, and as a template for minus-strand synthesis. During the replication cycle both parental dsRNA strands remain associated with the partially uncoated viral particle. Replication occurs in nascent subviral particles, and dsRNA or minus strand ssRNA are never found free in the infected cell. Subviral particles are formed in association with viral inclusions in the cytoplasm, termed viroplasms. The progeny virus particle matures by budding through the membrane of the ER where it acquires the outer capsid proteins VP4 and VP7, and the particles are then released by cell lysis. A schematic representation of the virus replication cycle is shown (Figure 1.4).

1.5.2 Virus attachment and entry

A variety of approaches have been used to study the initial stages of rotavirus replication. Only triple-layered particles containing VP4 have been shown to attach to cells (reviewed by Estes, 1996). It is unclear whether virus attachment is mediated by VP4 or VP7 or both, however increasing evidence favours VP4 (Ruggeri and Greenberg, 1991) (Ludert *et al.*, 1996). Recently it has been shown that the binding of virus-like particles to MA104 cells requires the presence of VP4 (Crawford *et al.*, 1994). Further, use of viral reassortants suggested that VP4 functions as the cell attachment protein both *in vitro* and *in vivo* (Ludert *et al.*, 1996). Binding to cells does

Figure 1.4 Schematic representation of the major features of the rotavirus replication cycle

The infecting (triple-layered) virus particle attaches to the cell membrane, probably by the interaction of VP4 with the cellular receptor (Hewish *et al.*, 2000), and is internalised either by endocytosis or direct penetration. A decrease in calcium concentration is thought to trigger the release of the outer coat proteins, however the mechanism by which this occurs is not yet clear (Ruiz *et al.*, 1997). Following the loss of the outer capsid, the RNA-dependent RNA polymerase (transcriptase) is activated and viral transcription occurs. The viral mRNAs have two functions: they are translated to produce viral proteins, and they also constitute the template for minus-strand synthesis in dsRNA replication. The mRNAs are translated to produce all the viral proteins required for replication. The mRNA segments undergo genome assortment and are transported to the viroplasm where RNA replication and assembly of single-shelled (double-layered) particles occurs. The single-shelled particle matures by budding through the ER membrane, and acquires the outer capsid proteins VP4 and VP7 in the ER. Mature progeny virions accumulate in the RER and are released following cell lysis. Adapted from Estes (1996).

Figure 1.4

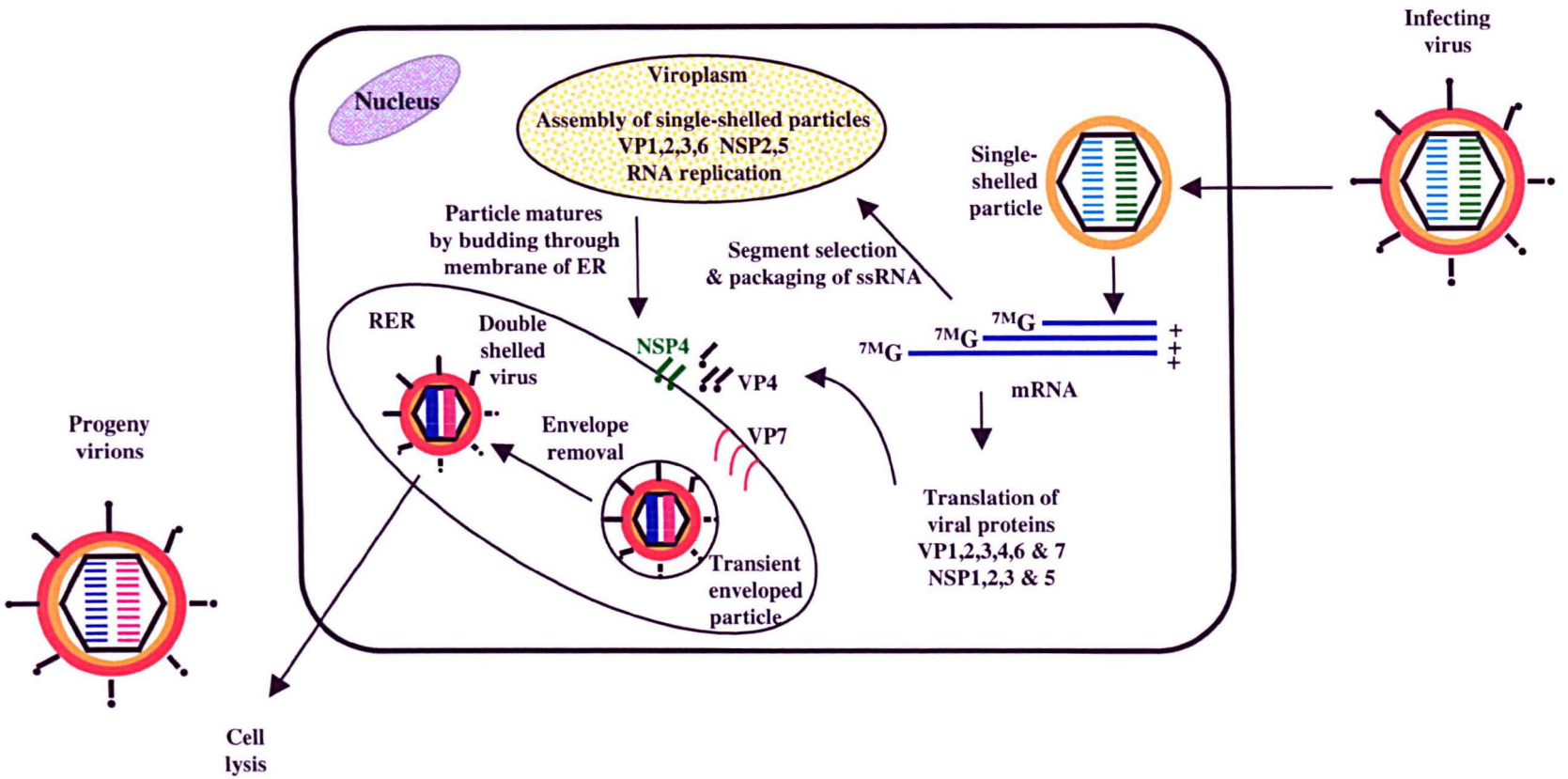
Infecting virus
Nucleus
Viroplasm
Assembly of single-shelled particles
VP1,2,3,6 NSP2,5
RNA replication
Single-shelled particle
Particle matures by budding through membrane of ER
Segment selection & packaging of ssRNA
RER
Double shelled virus
NSP4
VP4
VP7
7MG
7MG
7MG
+++
mRNA
Envelope removal
Transient enveloped particle
Translation of viral proteins VP1,2,3,4,6 & 7 NSP1,2,3 & 5
Progeny virions
Cell lysis

not require the proteolytic cleavage of VP4 to VP5* and VP8* (Fukuhara *et al.*, 1988), yet this is known to enhance infectivity in many, but not all, virus strains.

Until recently the cellular receptor for rotavirus was unknown. However, integrins $\alpha 2\beta 1$ and $\alpha 4\beta 1$ have now been implicated in rotavirus cell entry and infection (Coulson *et al.*, 1997), and it has since been demonstrated that these two integrins can act as cellular receptors for the SA11 strain of rotavirus (Hewish *et al.*, 2000). It was originally thought that binding of animal rotaviruses was dependent upon the presence of sialic acid residues in the membrane, while human rotavirus strains apparently initiated infection by a sialic acid-independent mechanism (Fukudome *et al.*, 1989). Neuraminidase treatment of red blood cells reduced virus binding, indicating a potential role for sialic acid in virus attachment for animal rotaviruses (Bastardo and Holmes, 1980). Human rotavirus strains were resistant to neuraminidase treatment (Fukudome *et al.*, 1989) (Yolken *et al.*, 1987). Sialic acid-resistant mutants retain full infectivity for cells, indicating that there are at least two binding sites for animal rotaviruses (Mendez *et al.*, 1994). Recent studies have however demonstrated that animal rotaviruses may also be able to infect permissive cells in a sialic acid-independent manner. Thus, it has been suggested that an initial interaction occurs, which might be sialic acid-dependent or independent, then virus entry proceeds by attachment to a common cellular receptor (Mendez *et al.*, 1998) (Ciarlet and Estes, 1999).

After binding to permissive cells, the virus is internalised. The penetration step is reportedly facilitated by the proteolytic cleavage of VP4, which is known to enhance infectivity (Clark *et al.*, 1981). Internalisation does not occur at less than 4°C, and therefore active cellular processes are required (Keljo and Smith, 1988). The mechanism of internalization is controversial since there is evidence to support both receptor-mediated endocytosis and direct penetration of the virus into the cell. Initial EM studies suggested that virus entry occurred by endocytosis into lysosomes (Ludert *et al.*, 1987) (Quan and Doane, 1983). It is known that viruses which initiate infection by receptor-mediated endocytosis often depend upon the acidification of endosomes for uncoating or cell entry (Estes, 1996). However, lysosomotrophic drugs (ammonium chloride, chloroquine, amantadine) have little inhibitory effect on virus replication (Ludert *et al.*, 1987), as do energy inhibitors (sodium azide, dinitrophenol) (Kaijot *et al.*, 1988), suggesting that conventional receptor-mediated endocytosis

might not represent the major entry route for productive infection. On the other hand, a model has been proposed recently for Ca^{2+}-dependent endocytosis of the virus particle that does not require acidification of the endosome for the infectious process (Ruiz *et al.*, 1997).

The mode of rotavirus entry into cells may differ depending on whether virus particles have been pre-treated with trypsin. EM studies showed that trypsin-treated virus entered by direct penetration of the cell membrane, while non-trypsin-treated particles were taken up by phagocytosis over a longer period of time though entry by phagocytosis was not thought to lead to viral replication (Suzuki *et al.*, 1985). Study of the kinetics of cell entry correlated with the EM studies described above on trypsin-treated and non-trypsin-treated rotavirus (Kaijot *et al.*, 1988). Trypsin-treated rotavirus was internalised with a half-time of 3-5 minutes, whereas non-trypsin-treated rotavirus had a half-time of 30-50 minutes. Only trypsin-activated virus resulted in a productive infection. Trypsin-treated virus was also shown to mediate the rapid release of ^{51}Cr from infected cells at 37 °C, but not at 4 °C. These data suggested that virus entry occurs by direct penetration of the cell membrane, resulting in permeabilisation of the cell membrane (Kaijot *et al.*, 1988). The proteolytic cleavage product of VP4, VP5*, has been shown to permeabilise membranes in the absence of other rotavirus proteins (Denisova *et al.*, 1999). The mechanism of rotavirus internalisation is therefore unclear, and it is possible that both endocytosis and direct penetration may be involved.

1.5.3 Transcription

Transcription of viral mRNA begins soon after virus entry and is at a maximum at 9 to 12 hours post-infection (p.i.) (Stacy-Phipps and Patton, 1987). Viral gene expression is regulated at the level of transcription as viral mRNAs are not produced in equimolar concentrations (Johnson and McCrae, 1989) (Stacy-Phipps and Patton, 1987). Regulation at the level of translation also occurs, as viral proteins are synthesised in the cell in relative concentrations that differ from those of viral mRNAs (Johnson and McCrae, 1989).

Transcription is asymmetric, and all transcripts are full-length plus strands transcribed from the minus strand of the dsRNA template (McCrae and McCorquodale, 1983). Viral mRNAs differ from cellular mRNAs in that they contain

a 5'-terminal methylated cap structure (Imai *et al.*, 1983), but lack 3' polyadenylate sequence (McCrae and McCorquodale, 1983). The site of transcription of viral mRNAs has not yet been localised either to the cytoplasm or the viroplasm. In other genera of the *Reoviridae*, such as bluetongue virus (BTV), transcription is believed to occur in viral inclusion bodies (VIBS) which form in the cytoplasm (Eaton *et al.*, 1990), as both parental and progeny virus particles are occluded within these structures. As yet, however, there is no firm evidence for the site of rotavirus transcription.

Transcription is mediated by an endogenous viral RNA-dependent RNA polymerase (transcriptase) that is a component of the virion (Mason *et al.*, 1980) (Sandino *et al.*, 1986). The conversion of triple-layered particles to double-layered particles activates the viral transcriptase activity and it is thought that transcription in cells occurs from such particles (Clark *et al.*, 1980). Other enzymatic activities known to be associated with the double-layered particle, such as nucleotide phosphohydrolase, guanylyltransferase, and methylase, are also required for RNA transcription (Estes, 1996). Rotavirus transcription requires a hydrolyzable form of ATP that may be necessary for initiation, or elongation, of RNA molecules (Spencer and Arias, 1981). The functions of some of the structural proteins associated with the transcriptase particle have been defined. VP1 is thought to be the RNA-dependent RNA polymerase (Section 1.4.1.1), although VP2 is also required for its activity (Section 1.4.1.2). VP3 is probably the guanylyltransferase (Section 1.4.1.1). VP6 is required for transcriptase activity (Sandino *et al.*, 1986), but its role in the process is unclear. It is possible that it acts as a scaffold protein in the composition of a functional transcriptase complex.

1.5.4 Replication

Analysis of the kinetics of RNA synthesis has shown that both plus- and minus-strand RNA synthesis can be detected in the cell by three hours p.i. (McCrae and Faulkner-Valle, 1981) (Stacy-Phipps and Patton, 1987). The level of minus-strand synthesis reaches a peak at 6 to 9 hours p.i. before the maximal level of plus-strand synthesis. As the level of replication does not increase in conjunction with the level of plus-strand synthesis, it is suggested that additional control factors must operate.

Replication is asymmetric with the viral plus-strand acting as a template for the synthesis of minus-strand RNA. The plus-strand RNA template is indistinguishable from viral mRNA (McCrae and McCorquodale, 1983). After synthesis, dsRNA remains associated with subviral particles and is not found free in the cell. Hence, genome assortment of viral mRNA must occur prior to RNA replication. During this process, each individual replicase particle acquires a single copy of each individual genome segment. The mechanism that controls genome assortment is unclear, however the presence of signal sequences on each of the eleven species of viral mRNA is a prerequisite for such an accurate process. Signals that allow differentiation between viral and host mRNAs, and also between each of the eleven genome segments would be required. The nature of these signals is unknown, but sequence analysis has shown that the 5' and 3' ends of the genome segments contain identical 5-10 base terminal sequences (McCrae and McCorquodale, 1983). Sequence analysis has also shown that the entire 5' and 3' untranslated regions (UTRs) of homologous genome segments are highly conserved (Clarke and McCrae, 1983) (Desselberger and McCrae, 1994). The site of genome assortment is unknown, but Patton (1995) has suggested that the accumulation of non-structural proteins with RNA-binding properties on the cytoskeleton could serve to concentrate mRNAs prior to packaging. The non-structural proteins may also have a function in transport of the viral mRNAs from their site of synthesis to the viroplasm for packaging and replication.

RNA replication probably occurs in the viroplasm (Petrie *et al.*, 1984). Similar structures (VIBs) in BTV-infected cells are also thought to be the site of viral genome replication (Eaton *et al.*, 1990). Characterisation of subviral particles with replicase activity identified three replication intermediates (RIs) in rotavirus-infected cells (Gallegos and Patton, 1989). The smallest RI (pre-core RI) contained the structural proteins VP1 and VP3, and the non-structural proteins NSP1, NSP2, NSP3 and NSP5, although only NSP1 and NSP3 reproducibly co-purify with the pre-core RIs (Patton, 1995). A second intermediate (core RI) contained the core structural proteins VP1, VP2 and VP3, and the non-structural proteins NSP2, NSP3 and NSP5. VP6 was then added to the core RI to form the largest RI (single-shelled RI). Thus, the replicase complex contains the core proteins VP1 and VP2, small amounts of VP6, and varying amounts of the non-structural proteins NSP1, NSP2, NSP3 and NSP5 (Gallegos and Patton, 1989). A model was proposed in which double-layered particles were

assembled by the sequential addition of VP2 and VP6 to the pre-core complex which occurred concurrently with genome replication. The positive sense RNA template appears to extend from the surface of early replicase particles and is then drawn into the particle as replication proceeds (Patton and Gallegos, 1990), supporting the hypothesis that morphogenesis and replication are related processes.

The use of temperature-sensitive mutants suggested that VP2, but not VP6, was an essential component of replicase particles (Mansell and Patton, 1990). The minimal replicase complex has since been shown to consist of VP1 and VP2 (Zeng *et al.*, 1996) (Patton *et al.*, 1997). VP1 is thought to be the RNA-dependent RNA polymerase. Despite the fact that VP2 is required for replicase activity, its exact function is still unknown (Patton, 1996). The function of the non-structural proteins in replication has not yet been fully defined, but they could be involved in genome assortment, transport and packaging of viral mRNA, and RNA synthesis.

A *cis*-acting signal involved in replication has been localised within the 26 3'-terminal non-coding nucleotides of a reporter template RNA in an *in vitro* replication system (Chen *et al.*, 1994). Wentz *et al.* (1996) then mapped the minimal promoter of minus-strand RNA synthesis to the 3'-terminal seven nucleotides. It has since been shown that this sequence must be single-stranded to allow efficient minus-strand synthesis (Chen and Patton, 1998). Further, the putative RNA-dependent RNA polymerase, VP1, has been shown to bind to the same region of viral mRNA (Patton, 1996). Additional enhancement signals for replication at the 5' and 3' ends of the viral mRNA have also been identified (Wentz *et al.*, 1996).

1.5.5 Virus assembly and release

Double-shelled particles are formed in the viroplasm, however the final stages of rotavirus morphogenesis, when the outer capsid proteins VP4 and VP7 are acquired, occurs in the ER. The double-shelled particles bud through the membrane of the ER and acquire a transient envelope, which is lost as the particles move towards the interior of the ER, and is replaced by the outer capsid to form a mature virion (Estes, 1996).

The glycoproteins VP7 and NSP4 are synthesised on ribosomes associated with the membrane of the ER. Signal sequences at the amino terminus of each protein direct their co-translational glycosylation and insertion into the ER membrane

(Whitteld *et al.*, 1987) (Kabcenell and Atkinson, 1985). The amino terminus of NSP4 is maintained in the membrane whilst the carboxy terminus extends into the cytoplasm of infected cells, where it is proposed to act as a receptor for double-layered particles and thus mediate their budding into the lumen of the ER (Chan *et al.*, 1988) (Petrie *et al.*, 1983). NSP4 has a binding site for VP4 (Au *et al.*, 1993) and forms homo-oligomers and heterooligomeric complexes with VP4 and VP7 (Maass and Atkinson, 1990). VP4 accumulates in the cytoplasm near the RER (Kabcenell *et al.*, 1988), and is thought to associate with the double-shelled particle before entry into the ER (Lopez *et al.*, 1985) (Mackow *et al.*, 1988). The exact details of particle budding across the ER membrane are, as yet, not well understood. The transient envelope acquired by budding particles in the ER is removed during virion morphogenesis, and glycosylated NSP4 may have a role in this process (Petrie, 1983) (Suzuki *et al.*, 1984).

Rotavirus maturation is a calcium-dependent process, as virus yields are decreased when produced in cells maintained in calcium-depleted medium (Shahrabadi and Lee, 1986). In addition, viruses produced in the absence of calcium do not bud into the ER and thus lack the outer capsid proteins (Shahrabadi *et al.*, 1987). It has been proposed that calcium is required both for the glycosylation of NSP4 and in the acquisition of the protein conformations necessary for the formation of hetero-oligomers (Poruchynsky *et al.*, 1991). Baculovirus-expressed NSP4 has been demonstrated to cause an increase in the intracellular calcium concentration (Tian *et al.*, 1994), and this increase has been proposed to be an important factor in virus maturation (Tian *et al.*, 1995). The presence of calcium may also stabilise or modulate the folding of glycosylated VP7 for subsequent assembly into virus particles (Shahrabadi *et al.*, 1987). VP7 has been shown to form hetero-oligomers with both VP4 and NSP4 in infected cells (Maass and Atkinson, 1990). Oligomer formation and interaction with calcium appear to be important in the assembly of VP7 into the outer capsid (Dormitzer and Greenberg, 1992) (Poruchynsky *et al.*, 1991) (Shahrabadi *et al.*, 1987). However, the precise mechanisms of transient envelope removal and outer capsid assembly remain poorly understood. The infectious cycle ends when progeny virus is released by host cell lysis (Altenburg *et al.*, 1980) (McNulty *et al.*, 1976).

1.6 Non-structural protein NSP1

1.6.1 Gene 5 shows high sequence divergence

NSP1 is unusual among the Group A rotavirus non-structural proteins in that it has a variable length of between 486 and 495 aa and its primary sequence has a low level of conservation (Hua *et al.*, 1993) (Patton, 1995). The nucleotide sequences of gene five from rotaviruses of different animal origin have been shown to be extremely diverse and range in size from 1564 to 1611 nucleotides (Hua *et al.*, 1993). Comparison of the gene segment five from the SA11 strain of simian rotavirus with that from the RF strain of bovine rotavirus revealed homologies of only 49 and 36 % at the nucleotide and amino acid levels respectively (Mitchell and Both, 1990a). By comparison, the other rotavirus non-structural proteins are highly conserved between isolates. For example, NSP2 has 78 % homology at the nucleotide level, and 83 % or greater homology at the amino acid level (Patton *et al.*, 1993). In fact, gene five appears to be more diverse than any other rotavirus gene, including those such as VP4 and VP7 which are subject to immune selection (Dunn *et al.*, 1994).

When viruses of different origin and serotype were compared, the gene five sequences appeared to exhibit a higher degree of sequence homology among viruses of the same serotype (Hua *et al.*, 1993). For example the bovine strains UK and RF, which are both serotype six, showed homology of 88 and 92 % at the nucleotide and amino acid levels respectively. This suggested a possible correlation between gene five sequence divergence and rotavirus serotype. In addition, a phylogenetic tree of the predicted amino acid sequences for NSP1 available at this time showed a clustering of the NSP1 genes according to host range (Hua *et al.*, 1993). Gene five sequences from viruses of the same host range were shown to be more closely related to each other than to those isolated from other species. Comparison of NSP1 amino acid sequences from isolates from more species revealed identities ranging from 36 to 92 % with the most evident sequence diversity between strains from different species (Dunn *et al.*, 1994). Analysis of the sequence homologies and phylogenetic relationships again showed that NSP1 sequences were clustered according to species origin, with one exception which was the inclusion of the human and porcine strains in a single group. This work suggested that NSP1 may have a role in determining host range restriction of rotavirus strains by an unknown mechanism (Section 1.6.5). It was proposed that NSP1 might interact with a host cytoplasmic protein that also varied

between species. The putative species-specific protein could possibly be of cytoskeletal origin, as NSP1 is known to accumulate in association with the cytoskeleton (Hua and Patton, 1994).

In contrast to this, analysis of the sequence of NSP1 from a larger range of isolates contradicted the work of Dunn *et al.* (1994) as it revealed that sequence conservation could not be correlated either with rotavirus serotype or the species of origin of the virus strain (Xu *et al.*, 1994). Many interspecies related strains were observed. For example, two simian rotavirus isolates, SA11 and RRV, exhibited amongst the highest levels of sequence divergence recorded, whilst a porcine and a human strain showed a similar level of conservation as two bovine strains. Hence, even if NSP1 interacted with a cellular protein, this interaction would not provide a major selective force for sequence divergence.

Finally, despite the fact that NSP1 shows considerable divergence of the primary sequence, the predicted secondary structure of the protein is remarkably conserved (Xu *et al.*, 1994). For example, proline residues, which are known to introduce bends in polypeptide chains, are conserved at eight separate positions in many strains (Kojima *et al.*, 1996). This implies the existence of a selective pressure to maintain the higher-order structure of the protein, despite the considerable sequence divergence, which is consistent with NSP1 having a role in the viral replication cycle (Xu *et al.*, 1994).

1.6.2 NSP1 has a highly conserved cysteine-rich region

Despite the unusually high sequence divergence, NSP1 does contain a well-conserved cysteine-rich sequence at the amino-terminus, between aa 37 and 81 (Mitchell and Both, 1990a). This short sequence is absolutely conserved in NSP1 from many sequenced strains, including human, bovine, simian, porcine and murine strains from both Group A and Group C rotavirus (Hua *et al.*, 1993) (Dunn *et al.*, 1994) (Xu *et al.*, 1994). The conserved sequence, $C\text{-}X_2\text{-}C\text{-}X_8\text{-}C\text{-}X_2\text{-}C\text{-}X_3\text{-}H\text{-}X\text{-}C\text{-}X_2\text{-}C\text{-}X_5\text{-}C$ (where C=cysteine; X= any amino acid) is a generalised motif for a metal binding domain (Hua *et al.*, 1993). It is possible that this region could form one or two zinc fingers, and the fact that it is highly conserved indicates that it is a potential functional domain. A second putative metal-binding domain, found between residues 315 and 328 in two bovine strains, UK and RF, was

not shown to be conserved when more strains were sequenced (Mitchell and Both, 1990a) (Kojima *et al.*, 1996).

1.6.3 The cysteine-rich region may function as a zinc finger

Mitchell and Both (1990a) proposed that the conserved cysteine-rich domain at the amino-terminus of NSP1 may form one or two zinc fingers. This prediction is supported by the fact that recombinant baculovirus-expressed NSP1 binds zinc with high affinity (Brottier *et al.*, 1992). The prototype zinc finger-containing protein TFIIIA has the conserved cysteine motif repeated up to nine times. However, several viral proteins which bind zinc, including the HIV tat protein (Frankel *et al.*, 1988) and the SV40 large T antigen (Loeber *et al.*, 1989), only have a single zinc finger element. The structure proposed for the cysteine-rich motif in NSP1 is a typical TFIIIA-like finger linked to a second atypical zinc finger by a short spacer sequence (Patton, 1995). Other similar proteins among the *Reoviridae* include the σ3 protein of reovirus, which has a zinc finger and has been shown to bind zinc (Schiff *et al.*, 1988). Several proteins with conserved cysteine-histidine-rich regions have also been identified, including μNS, σ2 and σNS of reovirus, and NS1 and NS2 of bluetongue virus (BTV) (Roy, 1989) (Weiner and Joklik, 1987) (Weiner *et al.*, 1989).

1.6.4 NSP1 has RNA-binding activity

NSP1 was first shown to interact with RNA by the high affinity binding of viral specific ssRNA probes by recombinant baculovirus-expressed NSP1 in a gel retardation assay (Brottier *et al.*, 1992). It also recognised non-rotavirus-specific RNA probes, indicating that the RNA-protein interaction was not RNA sequence-specific. In contrast to these findings, data were then presented to suggest that NSP1 might have specific affinity for rotavirus mRNAs (Hua *et al.*, 1994). Using NSP1 produced by *in vivo* expression systems and immobilised onto protein A-Sepharose with specific antiserum, it was shown that NSP1 bound all eleven rotavirus mRNAs. The addition of yeast tRNA had no effect on the viral specific RNA-binding activity of NSP1. It was suggested by the use of virus-specific RNA probes that NSP1 bound to the 5'-end of viral mRNAs. However, the probe consisted of 278 nucleotides of the 5'-end of genome segment five and a consensus binding sequence common to all viral

mRNAs was not identified. The putative specific binding site for NSP1 at the 5'-end of viral mRNAs has not been mapped more closely and its existence has not been substantiated (J. T. Patton, pers. comm.). Use of the viral RNA probes also demonstrated that NSP1 has non-specific RNA-binding activity, as binding of a 3'-end probe by NSP1 was not resistant to competition by non-specific viral mRNA.

Deletion mutagenesis of NSP1 and analysis of the RNA-binding activity of the mutants showed that the RNA-binding domain was located within the first 81 aa of the protein (Hua *et al.*, 1994), and the highly conserved cysteine-rich region at the amino-terminus was essential for RNA-binding activity. The putative zinc fingers found in the conserved cysteine-rich domain may function in the RNA-binding activity of NSP1, as analysis of such structures has shown that they generally impart specific nucleic acid-binding activities to proteins (Berg, 1990).

Rotavirus variants expressing a truncated NSP1 which lacks the carboxy terminus of the protein have been shown to be viable, non-defective mutants, supporting the theory that the functional domain of NSP1 resides at the amino terminus of the protein (Hua and Patton, 1994). However, the truncated mutants displayed a 9-60 fold lower titre in tissue culture than the wild-type virus, and a 50-fold reduction in mean plaque area (Tian *et al.*, 1993). Taniguchi and co-workers have identified non-defective rotavirus mutants carrying NSP1 that lacks the conserved cysteine-rich region (Taniguchi *et al.*, 1996). Their data contradicted previous findings by suggesting that the cysteine-rich region of NSP1 is not necessary for virus replication *in vitro*. However, given that the plaque sizes of the mutant viruses were extremely small, it is probable that possession of full length NSP1 confers some advantage upon the virus. More recently, subclones of these mutant viruses have been isolated which carry the truncated NSP1 described previously while retaining plaque size comparable to a normal clone (Taniguchi *et al.*, 1999). This suggested that, except for the amino-terminal 40 aa, NSP1 was not required for replication *in vitro*.

1.6.5 NSP1 may have a role in host species specificity

Rotaviruses exhibit marked species specificity. They are subject to host range restriction (HRR) and are, in general, unable to spread between species in nature. The gene, or genes, which confer HRR are unknown and different studies have yielded

varying results. Genetic reassortment studies suggested that gene five does not segregate randomly *in vivo* (Gombold and Ramig, 1986) (Broome *et al.*, 1993). Therefore, it may play a role in enhancing replication and conferring a selective growth advantage on the virus. A study of reassortant viruses produced *in vivo* by coinfecting mice with simian rotavirus (RRV) and murine rotavirus (EDIM-RW) implicated the gene five product NSP1 in HRR. Analysis of the virulence and species specificity of the reassortant viruses led to the conclusion that the major outer capsid proteins VP4 and VP7 were not primarily responsible for HRR (Broome *et al.*, 1993), but NSP1 was strongly associated with virulence and spread phenotypes, and was the only rotavirus gene to show this association. However, the association was not absolute as a few reassortants carrying the murine gene segment five had the virulence phenotype of the simian parent rotavirus. In contrast to these results, a study of porcine x human rotavirus reassortants in piglets did not implicate gene five in either virulence or HRR (Hoshino *et al.*, 1995).

In view of the conflicting results from the reassortant studies described previously, further investigation into the possible role of NSP1 in HRR was performed (Bridger *et al.*, 1998). A monoreassortant which possessed ten porcine rotavirus genes and the NSP1 gene from the UK strain of bovine rotavirus was analysed, and it was found that possession of a heterologous NSP1 gene did not affect the virulence or the ability of the monoreassortant virus to replicate *in vivo* as compared to the porcine parent virus. These findings did not support the original hypothesis that NSP1 may play a role in virulence and HRR. The sequence homology of the NSP1 genes used in the different studies could not be compared directly due to the lack of sequence data from the appropriate strains. However, by comparison of the sequences of NSP1 genes from other rotavirus strains from the same species (Xu *et al.*, 1994) (Dunn *et al.*, 1994) it was estimated that the sequence homology between the NSP1 genes was probably greater in the study by Bridger *et al.* (1998) than in the earlier study (Broome *et al.*, 1993). Thus, it was suggested that in the former study the heterologous NSP1 may be conserved enough to replace the parent NSP1 and allow similar levels of infection and replication. Virulence and HRR are probably multigenic phenotypes and a possible role for NSP1 remains elusive. Further studies are required to completely define the genetic basis of these phenotypes.

1.6.6 NSP1 accumulates in the cytoplasm and may be associated with the cytoskeleton

NSP1 is found in the cytoplasm of the infected cell where it accumulates in a punctate-like manner throughout the cytoplasm (Hua and Patton, 1994). Analysis of intracellular fractions derived from infected cells by gel electrophoresis and western blotting demonstrated that large amounts of NSP1 were present in the cytoplasm and also in association with the cytoskeleton (Hua *et al.*, 1994). Indirect immunofluorescence assays (IFA) with full-length NSP1 and a truncated NSP1 which lacked the carboxy half of the protein, revealed no difference in the distribution of the truncated protein in the infected cell compared to the full-length protein, suggesting that the subcellular localisation signal in NSP1 resides in the amino terminal half of the protein (Hua and Patton, 1994). Further analysis of mutant forms of NSP1 by IFA indicated that the intracellular localisation domain was between aa 84 and 176 in the amino-terminal half of NSP1 (Hua *et al.*, 1994). The distribution of NSP1 was shown to be similar to NSP3, which is also associated with the cytoskeleton of infected cells (Mattion *et al.*, 1992). However, the distribution of NSP1 throughout the cytoplasm was shown to be independent of any other viral protein (Hua *et al.*, 1994).

This data suggested that NSP1 might interact with a cytoskeletal protein. The possible identity of this putative cytoskeletal protein is unknown, though it has been shown by double-staining of infected cells with specific antibodies that NSP1 and the type III intermediate filament, vimentin, are similarly distributed within the cell (Patton, 1995). Thus, it has been suggested that perhaps NSP1 or NSP3 may be responsible for the selective reorganisation of vimentin observed in rotavirus-infected cells (Weclewicz *et al.*, 1994).

1.6.7 NSP1 is a component of early replication complexes

NSP1 is expressed at low levels early in infection and thus is thought to have a regulatory role in the viral replication cycle (Johnson and McCrae, 1989). A study to characterise intermediate structures in rotavirus replication identified three replication intermediates (RIs) in rotavirus-infected cells (Gallegos and Patton, 1989). The smallest RI (pre-core RI) contained the structural proteins VP1 and VP3 and the non-structural proteins NSP1, NSP2, NSP3 and NSP5, although only NSP1 and NSP3 reproducibly co-purified with the pre-core RI (Patton, 1995) (Section 1.5.4). The

presence of NSP1 in the pre-core RI suggested it had a function in the early stages of the viral replication cycle. Patton (1995) proposed a model to describe events in the early replication cycle, but the role of the non-structural proteins, including NSP1, in the process is still very unclear. As both NSP1 and NSP3 accumulate on the cytoskeleton and have RNA-binding activity, they could form a complex with mRNA that is a precursor of the pre-core RI. The pre-core RI would then be assembled on the cytoskeleton by the addition of VP1 and VP3 to the precursor complex. VP2 must then interact with the pre-core RI to form the core RI and induce the viral replicase activity. The sequential addition of VP2 to the pre-core RI and VP6 to the core RI was proposed as a mechanism for the assembly of rotavirus single-shelled particles, which might occur concurrently with genome replication.

2.1 Protein-protein interactions in RNA virus replication cycles

2.1.1 Introduction

Protein-protein interactions are intrinsic to all biological systems and have been implicated in a wide variety of cellular processes (Phizicky and Fields, 1995). In virus-infected cells, protein-protein interactions are fundamental to every stage of the virus replication cycle (Knipe, 1996). Interactions occur between viral proteins in the formation of transcription and replication complexes and their location to specific promoters (Zeng *et al.*, 1996). Further interactions occur in the assembly of progeny virions. By necessity, viral proteins must also associate with host cell proteins (Knipe, 1996). Interactions must occur between virus proteins and the cellular receptor (Hewish *et al.*, 2000), and also with the cellular transcription and translation apparatus (Ehrenfeld, 1993). During infection, interactions are likely to occur with the cytoskeleton that may be responsible for the movement of virus components and particles in the cell (Tyler *et al.*, 1986). Viral inclusions assembled in the cytoplasm of infected cells for synthesis of viral nucleic acids and assembly of virions may incorporate cytoskeleton components into the structure (Sharpe *et al.*, 1982). Proteins composed of more than one subunit are widespread. An example of this is provided by viral capsid proteins which are assembled into multimeric complexes (Bican *et al.*, 1982) (Prasad *et al.*, 1988). Transient protein-protein interactions, which often occur in the regulation of cellular processes, are by nature more difficult to characterise (Phizicky and Fields, 1995). A number of the techniques that can be used to study such interactions are described in Section 2.2.

2.1.2 Replicative strategy of RNA viruses with a segmented genome

2.1.2.1 The *Reoviridae*

The mammalian reoviruses are the prototype viruses of the genus *Orthoreovirus* in the family *Reoviridae* (Nibert *et al.*, 1996). They share many similar traits with the rotaviruses; indeed some details of the rotavirus replication cycle (Section 1.5) have been inferred from that of the closely related reovirus (Estes, 1996). The reovirus genome consists of ten segments of dsRNA which are replicated in the cytoplasm of the cell (Joklik, 1983). Following attachment of the virus to the

cellular receptor, particles are taken up by receptor-mediated endocytosis into vacuoles resembling endosomes and lysosomes (Sturzenbecker *et al.*, 1987). The outer capsid proteins then undergo specific proteolytic cleavage to form intermediate subviral particles (ISVPs) (Borsa *et al.*, 1981) (Sturzenbecker *et al.*, 1987). Subsequently, core particles derived from the ISVPs become transcriptionally active, leading to synthesis of the viral mRNAs. It is a notable feature of the replication cycle that transcription occurs within icosahedral viral particles and the mRNAs are then extruded from the particle (Shatkin *et al.*, 1983). In common with rotavirus, the virally encoded transcriptase particle produces transcripts that are methylated and possess a 5'-cap structure, but are not polyadenylated (Nibert *et al.*, 1996). The viral transcriptase and capping enzyme must be positioned close together in the core, as studies have demonstrated that capping of nascent mRNAs occurs when they are only 2 to 15 nucleotides long (Furuichi *et al.*, 1976) (Morgan and Kingsbury, 1981). The putative polymerase λ3 and guanylyltransferase λ2 have been shown to interact (Starnes and Joklik, 1993).

In common with rotavirus, reovirus mRNAs function both as templates for viral protein production and for minus-strand synthesis in dsRNA replication. Newly synthesised viral proteins are detected by 2 hours p.i. and as they increase the synthesis of cellular proteins declines (Zarbl and Millward, 1983). The mRNAs associate with newly made viral proteins to form progeny "RNA assortment complexes", but the mechanism by which the ten unique genome segments are packaged remains unknown (Zweerink, 1974) (Morgan and Zweerink, 1975). It is clear that assortment of both rotavirus and reovirus genome segments is a specific event, and that it is mRNAs that are assorted rather than dsRNA. Evidence to support selective assortment in reovirus includes a reported particle-to-pfu ratio as low as 1 (Spendlove *et al.*, 1970), and the fact that the central cavity of the reovirus particle is too small to accommodate many more than ten unique segments (Dryden *et al.*, 1993). The RNA and protein interactions that would be required to identify and package the ten unique viral mRNAs have not been identified.

Reovirus non-structural proteins σNS and μNS, and the outer capsid protein σ3, have been shown to associate with mRNAs soon after transcription to form small nucleoprotein complexes (Antczak and Joklik, 1992). Also, μNS is known to interact with σNS (Lee *et al.*, 1981). The μNS protein, which localises to the cytoskeleton

(Mora *et al.*, 1987), is the first protein to bind mRNAs post-synthesis (Antczak and Joklik, 1992). The cysteine-rich σNS protein probably binds ssRNA in a sequence-independent manner (Huismans and Joklik, 1976) (Gillian and Nibert, 1998), although there is some evidence that it selectively binds members of each mRNA size class (Stamatos and Gomatos, 1982). Both non-structural proteins are thought to play a role in condensing reovirus mRNAs into assortment complexes.

Comparisons have been made between the σNS protein of reovirus and the RNA-binding non-structural proteins of rotavirus (Gillian and Nibert, 1998). NSP2 forms multimeric complexes, as does σNS, and shows non-specific RNA-binding activity (Kattoura *et al.*, 1992). NSP3 forms oligomers (Mattion *et al.*, 1992), and binds viral mRNA (Poncet *et al.*, 1993). NSP1 also shows non-specific RNA-binding activity (Brottier *et al.*, 1992), and contains a cysteine-histidine-rich region, as do the reovirus proteins μNS and σNS. Despite what is known about both rotavirus and reovirus non-structural proteins, the mechanisms by which specific viral genome assortment and packaging occur remain unknown.

Following packaging of viral mRNA, dsRNA replication occurs. Newly synthesised dsRNA remains within the nascent progeny particle. Studies of reovirus replicase particles have revealed that the major protein components are the core proteins λ1, λ2, and λ3, together with μ1c, σ2 and σ3 (Joklik and Roner, 1995). The sedimentation coefficients of the replicase particles ranged in size from 180 to 550 S, but once minus-strand synthesis was complete, all particles sedimented with about 550S. Similar studies have been performed to identify replication intermediates (RIs) in rotavirus (Section 1.5.4). The RIs were also shown to undergo size changes, due to the recruitment of plus-strand mRNAs to the complex.

Recently it has been suggested that reovirus genome segment assortment may be linked more closely to replication than previously thought (Joklik and Roner, 1995). When the viral mRNAs associate with the non-structural proteins and σ3, as noted previously, the relative proportions of the individual RNA species reflects the population present in the infected cell, which differs from equimolarity. Four hours after infection, complexes appear which contain dsRNA and also proteins λ2 and λ3, in addition to the non-structural proteins and σ3. At this point, the relative proportions of the ten dsRNA species are equimolar, suggesting that assortment occurs concurrently with replication.

As in rotavirus-infected cells, reovirus-infected cells contain inclusion bodies in the cytoplasm (Anderson and Doane, 1966) (Gomatos *et al.*, 1962), as do other members of the *Reoviridae* such as bluetongue virus where the importance of these viral inclusion bodies (VIBs) in viral replication and morphogenesis have been demonstrated (Browne and Jochim, 1967) (Eaton *et al.*, 1990). Reovirus infection also causes disruption to the vimentin filament network (Sharpe *et al.*, 1982). It has been suggested that the non-structural protein μNS, which localises to the cytoskeleton, may associate with vimentin filaments to anchor structures involved in viral assembly to the network (Mora *et al.*, 1987). In rotavirus-infected cells, the viral non-structural protein NSP1 and vimentin are similarly distributed throughout the cytoplasm (Patton, 1995), and it has been proposed that NSP1 may be responsible for the selective reorganisation of vimentin in infected cells (Weclewicz *et al.*, 1994).

2.1.2.2 The *Orthomyxoviridae*

The *Orthomyxoviridae* have a segmented ssRNA genome, which is described as negative-sense since viral mRNAs are transcribed from the genome (Lamb and Krug, 1996). Influenza A and B have eight segments of RNA, while influenza C only has seven. The genome of influenza A encodes nine structural proteins and one non-structural protein. Influenza is unusual among RNA viruses in that both transcription and replication occur in the nucleus, rather than the cytoplasm (Barry *et al.*, 1962) (Rott *et al.*, 1965).

Following infection and uncoating, which is required for mRNA synthesis to occur, the virion RNAs (vRNAs) are both transcribed into mRNAs and replicated. Influenza encodes and packages an RNA-dependent RNA polymerase. The transcriptase complex consists of individual vRNAs associated with the nucleocapsid protein (NP) and the three polymerase proteins (PB1, PB2, and PA) (Ulmanen *et al.*, 1981). The P proteins interact to form a complex and are responsible for viral mRNA synthesis. The distinctive feature of viral mRNA synthesis is that it is primed by a 5'-cap structure derived from newly synthesised host cell transcripts (Bouloy *et al.*, 1978) (Krug *et al.*, 1979). Influenza viral mRNAs are polyadenylated as a result of the polymerase binding to the 5' end of the vRNA and reiteratively copying a short oligo(U) stretch found 17 nucleotides from the 5' end of the template (Li and Palese, 1994). An alternative form of transcription is required for replication to occur that

results in the production of full length copies of the vRNAs. Viral proteins, specifically the NP protein, must be synthesised before replication can proceed, and the switch between transcription and replication may be mediated by the binding of NP to the polymerase complex (Mena *et al.*, 1999). Full length template transcripts are replicated from the vRNAs, do not require the 5'-cap primer for initiation and are not terminated at the poly(A) site used during mRNA synthesis. The template RNAs are then copied into new vRNAs. The minimum components of the replicase complex, which would initiate synthesis of either template RNA or vRNA, are soluble NP, PB1, PB2 and PA (Huang *et al.*, 1990). Virus type-specific protein-protein interactions between the replicase components and the other structural proteins must be required for the formation of infectious virus particles, however, these are as yet poorly characterised (Gomez-Puertas *et al.*, 1999). The non-structural protein NS1 is not required for replication, but functions in regulation of nuclear export of mRNA and inhibition of pre-mRNA splicing.

Influenza has a segmented genome in common with the *Reoviridae*. In contrast with these viruses however, packaging of the influenza genome is thought to be a random process in terms of specific viral genome segments, although it is restricted to viral, and not cellular, RNAs. Evidence to support the random packaging theory is the fact that cells infected with a low multiplicity of infection (m.o.i.) of influenza virus sometimes lack the expression of some antigens, suggesting that some virions lack a full set of viral RNA segments (Martin and Helenius, 1991). Also, an engineered influenza virus has been obtained under selective conditions which contains nine RNA segments, suggesting that the virus is capable of packaging more than the minimum eight segments (Enami *et al.*, 1991). Calculation of the probability of randomly packaging the correct set of eight RNA segments reveals that, if 12 segments are packaged, 10 % of virions will have one copy of each of the eight segments (Enami *et al.*, 1991). Although evidence was presented in early reports to suggest that a specific assortment mechanism operated, the random packaging theory is generally favoured (Joklik and Roner, 1995).

2.2 The study of protein-protein interactions

2.2.1 Overview

An increasing array of methods are available to study protein-protein interactions and the formation of protein complexes in cells. A summary of common strategies to identify interacting proteins is given below. A more detailed and extensive review of both classical and recent developments in the study of protein-protein interactions can be found in Phizicky and Fields (1995).

2.2.2 Immunoprecipitation

Co-immunoprecipitation is a commonly used method of detecting protein-protein interactions. It relies on the fact that a specific antibody can precipitate a target protein from a complex mixture, and that heterologous proteins complexed to the target protein can be co-purified. The experimental procedure involves generating labelled cell lysates, the addition of either polyclonal or monoclonal antibody to precipitate the antigen, washing of the precipitate to remove adventitious material followed by elution and analysis of the bound proteins. As antibodies are usually non-precipitating, a reagent such as protein A-Sepharose is used to isolate the antibody-antigen complex.

Immunoprecipitation techniques have been used to study the protein composition of replicase complexes found in rotavirus-infected cells (Aponte *et al.*, 1996). By immunoprecipitation with a range of monoclonal antibodies and specific antisera against viral structural and non-structural proteins, it was determined that the non-structural protein NSP2 was a necessary component of an intermediate complex with replicase activity in the infected cell. A protein complex containing NSP2, VP1, VP2 and VP6, was precipitated by the monoclonal antibody specific for NSP2, however the reciprocal precipitation of NSP2 with antibodies against VP1, VP2 and VP6, was not observed. It was suggested that this finding could indicate that VP1, VP2 and VP6 are either buried in the complex or modified during the formation of viral protein-antibody complexes.

Immunoprecipitation from crude cell lysates has several advantages. The detection of a particular protein-protein interaction in the midst of all the competing proteins present in a crude lysate, implies a certain level of specificity.

Multicomponent protein complexes will already be in their natural state in the cell and can be readily co-precipitated. These sorts of complexes would be difficult to imitate *in vitro*, hence co-precipitation from cell lysates is the preferred method of detecting such protein complexes. Also, all the interacting proteins will be present in the same relative concentrations as found in the cell, and this avoids any artificial overproduction of the target protein associated with other methods. Finally, the normal posttranslational modification of proteins will have occurred, hence interactions that are dependent upon this will be realistically assessed. Analysis of the results of co-immunoprecipitation experiments should take account of the consideration that co-immunoprecipitating proteins may not necessarily represent a direct protein-protein interaction, since they may be components of a larger complex held together by other proteins and/or nucleic acid. Immunoprecipitation of proteins from *in vitro* transcription-translation reactions is an increasingly popular method to identify direct protein-protein interactions. However, the advantages noted previously for immunoprecipitation from crude cell lysates do not apply in experiments with extracts from *in vitro* translation reactions.

2.2.3 Immunofluorescence

Immunofluorescence is a technique commonly used to demonstrate co-localisation of proteins to a particular compartment of the cell. Specific proteins are detected in the cell using monoclonal antibodies conjugated to different fluorescence compounds that fluoresce at a specific wavelength when exposed to ultraviolet light. Experimentally, a cell monolayer can be fixed and stained with different fluorescent antibodies, thus locating specific proteins within the cell.

Localisation of the rotavirus non-structural proteins to either the viroplasm or the cytoplasm of infected cells has been demonstrated using immunofluorescence assays (Mattion *et al.*, 1992) (Hua *et al.*, 1994), and suggested interactions between these proteins appear to reflect their sub-cellular localisation (González *et al.*, 1998). Although co-localisation can be established by this method, it does not prove that a complex is formed or that direct interactions occur between the colocalised proteins.

2.2.4 Far-western blotting assay

Far-western blotting is a technique that allows the detection of protein-protein interactions between a specific protein probe and a range of proteins immobilised on a membrane. The method is similar to western blotting, but the probe is a specific protein other than an antibody. Proteins are separated by SDS-polyacrylamide gel electrophoresis and blotted onto a membrane. The SDS is then removed by dialysis to allow the immobilised, denatured proteins to regain some conformational structure. The incubation of a specific protein probe with the blot allows interactions to occur, whereby the protein probe will be retained on the membrane. The blot is then overlaid with an antibody against the protein probe, and the results are visualised in a similar manner to western blotting.

This technique was used in rotaviruses to detect interactions between the putative RNA-dependent RNA polymerase, VP1, and other proteins found in virus-like particles (Zeng *et al.*, 1998). The analysis showed that VP1 interacted with full length VP2. The use of truncated constructs of VP2 demonstrated that a domain within the amino-terminus of VP2 aa 1 to 25 was essential for binding VP1. It was thus postulated that this interaction was necessary for the encapsidation of VP1 and the suspected guanylyltransferase VP3 by the core protein VP2.

The fact that proteins are immobilised on a membrane for this method means that certain regions of the protein are not exposed, and therefore will not be able to interact or will only interact very weakly with the protein probe. This may mean that domains of the protein involved in the interaction are not detected. Despite the fact that dialysis is performed to allow the correct conformation of the proteins to reform, it is unlikely that the native structure will be regained when regions of the protein are attached to a membrane. The *in vitro* produced protein probe is also unlikely to exactly represent the native form of the protein found *in vivo*, due to a lack of posttranslational modification. While this method can be used to detect protein-protein interactions, the above considerations suggest that not every protein will be biologically active in such as assay and true protein-protein interactions may not always be detected.

2.3 The two-hybrid system

2.3.1 The principle of the two-hybrid system

The two-hybrid system is an *in vivo* method for the detection of protein-protein interactions. The system was originally developed by Fields and Song (1989) as a yeast-based genetic assay in *Saccharomyces cerevisiae*, where an interaction between two proteins of interest is detected by the activation of transcription of a reporter gene (Figure 2.1). The system makes use of a eukaryotic transcriptional activator, typically yeast GAL4, which consists of two physically discrete domains, one governing DNA binding and the second carrying the transcriptional activation function. The 881 aa GAL4 protein has a 147 aa DNA-binding domain at the immediate amino terminus of the protein. This region is involved in binding a 17 bp DNA target sequence called the galactose upstream activating sequence (UAS) (Keegan *et al.*, 1986). The carboxy region of the GAL4 protein has been shown to contain two separate activating domains, activating domain I (aa 148-196) and activating domain II (aa 768-881), both of which have a high content of acidic amino acids (Ma and Ptashne, 1987). The DNA-binding domain localises the transcription factor to specific DNA sequences upstream of the gene which is regulated by this factor. The activation domain interacts with other components of the transcription machinery required to initiate transcription. The presence of both domains is necessary to constitute a functional transcriptional activator. Normally the two domains are part of the same protein, however it has been demonstrated that a functional activator can be assembled *in vivo* from the separated domains expressed from plasmids, and this is the basis of the two-hybrid system (Ma and Ptashne, 1988) (Brent and Ptashne, 1985). The proteins of interest are fused to the separated domains. If there is an interaction between the two proteins of interest, then it will bring the two domains close together, resulting in restoration of the transcriptional activation function. Experimentally, the two hybrid plasmids expressing the GAL4 fusion proteins are co-transformed into a yeast host strain and transcriptional activation of expression of a reporter gene, typically *lacZ*, indicates a positive result.

The two-hybrid system has several advantages over more conventional methods. The assay is a sensitive method for detection of weak or transient

Figure 4.1 Schematic diagrams of the Yeast Two-Hybrid System cloning vectors, pGBT9 and pGAD424, showing the MCS sequence and unique restriction sites

Schematic diagrams of the main features of plasmid pGBT9 (panel A) and pGAD424 (panel B) are shown. pGBT9 generates a hybrid that contains the sequences for the GAL4 binding domain (amino acids 1-147) (GAL4 bd). pGAD424 generates a hybrid that contains the sequences for the GAL4 activation domain (amino acids 768-881) (GAL4 ad). The plasmids have unique restriction sites located in the MCS region at the 3' end of the open reading frame for either the DNA-binding or activation domain sequences. The gene encoding the protein of interest is ligated into the MCS in the correct orientation and with the correct reading frame, such that fusion proteins with the GAL4 domains are expressed. The sequence and reading frame of the MCS for pGBT9 and pGAD424 are shown in the boxes below the appropriate plasmid diagrams. The unique restriction sites in the MCS of each plasmid, which can be used for cloning purposes, are indicated. Fusion proteins are expressed from the constitutive ADH1 promoter (^{P}ADH1) and transcription is terminated at the ADH1 transcription termination signal (^{T}ADH1). The fusion proteins are targeted to the yeast nucleus by nuclear localisation sequences (▲). pGBT9 and pGAD424 plasmids replicate autonomously in both *E. coli* and *S. cerevisiae*. The selectable markers carried are the *bla* gene which confers resistance to ampicillin in *E. coli* (Amp^{R}), and a nutritional gene that allows yeast auxotrophs to grow on limiting synthetic media (TRP1 in pGBT9; LEU2 in pGAD424). This figure is adapted from the Clontech Matchmaker Two-Hybrid system protocol.

Figure 2.1

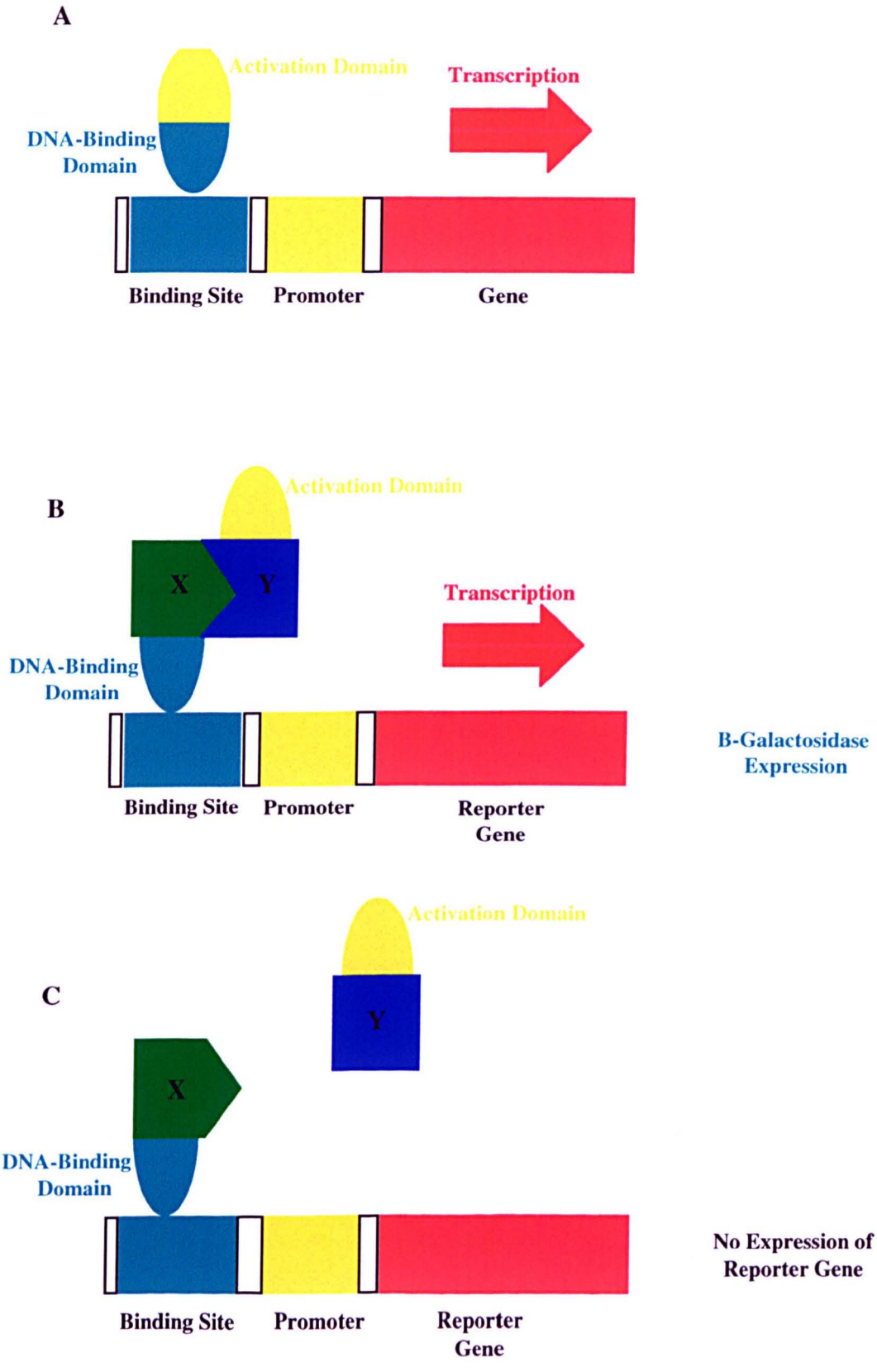
A
Activation Domain
Transcription
DNA-Binding Domain
Binding Site
Promoter
Gene
B
Activation Domain
X
Y
Transcription
DNA-Binding Domain
Binding Site
Promoter
Reporter Gene
B-Galactosidase Expression
C
Activation Domain
Y
X
DNA-Binding Domain
Binding Site
Promoter
Reporter Gene
No Expression of Reporter Gene

interactions. It also does not require the production of purified target proteins and antibodies to the desired proteins. In addition, the assay is performed *in vivo*, and consequently the proteins involved are more likely to be in their native conformations, albeit fused to a heterologous protein. The method has been used with a wide variety of proteins, including those that normally reside in the nucleus, cytoplasm, are peripherally associated with membranes or are extracellular (Fields and Sternglanz, 1994). Finally, an important development in the use of the two-hybrid system was its use to screen cDNA espression libraries to detect interacting host cell proteins (Chien *et al.*, 1991). The significance of this approach is that the cloned gene encoding the interacting protein can be rapidly isolated.

2.3.2 Development of the two-hybrid system

The original two-hybrid system, which was developed in yeast, utilised the DNA-binding and activation domains of the GAL4 protein (Fields and Song, 1989). Several developments on the original system have since been made. The LexA yeast two-hybrid system uses the DNA-binding domain of the bacterial repressor protein LexA. This required the engineering of the appropriate recognition sequence for LexA into the DNA of specific yeast strains (Vojtek *et al.*, 1993). An alternative LexA system has been developed which uses amino-terminal fusions to LexA of the protein of interest, rather than the more commonly used carboxy-terminal fusion (Beranger *et al.*, 1997). This system detects specific protein-protein interactions equally well, and could be of particular value when a 'free' amino-terminus of the protein of interest is required.

An alternative transactivation domain that has been successfully used is the VP16 transactivating protein from herpes simplex virus (Dalton and Treisman, 1992). In addition, the use of different reporter genes, such as selectable yeast genes such as *HIS3* and *LEU2*, allows the scope and sensitivity of the assay to be varied.

If an interaction is detected between two proteins, then deletion mutagenesis can be used to analyse the regions of the proteins containing the functional domains (Chien *et al.*, 1991). Point mutations can then be assayed to identify specific amino acid residues critical for the interaction (Li and Fields, 1993). The immediate availability of the cloned gene for the protein of interest aids this type of analysis. A reverse two-hybrid system has also been developed, whereby the interaction of the

two proteins of interest activates expression of a toxic gene (Leanna and Hannink, 1996). Thus, there is selective pressure against the interaction, facilitating identification of mutants that have lost the ability to interact.

The yeast system has been generally favoured, due to the ease of transformation of plasmids into yeast cells and the use of selectable transformation markers, however a mammalian cell system has also been successfully developed. The GAL4 DNA-binding domain and the VP16 transactivating domain from herpes simplex virus were used to develop a two-hybrid system in mammalian cells (Dang *et al.*, 1991) (Fearon *et al.*, 1992). Transfection of a variety of mammalian cell lines with plasmids expressing fusions of the proteins of interest with the DNA-binding and activation domains together with a reporter gene plasmid can be performed. The interaction of the proteins of interest activates transcription, which drives a reporter gene encoding chloramphenicol acetyltransferase (CAT). The CAT activity can be measured *in vitro* to quantify the protein interaction. The development of the mammalian cell systems allowed the detection of interactions that depend upon post-translational modifications which do not occur in yeast cells (e.g. tyrosine phosphorylation events).

An interesting development made recently is the description of the two-bait system in yeast. This system allows the characterisation of the interaction of two proteins fused to two different DNA-binding domains with a common protein fused to the activation domain. The use of two different reporter genes allows differentiation of the interacting protein pairs. Among other uses, this system allows the identification of interactions that depend upon a third protein (Xu *et al.*, 1997).

2.3.3 The use of the yeast two-hybrid system to study viral protein-protein interactions

Viral and cellular protein interactions are central to the replication process in the virus infectious cycle. Defining the protein-protein interactions that occur is an important step towards understanding the viral replication cycle. The two-hybrid system has been used to an increasing extent as an important tool to dissect viral protein-protein interactions. There are several applications of the system, including testing known proteins for an interaction and subsequently defining the domains or

amino acids that are critical for the interaction. The assay can also be used to screen libraries of cellular proteins for a protein that binds to a target viral protein.

One of the first examples of the use of the yeast two-hybrid system to investigate viral protein-protein interactions was in defining the multimerisation of the retroviral *gag* polyproteins (Luban *et al.*, 1992). Using the original GAL4 domain vectors (Fields and Song, 1989), Luban *et al.* (1992) determined that HIV-1 *gag* and Moloney murine leukemia virus *gag* polyproteins formed specific homo-oligomers, but not hetero-oligomers. Their experiments demonstrated that the interaction between the *gag* proteins was specific for a given species of virus. The yeast two-hybrid system has also been used to analyse specific interactions between viral structural proteins in the rice dwarf phytoreovirus (RDV) (Ueda *et al.*, 1997). RDV is a member of the *Reoviridae* and has a segmented genome consisting of 12 dsRNA segments. In order to investigate the process of viral morphogenesis and assembly, interactions among multiple structural proteins were dissected. Oligomerisation of the major core protein P3 was demonstrated with the yeast two-hybrid system, but additional interactions among the structural proteins were only revealed by far-western blotting, suggesting that the two-hybrid system should not be used in isolation when investigating protein-protein interactions.

A protein linkage map that documents a network of interactions between the non-structural cleavage products of the poliovirus P2 polyprotein has been determined using a combination of the GAL4 and the LexA yeast two-hybrid systems (Cuconati *et al.*, 1998). Homo-oligomeric and hetero-oligomeric protein interactions between the non-structural cleavage products 2BC, 2B and 2C, were described. Further analysis of the multimerisation of 2B by mutagenesis and selected deletion of regions of the protein, implicated the carboxy-terminus of the protein in the self-interaction. The homo-oligomerisation of 2B was thought to be required for replication of the positive-sense RNA genome of poliovirus. This study demonstrated the value of the two-hybrid system in determining the variety of different interactions that can occur between several viral proteins.

The assay has been used extensively to identify specific domains involved in interactions between viral proteins. Li and Fields (1993) demonstrated by mutagenesis of p53 and analysis of the interaction of the mutants with SV40 large T antigen, that the yeast two-hybrid system could be used to define residues in a protein required for binding. They advanced the idea that this approach could be generally applicable to

the analysis of protein-protein interactions. An interaction was demonstrated between the Rinderpest virus (RPV) nucleocapsid protein (N) and phosphoprotein (P) when the proteins were fused to the GAL4 domains and tested in the yeast two-hybrid system (Shaji and Shalia, 1999). Mapping of the domains of P protein involved in its interaction with N protein, revealed two domains, the amino-terminal 59 aa and the carboxy-terminal 32 aa, were involved in the interaction. Interestingly, the researchers found that a P protein mutant containing only the interaction domains, with all other regions of the protein deleted, retained its ability to interact with N protein. Similar studies on the interaction of the N and P proteins in human respiratory syncytial virus (hRSV) have also been performed using the two-hybrid system (Slack and Easton, 1998). Deletions in the carboxy-terminus of the P protein reduced its ability to interact with the N protein, suggesting that this region was functional in the interaction of N and P proteins. Use of the two-hybrid system to study the P protein of various negative-strand RNA viruses has revealed analogous results demonstrating that the assay can provide consistent data and allowing biologically relevant conclusions to be drawn.

The yeast two-hybrid system has proved to be a valuable research tool in the identification of cellular proteins that interact with specific viral proteins. For example, the assay was employed to search for cellular proteins that interacted with the influenza A virus NS1 protein (Wolff *et al.*, 1996). NS1 is the major non-structural protein expressed by influenza A and B viruses in infected cells, and although its precise function is unclear, it is thought to have a regulatory role in viral gene expression and/or replication. A HeLa cell library was screened using the yeast two-hybrid system and a cellular protein, NS1-I, which interacted with NS1 was identified. The interaction was shown to be conserved among six different human and avian influenza virus NS1 proteins, despite the fact that the sequence of NS1 is highly divergent between isolates, suggesting that the NS1-NS1-I interaction had an important function during the virus life cycle. Once interacting cellular proteins have been identified, binding domains on the proteins can be mapped. The data gained from such studies can lead towards further characterisation of viral protein function and delineation of the significance of the protein interactions in viral processes. For example, two cellular proteins shown to interact with the influenza virus NP protein have been found to be involved in the nuclear import of the NP protein and of viral RNA (Wang *et al.*, 1997). The cellular protein binding site was localised to the

amino-terminus of the NP using NP deletion mutants. It was then revealed that this region of the protein had nuclear localisation signal (NLS) activity, so the binding site for the cellular transport factors also functions as an NLS motif. Hence, binding of the cellular proteins to the NP protein may facilitate nuclear import.

Clearly, the development of the yeast-two hybrid system has allowed significant progress in the definition of interactions between viral and cellular proteins which can lead towards a greater understanding of viral processes.

2.4 Aims of the study

The rotavirus non-structural protein NSP1 is thought to have a function in the early stages of the virus replication cycle, although its exact role remains to be defined. Specific protein-protein interactions are essential for the processes involved in the replication cycle, including RNA replication, and assortment and packaging of the segmented genome. The aim of this project was to investigate potential protein-protein interactions between NSP1 and the viral proteins VP1, VP2, VP3, and NSP3, which are found associated with or subsequently added to a pre-core replication intermediate in the rotavirus-infected cell. A novel NSP1-containing complex found in rotavirus-infected cells was also examined. The overall objective was to further define the function of NSP1 in the virus replication cycle.

Materials and Methods

3.1 Materials

3.1.1 Standard solutions and buffers

5X Protein loading buffer: 10 % (w/v) SDS, 25 % (v/v) β-mercaptoethanol, 50 % (v/v) glycerol, 0.01 % (w/v) bromophenol blue.

5X Agarose gel loading buffer: 5X TAE/TBE, 50 % (v/v) glycerol, 0.01 % (w/v) bromophenol blue, 0.01 % (w/v) xylene cyanol ff.

Chloroform/Isoamyl alcohol (IAA): 96 % (v/v) chloroform, 4 % (v/v) isoamyl alcohol.

Phosphate Buffered Saline (PBS): 137 mM NaCl, 2.7 mM KCl, 4.3 mM $Na_2HPO_4.7H_2O$, 1.4 mM KH_2PO_4.

Phenol/Chloroform/Isoamyl alcohol: 48 % (v/v) phenol, 48 % (v/v) chloroform, 4 % isoamyl alcohol.

TAE Electrophoresis buffer (1X): 40 mM Tris Acetate, 2 mM EDTA pH 8.0.

TBE Electrophoresis buffer (1X): 89 mM Tris base, 89 mM Boric acid, 2 mM EDTA.

TE: 10 mM Tris-HCl pH 8.0, 1 mM EDTA pH 8.0.

Triton lysis solution: 2 % (v/v) Triton X-100, 50 mM Tris-HCl pH 8.0, 62.5 mM EDTA

3.1.2 Tissue culture media

Sterile PBS, trypsin (0.25 % in Tris saline), versene (0.02 % in PBS), L-glutamine (200 mM), 5 % $NaHCO_3$, penicillin and streptomycin sulphate (100,000,000 U/100 g in 200 ml PBS), 1.8 % Noble Agar, and tissue culture media including: Dulbecco's modification of Eagle's minimal essential medium (DMEM), Glasgow modification of Eagle's minimal essential medium (GMEM) plus non-essential amino acids (NEAA; 0.89 g L-alanine, 1.15 g L-asparagine.H_2O, 1.33 g L-aspartic acid, 0.75 g glycine, 1.45 g L-glutamic acid, 1.15 g L-proline and 1.05 g L-serine per litre) 1X, 2X, and GMEM minus methionine, valine, leucine and $NaHCO_3$, were all prepared by the media preparation staff of the Department of Biological Sciences, University of Warwick. Foetal Bovine Serum was purchased from Gibco BRL.

3.1.3 Cell lines

The tissue culture cell lines used in this study are shown in Table 3.1. Growth medium was supplemented with an appropriate concentration of FCS, L-glutamine (2 mM), penicillin (100 U/ml) and streptomycin (100 µg/ml).

3.1.4 Virus Strains

The bovine strain Compton UK tissue culture adapted (UKtc) (serotype 6) was originally provided by Dr M. Thouless, East Birmingham Hospital, Birmingham. Rotavirus was pre-treated with 10 µg/ml trypsin for 30 minutes at 37°C before propagation. The recombinant vaccinia virus VR5 containing the UKtc rotavirus gene 5 was produced by S. Stagg in the Rotavirus laboratory, University of Warwick.

3.1.5 Animals

The Half-Lop rabbit used for antibody production was obtained from Harlan UK and housed at the University of Warwick. Inoculation of the rabbit for production of antiserum was performed by Prof. N. J. Dimmock.

Table 3.1. Cell Lines

Cell Line	Origin	Tissue Culture Medium
BS-C-1	African Green Monkey Kidney (Supplied by Prof. M. A. McCrae, University of Warwick)	GMEM + 5 % FCS
MA104	Rhesus Monkey Kidney (Supplied by Prof. M. A. McCrae, University of Warwick)	GMEM + 5 % FCS
HeLa	Human cervical epitheloid carcinoma (Supplied by Prof. M. A. McCrae, University of Warwick)	DMEM + 10 % FCS
L-Cells	Mouse connective tissue (Supplied by Prof. M. A. McCrae, University of Warwick)	GMEM + 5 % FCS

3.1.6 Antiserum

The anti-NSP1 antiserum was obtained from Dr J. Cohen, Centre de Recherche Agronomique, France. The anti-UKtc rotavirus polyclonal serum (#2148) was produced by S. Thomas in the Rotavirus laboratory, University of Warwick. The anti-VP6 monoclonal antibody was obtained from Dr J. Howes at BioBest, Scotland. The anti-VP7 antiserum was obtained from Professor M. A. McCrae, University of Warwick.

3.1.7 Bacterial Strains

The bacterial strain *E. coli* MC1061 was obtained from Prof. M. A. McCrae, University of Warwick.

3.1.8 Bacterial Growth Conditions

The *E. coli* strain MC1061 was grown in LB media in the presence of appropriate antibiotics. Liquid media was converted to solid media by the addition of agar (15 g/L) prior to autoclaving.

LB media: 10 g Bacto-tryptone, 5 g Yeast extract, 5 g NaCl in 1 L water

3.1.9 Yeast Strains

Saccharomyces cerevisiae reporter host strains were obtained from Clontech Laboratories, Inc. as shown in Table 3.2.

Table 3.2 Yeast Strains

Strain	Genotype	Reporter(s)	Transformation Markers
SFY526	*MATa, ura3-52, his 3-200, ade 2-101, lys 2-801, trp 1-901 leu 2-3, 112, can^r, gal4-542, gal80-538, URA3::GAL1-lacZ*	*lacZ*	*trp1, leu2*
HF7c	*MATa, ura3-52, his3-200, lys2-801, ade2-101, trp1-901, leu2-3, 112, gal4-542, gal80-538, LYS2::GAL1-HIS3, URA3::(GAL4 17-*mers)$_3$-CYC1-lacZ	*HIS3, lacZ*	*trp1, leu2*

3.1.10 Yeast Growth Media

YPD Medium

20 g/l Difco peptone; 10 g/l Difco Yeast extract; 18 g/l Bacto-Agar (if needed for plates); filter-sterilised dextrose was added to 2 % after autoclaving.

SD Synthetic Medium (Dropout SD Medium)

6.7 g/l Difco yeast nitrogen base without amino acids; 20 g/l Agar; 10X Dropout solution to give final concentration 1X; filter-sterilised dextrose was added to 2 % after autoclaving.

10X Dropout solution

The Dropout solution is composed of essential amino acids required for yeast growth with one or more of the amino acids omitted such that only transformants carrying the appropriate nutritional genes can grow in the Dropout SD media. The concentrations of the amino acids are shown in the following table. The appropriate amino acid(s) for the Dropout SD medium required were omitted. The solution was autoclaved and stored at 4°C.

Amino Acid	mg/l
L-Isoleucine	300
L-Valine	1500
L-Adenine hemisulphate salt	200
L-Arginine HCl	200
L-Histidine HCl monohydrate	200
L-Leucine	1000
L-Lysine HCl	300
L-Methionine	200
L-Phenylalanine	500
L-Threonine	2000
L-Tryptophan	200
L-Tyrosine	300
L-Uracil	200

3.1.11 Vectors

The Yeast Two-Hybrid cloning vectors, plasmid pGBT9 and pGAD424, and the additional control plasmids were obtained from Clontech (Palo Alto, California, USA). The cloning vectors pTAg and pCR™II were obtained from Invitrogen (R & D Systems Ltd, Abingdon, Oxfordshire). Plasmids containing UKtc rotavirus genes 1, 2, 3, and 9 were obtained from Professor M. A. McCrae. Plasmids G5T7(TA), G5T7-TA1, T7-g5-blue, T7-p9Δ5, and T7Δ5G5blue were obtained from Dr Xu Li in the Rotavirus laboratory, University of Warwick. Plasmids pGBT9-N and pGAD424-P were obtained from M. Slack, University of Warwick.

3.1.12 Primers

The oligonucleotide primers utilised during this study are shown in Table 3.3. Primers were synthesised by Genosys Biotechnologies, Inc., Cambridge.

3.1.13 Suppliers

General chemicals were obtained from BDH Laboratory Supplies (Merck Ltd, Poole, Dorset), Fisons Scientific Equipment (Loughborough, Leicestershire), and Sigma Chemical Company Ltd (Poole, Dorset) and were of analytical or molecular biology grade. All water used was double distilled. Equipment and other reagents were obtained from the following suppliers.

Amersham International plc (Buckinghamshire).
^{32}P dCTP (111 TBq/mmol), ^{35}S Methionine (37 TBq/mmol), Full range Rainbow ™ Recombinant protein molecular weight markers, Shrimp Alkaline Phosphatase (SAP), Hybond™ N membrane, Amplify™ fluorographic reagent, Linked T7 *in vitro* transcription-translation system, Rabbit reticulocyte lysate system, Biotinylated goat anti-rabbit IgG (H + L), streptavidin/biotin horseradish peroxidase conjugate, ECL western blotting analysis system.

Table 3.3 Sequence of oligonucleotide primers.

Primer name	Sequence	Complimentary region location (red type)
Gene 5/5′	TCGAATTCGCTATGGCTACGTTCAAAGAC GCTTGCTATCATT	UKtc gene 5 nts 45-62
Rotgen 5 3′	CGATCGCGAATTCTGCAGGTCACATTTTAT	UKtc gene 5 nts 1567-1579
Gene 2/5′	CTGCAGAATTCGTAATGGCGTACAGGAA	UKtc gene 2 nts 16-30
Gene 2/3′	TCTAGATCTGCAGGTCACATCTGACCAGT GTG	UKtc gene 2 nts 2672-2691
Gene 3/5′	GACTGCAGGGATCCGGATGAAAGTATTAG CTTTAAG	UKtc gene 3 nts 50-69
Gene 3/3′	GAGCTCCGGATCCTGCAGGTCACATCTGA CCA	UKtc gene 3 nts 2576-2590
Gene 1/5′	CGCTGCAGGCCCGGGCATGGGGAAGTATA ATCTA	UKtc gene 1 nts 19-36
Gene 1/3′	AAGCCTCGAGCTCGGCCGCGGTCACATCT AAG	UKtc gene 1 nts 3290-3302
Gene 9/5′	TAGGATCCCTGCAGCTATGCTCAAGA	UKtc gene 9 nts 26-35
Gene 9/3′	CTTAAGCTTCAGCTGCAGGTCACATAACG	UKtc gene 9 nts 1065-1076
pTAg SEQ 5′	GCTATGACCATGATTACGCCAA	Plasmid pTAg, 84 bp upstream of insert site
pTAg SEQ 3′	TGTAAAACGACGGCCAGTGAA	Plasmid pTAg, 75 bp downstream of insert site
Primer 1	TCATCGGAAGAGAGTAG	Plasmid pGBT9, 31 bp from MCS start site
Primer 2	TACCACTACAATGGATG	Plasmid pGAD424, 56 bp from MCS start site

Bio-Rad (Hemel Hempstead, Hertfordshire).
Ammonium persulphate, N,N'-methylene-bis-acrylamide, TEMED.

Clontech (Palo Alto, California, USA).
MATCHMAKER Two-Hybrid system, Mammalian MATCHMAKER Two-Hybrid kit.

Difco Laboratories (Basingstoke, Hampshire).
Bacto-agar, Bacto-peptone, Bacto-tryptone, Yeast extract, Yeast nitrogen base w/o amino acids and ammonium sulphate.

Fuji Photo Film Co. Ltd (Tokyo, Japan).
Fuji medical x-ray film.

Gibco-BRL Life Technologies Ltd (Renfrewshire, Scotland).
Restriction and modification enzymes, Taq DNA polymerase, 1 Kb DNA ladder.

Harlan Sera-Lab Ltd (Crawley Down, UK).
FITC conjugate goat anti-rabbit Immunoglobulin.

Invitrogen (R & D Systems Ltd, Abingdon, Oxfordshire).
TA Cloning™ System, LigATor cloning kit.

Melford Laboratories Ltd (Ipswich, Suffolk).
5-Bromo-4-chloro-3-indolyl-β-D-galactoside (X-GAL)

New England Biolabs (UK) Ltd (Hampshire).
Restriction enzymes.

Promega (Madison, Wisconsin, USA).
TNT™ Coupled Reticulocyte Lysate System, TMB stabilised substrate for HRP, Taq DNA Polymerase.

Qiagen Ltd (Crawley, West Sussex).
QIAquick Gel extraction kit, QIAprep Spin Mini prep kit.

Stratagene (California, USA).
Cloned Pfu polymerase.

Whatman International Ltd (Maidstone, Kent).
Filter paper Grade 5 Qualitative (70mm).

3.2 Cell Culture

3.2.1 Maintenance of tissue culture cells

Mammalian cell lines were maintained at 37°C in either a 5 % CO_2 incubator in a humidified atmosphere (for 150 cm^2 flasks) or on a rolling bottle apparatus (Modular Cell Production Model III) (for 800 cm^2 roller bottles) using the appropriate media (see Table 3.1). When confluent, the cells were passaged as follows. Cells were detached by rinsing the monolayer twice with versene followed by incubation with trypsin/versene (1:5) and disaggregation. Cells were reseeded at a ratio of 1:4. Roller bottles were gassed with CO_2 to give a final concentration of 5 %. All manipulations were carried out under sterile conditions in a Class II Laminar Flow Cabinet using standard aseptic techniques.

3.2.2 Freezing and recovery of cell stocks

Cell stocks were prepared by suspending the cells from one 150 cm^2 flask in 2 ml of 8 % (v/v) dimethylsulphoxide (DMSO) and 30 % FCS in appropriate medium. Freezing vials were cooled slowly to -70 °C before immersion in liquid nitrogen for long term storage. Cell stocks were recovered by rapidly thawing at 37 °C, and adding the contents of one vial to a 150 cm^2 flask containing pre-warmed medium. The medium was changed or the cells passaged the following day.

3.3 Virus propagation and preparation

3.3.1 Large scale growth of rotavirus

Confluent BS-C-1 cell monolayers in roller bottles were infected at a m.o.i. of ≤0.1 and made up to a volume of 25 ml per bottle with GMEM (no FCS). Virus was harvested once complete c.p.e. was observed. Aprotinin (4 μg/ml) was added to the harvested virus to stabilise the triple layered virus particles (Keljo and Smith, 1988).

3.3.2 Large scale growth of recombinant vaccinia virus

Virus was propagated in confluent HeLa cell monolayers grown in 150 cm^2 flasks. The cells were infected at a m.o.i. of 0.1 and the virus inoculum was made up to 25 ml/flask with DMEM (1 % FCS). Virus was harvested following complete cpe and centrifuged at 25,000 rpm, 4°C for 90 minutes in a Beckman SW28 rotor and the pellets were resuspended in 1 ml 50 mM Tris-HCl pH 8.0.

3.3.3 Purification of recombinant vaccinia virus

The virus stock was subjected to 3 cycles of freeze/thawing and sonicated in a water bath for two periods of 15 seconds. The virus was then layered onto a 20-45 % sucrose gradient (allowing 1 flask/gradient), made up in 50 mM Tris-HCl pH 8.5, 0.5 M NaCl, 50 mM EDTA. The sucrose gradient was centrifuged at 18,000 rpm for 28 minutes at 4 °C in a Beckman SW28 rotor. Following centrifugation, a band of virus was visible in the centre of the gradient and a pellet, containing residual virus, was formed at the bottom of the tube. The band was recovered using a 19 gauge needle and a 5 ml syringe and pooled. Pooled virus bands were then pelleted in a Beckman SW28 rotor at 25,000 rpm for 90 minutes at 4 °C, and resuspended in 1 ml 50 mM Tris-HCl pH 8.0 overnight at 4 °C. Residual virus in the pellet from the sucrose gradient was extracted by a repeat banding on a 20-45 % sucrose gradient as follows. The pellet was resuspended in 1 ml 50 mM Tris-HCl pH 8.0 by cycles of freeze/thawing and sonication and centrifuged on a 20-45 % sucrose gradient at 18,000 rpm for 15 minutes at 4 °C. The virus band from this spin was recovered as before, pooled and pelleted in a Beckman SW28 rotor at 25,000 rpm for 90 minutes at 4 °C. The resulting pellet was resuspended in 1 ml 50 mM Tris-HCl pH 8.0 and

pooled with the virus collected initially. The virus stock was then subjected to a second cycle of purification in a smaller volume. 0.5 ml virus/tube was layered onto 20-45 % sucrose gradients, made up in 50 mM Tris-HCl pH 8.5, 0.5 M NaCl, 50 mM EDTA, and centrifuged in a SW41 Ti rotor at 18,500 rpm for 15 minutes at 4 °C. A virus band was collected as before and pelleted in a SW41 Ti rotor at 25,500 rpm for 90 minutes at 4 °C. The pellet was resuspended in 200 µl 50 mM Tris-HCl pH 8.0 and stored at -70 °C until required for titration and use.

3.3.4 Titration of virus stocks

Serial ten-fold dilutions of the virus stock were prepared in serum-free GMEM and 0.2 ml of virus dilution was added to confluent cell monolayers in 12-well dishes. After incubation at 37 °C for 1 hour, 2 ml of an overlay of GMEM containing 1.4 % agar, plus antibiotics, was added to each well and the cells incubated at 37 °C for 4-5 days. The cells were then fixed with formal-saline (30 % (v/v) formaldehyde in PBS) overnight. The agar was removed and the plaques visualised by staining the remaining cells with 0.1 % (w/v) crystal violet.

3.4 Molecular Biology Techniques

3.4.1 PCR amplification of viral genes

A standard PCR was performed in a final volume of 25 µl. This contained template DNA (approximately 100 ng), 1 µl primer mixture (100 ng/µl), 1X PCR mixture (2.5 µl 10X Cloned Pfu polymerase buffer, 250 µM dNTPs, sterile distilled water) and 1.5 units Pfu DNA polymerase. The solution was overlaid with 50 µl mineral oil and subjected to 30 cycles of 94°C for 1 min, 55°C for 1 min and 72°C for 5 min. 5 µl of the reaction was then analysed by agarose gel electrophoresis (Section 3.4.3). In some cases adjustment of the thermal cycling parameters were necessary to improve amplification specificity and target DNA yield.

3.4.2 Quantification of DNA

DNA was quantified by spectrophotometry. Absorbance readings were taken at 260 nm where an absorbance of 1.0 was taken as indicating a concentration of 50

µg/ml for double stranded DNA or 20 µg/ml for single stranded DNA primers. Digested and dilute DNA solutions were quantified using agarose gel electrophoresis (Section 3.4.3) by comparing the band intensity with 100 ng pBR322 plasmid DNA.

3.4.3 Agarose gel electrophoresis

DNA samples were analysed on agarose gels containing between 1.0 and 1.5 % agarose and 1 µg/ml ethidium bromide in 1X TAE/TBE. DNA samples and 1 Kb ladder were prepared by the addition of 1/5 volume of 5X TAE/TBE agarose gel loading buffer (Section 3.1.1) before being loaded into the preformed wells. Electrophoresis was performed at 70 mA in 1X TAE/TBE running buffer for 60-90 minutes. Bands were visualised using an UV Transilluminator Gel Documentation System (UVP), photographed using Grab-IT (UltraViolet Products Ltd, Cambridge), an annotating image capture system, and printed on a digital graphic printer.

3.4.4 Phenol/Chloroform extraction

An equal volume of phenol/chloroform/IAA was added to the DNA solution and mixed by vortexing. The phenol/chloroform/IAA fraction was separated from the aqueous phase by centrifugation for 1 minute in a microcentrifuge. The upper aqueous phase was removed and the lower phase discarded. The process was repeated and the resulting DNA solution was ethanol precipitated. An additional extraction using chloroform/IAA was performed before ethanol precipitation if additional purity was required.

3.4.5 Ethanol precipitation of nucleic acids

DNA was precipitated from solution by the addition of sodium acetate pH 5.2 to a final concentration of 0.3 M and 2.5 volumes of ice cold 100 % ethanol. After precipitation for 1 hour at -70°C, DNA was pelleted by centrifugation in a microcentrifuge for 10 min at 15,000 rpm. The pellet was washed with 70 % (v/v) ethanol, dried under vacuum and resuspended in 50 mM Tris-HCl pH 8.0 or TE buffer.

3.4.6 Restriction enzyme digestion of DNA

Restriction enzyme digests were performed under the manufacturer's recommended conditions using the supplied 10X buffer solutions.

3.4.7 Dephosphorylation of vector DNA

The 5' phosphate groups were removed from DNA using shrimp alkaline phosphatase (SAP) under the conditions recommended by the manufacturer. SAP was inactivated by heating to 65°C for 15 minutes. Calf intestinal alkaline phosphatase (CIP) was also used for dephosphorylation under the conditions recommended by the manufacturer.

3.4.8 Blunt-ending of DNA

Protruding 5′ extensions were filled using the Klenow fragment of *E. coli* DNA polymerase 1 (Maniatis *et al.*, 1982).

3.4.9 Recovery of DNA from agarose gels

DNA bands were excised from agarose gels under UV light using a sterile scalpel blade. The DNA was recovered using the QIAquick Gel Extraction Kit (Qiagen) according to the manufacturers instructions.

3.4.10 Ligation of DNA fragments

DNA fragments were ligated into dephosphorylated DNA vector molecules. Ligation was allowed to proceed at 15°C overnight and contained DNA (insert (20): vector (1) mix) 10X ligation buffer (0.66 M Tris-HCl pH 7.6, 50 mM $MgCl_2$, 50 mM DTT, 100 mM ATP) and 1 unit T4 DNA ligase in a total volume of 15 µl. The DNA ligation mixture was ethanol precipitated and the vacuum dried pellet resuspended in 10 µl of distilled water.

3.4.11 Preparation of competent cells for electroporation

Electro-competent *E. coli* cells were prepared by washing 200 ml of mid log phase bacteria (OD_{590} = 0.4-0.5) twice with sterile ice cold water. The bacteria were resuspended in 15 ml of ice cold water, washed again and resuspended in 0.5 ml sterile 10 % glycerol.

3.4.12 Transformation of DNA into bacteria by electroporation

50 µl electro-competent bacteria were mixed with 10 µl salt free ligated DNA or control DNA and pulsed in a BioRad Gene Pulser at 2.5 kV with 25 µF set as capacitance and 200 Ω set on the pulse controller. Cells were immediately transferred to 1.5 ml LB and allowed to recover by shaking for 30 minutes at 37 °C. The bacteria were then plated out onto selective agar plates and incubated overnight at 37 °C. Recombinant clones were identified by restriction enzyme analysis of mini-prep DNA or by Grunstein-Hogness filter hybridisation (Grunstein and Hogness, 1975).

3.4.13 Small scale preparation of plasmid DNA from bacteria (mini-prep)

Individual bacterial colonies were picked from agar plates into 5 ml LB medium containing appropriate antibiotics and incubated overnight with continuous shaking at 37 °C. For restriction enzyme analysis the plasmid DNA from 1.5 ml of culture was prepared using an alkaline lysis technique (Maniatis *et al.*, 1982) and the DNA pellets resuspended in 50 µl 50 mM Tris-HCl pH 8.0. For sequence analysis the plasmid DNA from 1.5 ml of culture was isolated using the QIAprep Spin Miniprep kit (Qiagen) according to the manufacturer's instructions and resuspended in 50 µl 10 mM Tris-HCl pH 8.0.

3.4.14 Large scale preparation of plasmid DNA from bacteria (maxi-prep)

The plasmid DNA from 1 L of bacterial culture was prepared using triton lysis followed by purification of plasmid DNA on a CsCl gradient (Maniatis *et al.*, 1982). The yield of low copy number plasmids was increased by using chloramphenicol amplification. 10 ml of LB containing ampicillin (final concentration of 100 µg/ml) was inoculated with a single colony and incubated overnight at 37 °C with shaking.

The overnight culture was subcultured into 1 L of LB plus ampicillin and incubated for 6-8 hours at 37 °C with shaking. Chloramphenicol was added to a final concentration of 150 μg/ml, the culture was incubated overnight at 37 °C with shaking then harvested.

3.4.15 Nick translation of DNA

DNA fragments purified following agarose gel electrophoresis were labelled with ^{32}P dCTP by nick translation with DNA polymerase I according to the method reported in Maniatis *et al.* (1982).

3.4.16 Grunstein-Hogness colony filter hybridisation assay

Large numbers of putative bacterial clones were screened by Grunstein-Hogness colony hybridisation (Grunstein and Hogness 1975) following the method published in Maniatis *et al.* (1982).

3.4.17 Direct cloning of PCR products

DNA fragments produced by PCR were cloned directly into the pTAg vector using the LigATor cloning kit (Invitrogen). The TA Cloning™ System (Invitrogen) was also used for direct cloning of PCR fragments. The manufacturers recommendations were followed in each case.

3.4.18 DNA Sequence Analysis

DNA cycle sequencing was carried out using the Applied Biosystems 373A Automated Sequencer by Mrs L. Ward, Department of Biological Sciences, University of Warwick, according to the manufacturers instructions.

3.5 Yeast Two-Hybrid Assay Methods

3.5.1 Preparation of competent yeast cells for transformation (Lithium acetate method)

50 ml YPD medium was inoculated with a single yeast colony (2-3 mm diameter) which was no more than 4 weeks old. The yeast culture was grown to stationary phase (OD600 ≥ 1.5) overnight (16-18 hours) at 30 °C with shaking (230-250 rpm). The culture was transferred to 250 ml YPD medium to give an OD_{600} reading between 0.2 and 0.3, and incubated as before for 3 hours. The cells were centrifuged in a Beckman J2-21 M/E centrifuge in a JA10 rotor at 1000 g (2400 rpm) for 5 minutes at room temperature. The cell pellet was resuspended by vortexing in 25-50 ml sterile, distilled water, and the cells centrifuged as before then resuspended in 1.5 ml of freshly prepared, sterile 1X TE/LiAc (0.01 M Tris-HCl; 1 mM EDTA; 0.1 M lithium acetate pH 7.5) and used for transformation immediately.

3.5.2 Transformation of yeast cells by heat shock

1 µg of each plasmid and 100 µg of denatured salmon sperm carrier DNA were mixed in an eppendorf tube. 100 µl of yeast competent cells were added and mixed well, then 600 µl of sterile PEG/LiAc (40 % PEG 4000; 0.01 M Tris-HCl; 1 mM EDTA; 0.1 M lithium acetate pH 7.5) was added to the tube and the contents vortexed. The reactions were incubated at 30 °C for 30 minutes with shaking (200 rpm), then 70 µl sterile DMSO was added to 10 % final concentration and mixed gently. The transformation reactions were heat shocked for 15 minutes at 42 °C, then chilled on ice and centrifuged for 5 seconds in a microcentrifuge. The cells were resuspended by pipetting in 0.5 ml of 1X TE buffer (0.01 M Tris-HCl; 1 mM EDTA pH 7.5). For single plasmid transformations, 100 µl of the transformation mixture was spread onto a 90 mm plate containing the appropriate SD selection medium. For double plasmid transformations, 250 µl of the transformation mixture was spread onto a 90 mm plate containing the appropriate double Dropout SD selection medium. Plates were incubated at 30 °C for 4-5 days until colonies appeared and then stored, sealed with Parafilm, at 4 °C for 3-4 weeks.

3.5.3 Colony lift filter assay for β-galactosidase

A sterile Whatman #5 filter (70 mm) was placed over the surface of the agar plate containing the freshly transformed colonies (1-2 mm diameter). Additional sterile Whatman #5 filters were pre-soaked in 2.5 ml of Z buffer/X-Gal solution.

Z Buffer

16.1 g/l Na2HPO4.7H2O; 5.5 g/l $NaH_2PO_4.H_2O$; 0.75 g/l KCl; 0.246 g/l $MgSO_4.7H_2O$ pH 7.0.

Z-Buffer/X-gal solution

100 ml Z-Buffer

0.27 ml β-mercaptoethanol

1.67 ml X-gal (5-bromo-4-chloro-3-indolyl-β-D-galactopyranoside) dissolved in N,N-dimethylformamide (DMF) at 20 mg/ml concentration.

The filter was carefully removed and submerged, colony side up, in liquid nitrogen for 10 seconds then allowed to thaw at room temperature. It was then placed, colony side up, on the filter which was pre-soaked in Z-buffer/X-gal solution and incubated at 30 °C until blue colonies appeared.

3.5.4 Liquid culture β-galactosidase assay

5 ml SD medium lacking the appropriate amino acids was inoculated with a freshly transformed yeast colony and incubated overnight at 30 °C with constant shaking (230-250 rpm). 8 ml YPD liquid medium was then inoculated with 2 ml of the overnight culture and incubated at 30 °C with shaking (230-250 rpm) for 3-5 hours until the culture was in mid-log phase (OD_{600} = 0.5-1.0). 1.5 ml of culture was removed in triplicate to microcentrifuge tubes and centrifuged in a benchtop microcentrifuge for 30 seconds (14,000 rpm). The pellet was washed in 1.5 ml of Z buffer and resuspended finally in 300 µl of Z buffer (concentration factor = 5). An aliquot of 100 µl was removed to a clean microcentrifuge tube and the tubes placed in liquid nitrogen until frozen, then thawed at 37 °C. A blank tube containing 100 µl of Z buffer only was prepared and 0.7 ml Z buffer plus β-mercaptoethanol (0.27 ml β-

mercaptoethanol added to 100 ml Z buffer) was added to all tubes. The timer was started immediately prior to adding 0.16 ml freshly prepared ONPG (o-nitrophenyl β-D-galactopyranoside) in Z buffer (4 mg/ml ONPG in Z buffer, pH 7.0) to the tubes. The reactions were incubated at 30 °C until a yellow colour was observed, then 0.4 ml 1 M Na_2CO_3 was added and the tubes were centrifuged for 10 minutes in a microcentrifuge at maximum speed to pellet the cell debris. The absorbance of the supernatants was measured at 420 nm relative to the blank and β-galactosidase units were calculated. 1 U β-galactosidase is defined as the amount which hydrolyses 1 μmole ONPG to o-nitrophenol and D-galactose per minute.

$$\beta\text{-galactosidase units} = 1000 \times OD_{420}/(t \times V \times OD_{600})$$

t = elapsed time (in minutes) of incubation

V = 0.1 ml × concentration factor

OD_{600} = Abs at 600 nm of 1 ml of culture

B-galactosidase units were calculated for each OD_{420} reading. The mean and standard deviation of β-galactosidase units were derived from the results of each transformation. Error bars were calculated using the 95 % confidence limits of the Students t test.

3.5.5 Preparation of yeast lysates for western blot analysis

Freshly transformed yeast colonies were used to inoculate 5 ml of dropout SD medium and the cultures were incubated at 30 °C until they reached mid-logarithmic phase (OD_{600} = 1.0). The cells were pelleted and the yeast lysates were prepared by boiling with acid washed glass beads and centrifugation as described previously (Li and Fields, 1993). The supernatants were fractionated on a 7.5 % SDS polyacrylamide gel (Section 3.6.5) and analysed by western blotting (Section 3.6.7).

3.6 Protein Expression and Analysis

3.6.1 In vitro protein expression

3.6.1.1 Zubay coupled transcription/translation

Zubay coupled transcription/translation was performed using the Linked T7 transcription-translation system (Amersham International plc, Buckinghamshire) following the manufacturers recommended protocol. The TNT™ Coupled Reticulocyte Lysate System (Promega, Madison, Wisconsin, USA) was also occasionally used for coupled transcription/translation following the manufacturers recommended protocol.

3.6.1.2 In vitro translation system

In vitro translation was performed using the rabbit reticulocyte lysate system (Amersham Pharmacia Biotech, Buckinghamshire) following the manufacturers recommended protocol.

3.6.1.3 Determination of *in vitro* translation efficiency by TCA precipitation

1 µl aliquots of the translation reaction were spotted onto filter paper discs, allowed to dry and transferred to 5 % (v/v) TCA-2 % (w/v) Cas-amino acid solution. The discs were boiled for 5 minutes in 5 % (v/v) TCA-2 % (w/v) Cas-amino acid solution under a fume hood, washed twice with 95 % (v/v) ethanol, twice with ether and allowed to dry. Incorporation of ^{35}S-methionine into protein was determined by measuring radioactivity in a scintillation counter.

3.6.2 Determination of protein concentration

The Bio-Rad protein assay™ was used according to the manufacturers instructions using bovine serum albumin (BSA) as a standard for comparison of protein concentrations.

3.6.3 Labelling of virus proteins in infected cells

A 12-well dish was seeded with 5×10^5 cells/well of BS-C-1 or MA104 cells and incubated overnight at 37 °C in a humidified 5 % CO_2 incubator. The following day the medium was removed from the cells and 0.2 ml high titre UKtc rotavirus, at a m.o.i. of approximately 20, was added to the cells and allowed to adsorb for 1 hour at 37 °C. The cells were then overlaid with 2 ml/well methionine-free GMEM and incubated for a further 6 hours at 37 °C. Following the incubation the medium was removed and the cells were labelled with 0.1 ml/well GMEM plus ^{35}S-methionine (500 µCi/ml) for 20 minutes at 37 °C. The label was removed and 0.5 ml/well 50 mM Tris-HCl pH 8 plus PMSF (0.2 mM final concentration) was added and the cells harvested using a rubber policeman. If a chase sample was required then after the label was removed 2 ml/well GMEM plus 100X unlabelled methionine was added to the cells and incubated at 37 °C for 2 hours before harvesting. The cells were subjected to 2 rounds freeze-thaw and sonication in a water bath. Centrifugation to separate the cell fractions was performed in a Beckman TL-100 ultracentrifuge using the TLS-55 rotor for 1 hour at 4 °C.

3.6.4 Immunoprecipitation

Immunoprecipitation was performed with infected cell lysates or *in vitro* translated protein samples. An equivalent volume of 2X IP3 buffer was added to the samples, followed by an aliquot of serum and the reactions were incubated at 4 °C for at least 2 hours on a rotating blood-wheel. 5 mg of Protein A-Sepharose was pre-prepared by soaking in 100 µl of IP3 buffer at 4 °C. The protein samples were added to the Protein A-Sepharose beads and incubated for a further 2 hours at 4 °C on a rotating blood-wheel. The samples were then centrifuged for 1 minute in a benchtop microcentrifuge and the beads resuspended in 1 ml of IP2 buffer, centrifuged again as before and then washed sequentially in IP2 buffer containing 1 M NaCl twice, IP3 buffer twice and IP1 buffer once. Finally the Protein A-Sepharose beads were resuspended in 40 µl of 50 mM Tris-HCl pH 8.0, 10 µl 5X protein loading buffer was added and the samples were boiled for 10 minutes prior to loading on a gel.

Immunoprecipitation (IP) Buffers:

IP1

20 mM Tris-HCL buffer pH 8.0; 100 mM NaCl; 1 mM EDTA; 1 % NP-40.

IP2

20 mM Tris-HCl buffer pH 8.0; 100 mM NaCl; 1 mM EDTA; 1 % NP-40; 1 % Na-deoxycholate; 20 mg/ml BSA.

IP3

20 mM Tris-HCl buffer pH 8.0; 100 mM NaCl; 1 mM EDTA; 1 % NP-40; 1 % Na-deoxycholate.

3.6.5 SDS-Polyacrylamide Gel Electrophoresis

Discontinuous single concentration and linear gradient (5-11 %) SDS-polyacrylamide gels were prepared and run in a vertical gel electrophoresis system according to the method of Laemmli (Laemmli, 1970). The composition of the separating and stacking gels was as shown below:

	4X Separating Gel Buffer pH 8.8	**4X Stacking Gel Buffer pH 6.8**
Tris base	36.3 g	12.1 g
SDS	0.8 g	0.8 g
Distilled H_2O to	200 ml	200 ml

Both buffers were adjusted to the correct pH with conc. HCl.

The composition of the gradient and linear polyacrylamide gels is shown in Tables 3.4 and 3.5.

Table 3.4 Composition of 5-11 % SDS Polyacrylamide gradient gels

	5 % Separating Gel Solution	11 % Separating Gel Solution	5 % Stacking Gel Solution
Acrylamide-Bis* (30:1.5)	8 ml	17.6 ml	2 ml
Glycerol	2.4 ml	4.8 ml	-
4X Buffer	12 ml	12 ml	3 ml
APS	6.6 %; 300 µl	6.6 %; 150 µl	0.28 %; 3 ml
TEMED	20 µl	20 µl	15 µl
Distilled H_2O to	48 ml	48 ml	12 ml

* Bis = N,N'-Methylene-bis-acrylamide

Table 3.5 Composition of 7.5 % Linear Gels

	7.5 % Separating Gel	5 % Stacking Gel
Acrylamide-Bis* (30:1.5)	12 ml	2 ml
Glycerol	3.3 ml	-
4X Buffer	12 ml	3 ml
APS	6.6 %; 300 µl	0.28 %; 3 ml
TEMED	20 µl	15 µl
Distilled H_2O to	48 ml	12 ml

* Bis = N,N'-Methylene-bis-acrylamide

Gradient gels were run at a constant current of 35 mA with variable voltage for 3-4 hours at 4 °C in a buffer containing 6.32 g/l Tris, 3.99 g/l glycine and 1 g/l SDS (buffer pH 8.9). Linear gels were run at 50 mA for 2-3 hours at room temperature.

3.6.6 Analysis of polyacrylamide gels

Gels containing proteins labelled with ^{35}S-methionine were fixed [10 % (v/v) acetic acid; 2 % (v/v) ethanol; 3 % (v/v) glycerol] overnight, treated for 15-30 minutes with Amplify (Amersham) for fluorographic enhancement of radioactive emissions, dried onto paper for 2 hours under vacuum at 80 °C and exposed to X-ray film in an autoradiography cassette at -70 °C. Quantification of protein bands was performed by phosphoimaging (Molecular Dynamics Corp.). Computer analysis of data was performed using Image Quant™ software.

3.6.7 Western Blotting

Polyacrylamide gels were soaked for 30 min in transfer buffer (25 mM Tris base, 192 mM glycine 2 % (v/v) methanol). Proteins were then electroblotted onto Hybond™ N membrane (Amersham International plc) using a Bio-Rad Trans-Blot™ device at 70 V for 3-4 hours. The membrane was then blocked with PBS containing 5 % milk powder for one hour at 37 °C. The membrane was probed with antibodies following suppliers recommendations. The blot was developed either using TMB stabilised substrate (Promega) dried and photographed, or using the ECL western blotting detection reagents (Amersham) and exposed to autoradiography film (Hyperfilm ECL, Amersham.).

3.7 Antibody Production

3.7.1 Inoculation procedure

The rabbit used for inoculation was obtained from a supplier (Harlan UK) who guaranteed that the animal was free from rotavirus infection. A pre-immune bleed was taken and tested to ensure no antibodies to rotavirus were present. The initial

inoculation was carried out subcutaneously with 1×10^7 pfu purified VR5 (Section 3.3.3) in 750 µl PBS. Bleeds were taken at intervals of 2 weeks after the initial inoculation and 10-20 ml of blood was usually obtained. Booster inoculations of an equivalent amount of virus were given at 13 weeks and 17 weeks after the initial inoculation and bleeds taken every two weeks as before. A final boost of 1×10^8 pfu of purified virus was given at 29 weeks after the initial inoculation and bleeds taken as before. All inoculations were performed with purified VR5 virus in PBS by subcutaneous route and the rabbit was housed in isolation at the University of Warwick after each inoculation.

3.7.2 Serum Collection

The blood was incubated overnight at 4 °C to allow the clot to form. The serum was then separated from the clot by centrifuging at 2000 rpm for 5 minutes at 4 °C. The blood clot was "ringed" using a pasteur pipette and the serum centrifuged again at 2000 rpm for 5 minutes at 4 °C. The serum supernatant was removed and stored in aliquots at -20 °C, or at -70 °C for long term storage.

3.7.3 Immunofluorescent labelling of infected cells

Confluent BS-C-1 cell monolayers on coverslips in 12-well dishes were infected at a m.o.i. of 0.1 (rotavirus) or 0.002 (VR5). At 16 hours post-infection the cells were washed four times in PBS and fixed with ice cold methanol on ice for 10 minutes. The solvent was removed and the fixed cells allowed to air dry. The cells were washed twice with PBS, then 50 µl of the primary antibody dilution was added to the coverslips and the plate incubated at 37 °C for 1 hour. After two washes with PBS, 50 µl of a 1/100 dilution of FITC conjugate goat anti-rabbit Ig was added to the coverslips and the plate incubated for 1 hour at 37 °C. The coverslips were washed twice with PBS, then placed cell side down onto a drop of 90 % glycerol and 10 % PBS on a glass microscope slide. Fluorescent staining was observed using a B-2H filter in a UV microscope (Nikon, Optiphot microscope). Photography was carried out using Ektachrome P1600 colour slide film (Kodak).

Results Chapter 1

Cloning of rotavirus genes

into yeast two-hybrid vectors

4.1 Aims

The overall objective of the project was to study protein-protein interactions between the rotavirus non-structural protein NSP1 and viral proteins found with it in pre-core complexes in the infected cell. The yeast two-hybrid system was chosen as one method of studying such protein-protein interactions. This chapter describes the strategies employed to generate fusion protein constructs between the rotavirus proteins found in pre-core complexes and both the GAL4 DNA-binding and activation domains for use in the yeast two-hybrid system.

4.2 Introduction

4.2.1 The yeast two-hybrid system

The yeast two-hybrid system is a genetic assay for detecting protein-protein interactions *in vivo* (Fields and Song, 1989). The system makes use of a eukaryotic transcriptional activator, classically the yeast GAL4 protein. This protein consists of two physically discrete domains, one governing DNA binding and the second carrying the transcriptional activation function (Keegan *et al.*, 1986), (Ma and Ptashne, 1987). To set up the assay, one of the two potentially interacting proteins is fused to the DNA-binding domain and the other to the activation domain. If there is an interaction between the two proteins under analysis, then it will bring the two GAL4 domains close together and result in the restoration of the transcriptional activation function (Ma and Ptashne, 1988), (Brent and Ptashne, 1985). Experimentally the two hybrid proteins are co-transformed into a yeast host strain and the activation of expression of a reporter gene, under the control of a GAL4 regulated promoter, is measured. The reporter gene used in this study was *lacZ*, and detection of β-galactosidase was an indication that the two proteins under study were interacting. The two-hybrid system has several advantages over more conventional biochemical methods. It is a sensitive method for the detection of weak and transient interactions that probably occur in complexes within an infected cell. Also, it is not dependent on the monospecific antibodies normally required for *in vitro* based methods of detecting protein-protein interactions. As the assay is performed *in vivo* the proteins are more likely to be in their native conformations. However, although the yeast two-hybrid assay has advantages over a bacterial expression system, it is still unlikely to represent the exact

conditions found in a mammalian cell. Further, as the proteins of interest are expressed as carboxy-terminal fusions of the GAL4 proteins in some cases this might adversely affect their normal folding and conformation, and also prevent detection of any interactions that require a free amino terminus of the protein.

4.2.2 Use of the two-hybrid system to test for rotavirus protein-protein interactions

The yeast two-hybrid assay has already been used successfully to study protein-protein interactions in viral systems (Luban *et al.*, 1992), (Takacs *et al.*, 1993), (Takacs and Banerjee, 1995), and in this project it was used for the study of rotavirus protein-protein interactions. NSP1 has been shown to be present, with other viral proteins and viral mRNA, in a pre-core replication intermediate (RI) in the infected cell (Patton, 1995). NSP1 could potentially interact with any member of this complex, however these interactions within the complex may be of a weak or transient nature, so a sensitive assay which could detect such interactions was required. The pre-core RI contains NSP1, NSP3 and the viral structural proteins VP1 and VP3. VP2 is then added to this complex to produce the core RI. It was therefore decided that the two-hybrid system should be used to test for interactions between NSP1 and the individual viral proteins VP1, VP2, VP3 and NSP3. The assay was also used to test for a potential dimerisation of NSP1. This two-hybrid assay would only detect a direct protein-protein interaction between NSP1 and a given protein, so therefore a potential interaction between NSP1 and a preformed complex of more than one protein would not be detected. Similarly, as viral mRNA cannot be added to the assay, if NSP1 interacted with a complex of proteins and RNA, or if it interacted directly with RNA, then these interactions would also not be detected by the two-hybrid assay.

The genes encoding all the required rotavirus proteins from the UKtc strain of bovine rotavirus had previously been cloned in the Rotavirus laboratory.

4.2.3 Cloning vectors for the production of GAL4 fusion proteins

The Matchmaker Yeast Two-Hybrid System (Clontech) was used to test for protein-protein interactions. In this system, sequences encoding the two functional

domains of the GAL4 transcriptional activator have been cloned into two different shuttle/expression vectors. The vector pGBT9 contains the sequences encoding the GAL4 DNA-binding domain, and pGAD424 contains the sequences encoding the GAL4 transcriptional activation domain (Bartel *et al.*, 1993) (Figure 4.1). Plasmid pGBT9 is therefore used to generate a fusion of the GAL4 DNA-binding domain with the target protein, while pGAD424 generates a fusion of the GAL4 activation domain with a candidate interacting protein. Plasmid pGBT9 carries the TRP1 nutritional gene which allows selection of transformant yeast colonies on limiting media lacking the amino acid tryptophan. Plasmid pGAD424 carries the LEU2 nutritional gene which allows selection on limiting media lacking the amino acid leucine. Transformant colonies carrying both pGBT9 and pGAD424 can be selected on double dropout media lacking both tryptophan and leucine. Both plasmids contain sequences encoding nuclear localisation signals, so that both hybrid proteins are targeted to the yeast nucleus. In pGAD424 the nuclear localisation sequence from SV40 T-antigen has been cloned into the vector between the ADH1 promoter and the GAL4 activation domain sequence (Chien *et al.*, 1991), whereas in pGBT9 it is an intrinsic part of the GAL4 DNA-binding domain (Silver *et al.*, 1984).

4.2.4 Production of fusion proteins

To study protein-protein interactions in the two-hybrid system, the rotavirus proteins must be expressed as fusion proteins with the GAL4 domains. In order to ensure correct expression of the fusion proteins, the gene encoding the protein of interest must be ligated into the multiple cloning site (MCS) of the vector such that the orientation is correct with respect to the GAL4 sequence. In addition, the reading frame must be preserved such that the GAL4 domain and the protein of interest are expressed contiguously to produce a fusion protein.

A further consideration was to ensure the sequences of the cloned genes were accurate so that genuine rotavirus proteins would be expressed. To ensure the fidelity of the PCR reactions, a thermostable DNA polymerase *Pfu* with 3' exonuclease, or "proof-reading", activity was used throughout. The 3' to 5' exonuclease activity of *Pfu* DNA polymerase can remove an incorrectly inserted base before continuing with the reaction. Thus, *Pfu* DNA polymerase has a 12-fold increase in fidelity of DNA synthesis over *Taq* DNA polymerase (Stratagene), and is recommended for high

Figure 4.1 Schematic diagrams of the Yeast Two-Hybrid System cloning vectors, pGBT9 and pGAD424, showing the MCS sequence and unique restriction sites

Schematic diagrams of the main features of plasmid pGBT9 (panel A) and pGAD424 (panel B) are shown. pGBT9 generates a hybrid that contains the sequences for the GAL4 binding domain (amino acids 1-147) (GAL4 bd). pGAD424 generates a hybrid that contains the sequences for the GAL4 activation domain (amino acids 768-881) (GAL4 ad). The plasmids have unique restriction sites located in the MCS region at the 3' end of the open reading frame for either the DNA-binding or activation domain sequences. The gene encoding the protein of interest is ligated into the MCS in the correct orientation and with the correct reading frame, such that fusion proteins with the GAL4 domains are expressed. The sequence and reading frame of the MCS for pGBT9 and pGAD424 are shown in the boxes below the appropriate plasmid diagrams. The unique restriction sites in the MCS of each plasmid, which can be used for cloning purposes, are indicated. Fusion proteins are expressed from the constitutive ADH1 promoter (^{P}ADH1) and transcription is terminated at the ADH1 transcription termination signal (^{T}ADH1). The fusion proteins are targeted to the yeast nucleus by nuclear localisation sequences (▲). pGBT9 and pGAD424 plasmids replicate autonomously in both *E. coli* and *S. cerevisiae*. The selectable markers carried are the *bla* gene which confers resistance to ampicillin in *E. coli* (Amp^{R}), and a nutritional gene that allows yeast auxotrophs to grow on limiting synthetic media (TRP1 in pGBT9; LEU2 in pGAD424). This figure is adapted from the Clontech Matchmaker Two-Hybrid system protocol.

Figure 4.1

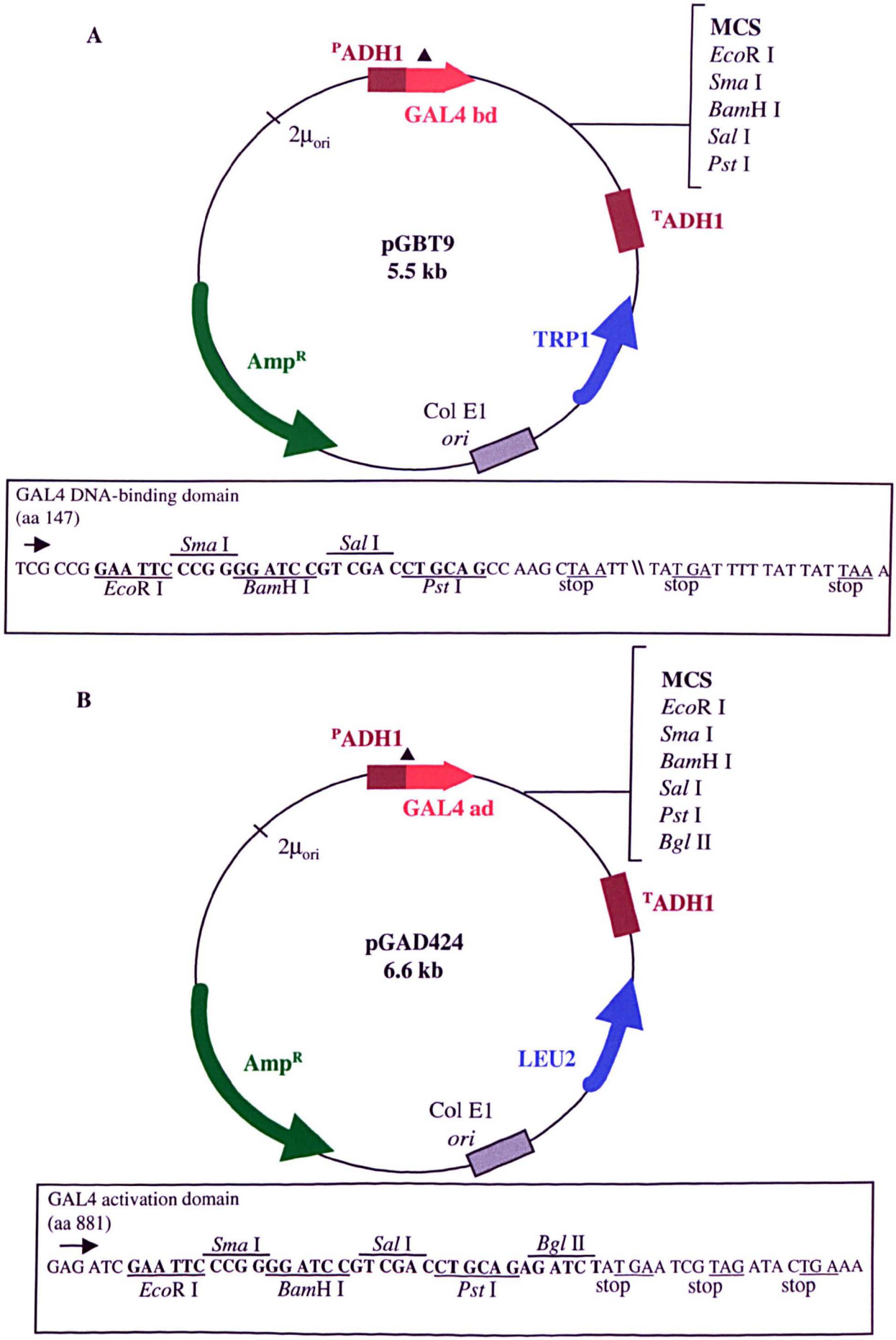
A
MCS
EcoR I
Sma I
BamH I
Sal I
Pst I
PADH1
GAL4 bd
2μori
TADH1
pGBT9
5.5 kb
TRP1
AmpR
Col E1
ori
GAL4 DNA-binding domain
(aa 147)
Sma I
Sal I
TCG CCG GAA TTC CCG GGG ATC CGT CGA CCT GCA GCC AAG CTA ATT \\ TAT GAT TTT TAT TAT TAA A
EcoR I
BamH I
Pst I
stop
stop
stop
B
MCS
EcoR I
Sma I
BamH I
Sal I
Pst I
Bgl II
PADH1
GAL4 ad
2μori
TADH1
pGAD424
6.6 kb
LEU2
AmpR
Col E1
ori
GAL4 activation domain
(aa 881)
Sma I
Sal I
Bgl II
GAG ATC GAA TTC CCG GGG ATC CGT CGA CCT GCA GAG ATC TAT GAA TCG TAG ATA CTG AAA
EcoR I
BamH I
Pst I
stop
stop
stop

fidelity and long PCR reactions. Sequencing was used to verify the junction regions and 5'-ends of each cloned rotavirus gene. In addition, genes cloned into TA vectors were expressed *in vitro* and full-length proteins were produced in each case (Section 4.4).

Attachment of the GAL4 domains to the proteins of interest can cause complications when the fusion proteins are expressed and tested in the two-hybrid system. In some cases an interaction may be observed if a protein of interest is fused to one GAL4 domain but not if it is fused to the other domain (Estojak *et al.*, 1995). Thus, if possible, each protein of interest should be tested as fusions with both GAL4 domains. A second possible complication arises if a protein of interest has intrinsic transcriptional activation properties and thus may activate transcription when fused to the GAL4 DNA-binding domain. This problem may produce a false positive result in the two-hybrid assay, but can be avoided by fusing the protein of interest to the GAL4 activation domain. The rotavirus genes encoding the proteins of interest were cloned into both two-hybrid vectors so that fusions of each protein with both GAL4 domains were generated.

4.3 Production of constructs to express NSP1-GAL4 domain fusion proteins

4.3.1 Strategy for production of NSP1-GAL4 domain fusion proteins

A cDNA of gene 5, which encodes NSP1, from the UKtc strain of bovine rotavirus, was used to produce NSP1-GAL4 domain fusion proteins by sub-cloning the gene 5 sequence into pGBT9 and pGAD424 (Figure 4.2). Fusions of NSP1 with both the DNA-binding and the transcriptional activation domains were produced. The most important considerations in the production of the fusion proteins were that gene 5 was ligated into the MCS of the vectors in the correct orientation with respect to the GAL4 domain sequence, and that the reading frame was maintained. The orientation of the gene was ensured by using a forced cloning procedure, whereby the gene was ligated into the MCS using different restriction sites at the 5' end and 3' end. To allow this, gene 5 sequences were amplified by PCR using specially designed primers to introduce specific restriction sites at the termini of the amplified sequences of the gene 5 cDNA. The introduced restriction sites could then be used for cloning the gene into both vectors. The sites were positioned such that, after ligation, the reading frame

Figure 4.2 Cloning strategy for construction of fusion proteins of NSP1 with the GAL4 DNA-binding and activation domain proteins

Gene 5 of the UKtc strain of bovine rotavirus, which encodes NSP1, was amplified by PCR with primers Gene 5/5' and Rotgen 5/3' (Table 3.3) (Section 3.4.1). Gene 5/5' was designed such that additional DNA sequence, including an *Eco*R I site, was added to the 5' end of the amplified DNA fragment. The addition of the *Eco*R I site allowed gene 5 to be cloned, in frame, into the MCS of either pGBT9 or pGAD424. Rotgen 5/3' added additional DNA sequence, including a *Pst* I site, to the 3' end of the amplified DNA fragment, which was used for cloning gene 5 into the MCS of either pGBT9 or pGAD424. The gene 5 PCR product was digested with *Eco*R I and *Pst* I (Section 3.4.6) and ligated into pGBT9 and pGAD424 that had also been digested with *Eco*R I and *Pst* I (Section 3.4.10). The framing of the junction region, between the GAL4 domain and gene 5, is shown.

Figure 4.2

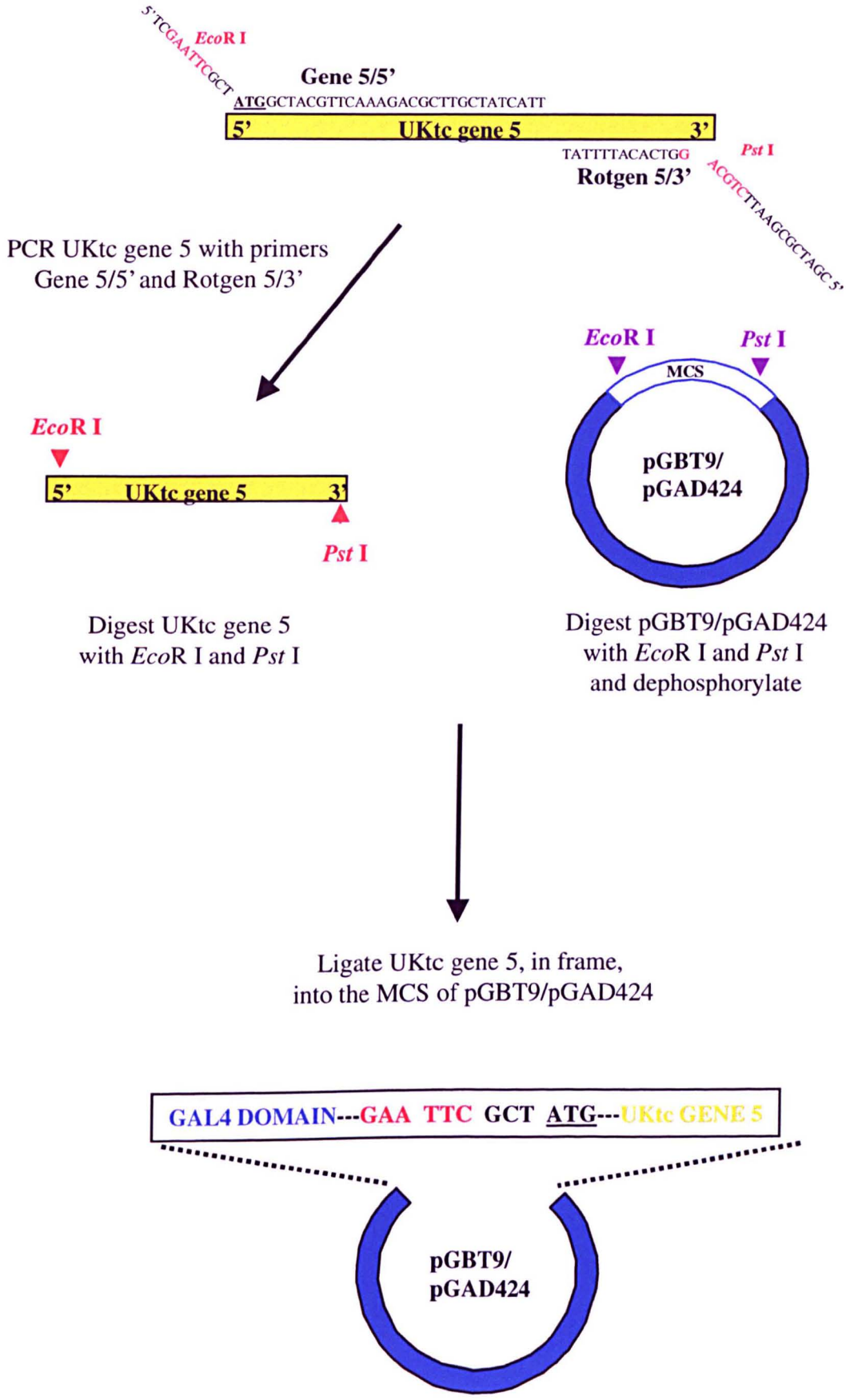
5'TCGAATTCGCT
EcoR I
Gene 5/5'
ATGGCTACGTTCAAAGACGCTTGCTATCATT
5'
UKtc gene 5
3'
TATTTTACACTGG
Rotgen 5/3'
Pst I
ACGTCTTAAGCGGCTAGC 5'
PCR UKtc gene 5 with primers
Gene 5/5' and Rotgen 5/3'
EcoR I
Pst I
MCS
pGBT9/
pGAD424
EcoR I
5'
UKtc gene 5
3'
Pst I
Digest UKtc gene 5
with EcoR I and Pst I
Digest pGBT9/pGAD424
with EcoR I and Pst I
and dephosphorylate
Ligate UKtc gene 5, in frame,
into the MCS of pGBT9/pGAD424
GAL4 DOMAIN---GAA TTC GCT ATG---UKtc GENE 5
pGBT9/
pGAD424

of the GAL4 domain sequence was maintained and thus a fusion protein would be expressed. Following isolation of the fusion constructs, the junction region between the GAL4 domain and gene 5 was sequenced to ensure that the reading frame was correct. In each case, approximately 200-300 bp at the 5' end of each rotavirus gene was also checked against the original sequence data to ensure accuracy. The ligation of gene 5 into both pGBT9 and pGAD424 allowed the hypothesis that NSP1 interacts with itself to form dimers to be tested. It also provided for the possibility, discussed in Section 4.2.4, that one of the rotavirus proteins to be tested might have intrinsic transcriptional activating properties thus forcing the use of a particular vector.

4.3.2 Cloning of gene 5 into the GAL4 DNA-binding domain vector pGBT9 to generate construct pGBT9-Gene 5

Gene 5 of the UKtc strain of bovine rotavirus was amplified by PCR using primers Gene 5/5' and Rotgen 5/3' (Figure 4.3). A band on the gel corresponding to gene 5 (1579 bp) can be clearly seen. The larger band at approximately 5000 bp in the G5 lane was not identified. The gene 5 band was gel purified prior to cloning to avoid contamination with this larger PCR product. The Gene 5/5' primer was designed to introduce an *Eco*R I restriction enzyme site to the 5' end of the gene, immediately prior to the ATG start site. *Eco*R I was chosen because it was also present in the MCS of the yeast two-hybrid vectors, thus it could be utilised for cloning purposes. The framing of the *Eco*R I site in relation to the ATG of gene 5 and the ORF of the GAL4 domain was designed to maintain the reading frame when gene 5 was cloned into the vector, resulting in the production of a fusion protein of the GAL4 domain and the gene 5 product NSP1. The vector pGBT9, which contains sequence encoding the GAL4 DNA-binding domain, was digested with *Eco*R I and *Pst* I and dephosphorylated with calf intestinal alkaline phosphatase (CIP) to reduce recircularisation of the vector. The amplified DNA fragment, which had been similarly digested with *Eco*R I (5' end) and *Pst* I (3' end), was ligated into the prepared vector pGBT9 to generate a pGBT9-Gene 5 construct. Recombinant clones were screened by double-digestion with *Eco*R I and *Pst* I which released the gene 5 insert. Two clones containing gene 5 inserts were identified: G5(7) and G5(10) (Figure 4.4). Further restriction enzyme digestions with *Xho* I and *Xba* I were performed to confirm the positive orientation of the gene 5 insert with respect to the

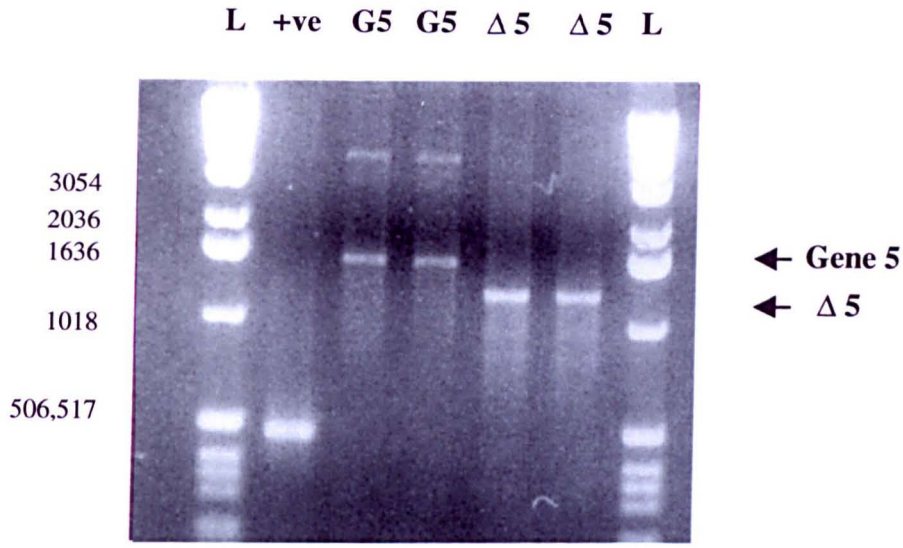

Figure 4.3 Amplification of the UKtc strain of bovine rotavirus gene 5 from plasmid G5T7(TA), and gene Δ5 from plasmid p9DΔ5, with primer pair Gene 5/5' and Rotgen 5/3'

5 µl of the PCR products amplified using primers Gene 5/5' and Rotgen 5/3' (Table 3.3) were analysed by electrophoresis on a 1.5 % TAE agarose gel (Section 3.4.3). The predicted size of the gene 5 DNA fragment (G5) is 1579 bp, and the predicted size of the gene Δ5 fragment is 1271 bp. +ve refers to the positive control for the PCR reaction which is adenovirus DNA of approximately 500 bp. Lanes marked L were loaded with 1 Kb DNA ladder. The sizes of the markers are given in base pairs.

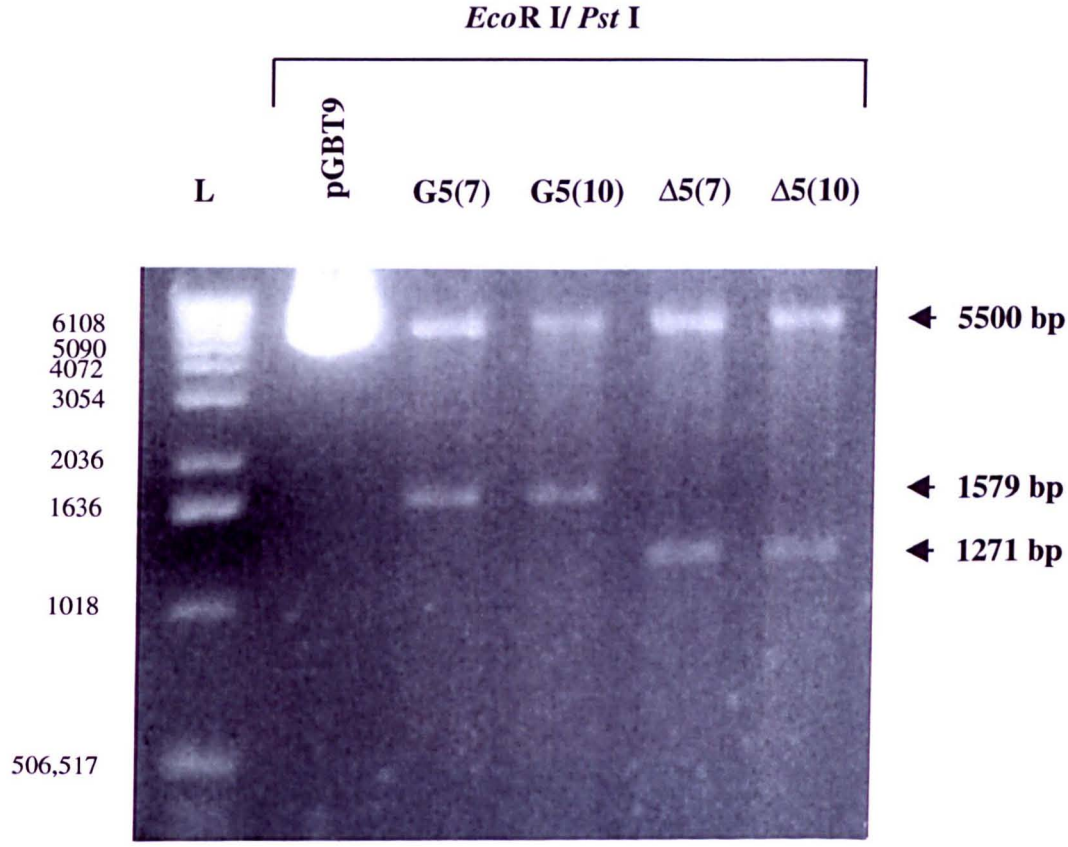

Figure 4.4 Identification of recombinant clones pGBT9-gene 5 and pGBT9-gene Δ5 by restriction enzyme digestion

Plasmid DNA from 20 independent clones, created following the ligation reactions between pGBT9 and either PCR amplified gene 5 or gene Δ5, was prepared by mini-prep (Section 3.4.13) and double-digested with *Eco*R I and *Pst* I (Section 3.4.6). The products were analysed by electrophoresis on a 1.5 % TAE agarose gel (Section 3.4.3). Double-digestion of pGBT9 with *Eco*R I and *Pst* I resulted in linearisation of the plasmid and a band at 5500 bp. Gene 5 inserted into PGBT9 was released by double digestion with *Eco*R I and *Pst* I resulting in bands at 5500 bp and 1579 bp. Two clones of pGBT9-gene 5 were identified [G5(7); G5(10)]. Gene Δ5 inserted into pGBT9 was released by double digestion with *Eco*R I and *Pst* I resulting in bands at 5500 bp and 1271 bp. Two clones of pGBT9-gene Δ5 were identified [Δ5(7); Δ5(10)]. Lanes marked L were loaded with 1 Kb DNA ladder. The sizes of the markers are given in base pairs.

GAL4 domain sequence in pGBT9 in both clones (Figure 4.5). The junction region between the GAL4 domain sequence and gene 5 was also sequenced. Initially, sequencing of both G5(7) and G5(10) revealed that additional sequence (68 bp) had been incorporated into the construct at the 5' end of gene 5 (Figure 4.6A). The presence of this additional 68 bp of sequence resulted in the ATG start site of gene 5 being out-of-frame with respect to the GAL4 domain sequence in pGBT9 hence the desired fusion protein would not be produced. As the additional sequence was short (68 bp) and did not disrupt the restriction sites, it was not observed during electrophoretic examination of the clones (Figures 4.4 and 4.5), and was only discovered by sequencing. The additional sequence corresponded to the T7 vector, primer and leader sequence of gene 5 from plasmid G5T7(TA) from which gene 5 was amplified. It was thought that the presence of this sequence was due to incorrect priming during the PCR reaction. The sequence was excised by restriction enzyme digestion with *Nco* I and *Eco*R I, which cut at unique sites either side of it, and the free ends were blunt-ended and religated (Figure 4.6B). The correct clones were identified by digestion with a restriction enzyme (*Acc* I) which had lost a site during the procedure so that different sized bands were now produced. Sixteen new clones were identified (Figure 4.6B), and clones G5(1) and G5(5) were sequenced. The procedure resulted in the correct junction region and the establishment of a contiguous reading frame between the GAL4 domain sequence and gene 5 (Figure 4.6C). In addition, approximately 300 bp at the 5' end of gene 5 was compared with the original sequence data, and it was verified that the sequence was accurate.

4.3.3 Cloning of a mutant gene 5 (gene Δ5) into the DNA-binding domain vector pGBT9 to generate construct pGBT9-Δ5

A truncated variant of gene 5, p9Δ5, has been described (Tian *et al.*, 1993). This gene 5 (Δ5) variant has a single 308 bp deletion, between nucleotides 460 and 768, in the centre of the wild-type gene 5 sequence. This deletion causes a frameshift in the gene, introducing a stop codon, so that a truncated protein consisting only of the amino-terminal third of the protein is produced. This variant was studied in addition to the full-length protein, as it contains the conserved regions of NSP1 which are thought to be the functional domains (Xu *et al.*, 1994).

Figure 4.5 Confirmation of correct cloning and orientation of the UKtc strain of bovine rotavirus gene 5 and gene Δ5 in pGBT9

Clones suspected to contain gene 5 or gene Δ5 ligated into the MCS of pGBT9 were analysed by restriction enzyme double-digest with *Xho* I and *Xba* I to confirm the orientation of the insert. The products were analysed by electrophoresis on a 1.5 % TAE agarose gel (Section 3.4.3) (Panel A). The lane marked pGBT9 is the vector only, digested with the enzymes indicated. The lanes marked G5(7) and G5(10) are specific clones of pGBT9-gene 5, digested with the enzymes indicated. The lanes marked Δ5(7) and Δ5(10) are specific clones of pGBT9-gene Δ5, digested with the enzymes indicated. Lanes marked L were loaded with 1 Kb DNA ladder. The sizes of the markers are given in base pairs. The predicted sizes of the fragments obtained with each digest are shown below.

Plasmid	**Restriction enzyme digest**	**Predicted fragment sizes (bp) correct orientation**
pGBT9	*Xho* I / *Xba* I	4404 + 1096
pGBT9-Gene 5	*Xho* I / *Xba* I	4430, 1449 + 1200
pGBT9-Δ5	*Xho* I / *Xba* I	4430, 1209 + 1132

Panel B is a schematic diagram to show cloning of gene 5 (1579 bp) and gene Δ5 (1271 bp) into pGBT9 (5500 bp). The *Eco*R I site (879 bp) and the *Pst* I site (905 bp) in the MCS of pGBT9 were used for cloning purposes. The positions of the other restriction enzyme sites in pGBT9 and gene 5 /gene Δ5 which were used for analysis are indicated.

Figure 4.5

A

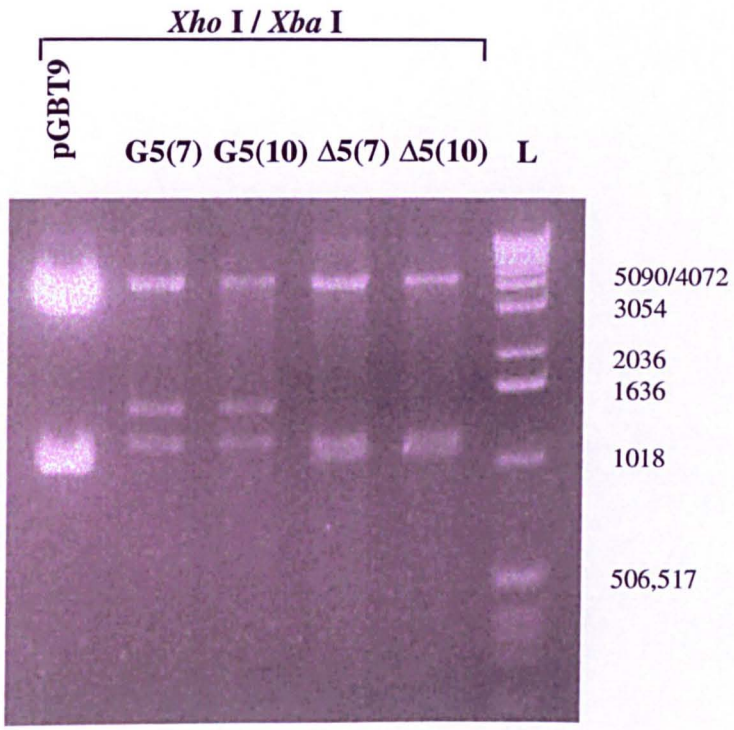
Xho I / Xba I
pGBT9
G5(7) G5(10) Δ5(7) Δ5(10) L
5090/4072
3054
2036
1636
1018
506,517

B

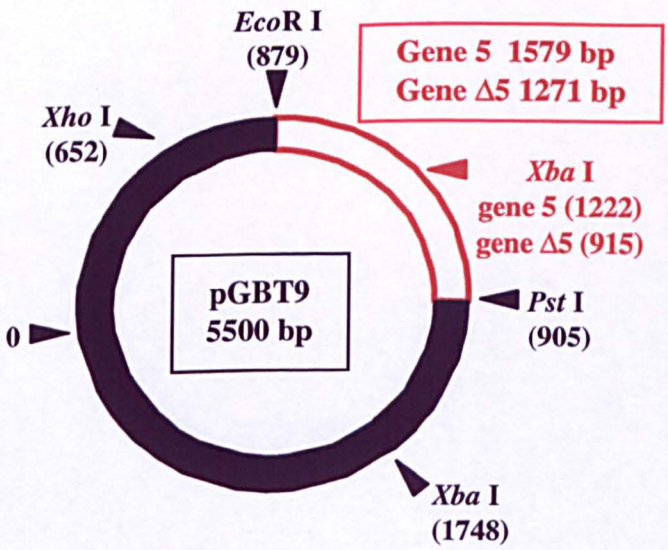
EcoR I
(879)
Gene 5 1579 bp
Gene Δ5 1271 bp
Xho I
(652)
Xba I
gene 5 (1222)
gene Δ5 (915)
pGBT9
5500 bp
Pst I
(905)
0
Xba I
(1748)

Figure 4.6 Sequence analysis of the junction region of clone pGBT9-gene 5

A. Sequence analysis of clone pGBT9-gene 5 [G5(7)] showing additional sequence at the junction region resulting in an out-of-frame ATG site

Clone pGBT9-Gene 5 [G5(7)] DNA was amplified and purified by maxi-prep (Section 3.4.14) and sequenced using Primer 1 (Table 3.3) which recognizes sequence 31 bp upstream of the MCS start site in pGBT9 (Figure 4.1). Sequence analysis (Section 3.4.18) was performed to confirm the orientation and framing of gene 5 at the junction between the GAL4 domain sequence in pGBT9 and gene 5. The analysis revealed that additional sequence had been incorporated into the junction region between pGBT9 and gene 5. As a result the ATG site of gene 5 was out-of-frame with respect to the pGBT9 sequence.

B. Cloning strategy to remove additional sequence and restore reading frame, and identification of new clones pGBT9-gene 5

The presence of unique restriction sites *Eco*R I and *Nco* I at the junction region allowed the additional unwanted sequence to be precisely excised. The plasmid DNA was digested with *Eco*R I and *Nco* I and gel purified to remove the excised sequence. Following treatment with the Klenow fragment of *E. coli* DNA polymerase I to produce blunt ends (Section 3.4.8), the ends of the plasmid were re-ligated (Section 3.4.10).

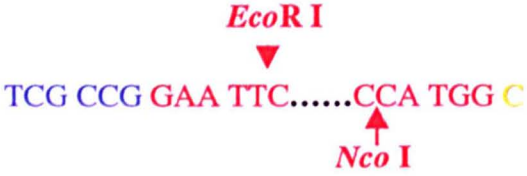

Plasmid DNA from 21 independent clones was prepared by mini-prep (Section 3.4.13), and positive clones were identified by restriction enzyme digest analysis with *Acc* I. The products were analysed by electrophoresis on a 1.5 % TAE agarose gel (Section 3.4.3). An *Acc* I site was destroyed during the procedure to remove the extra sequence, so digestion of the new clones with this enzyme produced a different pattern of bands to the original clone:

pGBT9-gene 5 [G5(7)]	3800, 900, 860, 670, 500, 280 bp
pGBT9-gene 5 new clones	3800, 1500, 900, 500,280 bp

Lanes marked L were loaded with 1 Kb ladder. The sizes of the markers are given in base pairs.

C. Sequence analysis of clone pGBT9-gene 5 [G5(1)new]

Clone pGBT9-gene 5 [G5(1)new] DNA was amplified and purified by maxi-prep (Section 3.4.14) and sequenced using Primer 1 as before. Sequence analysis (Section 3.4.18) was performed to confirm that the additional sequence had been successfully removed, and that the orientation and framing of gene 5 at the junction between the GAL4 domain sequence in pGBT9 and gene 5 was now correct (Figure 4.2). Approximately 300 bp of sequence at the 5' end of gene 5 was also checked. Sequence analysis was repeated twice.

Figure 4.6

A.

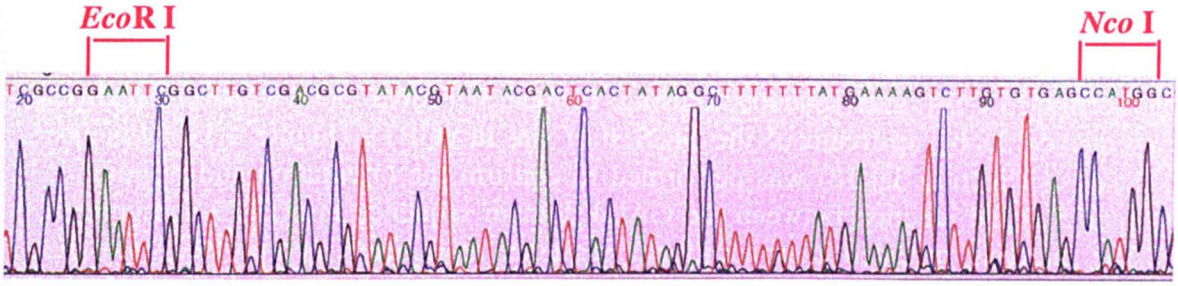

GAL4 DNA-binding domain *Eco*R I **T7 vector** **5G5T7 primer**

TCG CCG GAA TTC GGC TTG TCG ACG CGT ATA CGT AAT ACG ACT CAC TAT AGG

CTT TTT TTA TGA AAA GTC TTG TGT GAG CCA TGG C **UKtc gene 5**

Gene 5 leader sequence **CCATGG** ***Nco* I**

B.

C.

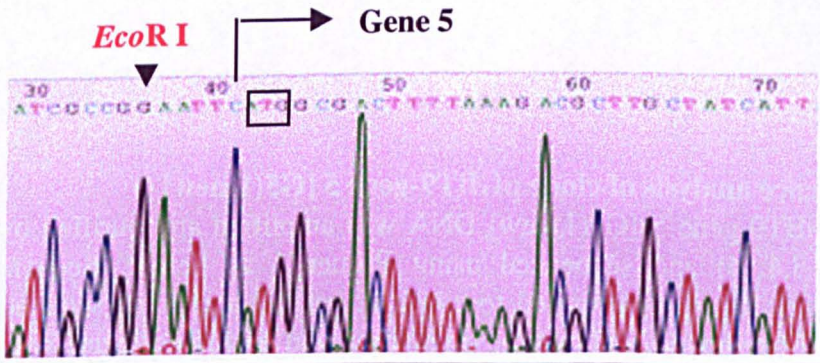

GAL4 DNA-binding domain *Eco*R I **UKtc gene 5**

TCG CCG GAA TTC ATG GCG ACT TTT AAA GAC GCT TGC TAT CAT TAC

Gene Δ5 was amplified from plasmid p9Δ5 by PCR using primers Gene 5/5' and Rotgen 5/3' (Figure 4.3) as described previously (Section 4.3.1). The primers which were used for the full length gene 5 could also be used for p9Δ5 as the deletion is in the centre of the gene while the 5' and 3' ends are conserved. The vector pGBT9 was digested with *Eco*R I and *Pst* I and dephosphorylated with CIP. The amplified DNA was digested with *Eco*R I and *Pst* I and ligated into the prepared vector pGBT9 to generate a pGBT9-gene Δ5 construct. Recombinant clones were screened by double-digestion with *Eco*R I and *Pst* I which released the gene Δ5 insert. Two clones containing gene 5 inserts were identified: Δ5(7) and Δ5(10) (Figure 4.4). Further restriction enzyme digestions with *Xho* I and *Xba* I were performed to confirm the positive orientation of the gene Δ5 insert with respect to the GAL4 domain sequence in pGBT9 in both clones (Figure 4.5). The junction region of Δ5(10) was sequenced, and it was confirmed that the reading frame between the GAL4 domain sequence and gene Δ5 was maintained, ensuring the production of the desired fusion protein (Figure 4.7). In addition, approximately 250 bp at the 5' end of gene Δ5 was compared with the original sequence data, and it was verified that the sequence was accurate.

4.3.4 Cloning of gene 5 into the activation domain vector pGAD424 to generate construct pGAD424-Gene 5

A cDNA of gene 5 from the UKtc strain of bovine rotavirus was amplified by PCR using primers Gene 5/5' and Rotgen 5/3' (Figure 4.3) as described previously (Section 4.3.1). The vector pGAD424, which contains sequence encoding the GAL4 activation domain, was digested with *Eco*R I and *Pst* I and dephosphorylated with CIP. The amplified DNA was digested with *Eco*R I and *Pst* I, and ligated into the prepared vector pGAD424 to generate construct pGAD424-gene 5. Two recombinant clones were identified by restriction enzyme digestion with *Eco*R I and *Pst* I which released the gene 5 insert: pGAD424-gene5(15) and pGAD424-gene5(18) (Figure 4.8, Panel A). Further restriction enzyme digestion with *Hind* III was performed to confirm the orientation of the insert in pGAD424. Bands at 5900 bp and 2250 bp were produced, confirming the correct orientation of the gene 5 insert with respect to the GAL4 domain sequence in pGAD424-gene5(15) (Figure 4.8, Panel B). The junction region of pGAD424-gene5(15) was sequenced to confirm that the reading frame

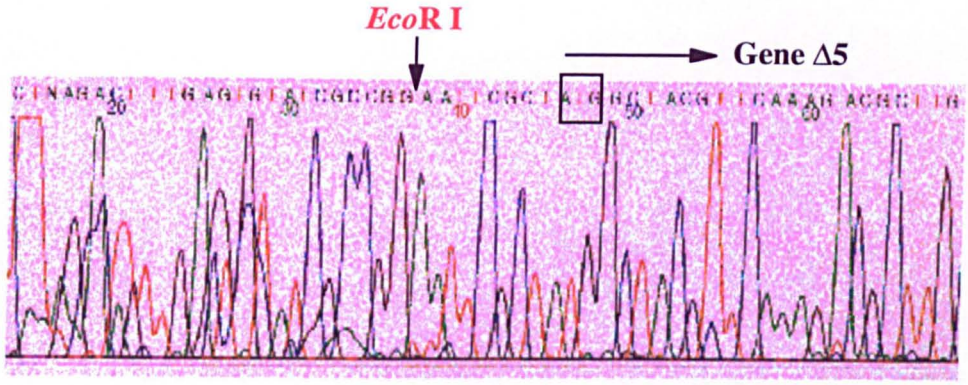

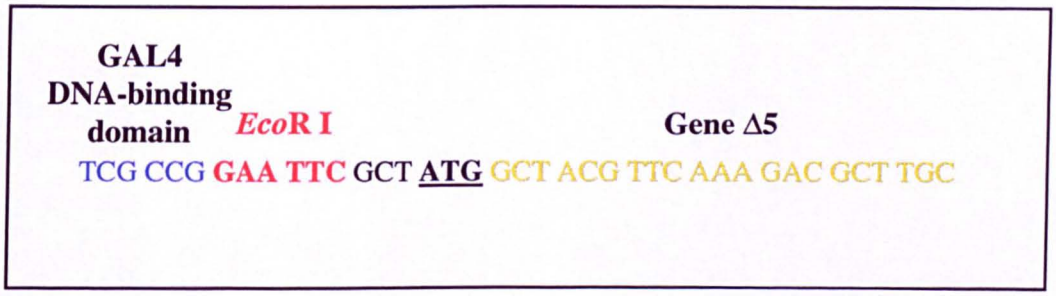

Figure 4.7 Sequence analysis of the junction region of clone pGBT9-gene Δ5

Clone pGBT9-Δ5(10) DNA was amplified and purified by maxi-prep (Section 3.4.14) and sequenced using Primer 1 (Table 3.3) which recognizes sequence 31 bp upstream of the MCS start site in pGBT9 (Figure 4.1). Sequence analysis (Section 3.4.18) was performed to confirm the orientation of gene Δ5, and the framing at the junction between the GAL4 domain sequence in pGBT9 and gene Δ5. The *Eco*R I site preceding the ATG site of gene Δ5 was introduced by PCR and allowed the gene to be cloned, in frame, into pGBT9. The sequence analysis revealed that the reading frame was maintained (Figure 4.2). Approximately 250 bp at the 5' end of gene Δ5 was compared with the original sequence data, and it was verified that the sequence was accurate. Sequence analysis was repeated twice.

Figure 4.8 Identification of recombinant clones pGAD424-gene 5 by restriction enzyme digestion analysis

Panel A. Plasmid DNA from 20 independent clones, created following the ligation reaction between pGAD424 and PCR amplified gene 5, was prepared by mini-prep (Section 3.4.13) and double-digested with *Eco*R I and *Pst* I (Section 3.4.6). The products were analysed by electrophoresis on a 1.5 % TAE agarose gel (Section 3.4.3) (lanes 1-20). Double-digestion of pGAD424 with *Eco*R I and *Pst* I resulted in linearisation of the plasmid and a band at 6600 bp. Gene 5 inserted into pGAD424 was released by double digestion with *Eco*R I and *Pst* I resulting in bands at 6600 bp and 1579 bp. The arrow indicates the band at 1579 bp in lanes 15 and 18.

Panel B. Clones 15 and 18 (as indicated in Panel A) were digested with *Eco*R I/*Pst* I and *Hind* III (Section 3.4.6) and analysed by electrophoresis on a 1.5 % TAE agarose gel (Section 3.4.3). Digestion of pGAD424 with *Hind* III resulted in bands at 5900 bp and 695 bp. Digestion of clone G5(15) with *Hind* III resulted in bands at 5900 bp and 2250 bp. Lanes marked L were loaded with 1 Kb DNA ladder. The sizes of the markers are given in base pairs.

The schematic diagram (see below) shows the restriction enzyme sites *Eco*R I and *Pst* I in the MCS of pGAD424 which were used for cloning of gene 5. The position of the *Hind* III sites in pGAD424 which were used for analysis are also shown.

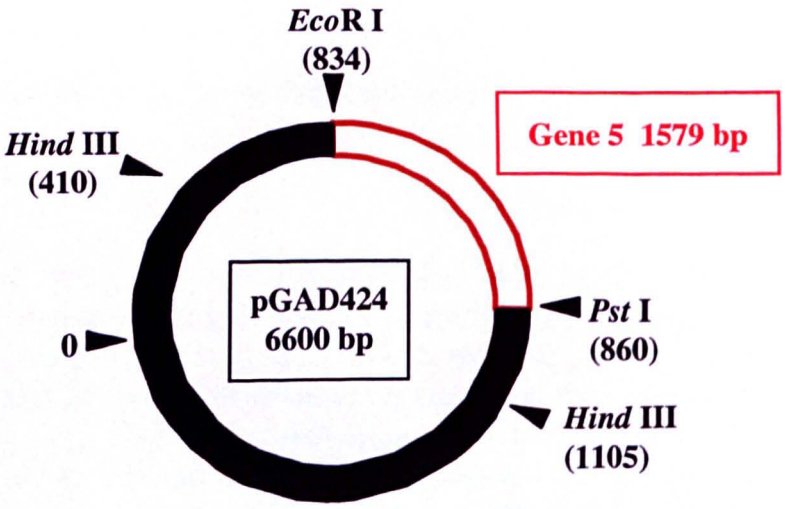

Figure 4.8

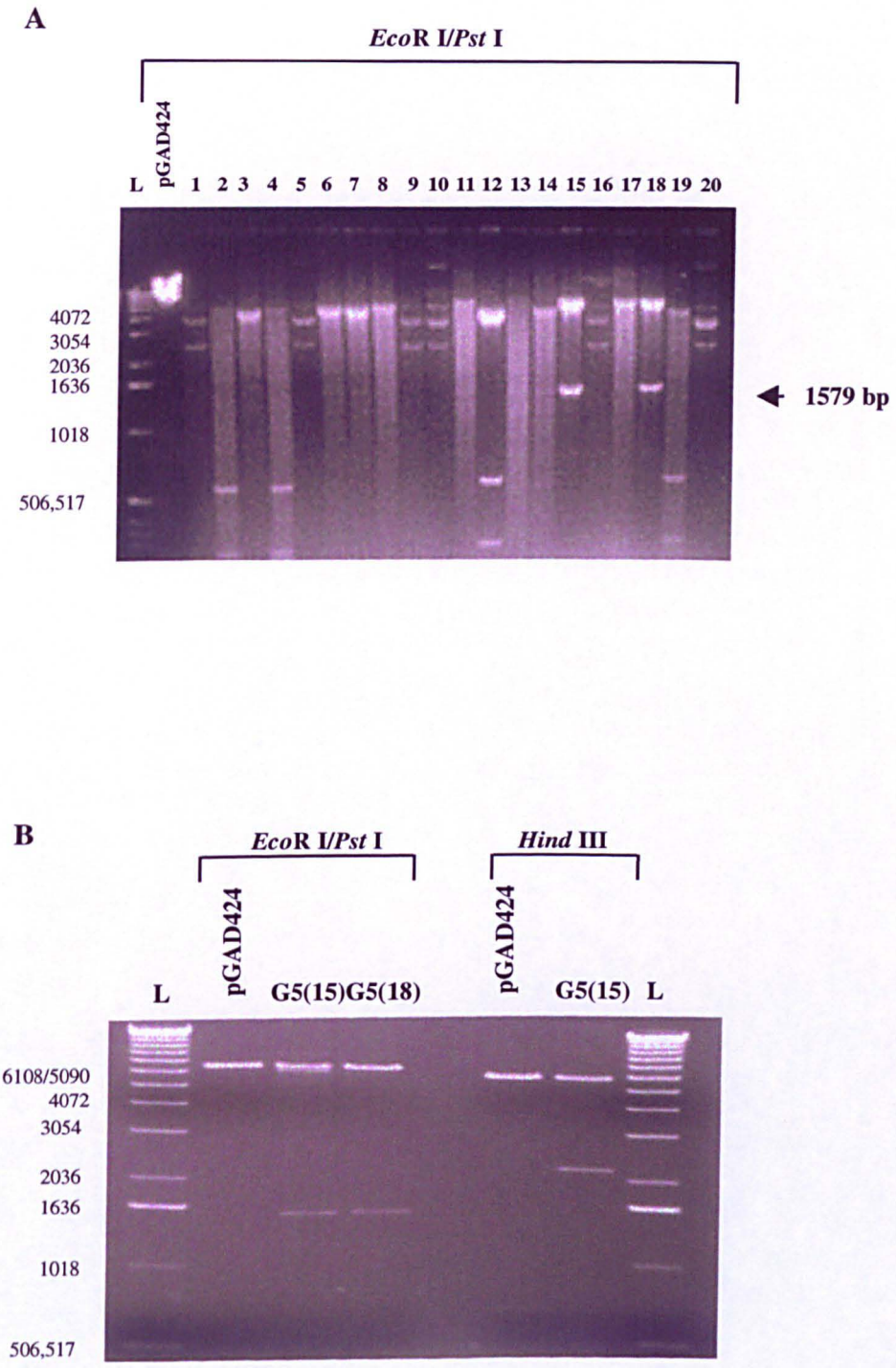
A
EcoR I/Pst I
L
pGAD424
1 2 3 4 5 6 7 8 9 10 11 12 13 14 15 16 17 18 19 20
4072
3054
2036
1636
1018
506,517
1579 bp
B
EcoR I/Pst I
Hind III
L
pGAD424
G5(15)G5(18)
pGAD424
G5(15)
L
6108/5090
4072
3054
2036
1636
1018
506,517

between the GAL4 domain sequence and gene 5 was maintained, ensuring the production of the desired fusion protein (Figure 4.9). In addition, approximately 250 bp at the 5' end of gene 5 was compared with the original sequence data, and it was verified that the sequence was accurate.

4.4 Production of constructs to express viral core proteins as GAL4 domain fusion proteins

4.4.1 Strategy for production of GAL4 domain fusion proteins with viral core proteins VP1, VP2 and VP3

The genes encoding the viral core proteins VP1 (gene 1), VP2 (gene 2) and VP3 (gene 3), were cloned into the vectors pGBT9 and pGAD424 in order to produce GAL4 domain fusion proteins. Fusions of each protein with both the GAL4 DNA-binding domain and the GAL4 transcriptional activation domain were produced. The genes were cloned into both vectors to allow for the possibility that one of the rotavirus proteins under investigation had intrinsic transcriptional activating properties thereby negating the use of one of the vectors.

A sub-cloning procedure was followed for each gene whereby, after PCR amplification of the gene, it was ligated directly into a TA vector without the need for restriction enzyme digestion (Figure 4.10). Each gene was then excised from the TA vector with the appropriate restriction enzymes and ligated into the two-hybrid vectors. This approach was found to be considerably more successful than attempting to ligate the PCR product directly into the two-hybrid vectors.

The most important considerations in the production of the fusion proteins were that each gene was ligated into the MCS of the vectors in the correct orientation with respect to the GAL4 domain sequence, and that the reading frame was maintained. The orientation of each gene was ensured by using a forced cloning procedure, whereby the genes were ligated into the MCS using specific restriction sites at the 5' and 3' ends. The genes were amplified by PCR using primers designed to introduce particular restriction sites which could then be used for cloning into the MCS of each vector. The sites were positioned such that, after ligation, the reading frame of the GAL4 domain sequence would be maintained and fusion proteins would be expressed. The junction regions, between the GAL4 domain sequence and the 5'

Figure 4.9

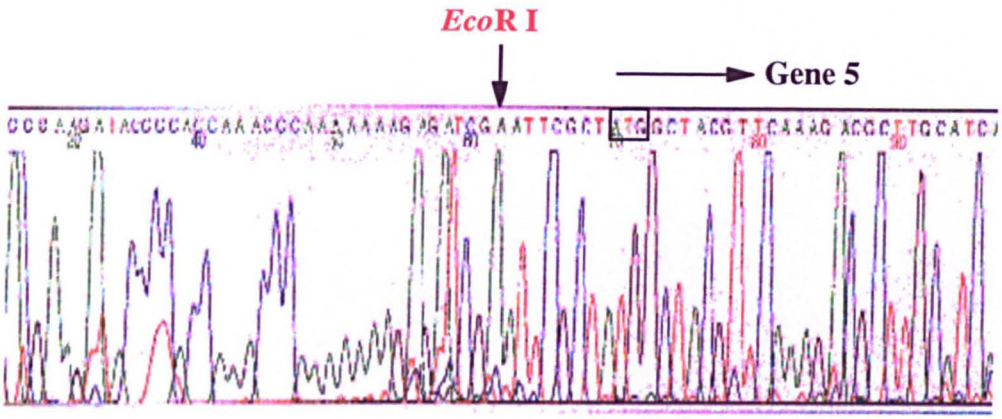

GAL4 activation domain | *Eco*R I | UKtc gene 5

CCA AAA AAA GAG ATC GAA TTC GCT ATG GCT ACG TTC AAA GAC GCT TGC

Figure 4.9 Sequence analysis of the junction region of clone pGAD424-gene 5

Clone pGAD424-gene5(15) DNA was amplified and purified by maxi-prep (Section 3.4.14) and sequenced using Primer 2 (Table 3.3) which recognizes sequence 56 bp upstream of the MCS start site in pGAD424 (Figure 4.1). Sequence analysis (Section 3.4.18) was performed to confirm the orientation of gene 5, and the framing at the junction between the GAL4 domain sequence in pGAD424 and gene 5. The *Eco*R I site preceding the ATG site of gene 5 was introduced by PCR and allowed the gene to be cloned, in frame, into pGAD424. The sequence analysis revealed that the reading frame was maintained (Figure 4.2). Approximately 250 bp at the 5'-end of gene 5 was compared with the original sequence data, and it was verified that the sequence was accurate. Sequence analysis was repeated twice.

Figure 4.10 Sub-cloning strategy employed for cloning of the UKtc strain of bovine rotavirus genes into pTAg and two-hybrid vectors pGBT9 and pGAD424

An overview of the sub-cloning strategy used to clone rotavirus genes 1, 2, 3 and 9, first into the TA vector pTAg, and subsequently into the two-hybrid cloning vectors, pGBT9 and pGAD424, is shown. The rotavirus genes were amplified by PCR using primers designed to introduce specific restriction sites to the 5' and 3' ends of the gene. The PCR amplified genes were ligated directly into pTAg by means of the single A overhangs added by the *Taq* enzyme during PCR amplification. The pTAg vector has complementary T overhangs which can be used for direct ligation to the PCR product. If a proof-reading DNA polymerase (e.g. *Pfu),* which has a 3' to 5' exonuclease activity, is used for PCR amplification then the product will not have 3' A overhangs. However, the vector can still be used, provided a dA tailing reaction with *Taq* is performed after amplification. The pTAg vector has a versatile polylinker (MCS) including the following restriction sites: *Eco*R I, *Bam*H I, *Mlu* I, *Pst* I, *Sph* I, *Kpn* I (5' end); *Sal* I, *Hind* III, *Xho* I, *Xba* I (3' end). The *LacZ* gene facilitates blue/white screening for recombinants. The presence of white colonies indicates interruption of the *LacZ* gene caused by the insertion of the gene into the vector. The vector has two selectable markers, ampicillin resistance (Amp^R) and kanamycin resistance (Kan^R), which can be used as appropriate to avoid the selection of false positive colonies. The vector also contains the T7 promoter.

The pTAg clones were used for sub-cloning genes into the two-hybrid vectors pGBT9 and pGAD424. The genes were excised from pTAg by cutting at the restriction sites introduced by PCR, and were cloned into the relevant restriction sites in the MCS of the two-hybrid vectors. This procedure ensured that the genes were cloned in frame into the two-hybrid vectors, with respect to the GAL4 domain sequence. The orientation and framing of the inserts were analysed by restriction enzyme digestion and sequencing.

Figure 4.10

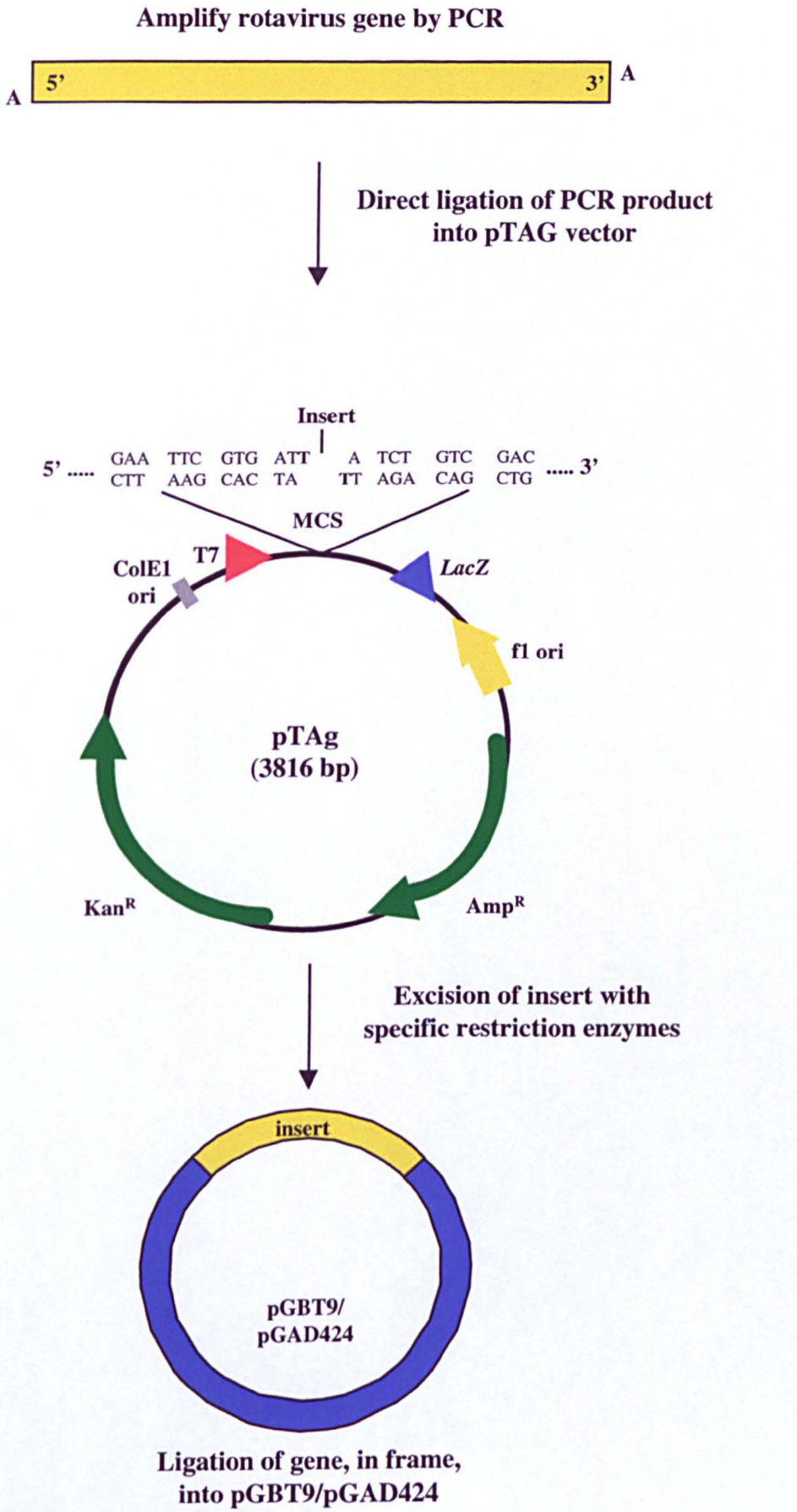
Amplify rotavirus gene by PCR
A
5'
3'
A
Direct ligation of PCR product into pTAG vector
Insert
5' ..... GAA TTC GTG ATT A TCT GTC GAC ..... 3'
CTT AAG CAC TA TT AGA CAG CTG
MCS
T7
ColE1 ori
LacZ
f1 ori
pTAg (3816 bp)
Kan^R
Amp^R
Excision of insert with specific restriction enzymes
insert
pGBT9/ pGAD424
Ligation of gene, in frame, into pGBT9/pGAD424

end of each rotavirus gene, were sequenced to ensure that the reading frames were correct. The data generated by this sequencing also allowed approximately 200-300 bp at the 5' end of each cloned rotavirus gene to be checked against the original sequence data to ensure that it was correct. In addition, each rotavirus gene that was cloned into a TA vector was expressed *in vitro* to produce a full-length protein product of the expected size (Chapter 6). This data indicates that mutations encoding stop codons were not introduced during PCR of the rotavirus genes, and lends support to the assumption that full-length rotavirus proteins would be expressed as GAL4 fusions following cloning into the two-hybrid vectors.

4.4.2 Cloning of Gene 1 into pGBT9 and pGAD424

A cDNA of gene 1 from the UKtc strain of bovine rotavirus, which encodes VP1, was amplified by PCR (Section 3.4.1) using primers Gene 1/5' and Gene 1/3' (Table 3.3). The Gene 1/5' primer was designed to introduce a specific restriction enzyme site, *Sma* I, to the 5' end of the gene immediately prior to the ATG start site. A *Sma* I restriction site is also present in the MCS of both yeast two-hybrid vectors, so it could be utilised for cloning purposes. The framing of the *Sma* I site, in relation to the ATG of gene 1 and the ORF of the GAL4 domain, was designed such that the reading frame would be maintained when gene 1 was cloned into either vector, resulting in the production of fusion proteins of the GAL4 domains with the gene 1 product VP1. The PCR amplified gene 1 was ligated directly into the pTAg vector using the Invitrogen LigATor cloning kit (Section 3.4.16). This sub-cloning approach was followed as earlier attempts at direct cloning of gene 1 into pGAD424 were unsuccessful. A full-length protein product corresponding to VP1 was expressed *in vitro* from pTAg-gene1 (Figure 6.12). Gene 1 was excised from pTAg-Gene 1 by digestion with *Sma* I, which cuts at the 5' end of gene 1, and *Xho* I, which cuts at the 3' end of gene 1. Vector pGAD424 was digested with *Sma* I and *Sal* I (*Sal* I and *Xho* I are compatible restriction sites). Gene 1 was ligated into the MCS of pGAD424 to generate clone pGAD424-gene 1. Recombinant clones were identified by Grunstein-Hogness colony hybridisation assay (Section 3.4.15), as the frequency of recombination appeared to be extremely low, and confirmed by restriction enzyme digestion with *Sma I/ Pst* I which released the gene 1 insert (Figure 4.11, Panel A). The orientation of gene 1 in the positive clones was confirmed by restriction enzyme

Figure 4.11 Analysis of pGAD424-Gene 1 by restriction enzyme digestion and sequencing of the junction region

A. Restriction enzyme digestion analysis of pGAD424-gene 1

Plasmid DNA from a clone created following the ligation of gene 1 into the *Sma* I and *Sal* I sites of pGAD424 was prepared by mini-prep (Section 3.4.13) and analysed by restriction enzyme digestion (Section 3.4.6). The products of the digests were analysed by electrophoresis on a 1.0 % TAE agarose gel (Section 3.4.3). Lanes marked pGAD424 contain the vector digested with the enzymes indicated. Lanes marked G1 contain the clone pGAD424-gene 1 digested with the enzymes indicated. Digestion of pGAD424 with *Sma* I/*Pst* I linearises the plasmid (6600 bp). Digestion of pGAD424-gene 1 with *Sma* I/*Pst* I releases the insert (6600 bp and 3300 bp). Digestion of pGAD424 with *Eco*R I linearises the plasmid (6600 bp). Predicted band sizes for digestion of pGAD424-gene 1, containing positively orientated gene 1, with *Eco*R I are 8400 bp, 850 bp and 650 bp. Lanes marked L were loaded with 1 kb DNA ladder. The sizes of the markers are given in base pairs.

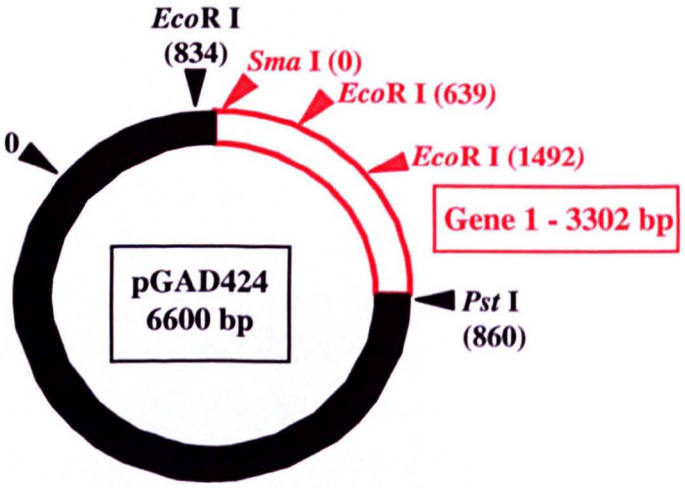

B. Sequence analysis of pGAD424-gene 1 junction region

The junction region of plasmid pGAD424-gene1 [6(1)] at the 5' end of gene 1 was sequenced (Section 3.4.18) using Primer 2 (Table 3.3) to ensure the correct framing for the production of the desired fusion protein. An original sequence trace and a schematic diagram of the junction region are shown. The sequence at the junction region, which includes the GAL4 activation domain sequence (blue on the schematic diagram), the UKtc gene 1 sequence (yellow) and the *Sma* I cloning site (red) which was used to produce the in-frame clone, is shown. The ATG start site in gene 1 is underlined in bold. Approximately 300 bp of sequence at the 5' end of gene 1 was also checked in this analysis. The sequence analysis was repeated at least twice to confirm the sequence of the junction region.

Figure 4.11

A

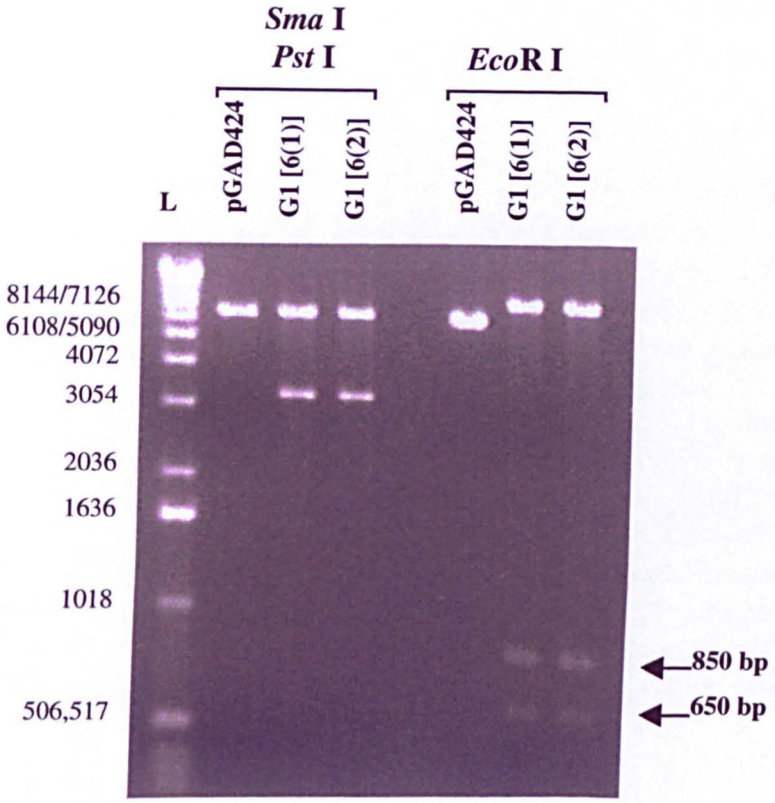

B. pGAD424-Gene 1 junction region sequence

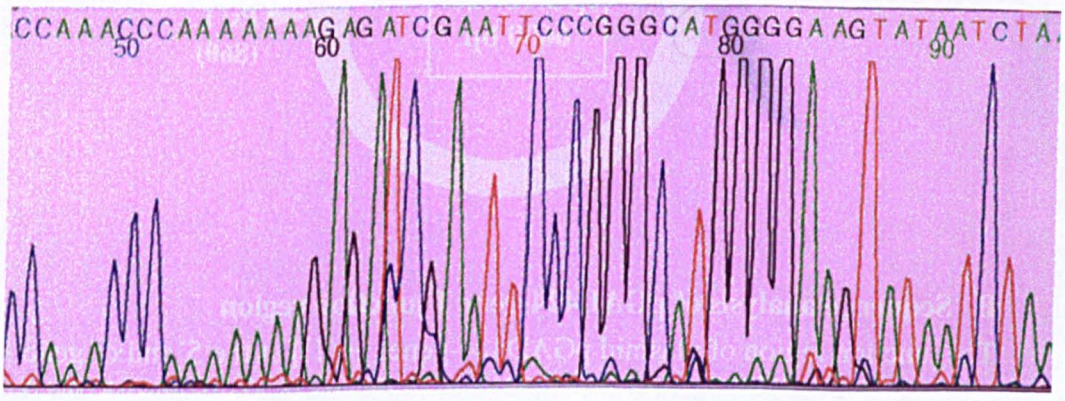

GAL4 activation domain — *Sma* I — **UKtc gene 1**

CCA AAC CCA AAA AAA GAG ATC GAA TTC CCG GGC ATG GGG AAG TAT AAT CTA

digestion analysis with *Eco*R I. Bands of 8400 bp, 850 bp and 650 bp were produced when the orientation of the gene 1 insert was correct (Figure 4.11, Panel A). The junction region was sequenced to confirm that the reading frame between the GAL4 domain sequence and gene 1 was maintained, ensuring the production of the desired fusion protein (Figure 4.11, Panel B). In addition, approximately 300 bp at the 5' end of gene 1 was also sequenced and checked against the original sequence (data not shown).

Plasmid pGBT9-Gene 1 was produced by sub-cloning from pGAD424-Gene 1. Gene 1 was excised from pGAD424-Gene 1 by *Sma* I (5' end) and *Pst* I (3' end). Vector pGBT9 was digested with *Sma* I and *Pst* I and dephosphorylated with shrimp alkaline phosphatase (SAP) (Section 3.4.6). Gene 1 was then ligated into pGBT9 to generate clone pGBT9-Gene 1. Recombinant clones were screened and identified by restriction enzyme digestion with *Sma I/ Pst* I which released the insert (Figure 4.12, Panel A). The orientation of gene 1 in the positive clones was confirmed by restriction enzyme digestion with separate reactions of *Eco*R I and *Eco*R V. The reactions with *Eco*R I (bands of 7300 bp, 860 bp and 640 bp) and EcoR V (bands of 7400 bp and 1400 bp) confirmed the positive orientation of the gene 1 insert in the two clones (Figure 4.12, Panel A). The junction region was sequenced to confirm that the reading frame between the GAL4 domain sequence and gene 1 was maintained, ensuring the production of the desired fusion protein (Figure 4.12, Panel B). In addition, approximately 300 bp at the 5' end of gene 1 was also sequenced and checked against the original sequence (data not shown).

4.4.3 Cloning of Gene 2 into pGBT9 and pGAD424

A cDNA of gene 2 from the UKtc strain of bovine rotavirus, which encodes VP2, was amplified by PCR (Section 3.4.1) using primers Gene 2/5' and Gene 2/3' (Table 3.3). The Gene 2/5' primer was designed to introduce an *Eco*R I restriction site to the 5' end of gene 2 immediately prior to the ATG start site. An *Eco*R I site is also present in the MCS of both of the yeast two-hybrid vectors. The framing of the *Eco*R I site, in relation to the ATG of gene 2 and the ORF of the GAL4 domain, was designed to maintain the reading frame when gene 2 was cloned into either vector, resulting in the production of fusion proteins of the GAL4 domains with the gene 2 product VP2. The PCR amplified gene 2 was ligated directly into the pTAg vector

Figure 4.12 Analysis of pGBT9-Gene 1 by restriction enzyme digestion and sequencing of the junction region

A. Restriction enzyme digestion analysis of clone pGBT9-Gene 1

Plasmid DNA from the sub-cloning of gene 1 into the *Sma* I (5' end) and *Sal* I (3' end) sites of pGBT9 was prepared by mini-prep (Section 3.4.13) and analysed by restriction enzyme digestion (Section 3.4.6). The products of the digests were analysed by electrophoresis on a 1.0 % TAE agarose gel (Section 3.4.3). The lane marked pGBT9 contains the vector digested with *Sma* I/ *Pst* I. Lanes marked G1 contain the clones of pGBT9-gene1 [G1(5); G1(6)] digested with the enzymes indicated. Digestion of pGBT9 with *Sma* I/*Pst* I linearises the plasmid (5500 bp). Digestion of pGBT9-gene1 with *Sma* I/*Pst* I releases the insert (5500 bp and 3300 bp). Predicted band sizes for digestion of pGBT9-gene1, containing positively orientated gene 1, with *Eco*R I are 7300 bp, 860 bp and 640 bp. Predicted band sizes for digestion of pGBT9-gene 1, containing positively orientated gene 1, with *Eco*R V are 7400 bp and 1400 bp. Lanes marked L were loaded with 1 kb DNA ladder. The sizes of the markers are given in base pairs.

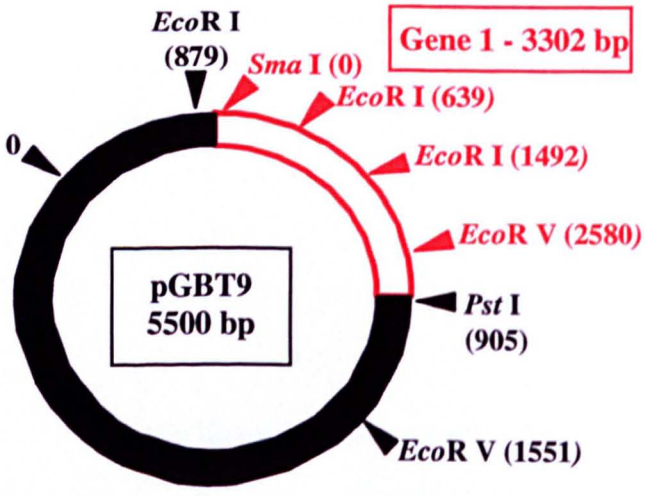

B. Sequence analysis of pGBT9-Gene 1 junction region.

The junction regions of both clones [G1(5); G1(6)] of plasmid pGBT9-gene1 at the 5' end of gene 1 was sequenced (Section 3.4.18) using Primer 1 (Table 3.3) to ensure the correct framing for the production of the desired fusion protein. An original sequence trace of G1(5), and a schematic diagram of the junction region are shown. The sequence at the junction region, which includes the GAL4 DNA-binding domain sequence (blue on the schematic diagram), the UKtc gene 1 sequence (yellow) and the *Sma* I cloning site (red) which was used to produce the in-frame clone, is shown. The ATG start site in gene 1 is underlined in bold. Approximately 300 bp of sequence at the 5' end of gene 1 was also checked in this analysis. The sequence analysis was repeated at least twice to confirm the junction region sequence.

Figure 4.12

A

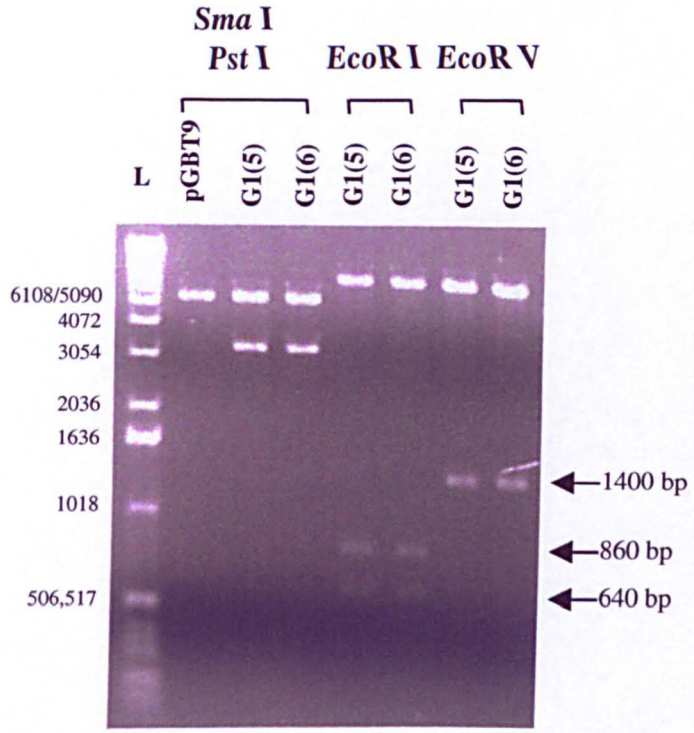

B. pGBT9-Gene1 junction region sequence

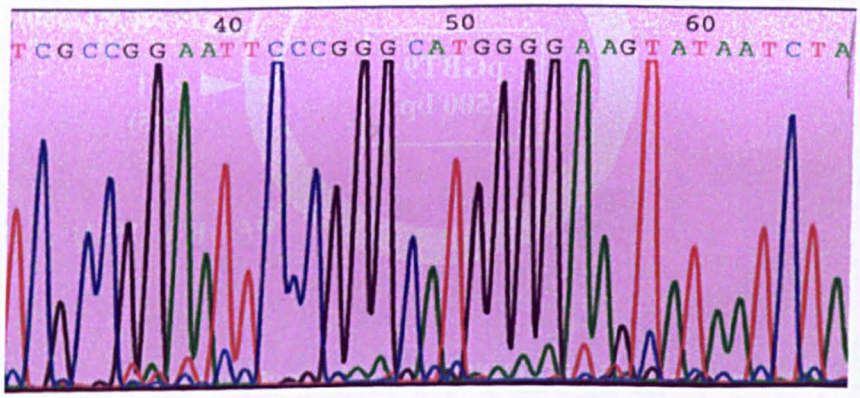

GAL4 DNA-binding domain | ***Sma* I** | **UKtc Gene 1**

TCG CCG GAA TTC CCG GGC ATG GGG AAG TAT AAT CTA

using the Invitrogen LigATor cloning kit (Section 3.4.16). This sub-cloning approach was followed as earlier attempts to directly clone gene 2 into pGAD424 were unsuccessful. This produced clones with inserts ligated into pTAg in both a positive and negative orientation. Plasmid pTAg-gene2, containing gene 2 in a positive orientation, was used for *in vitro* expression studies and a full-length protein product corresponding to VP2 was produced indicating that no deleterious mutations were introduced during PCR (Figure 6.11). A clone containing gene 2 in the negative orientation in pTAg was used for the sub-cloning procedure into pGAD424. To excise the insert the clone was digested with *Eco*R I since it cuts at the 5' end of PCR amplified gene 2 and also in the MCS of pTAg at the 3' end of gene 2 when in the negative orientation. Vector pGAD424 was digested with *Eco*R I and dephosphorylated with CIP. Gene 2, digested with *Eco*R I, was then ligated into the *Eco*R I site of pGAD424 to generate clone pGAD424-gene 2. Recombinant clones were screened and identified by restriction enzyme digestion analysis. A clone containing gene 2 was identified by digestion with *Eco*R I which released the insert (Figure 4.13, Panel A). The positive orientation of gene 2, with respect to the GAL4 domain sequence in pGAD424, was then confirmed by carrying out further restriction enzyme digestions. Digestion with *Eco*R V (bands of 5900 bp and 3400 bp), *Eco*R I/*Pst* I (bands of 6600 bp, 1900 bp and 800 bp) and *Cla* I/*Mlu* I (bands of 4800 bp, 3600 bp and 800 bp) identified the correct orientation of gene 2 in clone pGAD424-gene 2 (Figure 4.13, Panel A). The junction region was sequenced to confirm that the reading frame between the GAL4 domain sequence and gene 2 was maintained, ensuring the production of the desired fusion protein (Figure 4.13, Panel B). The nucleotide sequence of the gene 2 insert was compared with the published sequence for gene 2 from the UKtc strain of bovine rotavirus (Tian *et al.*, 1990). Nucleotide sequence variation, resulting in three amino acid changes at the amino-terminus, was found in the gene 2 insert compared to the published sequence. These changes were probably introduced during the PCR amplification of gene 2. However, these three amino acid changes were present in the gene 2 sequence from the SA11 strain of simian rotavirus, suggesting that this low level of sequence variability is acceptable.

Plasmid pGBT9-Gene 2 was produced by sub-cloning from pGAD424-Gene 2. Gene 2 was excised from pGAD424-Gene 2 by digestion with *Eco*R I. Vector pGBT9 was digested with *Eco*R I and dephosphorylated with SAP (Section 3.4.6).

Figure 4.13 Analysis of pGAD424-Gene 2 by restriction enzyme digestion and sequencing of the junction region

A. Restriction enzyme digestion analysis of pGAD424-Gene2 [G2(10)]

Plasmid DNA from a clone [G2(10)] created following the ligation of gene 2 into the *Eco*R I site of the MCS of pGAD424, was prepared by mini-prep (Section 3.4.13) and digested with combinations of restriction enzymes (Section 3.4.6). The products of the digests were analysed by electrophoresis on a 0.8 % TAE agarose gel (Section 3.4.3). Lanes marked pGAD424 contain the vector only digested with the enzymes indicated. Lanes marked G2 contain pGAD424-gene 2 [G2(10)] digested with the enzymes indicated. Digestion of pGAD424 with *Eco*R I linearises the plasmid (6600 bp). Digestion of pGAD424-gene 2 with *Eco*R I releases the insert (6600 bp and 2700 bp). Predicted band sizes for digestion of pGAD424-gene 2 containing positively orientated gene 2, with *Eco*R V are 5900 bp and 3400 bp, and with *Eco*R I/ *Pst* I are 6600 bp, 1900 bp and 800 bp. Digestion of pGAD424 with *Cla* I/ *Mlu* I results in bands of 4800 bp and 1800 bp. Predicted band sizes for digestion of pGAD424-gene 2 containing positively orientated gene 2, with *Cla* I/ *Mlu* I are 4800 bp, 3600 bp and 800 bp. Lanes marked L were loaded with 1 kb DNA ladder. The sizes of the markers are given in base pairs.

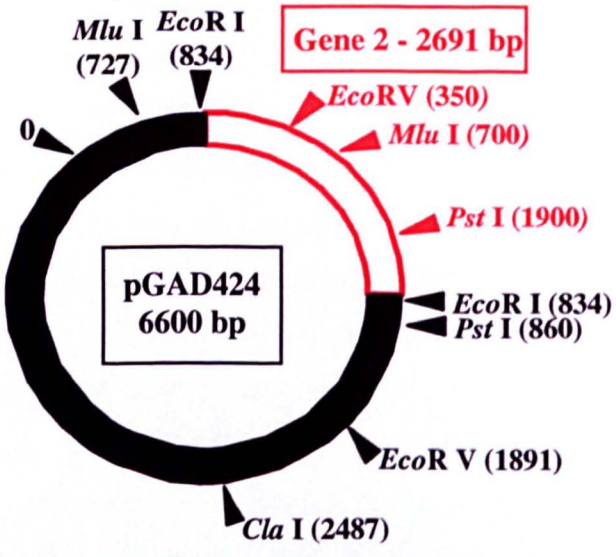

B. Sequence analysis of pGAD424-Gene2 junction region

The junction region of plasmid pGAD424-gene2 [G2(10)] at the 5' end of gene 2 was sequenced (Section 3.4.18) using Primer 2 (Table 3.3) to ensure the correct framing for the production of the desired fusion protein. An original sequence trace and a schematic diagram of the junction region are shown. The sequence at the junction region, which includes the GAL4 activation domain sequence (blue on the schematic diagram), the UKtc gene 2 sequence (yellow) and the *Eco*R I cloning site (red) which was used to produce the in-frame clone, is shown. The ATG start site in gene 2 is underlined in bold. Approximately 250 bp of sequence at the 5' end of gene 2 was also checked in this analysis. The sequence analysis was repeated at least twice to confirm the junction region sequence.

Figure 4.13

A.

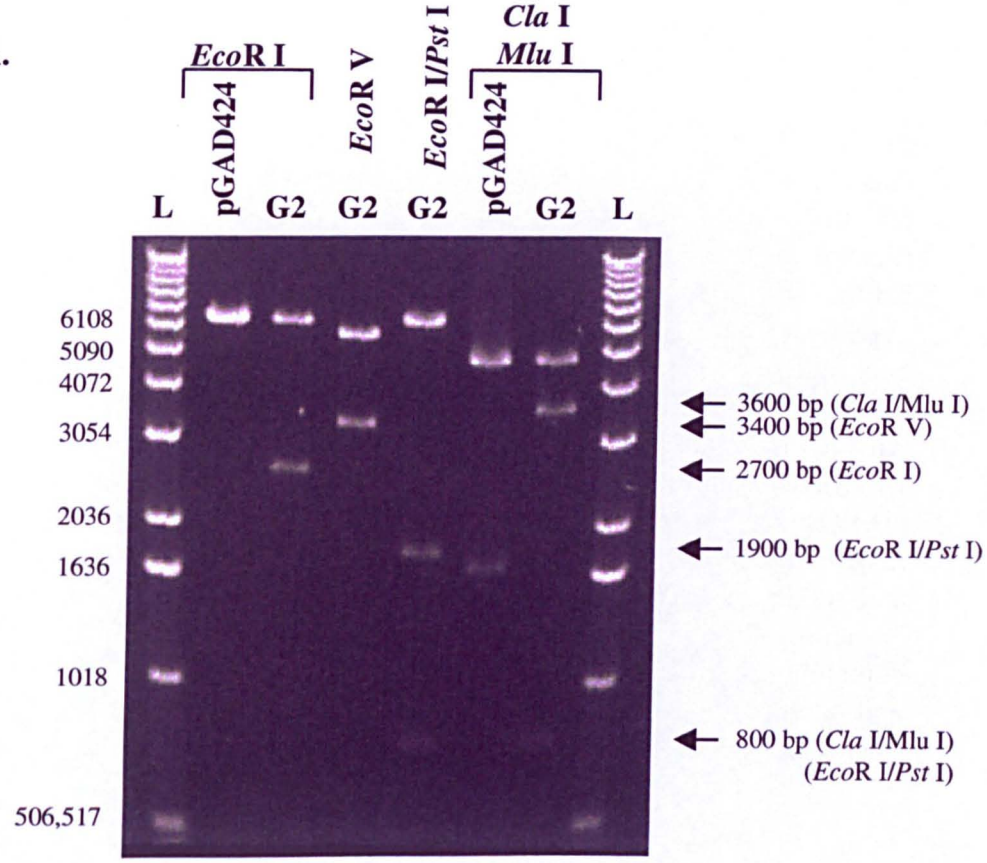

B. pGAD424-Gene 2 junction region sequence

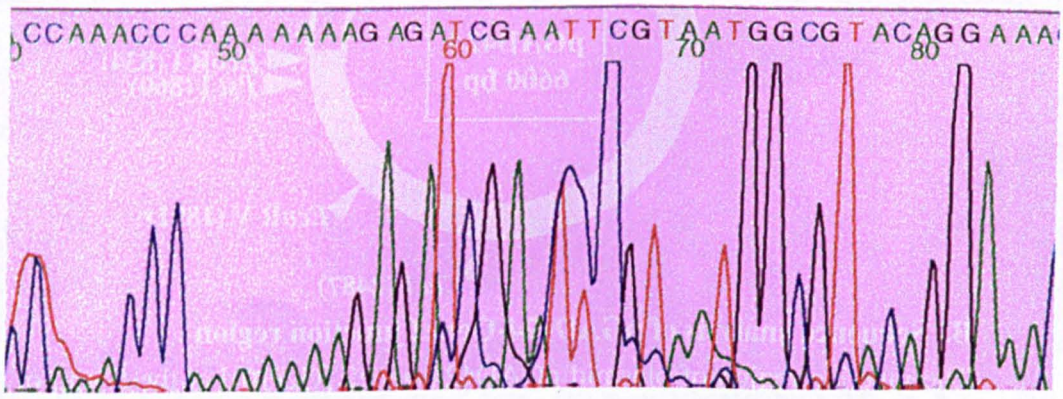

GAL4 activation domain ***Eco*R I** **UKtc gene 2**

CCA AAC CCA AAA AAA GAG ATC GAA TTC GTA **ATG** GCG TAC AGG AAA

Gene 2 was then ligated into the *Eco*R I site of the MCS of pGBT9 to generate clone pGBT9-Gene 2. Recombinant clones were screened and identified by restriction enzyme digestion with *Eco*R I which released the insert (Figure 4.14, Panel A). A clone containing gene 2 in a positive orientation, with respect to the GAL4 domain sequence in pGBT9, was identified by digestion with *Eco*R V which produced bands sized 5200 bp and 3000 bp with the correct pGBT9-gene 2 clone (Figure 4.14, Panel B). The junction region was sequenced to confirm that the reading frame between the GAL4 domain sequence and gene 2 was maintained, ensuring the production of the desired fusion protein (Figure 4.14, Panel C). In addition, approximately 350 bp at the 5' end of gene 2 was also sequenced and checked against the original sequence (data not shown).

4.4.4 Cloning of Gene 3 into pGBT9 and pGAD424

A cDNA of gene 3 from the UKtc strain of bovine rotavirus was amplified by PCR (Section 3.4.1) from plasmid pGS62-gene 3 with primers Gene 3/5' and Gene 3/3' (Table 3.3). The Gene 3/5' primer was designed to introduce a *Bam*H I restriction site at the 5' end of gene 3, immediately prior to the ATG start site. A *Bam*H I site is also present in the MCS of both of the yeast two-hybrid vectors. The framing of the *Bam*H I site, in relation to the ATG of gene 3 and the ORF of the GAL4 domain, was designed to maintain the reading frame when gene 3 was cloned into either vector, resulting in the production of fusion proteins of the GAL4 domains with the gene 3 product VP3. The PCR amplified gene 3 was ligated directly into the pTAg vector using the Invitrogen LigATor cloning kit (Section 3.4.16). This sub-cloning approach was followed as earlier attempts to directly clone gene 3 into pGAD424 were unsuccessful. A full-length protein product corresponding to VP3 was expressed *in vitro* from pTAg-gene3 (Figure 6.15), indicating that no deleterious mutations were introduced during PCR. To sub-clone gene 3 into pGAD424, the gene was excised from pTAg by restriction enzyme digestion with *Bam*H I (5' end) and *Bgl* II (3' end). Vector pGAD424 was digested with *Bam*H I and *Bgl* II and dephosphorylated with SAP. The digested gene 3 was ligated into the MCS of pGAD424 to generate a pGAD424-gene 3 construct. Recombinant clones were identified by restriction enzyme digestion analysis. Digestion with enzymes *Bam*H I plus *Bgl* II linearised all the recombinant plasmids rather than releasing the gene 3 insert as expected. This

Figure 4.14 Analysis of pGBT9-Gene2 by restriction enzyme digestion and sequencing of the junction region

A. Identification of clones containing the gene 2 insert by restriction enzyme digestion with *Eco*R I

Plasmid DNA from the sub-cloning of gene 2 into the *Eco*R I site of the MCS of pGBT9 was prepared by mini-prep (Section 3.4.13) and digested with *Eco*R I (Section 3.4.6). The products of the digests were analysed by electrophoresis on a 1.0 % TAE agarose gel (Section 3.4.3). The lane marked pGBT9 contains the vector digested with *Eco*R I (5500 bp). Lanes 1-10 contain plasmid DNA from the sub-cloning digested with *Eco*R I. Digestion with *Eco*R I linearises pGBT9 (5500 bp) and releases the gene 2 insert (5500bp and 2700 bp). The identity of the 3.5kb bands in lanes 3 and 8 was not determined and this plasmid DNA was discarded. Lanes marked L were loaded with 1 kb DNA ladder. The sizes of the markers are given in base pairs.

B. Determination of the orientation of the gene 2 insert in pGBT9 by restriction enzyme digestion with *Eco*R V

Plasmid DNA, as described above (A), was digested with *Eco*R V (Section 3.4.6). The products of the digests were analysed by electrophoresis on a 1.0 % TAE agarose gel. The lane marked pGBT9 contains the vector digested with *Eco*R V (5500 bp). Lanes 1,2 and 4-6 contain plasmid DNA from the sub-cloning digested with *Eco*R V. The predicted band sizes for digestion of pGBT9-gene 2 with *Eco*R V are 5200 bp and 3000 bp (positive orientation) and 7200 bp and 1000 bp (negative orientation).

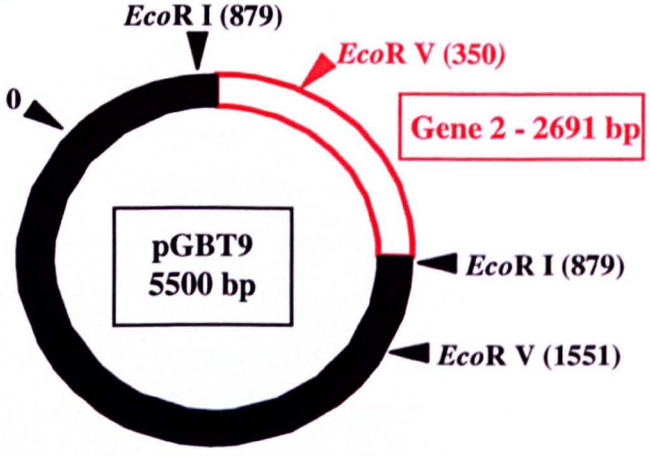

C. Sequence analysis of pGBT9-Gene2 junction region

The junction region of plasmid pGBT9-gene2 [G2(2)] at the 5' end of gene 2 was sequenced (Section 3.4.18) using Primer 1 (Table 3.3) to ensure correct framing for the production of the desired fusion protein. An original sequence trace and a schematic diagram of the junction region are shown. The sequence at the junction region, which includes the GAL4 DNA-binding domain sequence (blue in the schematic diagram), the UKtc gene 2 sequence (yellow) and the *Eco*R I cloning site (red) which was used to produce the in-frame clone, is shown. The ATG start site in gene 2 is underlined in bold. The nucleotide at position 55 on the sequence trace has been incorrectly assigned and should be A. Approximately 350 bp of sequence at the 5' end of gene 2 was also checked in this analysis. The sequence analysis was repeated at least twice to confirm the junction region sequence.

Figure 4.14

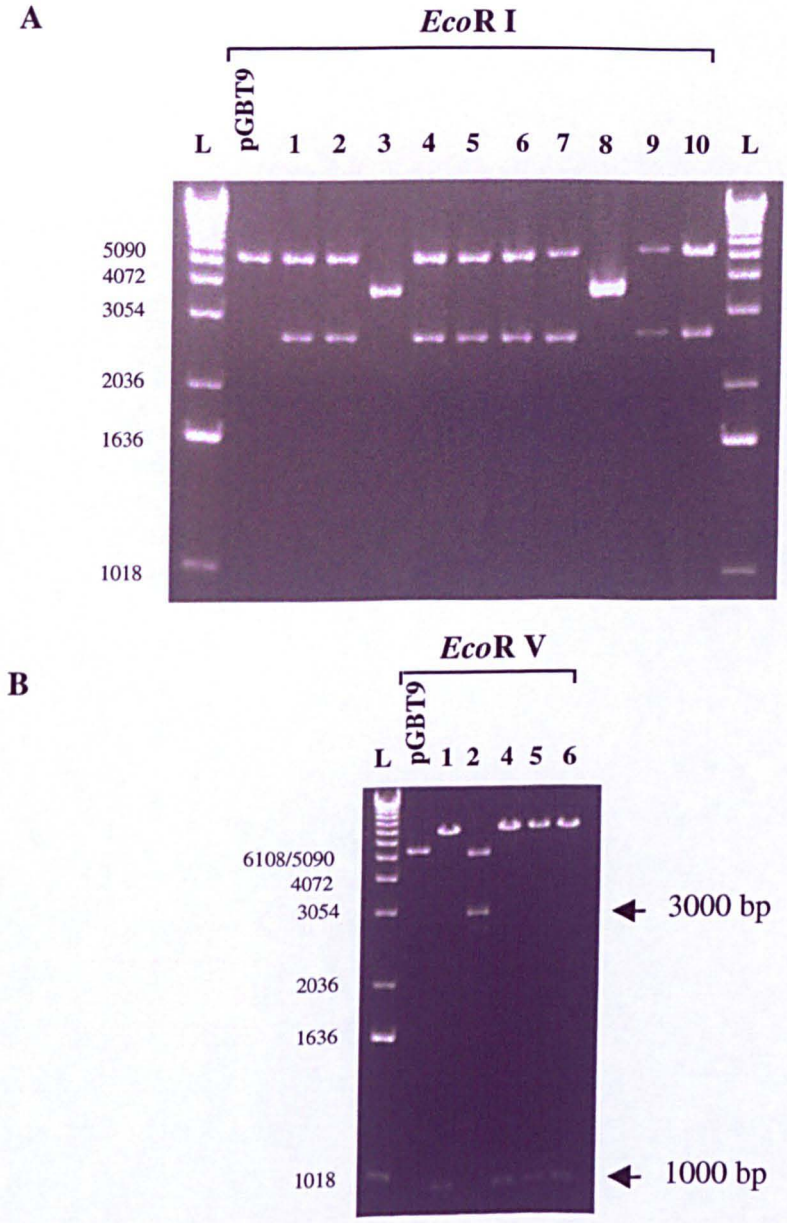
A
EcoR I
L
pGBT9
1
2
3
4
5
6
7
8
9
10
L
5090
4072
3054
2036
1636
1018
B
EcoR V
L
pGBT9
1
2
4
5
6
6108/5090
4072
3054
2036
1636
1018
3000 bp
1000 bp
C
40
50
60
GAL4
DNA-binding
domain
UKtc gene 2
TCG CCG GAA TTC GTA ATG GCG TAC AGG AA
EcoR I

suggested that one of the enzyme sites in the recombinant plasmids had been destroyed. Digestion with enzymes *Bgl* II plus *Eco*R I produced bands consistent with an *Eco*R I only digest, suggesting that the *Bgl* II site, which should lie at the 3' end of gene 3 in the recombinant plasmids, had been destroyed during the cloning procedure. Hence, a series of digests with other restriction enzymes were used to identify positive clones. Clones containing gene 3 in a positive orientation, with respect to the GAL4 domain sequence in pGAD424, were identified by restriction enzyme digestion analysis with *Bam*H I/*Sph* I (bands 5200 bp, 3200 bp and 800 bp) and *Eco*R I (7200 bp and 1800 bp) (Figure 4.15, Panel A). The junction region was sequenced to confirm that the reading frame between the GAL4 domain sequence and gene 3 was maintained, ensuring the production of the desired fusion protein (Figure 4.15, Panel B). In addition, approximately 250 bp at the 5' end of gene 3 was also sequenced and checked against the original sequence (data not shown).

Plasmid pGBT9-Gene 3 was produced by sub-cloning from pGAD424-Gene 3. Gene 3 was excised from pGAD424-Gene 3 by digestion with *Bam*H I (5' end) and *Pst* I (3' end). Vector pGBT9 was digested with *Bam*H I and *Pst* I and dephosphorylated with SAP (Section 3.4.6). Gene 3 was ligated into the MCS of pGBT9 to generate a pGBT9-gene 3 construct. Recombinant clones were screened and identified by restriction enzyme digestion with *Bam*H I/*Pst* I which released the insert (Figure 4.16, Panel A). Clones containing gene 3 in a positive orientation, with respect to the GAL4 domain sequence in pGBT9, were identified by digestion with *Eco*R I which produced bands sized 6100 bp, 1900 bp and 180 bp with the correct pGBT9-gene 3 clones (Figure 4.16, Panel A). The junction region was sequenced to confirm that the reading frame between the GAL4 domain sequence and gene 3 was maintained, ensuring the production of the desired fusion protein (Figure 4.16, Panel B). In addition, approximately 250 bp at the 5' end of gene 3 was also sequenced and checked against the original sequence (data not shown).

Figure 4.15 Analysis of pGAD424-Gene 3 by restriction enzyme digestion and sequencing of the junction region

A. Restriction enzyme digestion analysis of clone pGAD424-Gene3

Plasmid DNA from a clone created following the ligation of gene 3 into the *Bam*H I and *Bgl* II sites of the MCS of pGAD424 was prepared by mini-prep (Section 3.4.13) and analysed by restriction enzyme digestion (Section 3.4.6). The products of the digests were analysed by electrophoresis on a 0.8 % TAE agarose gel (Section 3.4.3). Lanes marked pGAD424 contain the vector digested with the enzymes indicated. Lanes marked G3 contain the clone pGAD424-gene 3 digested with the enzymes indicated. Digestion of pGAD424 with *Bam*H I/*Sph* I results in bands of 5200 bp, 800 bp and 600 bp. Predicted band sizes from the digestion of pGAD424-gene 3, containing positively orientated gene 3, with *Bam*H I/*Sph* I are 5200 bp, 3200 bp and 800 bp. Digestion of pGAD424 with *Eco*R I linearises the plasmid (6600 bp). Predicted band sizes from the digestion of pGAD424-gene 3, containing positively orientated gene 3, with *Eco*R I are 7200 bp, 1800 bp and 150 bp. Lanes marked L were loaded with 1 kb DNA ladder. The sizes of the markers are given in base pairs.

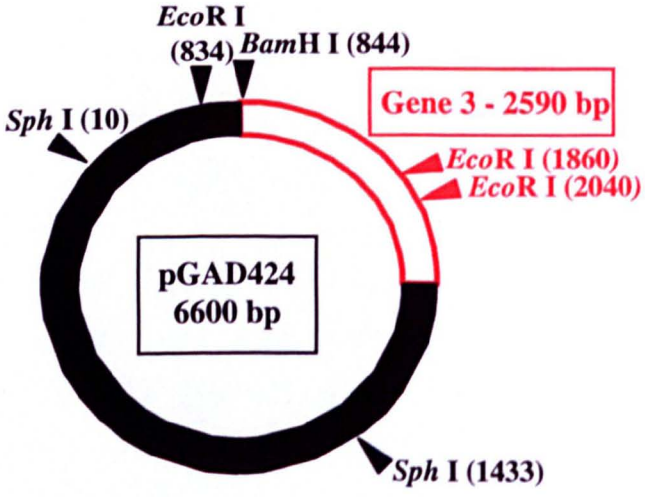

B. Sequence analysis of pGAD424-Gene 3 junction region

The junction region of plasmid pGAD424-gene3 [G3(4)], at the 5' end of gene 3, was sequenced (Section 3.4.18) using Primer 2 (Table 3.3) to ensure the correct framing for the production of the desired fusion protein. An original sequence trace and a schematic diagram of the junction region are shown. The sequence at the junction region, which includes the GAL4 activation domain sequence (blue on the schematic diagram), the UKtc gene 3 sequence (yellow) and the *Bam*H I cloning site (red) which was used to produce the in-frame clone, is shown. The ATG start site in gene 3 is underlined in bold. Approximately 250 bp of sequence at the 5' end of gene 3 was also checked in this analysis. The sequence analysis was repeated at least twice to confirm the junction region sequence.

Figure 4.15

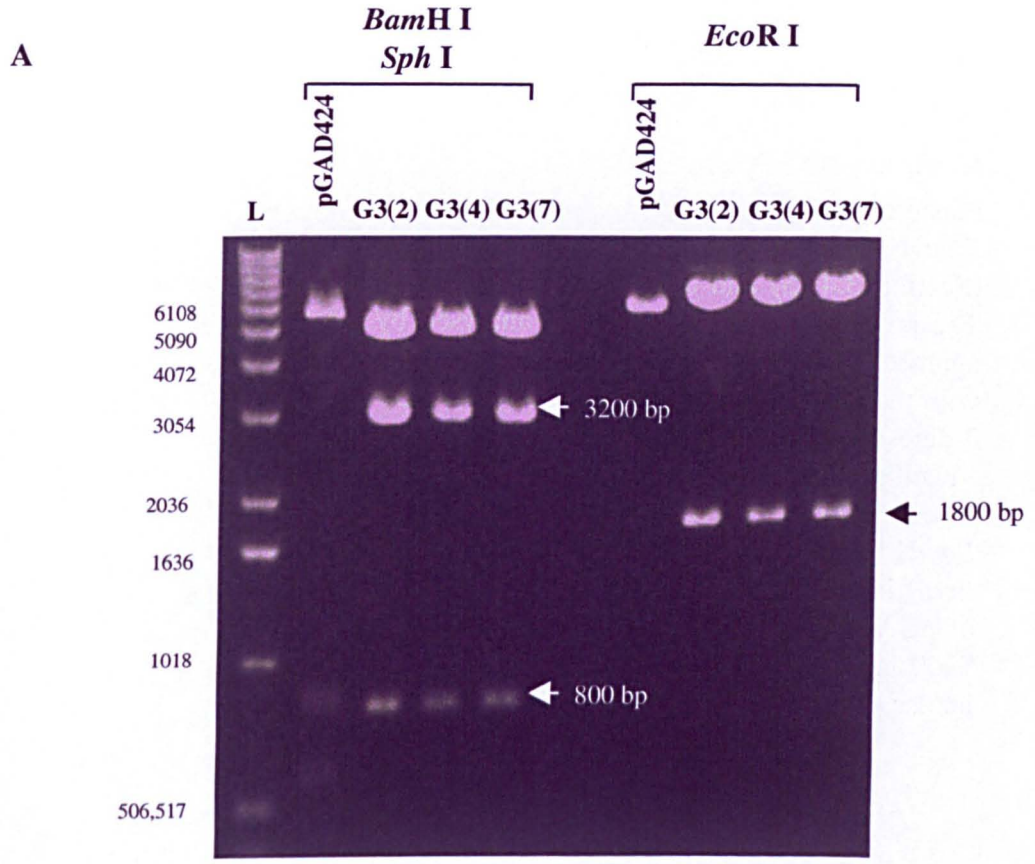

B. pGAD424-Gene 3 junction region sequence

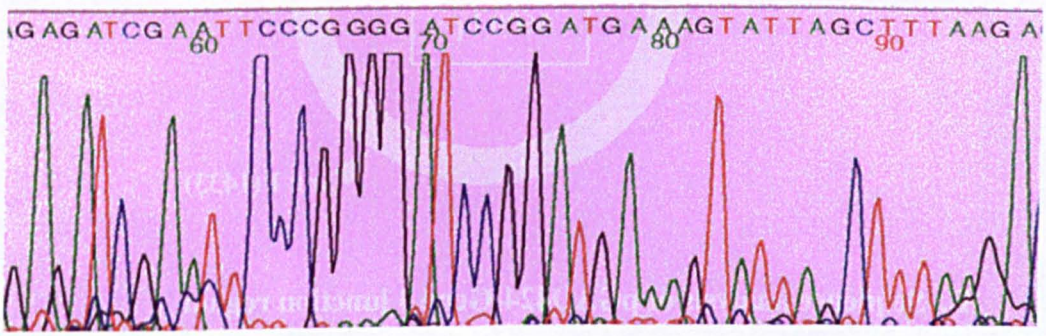

GAL4 activation domain **UKtc gene 3**

GAG ATC GAA TTC CCG GGG ATC CGG ATG AAA GTA TTA GCT TTA AGA

*Bam*H I

Figure 4.16 Analysis of pGBT9-Gene 3 by restriction enzyme digestion and sequencing of the junction region

A. Restriction enzyme digestion analysis of clone pGBT9-Gene 3

Plasmid DNA from the sub-cloning of gene 3 into the *Bam*H I (5' end) and *Pst* I (3' end) sites of the MCS of pGBT9 was prepared by mini-prep (Section 3.4.13) and analysed by restriction enzyme digestion (Section 3.4.6). The products of the digests were analysed by electrophoresis on a 1.0 % TAE agarose gel (Section 3.4.3). The lane marked pGBT9 contains the vector digested with *Bam*H I/*Pst* I. Lanes marked G3(2) and G3(3) contain clones of pGBT9-gene3 digested with the enzymes indicated. Digestion of pGBT9 with *Bam*H I/*Pst* I linearises the plasmid (5500 bp). Digestion of pGBT9-gene3 with *Bam*H I/*Pst* I releases the insert (5500 bp and 2590 bp). Predicted band sizes from the digestion of pGBT9-gene 3, containing positively orientated gene 3, with *Eco*R I are 6100 bp, 1900 bp and 180 bp. The 180 bp band is too faint to be seen on this gel. Lanes marked L were loaded with 1 kb DNA ladder. The sizes of the markers are given in base pairs.

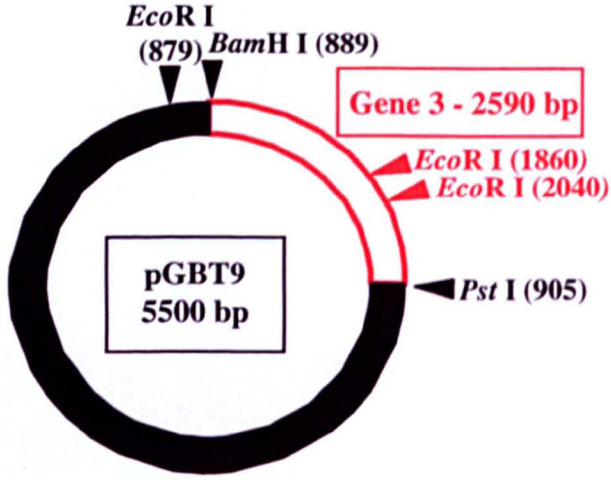

B. Sequence analysis of pGBT9-Gene 3 junction region

The junction region of plasmid pGBT9-gene3 [G3(2)], at the 5' end of gene 3, was sequenced (Section 3.4.18) using Primer 1 (Table 3.3) to ensure the correct framing for the production of the desired fusion protein. An original sequence trace and a schematic diagram of the junction region are shown. The sequence at the junction region, which includes the GAL4 DNA-binding domain sequence (blue on the schematic diagram), the UKtc gene 3 sequence (yellow) and the *Bam*H I cloning site (red) which was used to produce the in-frame clone, is shown. The ATG start site in gene 3 is underlined in bold. Approximately 250 bp of sequence at the 5' end of gene 3 was also checked in this analysis. The sequence analysis was repeated at least twice to confirm the junction region sequence.

Figure 4.16

A

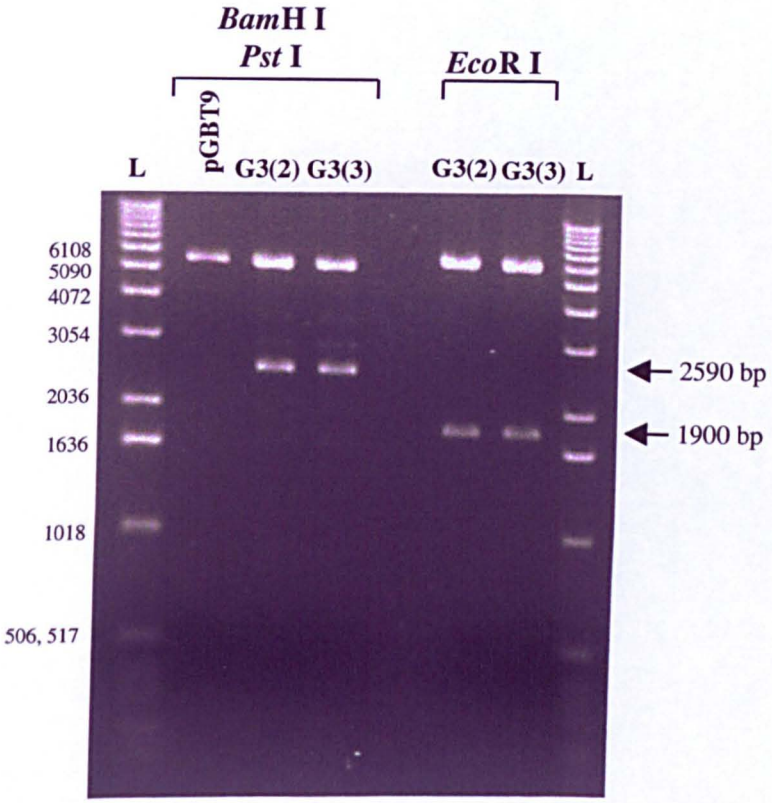

B. pGBT9-Gene3 junction region sequence

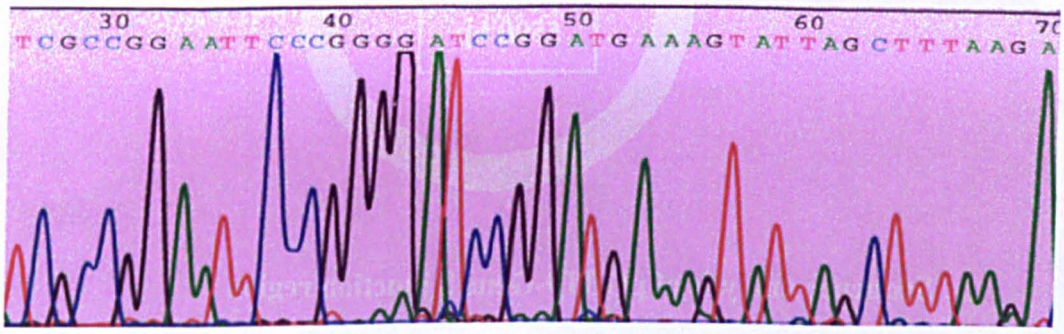

GAL4 DNA-binding domain | ***Bam*H I** | **UKtc Gene 3**

TCG CCG GAA TTC CCG GGG ATC CGG ATG AAA GTA TTA GCT TTA AGA

4.5 Production of constructs to express rotavirus protein NSP3 as GAL4 domain fusion proteins

4.5.1 Strategy for production of GAL4 domain fusion proteins with NSP3

A cDNA of gene 9 from the UKtc strain of bovine rotavirus, which encodes the rotavirus non-structural protein NSP3, was used to produce NSP3-GAL4 domain fusion proteins. The PCR amplified gene 9 sequence was initially ligated directly into the TA vector pCR2.1^{TM} (Invitrogen) and the rotavirus cDNA was then sub-cloned into the two-hybrid vectors pGBT9 and pGAD424 to create fusion proteins with the GAL4 DNA-binding and transcriptional activation domains respectively. The same considerations made when cloning the viral core proteins (Section 4.4.1), which were the correct orientation of the cloned rotavirus cDNA with respect to the GAL4 domain sequence and the maintenance of the reading frame, were also applied here. In addition, sequence at the 5' end of gene 9 was also checked to ensure that errors had not been introduced during PCR amplification of the gene.

The NSP3-GAL4 domain fusion proteins were created to investigate the hypothesis that NSP3 interacts with NSP1. Both proteins are found in the pre-core RI in the rotavirus-infected cell and it was postulated that an interaction could occur between them. In addition, previous work suggested that NSP3 formed dimers in the infected cell (Mattion *et al.*, 1992). The two-hybrid system could be used to demonstrate a direct, independent self-interaction of NSP3, and this could then be used as an internal positive control in the two-hybrid assay screen for further rotavirus protein-protein interactions. NSP3-GAL4 domain fusion proteins were created with both GAL4 domains such that the dimerisation of NSP3 could be investigated.

4.5.2 Cloning of gene 9 into pGBT9 and pGAD424

A cDNA of gene 9 from the UKtc strain of bovine rotavirus was amplified by PCR (Section 3.4.1) from plasmid pGS62-gene 9 with primers Gene 9/5' and Gene 9/3' (Table 3.3). The Gene 9/5' primer was designed to introduce *Bam*H I and *Pst* I restriction enzyme sites to the 5' end of gene 9. These restriction enzyme sites are also present in the MCS of both of the yeast two-hybrid vectors. The framing of the restriction sites in relation to the ATG of gene 9 and the ORF of the GAL4 domain was designed to maintain the reading frame when gene 9 was cloned into either

vector, resulting in the production of fusion proteins of the GAL4 domains with the gene 9 product NSP3. The PCR amplified gene 9 was ligated directly into the pCR2.1^{TM} TA vector using the Invitrogen PCR cloning kit (Section 3.4.16) and positive clones containing the insert were identified by restriction enzyme digestion analysis.

Plasmids pGBT9-gene 9 and pGAD424-gene 9 were produced by sub-cloning from the TA vector containing gene 9. The *Pst* I sites at the 5' end and 3' end of gene 9, which were introduced by PCR, were used for cloning into the two-hybrid vectors. However, gene 9 could not be excised from the TA vector with *Pst* I as digestion of the TA vector with this enzyme produced a band of a similar size to gene 9, which made gel purification of the gene difficult. Hence, gene 9 was initially excised from the TA vector by digestion with *Bst*X I which produced a uniquely sized band. Gene 9 was then digested with *Pst* I to produce the correct ends for ligation into the two-hybrid vectors. Vector pGBT9 was digested with *Pst* I and dephosphorylated with SAP (Section 3.4.6). Gene 9 was ligated into the *Pst* I site of pGBT9 to generate clone pGBT9-gene 9. Recombinant clones were screened and identified by restriction enzyme digestion with *Pst* I which released the insert (Figure 4.17, Panel A). Clones containing gene 9 in a positive orientation, with respect to the GAL4 domain sequence in pGBT9, were identified by digestion with *Eco*R I which produced bands sized 5725 bp and 825 bp with the correct pGBT9-gene 9 clones (Figure 4.17, Panel A). The junction region was sequenced to confirm that the reading frame between the GAL4 domain sequence and gene 9 was maintained, ensuring the production of the desired fusion protein (Figure 4.17, Panel B). In addition, approximately 100 bp at the 5' end of gene 9 was also sequenced and checked against the original sequence (data not shown).

Plasmid pGAD424-gene 9 was produced as described for pGBT9-gene 9, by cloning gene 9 into the *Pst* I site of vector pGAD424. Recombinant clones were screened and identified by restriction enzyme digestion with *Pst* I which released the insert (Figure 4.18, Panel A). Clones containing gene 9 in a positive orientation, with respect to the GAL4 domain sequence in pGAD424, were identified by digestion with *Eco*R I which produced bands sized 6825 bp and 825 bp with the correct pGAD424-gene 9 clones (Figure 4.18, Panel A). The junction region was sequenced to confirm that the reading frame between the GAL4 domain sequence and gene 9 was maintained, ensuring the production of the desired fusion protein (Figure 4.18,

Figure 4.17 Analysis of pGBT9-Gene 9 by restriction enzyme digestion and sequencing of the junction region

A. Restriction enzyme digestion analysis of clone pGBT9-Gene 9

Plasmid DNA from the sub-cloning of gene 9 into the *Pst* I site in the MCS of pGBT9 was prepared by mini-prep (Section 3.4.13) and analysed by restriction enzyme digestion (Section 3.4.6). The products of the digests were analysed by electrophoresis on a 1.0 % TAE agarose gel (Section 3.4.3). The lanes marked pGBT9 contain the vector digested with the enzymes indicated. Lanes marked G9 contain clones of pGBT9-gene9 digested with the enzymes indicated. Digestion of pGBT9 with *Pst* I or *Eco*R I linearises the plasmid (5500 bp). Digestion of pGBT9-gene 9 with *Pst* I releases the insert (5500 bp and 1076 bp). Predicted band sizes from the digestion of pGBT9-gene 9 with *Eco*R I are 5725 bp and 825 bp (positive orientation; clones 3, 6, and 7) and 6300 bp and 250 bp (negative orientation; clones 8 and 9). Lanes marked L were loaded with 1 kb DNA ladder. The sizes of the markers are given in base pairs.

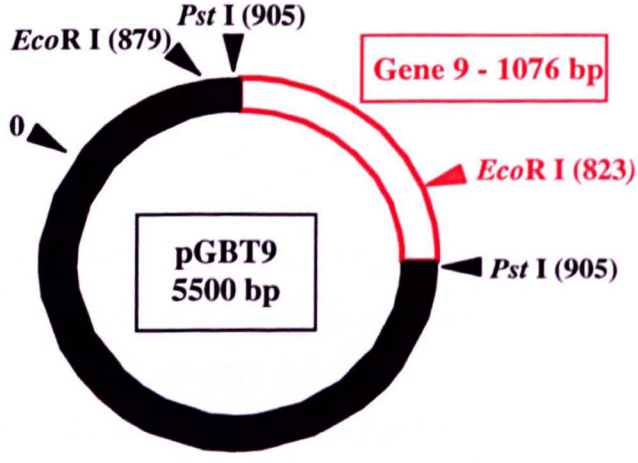

B. Sequence analysis of pGBT9-Gene 9 junction region

The junction region of plasmid pGBT9-gene9 [G9(3)], at the 5' end of gene 9, was sequenced (Section 3.4.18) using Primer 1 (Table 3.3) to ensure the correct framing for the production of the desired fusion protein. An original sequence trace and a schematic diagram of the junction region are shown. The sequence at the junction region, which includes the GAL4 DNA-binding domain sequence (blue on the schematic diagram), the UKtc gene 9 sequence (yellow) and the *Pst* I cloning site (red) which was used to produce the in-frame clone, is shown. The ATG start site in gene 9 is underlined in bold. The nucleotides at positions 56 and 57 on the sequence trace have been incorrectly assigned and should read C and G. Approximately 100 bp of sequence at the 5' end of gene 9 was also checked in this analysis. The sequence analysis was repeated at least twice to confirm the junction region sequence.

Figure 4.17

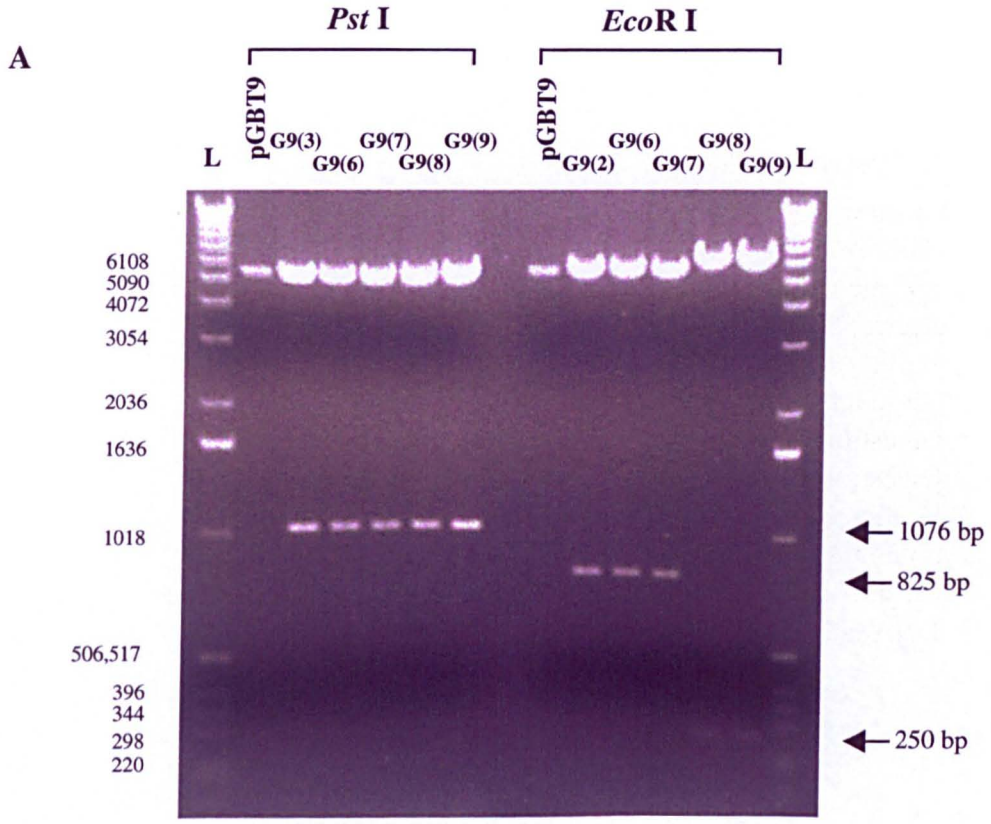

B. pGBT9-Gene 9 junction region sequence

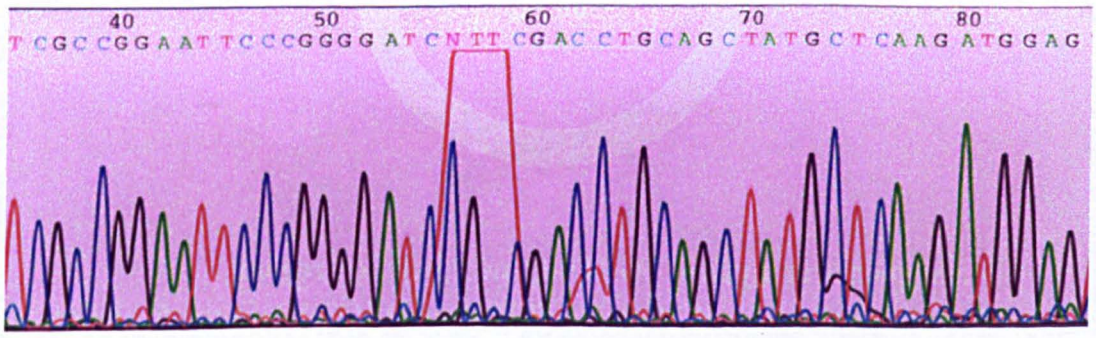

GAL4 DNA-binding domain *Pst* I **UKtc gene 9**

TCG CCG GAA TTC CCG GGG ATC CGT CGA C**CT GCA G**CT **ATG** CTC AAG ATG GAG

Figure 4.18 Analysis of pGAD424-Gene 9 by restriction enzyme digestion and sequencing of the junction region

A. Restriction enzyme digestion analysis of clone pGAD424-Gene 9

Plasmid DNA from clones created following the ligation of gene 9 into the *Pst* I site of the MCS of pGAD424, was prepared by mini-prep (Section 3.4.13) and analysed by restriction enzyme digestion (Section 3.4.6). The products of the digests were analysed by electrophoresis on a 1.0 % TAE agarose gel (Section 3.4.3). Lanes marked pGAD424 contain the vector digested with the enzymes indicated. Lanes marked G9 contain clones of pGAD424-gene9 digested with the enzymes indicated. Digestion of pGAD424 with *Pst* I or *Eco*R I linearises the plasmid (6600 bp). Digestion of pGAD424-gene 9 with *Pst* I releases the insert (6600 bp and 1076 bp). Predicted band sizes from the digestion of pGAD424-gene 9 with *Eco*R I are 6825 bp and 825 bp (positive orientation; clones 3, 4, 7 and 10) and 7400 bp and 250 bp (negative orientation; clones 2 and 9). One clone had bands at both 825 bp and 250 bp (clone 6). Lanes marked L were loaded with 1 kb DNA ladder. The sizes of the markers are given in base pairs.

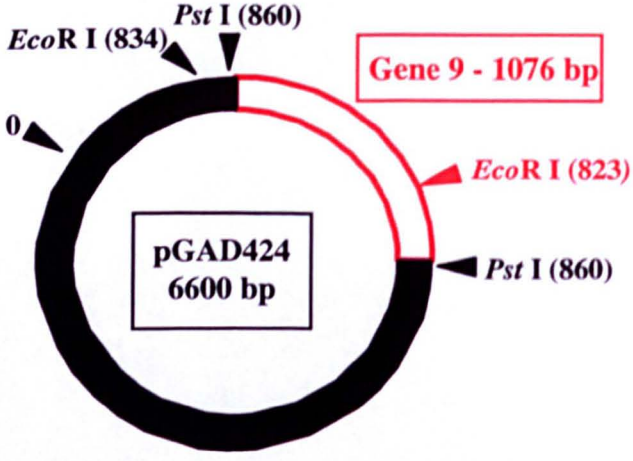

B. Sequence analysis of pGAD424-Gene 9 junction region

The junction region of plasmid pGAD424-gene9 [G9(3)], at the 5' end of gene 9, was sequenced (Section 3.4.18) using Primer 2 (Table 3.3) to ensure the correct framing for the production of the desired fusion protein. An original sequence trace and a schematic diagram of the junction region are shown. The sequence at the junction region, which includes the GAL4 activation domain sequence (blue on the schematic diagram), the UKtc gene 9 sequence (yellow) and the *Pst* I cloning site (red) which was used to produce the in-frame clone, is shown. The ATG start site in gene 9 is underlined in bold. The nucleotides at positions 57-60 on the sequence trace have been incorrectly assigned and should all read A. Approximately 50 bp of sequence at the 5' end of gene 9 was also checked in this analysis. The sequence analysis was repeated at least twice to confirm the junction region sequence.

Figure 4.18

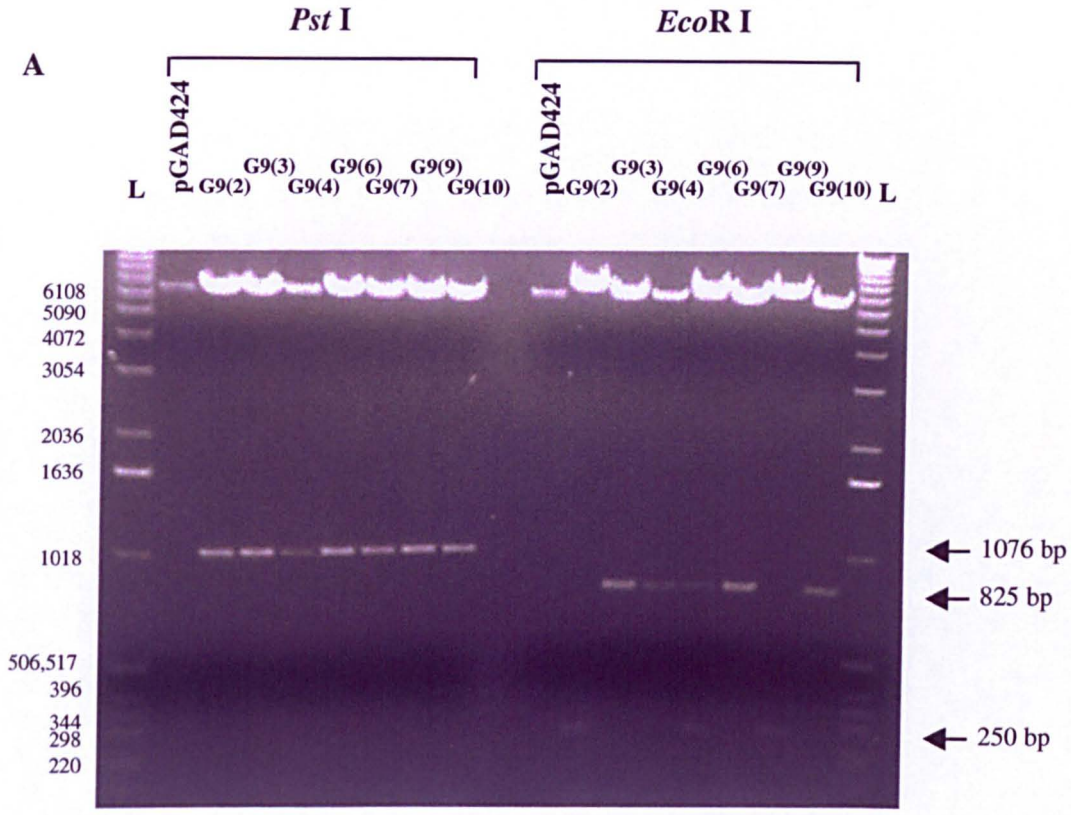

B. pGAD424-Gene 9 junction region sequence

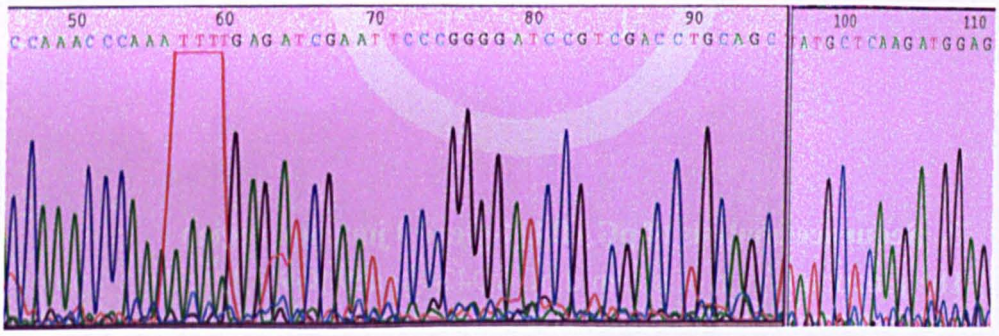

GAL4 activation domain

CCA AAC CCA AAA AAA GAG ATC GAA TTC CCG GGG ATC CGT

CGA CCT GCA GCT ATG CTC AAG ATG GAG

Pst I UKtc gene 9

Panel B). In addition, approximately 50 bp at the 5' end of gene 9 was also sequenced and checked against the original sequence (data not shown).

4.6 Conclusions

This chapter describes the cloning of rotavirus genes from the UKtc strain of bovine rotavirus into the yeast two-hybrid vectors (pGBT9 and pGAD424) to create constructs which could express fusion proteins of the GAL4 DNA-binding and activation domains with the proteins VP1 (gene 1), VP2 (gene 2), VP3 (gene 3), NSP1 (gene 5) and NSP3 (gene 9). A complete list of all the clones generated is given (Table 4.1). The constructs created were all analysed by restriction enzyme digestion to ensure the correct orientation of the insert. The junction region between the GAL4 domain and the rotavirus gene in each case was sequenced to ensure that the reading frame was maintained and thus the relevant fusion protein would be produced. Sequence at the 5' end of each rotavirus gene was checked against the original sequence data to ensure that no deleterious mutations had been introduced during PCR amplification. Further, the expression of some of the PCR amplified rotavirus genes was verified in an *in vitro* expression system when full-length proteins of the appropriate size were produced.

Table 4.1 Identification of clones generated during construction of plasmids for use in the yeast two-hybrid assay

Plasmids	Total clones generated	Identification	Sequence data	Additional notes
pGBT9-gene5	2	G5(7) G5(10)	Both clones contained additional sequence at 5'-end	G5(7) used for subsequent cloning to produce correct 5'-end
	16	G5(1);G5(2); G5(5);G5(7);G5(9)	All clones had correct 5'-end and junction region	G5(1) used for assays
pGBT9-geneΔ5	2	Δ5(7);Δ5(10)	Δ5(10)-correct junction region	Δ5(10) used in assays
pGAD424-gene5	2	G5(15); G5(18)	G5(15)–correct junction region	G5(15) used in assays
pTAg-gene1	6	G1(6):(8):(12): (14):(15):(17).	-	G1(8) used for sub-cloning
pGAD424-gene1	1	Clone 6: 6(1); 6(2)	6(1)-correct junction region	Clone 6 identified by Grunstein assay (3.4.16). Stock 6(1) used in assays
pGBT9-gene1	2	G1(5); G1(6)	Both clones correct junction	Sub-cloned from 6(1); G1(5) used in assays
pTAg-gene2	13	G2(2):(4-6): (8):(10-16):(20)	-	G2(6), G2(8) (negative orientation) used for sub-cloning
pGAD424-gene2	1	G2(10)	Correct junction	G2(10) used for assays and sub-cloning
pGBT9-gene2	1	G2(2)	Correct junction	G2(2) used for assays
pTAg-gene3	4	G3(1):(10):(15): (17)	-	G3(17) used for sub-cloning
pGAD424-gene3	3	G3(2);G3(4);G3(7)	Correct junction	-
pGBT9-gene3	7	G3(2);G3(3); G3(4);G3(7);G3(9; G3(10);G3(11).	G3(2);G3(3)- correct junction region	G3(2) used in assays
pCR2.1-gene9	5	G9(1):(3):(5):(6): (7)	-	G9(3) used for sub-cloning
pGBT9-gene9	3	G9(3);G9(6);G9(7)	G9(3) sequenced-correct junction	G9(3) used in assays
pGAD424-gene9	4	G9(3);G9(4); G9(7);G9(10).	G9(3) sequenced-correct junction	G9(3) used in assays

Results Chapter 2

Analysis of rotavirus protein-protein interactions using the yeast two-hybrid system

5.1 Aims

This chapter describes the use of the yeast two-hybrid system to analyse rotavirus protein-protein interactions. The aim was to determine if direct protein-protein interactions occurred between the rotavirus non-structural protein NSP1 and other viral proteins. The proteins which were chosen for analysis were either those found in an initial complex with NSP1 identified in infected cells (Patton, 1995), or those added to the complex at later times in the replication cycle. A secondary aim was to determine if NSP1 interacted with itself to form dimers.

5.2 Introduction

The exact functions of the viral-encoded non-structural proteins in the rotavirus replication cycle are, as yet, unknown. However, it is probable that they are involved in a variety of events, such as genome replication and gene assortment. The viral non-structural protein NSP1 is expressed at low levels early in infection and is thought to function at an early stage of viral replication (Johnson and McCrae, 1989). It has been identified as a component of a pre-core replication intermediate (RI) together with the viral proteins VP1, VP3 and NSP3 (Gallegos and Patton, 1989). The core RI is formed by the addition of VP2 to the pre-core RI. In order to gain insight into the role that NSP1 plays in the viral replication cycle, potential protein-protein interactions between NSP1 and the other components of the pre-core and core RIs were investigated using the yeast two-hybrid system, which has been shown to be a sensitive method for detection of protein-protein interactions *in vivo* (Fields and Song, 1989) (Section 4.2.1).

The cDNAs of selected genes from the UKtc strain of bovine rotavirus were cloned into two-hybrid vectors in order to produce fusions of each rotavirus protein with both the GAL4 DNA-binding and activation domains (Chapter Four). The objective was then to test these constructs in the yeast two-hybrid system and investigate potential interactions between NSP1 and the other components of the pre-core RI, VP1, VP3 and NSP3, and also VP2 which is added subsequently to form the core RI. Possible dimerisation of the non-structural proteins, NSP1 and NSP3, was also investigated.

A cDNA of a mutant gene 5, encoding a truncated NSP1 consisting of only the amino terminal third of the protein, was also utilised to produce GAL4 fusion proteins. The mutant gene 5, p9Δ5, was obtained during plaque purification undertaken as part of the biological cloning of a field isolate of virus (Tian *et al.*, 1993). It has a single 308 bp deletion in the centre of the normal gene 5 sequence, which causes a frameshift resulting in a stop codon eight amino acids (aa) downstream of the deletion. The resulting truncated protein product has a predicted size of 150 aa compared to the normal size of NSP1 of 490 aa. Viruses containing this truncated mutant gene 5 (Δ5) are non-defective in tissue culture (Tian *et al.*, 1993), indicating that the carboxy terminus of the protein may not be essential for gene function in tissue culture, although it might still have an important function in natural infections. A highly conserved cysteine-rich region, which contains a generalised motif for a metal binding domain, has been recognised near the amino terminal end of the gene (Mitchell and Both, 1990a). The fact that this region is conserved may be indicative of its functional importance. The truncated mutant NSP1 was studied as it is viable *in vivo* and contains the proposed functional domains of the protein.

Yeast strains were transformed with the constructs and transformant colonies were selected on limiting media according to the nutritional gene (TRP1 or LEU2) carried on the plasmids encoding the GAL4 fusion proteins (Figure 4.1). In the assay for protein-protein interactions, colonies co-transformed with constructs expressing fusions with both GAL4 domains were selected on limiting media lacking both the amino acids tryptophan and leucine. As the reporter gene used in the assay was *lacZ*, an assay for β-galactosidase activity was then used to determine if a protein-protein interaction was occurring.

Blue/white screening of transformant yeast colonies, using a colony lift filter assay for β-galactosidase, was most commonly used to detect expression of the reporter gene. A liquid β-galactosidase assay was also used to provide a quantitative evaluation of the level of expression of *lacZ*, which has been suggested to reflect semi-quantitatively the stability of the interaction between the proteins under study (Li and Fields, 1993) (Estojak *et al.*, 1995). The filter assay for β-galactosidase used X-gal as the chromogenic substrate, which is approximately 10^6 times more sensitive than ONPG, which was the substrate for the liquid assay. Transient or weak two-hybrid interactions may not be quantifiable by ONPG. Hence, the filter assay

with X-gal was used to screen for protein interactions, which once identified were subsequently quantified using the liquid assay with ONPG.

Before screening for protein-protein interactions commenced, the GAL4 fusion constructs were tested alone in the yeast two-hybrid system. It is important to ensure, prior to analysis, that the proteins under test do not have intrinsic DNA-binding or transcriptional activating properties that would produce a false positive in the assay. If a protein does have intrinsic DNA-binding or transcriptional activating properties, which can compensate for the missing function of the other GAL4 domain, then transcription of the reporter gene will be activated and a false positive result will be obtained. Thus, to obtain meaningful results in the assay, each construct was tested to ensure it did not activate the reporter gene when present alone.

5.3 Preliminary control experiments for the yeast two-hybrid system

5.3.1 Yeast reporter strains

The genotypes of the *Saccharomyces cerevisiae* yeast reporter strains, which were used in this study, have been described previously (Table 3.2). The *Saccharomyces cerevisiae* strain SFY526 was recommended for use when testing for an interaction between known proteins, and was the strain most frequently used in this study. A second *Saccharomyces cerevisiae* strain, HF7c, was also used to verify the initial results. The main difference between the strains for the purpose of this study was in the promoter elements for the reporter gene *lacZ*. In SFY526, the GAL1 upstream activating sequence (UAS) and the TATA portion of the GAL1 promoter are fused to the *lacZ* reporter gene. In HF7c, three copies of the GAL4 17-mer consensus sequence and the TATA portion of the CYC1 promoter are fused to the *lacZ* reporter gene. The GAL1 UAS and the GAL4 17-mers are both responsive to the GAL4 transcriptional activator. Thus, the promoter elements in the yeast strains differ significantly with only the GAL4-responsive element in common. Therefore, a positive interaction which is observed in both yeast strains must be the result of the GAL4 DNA-binding domain binding specifically to the GAL4-responsive elements. As the promoter strengths differ between the two yeast strains, interactions which are observed in SFY526 may not be observed in HF7c. SFY526 gives stronger β-

galactosidase signals due to the GAL1 promoter driving expression of the *lacZ* gene, thus it was the reporter strain of choice in the study.

5.3.2 Phenotype verification of the yeast reporter strains

The nutritional requirement phenotypes of the yeast reporter strains SFY526 and HF7c were verified prior to transformation with the experimental two-hybrid plasmids. These two yeast strains are auxotrophic for both tryptophan and leucine, hence the untransformed yeast strains should not grow on media lacking these amino acids. Both yeast strains also have deletions in the *his3* gene, hence they will not grow on media lacking histidine. Strain HF7c contains the *HIS3* reporter gene under control of GAL4-responsive sequences, which are the GAL1 UAS and the TATA portion of the GAL1 promoter. This reporter gene is expressed in the presence of the GAL4 transcriptional activator.

Freshly grown yeast colonies were streaked onto plates containing the appropriate SD medium for testing each of the following four nutritional requirements: tryptophan (Trp), leucine (Leu), histidine (His) and uracil (Ura). After 6 days incubation at 30 °C both yeast strains had grown on the plates without Ura but not on the other three media as expected. Slow growth of strain HF7c was observed on the media lacking His, which was due to a low level leaky expression of the *HIS3* reporter gene. This test confirmed the nutritional requirement phenotypes of the yeast reporter strains.

5.3.3 Two-hybrid system control plasmids

Positive and negative control reactions were included in each two-hybrid assay. The control plasmids used are described in Table 5.1. The positive control plasmid for the assay, pCL1, encodes and expresses the full-length, wild-type GAL4 protein (Fields and Song, 1989). A second positive control used was a model of interacting proteins provided by plasmids pVA3 and pTD1. Plasmid, pVA3, encodes a fusion of the GAL4 DNA-binding domain with murine p53 (Iwabuchi *et al.*, 1993), and pTD1 encodes a fusion of the GAL4 activation domain with SV40 large T-antigen (Li and Fields, 1993) (Chien *et al.*, 1991). Murine p53 and SV40 large T-antigen have been shown to interact; indeed p53 was originally identified as a protein

Plasmid	Control	Description
pCL1	positive control plasmid	wild-type, full-length GAL4 gene LEU2, amp^R
pVA3	positive control plasmid	murine $p53_{(72-390)}$ in pGBT9 TRP1, amp^R
pTD1	positive control plasmid	SV40 large T-$antigen_{(84-708)}$ in pGAD3F LEU2, amp^R
pLAM5'	false positive detection plasmid	Human lamin $C_{(66-230)}$ in pGBT9 TRP1, amp^R

Table 5.1 Yeast two-hybrid system control plasmids

The table shows the control plasmids used to provide positive and negative controls in the yeast two-hybrid system. A description of each plasmid is given, detailing the type of control reaction it was used for and the genes carried on the plasmid. The abbreviations LEU2 and TRP1 refer to the wild-type genes for Leucine and Tryptophan. Amp^R refers to the resistance gene for ampicillin. The plasmids were provided in the Matchmaker Two-Hybrid System (Clontech).

bound to large T-antigen in SV40-transformed cells (Lane and Crawford, 1979) (Linzer and Levine, 1979). Thus, the purpose of this positive control transformation was to verify that the system was detecting an expected protein-protein interaction between two known interacting proteins. The plasmid pLAM5' encodes a human Lamin C/GAL4 DNA-binding domain hybrid (Bartel *et al.*, 1993). The transformation of yeast with pLAM5' and pTD1 was used as a negative control, as human Lamin C does not interact with SV40 large T-antigen.

5.3.4 Interaction of the human respiratory syncytial virus N and P proteins in the yeast two-hybrid system

A second positive control was used in addition to those provided in the Matchmaker Two-Hybrid System (Clontech). The yeast two-hybrid system was used to characterise an interaction between the phosphoprotein (P) and the nucleocapsid protein (N) of the human respiratory syncytial virus (hRSV) (Slack and Easton, 1998). The yeast strain SFY526 was transformed with plasmids encoding fusions of the two hRSV proteins (pGBT9-N and pGAD424-P) and an interaction was detected in the two-hybrid system.

5.3.5 Transformation of SFY526 with control fusion plasmids

Table 5.2 shows the results of the initial two-hybrid assay control experiments which were performed in the SFY526 yeast host strain. These control reactions were subsequently performed for each two-hybrid assay screening for rotavirus protein-protein interactions. The SFY526 yeast reporter strain was transformed with 1 μg of each plasmid, as indicated in the table. Initially 0.1 μg of each plasmid was used, however 1 μg was found to give a greater transformation efficiency. Transformant colonies were selected on dropout SD medium according to the nutritional gene (TRP1 or LEU2) carried on the plasmid. The following results were obtained in a β-galactosidase filter assay. Yeast colonies transformed with pCL1 expressed high β-galactosidase levels, as indicated by the fact that transformants turned blue in the presence of X-Gal in the filter assay within 15 minutes of the assay start time. Transformants carrying the positive control plasmids pVA3 and pTD1, which encode a model of interacting proteins, turned blue in the presence of X-Gal

Plasmid 1 DNA-Binding Domain	Plasmid 2 Activation Domain	Control	Selection on SD medium	Result in B-Galactosidase Assay
pCL1	-	Positive	- Leu	+ + +
pGBT9	pGAD424	Negative	- Leu, - Trp	-
pVA3	pGAD424	Negative	- Leu, - Trp	-
pGBT9	pTD1	Negative	- Leu, - Trp	-
pVA3	pTD1	Positive	- Leu, - Trp	+ +
pLAM5'	pTD1	Negative	- Leu, - Trp	-
pGBT9-N	pGAD424-P	Positive	- Leu, - Trp	+ + +

Table 5.2 Results of the two-hybrid system control reactions in strain SFY526

The table shows the results of a β-galactosidase filter assay performed with colonies of the yeast reporter strain SFY526 transformed with the two-hybrid system control plasmids. The yeast two-hybrid system control plasmids and the control reactions they provide are shown. Transformation of SFY526 with the hybrid plasmids indicated in the table was performed by the lithium acetate/heat shock method as described (Section 3.5.1 and 3.5.2). The transformed yeast were plated on SD selection media (Section 3.1.10) lacking the amino acids leucine (-Leu) and/or tryptophan (-Trp). The β-galactosidase filter assay was performed using plates containing the freshly transformed colonies (Section 3.5.3), and the filters were incubated in the Z buffer/X-gal solution at 30 °C until blue colonies appeared or until background expression of the reporter gene was observed at 480 minutes (8 hours). The colour of the colonies was described as white (negative) (-) or blue (positive) (+, + +, or + + +) depending on the relative strength of the blue colour reaction.

within 30 minutes. Transformants carrying pGBT9-N and pGAD424-P, which encode a model of interacting proteins from hRSV, also turned blue in the presence of X-Gal in less than 30 minutes. Thus, all positive control reactions gave the expected result in the β-galactosidase filter assay. The human Lamin C protein, encoded by pLAM5', does not interact with SV40 large T-antigen, so the reaction with plasmids pLAM5' and PTD1 was included to detect false positives. In addition, SFY526 was co-transformed with the vectors pGBT9 and pGAD424 to ensure that the reporter gene was not activated when the GAL4 domains were expressed separately. Additional negative control reactions were also performed as described in Table 5.2. All the control reactions gave the expected results, indicating that the assay was functioning correctly.

In addition to the control two-hybrid reactions, it was also necessary to transform the SFY526 yeast reporter strain with the experimental hybrid constructs alone (e.g. pGBT9-gene9) and together with the opposing empty vector (e.g. pGBT9-gene9 plus pGAD424), prior to screening for protein-protein interactions. These transformations were performed to verify that the experimental hybrid constructs did not activate the reporter gene when present alone to give a false positive result in the assay. It was a test for any inherent DNA-binding or transcriptional activation properties in the rotavirus proteins cloned into the two-hybrid vectors. Transformation of the constructs with the opposing empty vectors was performed to detect any false positives generated by an interaction between the protein of interest and either of the GAL4 domains. In most cases the results of these experimental transformations were negative, with the notable exception of the transformation of pGBT9-gene 9 (Section 5.4.2). These results are fully discussed with the results of the appropriate two-hybrid assay (Sections 5.4 -5.7).

5.3.6 Expression of two-hybrid fusion proteins in the yeast reporter strain SFY526

The cDNAs encoding each rotavirus protein to be studied were cloned into the two-hybrid vectors so that a fusion protein would be produced with each GAL4 domain. The junction regions between the genes encoding the GAL4 domain and the rotavirus protein were checked by sequence analysis for each construct to ensure that a fusion protein would be produced. It was also desirable that the expression of each

GAL4 fusion protein in yeast was confirmed. Expression of the fusion proteins can be verified by western blotting provided specific antibodies are available. The fusion proteins must be stably expressed in the yeast cell for the two-hybrid assay to function. However, the fusion proteins are expressed from a truncated ADH1 promoter and the low level of expression means they can be extremely difficult to detect on a western blot. In addition, monoclonal antibodies that bind specifically to the major activation domain (aa 768-881) or the DNA-binding domain (aa 1-147) of the yeast GAL4 protein do not detect fusion proteins generated with the low expression GAL4 two-hybrid cloning plasmids pGBT9 and pGAD424 on a western blot. Despite this fact, other researchers have proven protein-protein interactions using constructs generated with pGBT9 and pGAD424 when expression could not be detected by western blotting (Slack, 1998).

Analysis of expression of the fusion proteins in yeast reporter strain SFY526 was attempted using antibodies raised against rotavirus proteins. To detect fusion proteins of NSP1, a monospecific anti-NSP1 serum was used. A polyclonal serum raised against the UKtc strain of bovine rotavirus was used to analyse expression of GAL4 fusion proteins of VP1, VP2 and VP3. A biotinylated goat anti-rabbit IgG antibody was used as the secondary antibody in each case. However, analysis of the western blot did not reveal any unique bands corresponding to GAL4 fusion proteins (data not shown). The failure to detect the GAL4 fusion proteins on western blots was probably due to the low expression of the proteins from the two-hybrid plasmids. However, despite the low expression of the fusion proteins the fact that positive interactions were detected in some cases demonstrates that this system could be successfully used to detect interactions between rotavirus proteins (Section 5.4).

5.4 Analysis of dimerisation of NSP3 in the yeast two-hybrid system

5.4.1 NSP3 may form dimers in rotavirus-infected cells

The rotavirus non-structural protein NSP3 has been shown to form oligomers in rotavirus-infected cells, insect cells and in a cell-free translation system (Mattion *et al.*, 1992). NSP3 is encoded by gene 7 in the SA11 4F strain of simian rotavirus and by gene 9 in the UKtc strain of bovine rotavirus. Mattion *et al.* (1992) described homo-oligomers of NSP3 in insect cells infected with a baculovirus expression vector

expressing the SA11 4F gene 7 product NSP3. They found different sized oligomers, C1 and C2, by analysis of complexes from infected cells on non-reducing gels and by western blotting. C2 was thought to be a homodimer, while C1 was likely to be a multimer of NSP3. Both homo-oligomers were also seen in a cell-free translation system, however in SA11-infected MA104 cells only the dimer of NSP3 (C2) was seen. A complex thought to be a dimer of NSP3 was detected in SA11-infected MA104 cells on a non-reducing gel by western blotting with antiserum produced against recombinant NSP3. The complex which was detected migrated to the same position on the gel as C2, and therefore was thought to be analogous to it. However, this result did not confirm a direct self-interaction of NSP3 in mammalian cells, or rule out the possible presence of small amounts of another protein(s) in this complex. A conserved region of hydrophobic repeats and a leucine zipper at the carboxy terminus of the protein was implicated in the oligomerisation. It has also been suggested that conserved cysteine residues in the protein may form disulphide bridges, thus stabilising the intermolecular interaction. However, given the highly reducing environment of the cytoplasm, it is possible that disulphide-linked oligomers might be formed following cell lysis and are not actually present in the cell (Piron *et al.*, 1999). Therefore, dimerisation of NSP3 *in vivo* was not directly demonstrated.

5.4.2 Dimerisation of NSP3 can be quantified in the yeast two-hybrid system

Previous work has suggested that NSP3 forms a dimer in SA11 rotavirus-infected cells (Mattion *et al.*, 1992). Hence, it was expected that dimerisation of NSP3 would also occur with the protein from the UKtc strain of bovine rotavirus. The yeast two-hybrid system was used to demonstrate a direct self-interaction of NSP3 from the UKtc strain. Plasmids encoding fusions of the GAL4 DNA-binding and activation domains with NSP3 were created (Section 4.5) and tested alone in the two-hybrid system. A β-galactosidase filter assay showed SFY526 colonies transformed with pGBT9-gene 9 alone produced a blue colour, indicating activation of the reporter gene, after 120 minutes incubation at 30 °C. By contrast, colonies transformed with the plasmid pGAD424-gene 9 gave a negative result, even after a maximum incubation time of eight hours. This positive result was repeated in the HF7c yeast reporter strain, although the time taken for the blue colour to appear in colonies transformed with pGBT9-gene 9 was longer (4 hours). This may

have been due to the weaker promoter in the HF7c strain. This result suggested that NSP3 may have some intrinsic transcriptional activation properties, which can complement the DNA-binding activity of the GAL4 domain expressed by pGBT9, to activate the reporter gene.

A two-hybrid assay was performed to determine if dimerisation of NSP3 could be detected *in vivo*. The SFY526 yeast reporter strain was transformed with the two-hybrid plasmids encoding NSP3, pGBT9-gene 9 and pGAD424-gene 9, and the appropriate control plasmids. Co-transformation efficiencies were approximately 10^3 cfu/μg DNA (see Appendix 1.2 for equation) and thus within the expected range of 10^3-10^4 cfu/μg DNA for the double plasmid transformation. The transformed colonies were screened using a β-galactosidase filter assay to detect expression of the *lacZ* reporter gene (Table 5.3). Colonies co-transformed with the two plasmids encoding fusions of NSP3 (pGBT9-gene 9 and pGAD424-gene 9) turned blue within 30 minutes of the assay start time, indicating that a dimerisation of NSP3 was occurring. The control plates containing colonies transformed with pGBT9-gene 9 alone turned blue 120 minutes after the assay start time which was a false positive result. As the gap between the appearance of the blue colour in the colonies co-transformed with both gene 9 hybrid plasmids and the false positive of pGBT9-gene 9 alone was considerable, it seems likely that a true self-interaction of NSP3 did occur. If it were merely a false positive, then the colonies transformed with both constructs and those transformed with a single construct would be expected to turn blue at a similar time.

To confirm and quantify this result, a liquid culture β-galactosidase assay (ONPG assay) was performed. Colonies screened by the β-galactosidase filter assay were allowed to regrow, then picked into SD selection media and the ONPG assay was performed as described (Table 5.3). B-galactosidase units were calculated for each transformation. Colonies transformed with the positive control plasmid pCL1, which is a wild-type GAL4 control, produced a very high level of β-galactosidase (466.1 ± 52.2 β-galactosidase units) as expected. The model of interacting proteins provided by pVA3 and pTD1 also produced a high level of β-galactosidase (78.9 ± 22 β-galactosidase units). Although the margin of error appears to be quite large, it is in fact less than the variation reported by other researchers (Iwabuchi *et al.*, 1993) (Chien *et al.*, 1991). Results equating to extremely low levels of β-galactosidase (β-galactosidase units ≤ 0.1), such as those obtained for the control transformation,

Table 5.3

DNA-binding domain hybrid plasmid	Activation domain hybrid plasmid	Selection on SD medium	Result of β-galactosidase filter assay	Time elapsed in β-galactosidase filter assay (minutes)	Result of ONPG assay (β-galactosidase units)
pCL1	-	-Leu	+ + +	30	466.1 ± 52.2
pVA3	pTD1	-Leu, -Trp	+ +	30	78.9 ± 22
pGBT9	pGAD424	-Leu, -Trp	-	360	0.02 ± 0.006
pGBT9-Gene9	-	-Trp	+ +	120	0.57 ± 0.07
-	pGAD424-Gene9	-Leu	-	360	0.02 ± 0.001
pGBT9-Gene9	pGAD424	-Leu, -Trp	+ +	120	0.59 ± 0.09
pGBT9	pGAD424-Gene9	-Leu, -Trp	-	360	0.07 ± 0.03
pGBT9-Gene9	pGAD424-Gene9	-Leu, -Trp	+ +	30	37.3 ± 7.5

Table 5.3 Dimerisation of NSP3 can be quantified in the yeast two-hybrid system

The results of a yeast two-hybrid assay to analyse and quantify the dimerisation of NSP3 are shown. Transformation of SFY526 with the hybrid plasmids indicated in the table was performed by the lithium acetate/heat shock method as described (Section 3.5.1 and Section 3.5.2). The transformed yeast were plated on SD selection media (Section 3.1.10) lacking the amino acids leucine (-Leu) and/or tryptophan (-Trp). All the control reactions detailed previously (Table 5.2) were performed in conjunction with the experimental reactions and gave the expected results. The β-galactosidase filter assay was performed using plates containing the freshly transformed colonies (Section 3.5.3), and the filters were incubated in the Z buffer/X-gal solution at 30 °C until blue colonies appeared or until background expression of the reporter gene was observed at 360 minutes (6 hours). The colour of the colonies was described as white (negative) (-) or blue (positive) (+, + +, or + + +) depending on the relative strength of the blue colour reaction. The liquid culture β-galactosidase assay (ONPG assay) was performed as described (Section 3.5.4). SD medium was inoculated with yeast colonies transformed with the hybrid plasmids and the cultures incubated overnight at 30 °C with shaking. The overnight culture was then used to inoculate fresh YPD medium and the culture was incubated as before for approximately 240 minutes (four hours) until the required OD_{600} reading (OD_{600} = 0.5-1.0) was obtained. The ONPG assay was performed in triplicate with two dilutions of the culture (concentration factor = 5 and concentration factor = 3) for each transformation (i.e. six times for each transformation). The assay was stopped when the yellow colour developed and OD_{420} readings were taken (OD_{420} = 0.02-1.0). OD_{420} readings must be within the margin 0.02-1.0 in order for β-galactosidase units to be calculated accurately. The assay was incubated overnight to allow weaker interactions to develop. B-galactosidase units were calculated from the OD_{420} readings obtained. The mean was derived and error bars were calculated within the 95 % confidence limits of the Students t test. (Appendix 1.1).

pGBT9 plus pGAD424, were considered negative. The β-galactosidase levels for the controls of pGBT9-gene 9 alone or with vector pGAD424, which gave false positive results in the filter assay, were considerably less than that reported for the co-transformation (β-galactosidase units < 1) and were considered to be negative. The result for the colonies co-transformed with pGBT9-gene 9 and pGAD424-gene 9 in the ONPG assay was 37.3 ± 7.5 β-galactosidase units. This was a sufficient increase in the level of β-galactosidase activity for the interaction to be considered a true positive. Indeed, a two to four fold increment from background activity has been considered significant, as such increments in activity from background enzyme levels have previously been associated with specific protein-protein interactions (Li and Fields, 1993) (Rossi *et al.*, 1996).

The NSP3 fusion proteins were expressed in yeast, and interacted to form a dimer such that the interaction could be detected in the yeast two-hybrid system. A positive result was produced both in a colony lift filter β-galactosidase assay and in a liquid (ONPG) β-galactosidase assay. The interaction was quantified as 37.3 ± 7.5 β-galactosidase units. This result suggests that the self-interaction of NSP3 is approximately half as strong as the interaction between p53 and SV40 large T-antigen in this assay. The interaction of the NSP3 protein could be considered as an internal positive control in two-hybrid assays for protein interactions between other rotavirus proteins.

5.5 Analysis of NSP1 using the yeast two-hybrid system

5.5.1 Two-hybrid assay to determine whether NSP1 forms dimers

The yeast two-hybrid system was employed to examine the hypothesis that NSP1 may interact with itself to form a dimer. Dimerisation of NSP3, which is present in early replication complexes with NSP1, has already been shown (Section 5.4.2.). However, the possibility that NSP1 may also undergo dimerisation has not been previously investigated.

Plasmids encoding fusions of the GAL4 DNA-binding and activation domains with both full length and truncated NSP1 were created (Section 4.3) and tested in the two-hybrid system. When the SFY526 yeast reporter strain was transformed with each experimental plasmid alone, a negative result was obtained in the β-galactosidase

filter assay (Table 5.4). This result was repeated with the HF7c yeast strain transformed with the plasmids separately and tested in a β-galactosidase filter assay with a maximum incubation time of eight hours (data not shown).

A two-hybrid assay was performed with yeast strain SFY526 which was co-transformed with the two-hybrid plasmids encoding full length NSP1 (pGBT9-gene 5 and pGAD424-gene 5) and the truncated mutant of NSP1 (pGBT9-gene Δ5 and pGAD424-gene 5), together with the appropriate control plasmids. Co-transformation efficiencies for the experimental plasmids were approximately 10^3 cfu/μg DNA (see Appendix 1.2). The transformed colonies were screened using a β-galactosidase filter assay to detect expression of the *lacZ* reporter gene (Table 5.4). Colonies transformed with the control reaction of plasmids pGBT9-gene Δ5 and pGAD424 turned very pale blue 240 minutes after the assay start time. This false positive result was probably due to a low level leaky expression of the reporter gene which occasionally occurred. The control co-transformation of pGBT9 and pGAD424-gene 5 also gave a false positive result after 300 minutes incubation. The co-transformation of the experimental constructs, pGBT9-gene Δ5 and pGAD424-gene 5, gave a weakly positive result, as indicated by faint blue colonies, after 300 minutes. However, this was also thought to be a false positive result and due to leaky expression of the reporter gene, as with the control reactions. Colonies co-transformed with the two plasmids encoding fusions of full length NSP1 remained white, even after a maximum assay incubation time of eight hours. This negative result suggested that a dimerisation of NSP1 did not occur. In conclusion, dimerisation of NSP1 was not detected, either between full length NSP1 or with the amino terminus of the protein only, under the conditions of the two-hybrid assay.

5.6 Investigation of protein-protein interactions between NSP1 and NSP3

5.6.1 Assay for a potential interaction between NSP1 and NSP3

The yeast two-hybrid system was employed to test for a potential interaction between the viral non-structural proteins NSP1 and NSP3. Both proteins are found in the pre-core RI at an early stage of the viral replication cycle (Section 5.2). Although NSP1 and NSP3 both localise to the cytoplasm and are known to bind mRNA, it was not known whether a protein-protein interaction occurred between the two proteins.

DNA-binding domain hybrid plasmid	Activation domain hybrid plasmid	Selection on SD medium	Result of β-galactosidase filter assay	Time elapsed in β-galactosidase filter assay (minutes)
pCL1	-	-Leu	+ + +	30
pGBT9	pGAD424	-Leu, -Trp	-	300
pVA3	pTD1	-Leu, -Trp	+ +	30
pLAM5'	pTD1	-Leu, -Trp	-	300
pGBT9-N	pGAD424-P	-Leu, -Trp	+ + +	30
pGBT9-gene 5	-	-Trp	-	300
pGBT9-gene Δ5	-	-Trp	-	300
-	pGAD424-gene 5	-Leu	-	300
pGBT9-gene 5	pGAD424	-Leu, -Trp	-	300
pGBT9-gene Δ5	pGAD424	-Leu, -Trp	+ / -	240
pGBT9	pGAD424-gene 5	-Leu, -Trp	+/-	300
pGBT9-gene 5	pGAD424-gene 5	-Leu, -Trp	-	300
pGBT9-gene Δ5	pGAD424-gene 5	-Leu, -Trp	+/-	300

Table 5.4 Two-hybrid assay for potential dimerisation of NSP1

The results of a yeast two-hybrid assay for a potential dimerisation of NSP1 are shown. Transformation of SFY526 with the hybrid plasmids indicated in the table was performed by the lithium acetate/heat shock method as described (Section 3.5.1 and 3.5.2). The transformed yeast were plated on SD selection media (Section 3.1.10) lacking the amino acids leucine (-Leu) and/or tryptophan (-Trp). All the control reactions detailed previously (Table 5.2) were performed in conjunction with the experimental reactions and gave the expected results. The β-galactosidase filter assay was performed using plates containing the freshly transformed colonies (Section 3.5.3), and the filters were incubated in the Z buffer/X-gal solution at 30 °C until blue colonies appeared or until background expression of the reporter gene was observed at 300 minutes. The colour of the colonies was described as white (negative) (-) or blue (positive) (+, + +, or + + +) depending on the relative strength of the blue colour reaction. A faint blue colour, which appeared after several hours incubation and was thought to be background was also described (+/-). The results presented represent three repeats of the experiment.

The yeast reporter strain SFY526 was transformed with plasmids expressing fusions of NSP1 and NSP3 with both the GAL4 DNA-binding and activation domains in all possible combinations and with the appropriate controls, and a β-galactosidase filter assay was used to screen for potential interactions. The efficiency of the double plasmid co-transformation was calculated to be approximately 5 x 10^2 cfu/μg DNA and was found to be slightly higher for the experimental constructs compared to the control constructs.

The results of the β-galactosidase filter assay for the controls and experimental transformations are shown (Table 5.5). All the control transformations gave the expected results. After 120 minutes incubation, colonies transformed with plasmid pGBT9-gene 9 alone or together with vector pGAD424, gave a false positive result. As discussed previously (Section 5.4.2), this was due to activation of the reporter gene by NSP3 fused to the GAL4 DNA-binding domain, and was thought to be due to a transcriptional activation property of NSP3. Colonies co-transformed with pGBT9-gene 9 and the construct expressing a fusion of NSP1 with the GAL4 activation domain (pGAD424-gene 5), turned blue after 180 minutes incubation. However, colonies transformed with constructs expressing the proteins fused to the opposite GAL4 domains (i.e. pGBT9-gene 5 and pGAD424-gene 9), produced a negative result. Hence, a true protein-protein interaction was not detected between NSP1 and NSP3. A liquid (ONPG) β-galactosidase assay also failed to detect an interaction between NSP1 and NSP3. A similar level of β-galactosidase was obtained for yeast colonies transformed with pGBT9-gene 9, irrespective of whether pGAD424-gene 5 was present. This indicated that the positive result which was observed in the filter assay was probably due to the activation of the reporter gene by NSP3 in yeast colonies transformed with plasmid pGBT9-gene 9, and thus a false positive result. A co-transformation was also performed with pGAD424-gene 9 and the plasmid expressing the truncated mutant of NSP1, pGBT9-gene Δ5 (Section 4.3.3). The results of the β-galactosidase assay for this co-transformation were also negative, confirming that an interaction could not be detected between NSP1 and NSP3.

Table 5.5

DNA-binding domain hybrid plasmid	Activation domain hybrid plasmid	Selection on SD medium	Result of β-galactosidase filter assay	Time elapsed in β-galactosidase filter assay (minutes)	Result of ONPG assay (β-galactosidase units)
pCL1	-	-Leu	+ + +	30	466.1 ± 52.2
pVA3	pTD1	-Leu, -Trp	+ +	30	78.9 ± 22
pGBT9	pGAD424	-Leu, -Trp	-	360	0.02 ± 0.006
pGBT9-Gene9	-	-Trp	+ +	120	0.57 ± 0.07
-	pGAD424-Gene9	-Leu	-	360	0.02 ± 0.001
pGBT9-Gene5	-	-Trp	-	360	-
-	pGAD424-Gene5	-Leu	-	360	-
pGBT9-Gene9	pGAD424	-Leu, -Trp	+ +	120	0.59 ± 0.09
pGBT9	pGAD424-Gene9	-Leu, -Trp	-	360	0.07 ± 0.03
pGBT9-Gene5	pGAD424	-Leu, -Trp	-	360	-
pGBT9	pGAD424-Gene5	-Leu, -Trp	-	360	0.08 ± 0.01
pGBT9-Gene5	pGAD424-Gene9	-Leu, -Trp	-	360	-
pGBT9-Gene9	pGAD424-Gene5	-Leu, -Trp	+ +	180	0.6 ± 0.05

Table 5.5 Yeast two-hybrid analysis of a potential protein-protein interaction between NSP1 and NSP3

The results of a yeast two-hybrid assay to analyse and quantify a potential interaction between NSP1 and NSP3 are shown. Transformation of SFY526 with the hybrid plasmids indicated in the table was performed by the lithium acetate/heat shock method as described (Section 3.5.1 and 3.5.2). The transformed yeast were plated on SD selection media (Section 3.1.10) lacking the amino acids leucine (-Leu) and/or tryptophan (-Trp). All the control reactions detailed previously (Table 5.2) were performed in conjunction with the experimental reactions and gave the expected results. The β-galactosidase filter assay was performed using plates containing the freshly transformed colonies (Section 3.5.3), and the filters were incubated in the Z buffer/X-gal solution at 30 °C until blue colonies appeared or until background expression of the reporter gene was observed at 360 minutes (6 hours). The colour of the colonies was described as white (negative) (-) or blue (positive) (+, + +, or + + +) depending on the relative strength of the blue colour reaction. The results presented represent three repeats of the experiment. The liquid culture β-galactosidase assay (ONPG assay) was performed as described (Section 3.5.4). SD medium was inoculated with yeast colonies transformed with the hybrid plasmids and the cultures incubated overnight at 30 °C with shaking. The overnight culture was then used to inoculate fresh YPD medium and the culture was incubated as before for approximately 240 minutes (four hours) until the required OD_{600} reading (OD_{600} = 0.5-1.0) was obtained. The ONPG assay was performed in triplicate with two dilutions of the culture (concentration factor = 5 and concentration factor = 3) for each transformation (i.e. six times for each transformation). The assay was stopped when the yellow colour developed and OD_{420} readings were taken (OD_{420} = 0.02-1.0). The assay was incubated overnight to allow weaker interactions to develop. B-galactosidase units were calculated from the OD_{420} readings obtained. OD_{420} readings must be within the margin 0.02-1.0 in order for β-galactosidase units to be calculated accurately. When the OD_{420} readings were less than 0.02, β-galactosidase units could not be calculated and no result is given for the ONPG assay. The mean value of β-galactosidase units was derived and error bars were calculated within the 95 % confidence limits of the Students t test. (Appendix 1.1).

5.6.2 Conclusions

A protein-protein interaction was not detected between NSP3 and either the full-length NSP1 or the truncated mutant NSP1. The results of a solid phase β-galactosidase filter assay and a liquid β-galactosidase assay (ONPG assay) confirmed this observation. In contrast to this result, an interaction between NSP1 and NSP3 from the YM strain of porcine rotavirus has been shown recently (González *et al.*, 1998). An interaction producing 3.4 units of β-galactosidase was detected in the yeast two-hybrid system. Although this value was only approximately two to four fold above background activity, it was considered to be significant and associated with a specific protein-protein interaction. It is not clear why different results were obtained in the yeast two-hybrid assays for an NSP1-NSP3 interaction, although it is not without precedent as a failure to detect demonstrated protein-protein interactions in the two-hybrid system has been documented previously (Van Aelst *et al.*, 1993) (Fields and Sternglanz, 1994). The results may have been due to differences in the virus strains used, leading to the production of fusion products which interact with differing affinities or are unable to interact. The nucleotide sequence of gene 5 from the YM strain of porcine rotavirus, which was used in the study by González *et al.* (1998), has not been published. Therefore, a direct comparison of the sequence differences with gene 5 from the UKtc strain of bovine rotavirus used in this study was not possible. However, previous studies have shown considerable sequence divergence between the bovine UKtc strain and other porcine strains, such as OSU (Xu *et al.*, 1994). On the basis of these observations, it is conceivable that the sequences of gene 5 from the strains used in the two studies were sufficiently different such that the resulting proteins might have different properties.

5.7 Investigation of potential protein-protein interactions between NSP1 and structural proteins of the virus core

5.7.1 Assay for a potential interaction between NSP1 and VP1

The yeast two-hybrid system was used to screen for a potential protein-protein interaction between NSP1 and the viral structural protein VP1, both of which are found in the viral pre-core RI. The yeast reporter strain SFY526 was transformed with experimental plasmids encoding fusions of NSP1 and VP1 with both the GAL4

DNA-binding and activation domains (Chapter Four) in all possible combinations and with the appropriate controls, and a β-galactosidase filter assay was used to screen for potential interactions (Table 5.6). The efficiency of the double plasmid co-transformation was calculated and it was found to be in the range 10^2-10^3 cfu/μg DNA and thus slightly lower than the expected range of 10^3-10^4 cfu/μg DNA. It was particularly notable that the transformation efficiency for the plasmid pGAD424-gene 1 was consistently lower compared to the other plasmids. It is possible that VP1 may have a slightly toxic effect when expressed in the yeast cell as a fusion protein with the GAL4 activation domain. This may account for the low transformation efficiency obtained with this particular plasmid.

The results of the β-galactosidase filter assay for the controls and experimental transformations are shown (Table 5.6). All the control transformations gave the expected results. After 240 minutes incubation the appearance of a very pale blue colour was observed with colonies that had been transformed with the experimental constructs alone, or together with the two-hybrid vector. False positive results can arise after prolonged incubation and may be due to a low level leaky expression of the reporter gene. It was observed that colonies transformed with the experimental constructs expressing NSP1 and VP1 in either GAL4 domain remained white. This result indicated that a protein-protein interaction was not detected between full length NSP1 and VP1 in the yeast two-hybrid system. The results of a liquid (ONPG) β-galactosidase assay also confirmed that an interaction could not be detected between NSP1 and VP1. It was not possible to calculate β-galactosidase units for the strength of the interactions, as the OD_{420} readings obtained in the assay were too low to be analysed ($OD_{420} < 0.02$) (data not shown).

The SFY526 yeast reporter strain was transformed with plasmids pGBT9-gene Δ5 and pGAD424-gene 1, which express GAL4 fusion proteins with truncated NSP1 and VP1 respectively. A β-galactosidase assay was performed and it was observed that colonies transformed with both the experimental constructs remained white, indicating that an interaction between NSP1 and VP1 did not occur (Table 5.7). In conclusion, protein-protein interactions between VP1 and both full-length and truncated NSP1 were not detected in the two-hybrid system.

DNA-binding domain hybrid plasmid	Activation domain hybrid plasmid	Selection on SD medium	Result of β-galactosidase filter assay	Time elapsed in β-galactosidase filter assay (minutes)
pCL1	-	-Leu	+ + +	15
pGBT9	pGAD424	-Leu, -Trp	-	360
pVA3	pTD1	-Leu, -Trp	+ +	30
pLAM5'	pTD1	-Leu, -Trp	-	360
pGBT9-N	pGAD424-P	-Leu, -Trp	+ + +	30
pGBT9-gene 1	-	-Trp	-	360
-	pGAD424-gene 1	-Leu	+/-	240
pGBT9-gene 5	-	-Trp	-	360
-	pGAD424-gene 5	-Leu	-	360
pGBT9-gene 1	pGAD424	-Leu, -Trp	+/-	240
pGBT9	pGAD424-gene 1	-Leu, -Trp	-	360
pGBT9-gene 5	pGAD424	-Leu, -Trp	-	360
pGBT9	pGAD424-gene 5	-Leu, -Trp	-	360
pGBT9-gene 1	pGAD424-gene 5	-Leu, -Trp	-	360
pGBT9-gene 5	pGAD424-gene 1	-Leu, -Trp	-	360

Table 5.6 Two-hybrid assay for a potential interaction between NSP1 and VP1

The results of a yeast two-hybrid assay for a potential interaction between NSP1 and VP1 are shown. Transformation of SFY526 with the hybrid plasmids indicated in the table was performed by the lithium acetate/heat shock method as described (Section 3.5.1 and 3.5.2). The transformed yeast were plated on SD selection media (Section 3.1.10) lacking the amino acids leucine (-Leu) and/or tryptophan (-Trp). All the control reactions detailed previously (Table 5.2) were performed in conjunction with the experimental reactions and gave the expected results. The β-galactosidase filter assay was performed using plates containing the freshly transformed colonies (Section 3.5.3), and the filters were incubated in the Z buffer/X-gal solution at 30 °C until blue colonies appeared or until background expression of the reporter gene was observed at 360 minutes (6 hours). The colour of the colonies was described as white (negative) (-) or blue (positive) (+, + +, or + + +) depending on the relative strength of the blue colour reaction. A faint blue colour, which appeared after several hours incubation and was thought to be background was also described (+/-). The results presented represent three repeats of the experiment.

DNA-binding domain hybrid plasmid	Activation domain hybrid plasmid	Selection on SD medium	Result in β-galactosidase filter assay	Time elapsed in β-galactosidase filter assay (minutes)
pCL1	-	-Leu	+ + +	30
pGBT9	pGAD424	-Leu, -Trp	-	480
pVA3	pTD1	-Leu, -Trp	+ +	60
pLAM5'	pTD1	-Leu, -Trp	-	480
pGBT9-N	pGAD424-P	-Leu, -Trp	+ + +	30
pGBT9-gene Δ5	-	-Trp	-	480
-	pGAD424-gene 1	-Leu	-	480
pGBT9-gene Δ5	pGAD424-gene 1	-Leu, -Trp	-	480

Table 5.7 Two-hybrid assay for a potential interaction between truncated NSP1 and VP1

The results of a yeast two-hybrid assay to detect a potential interaction between a truncated mutant of NSP1, encoded by gene Δ5, and VP1 are shown. Gene Δ5 encodes a protein consisting of the amino terminal third of the full-length NSP1 protein. Transformation of SFY526 with the hybrid plasmids indicated in the table was performed by the lithium acetate/heat shock method as described (Section 3.5.1 and 3.5.2). The transformed yeast were plated on SD selection media (Section 3.1.10) lacking the amino acids leucine (-Leu) and/or tryptophan (-Trp). All the control reactions detailed previously (Table 5.2) were performed in conjunction with the experimental reactions and gave the expected results. The β-galactosidase filter assay was performed using plates containing the freshly transformed colonies (Section 3.5.3), and the filters were incubated in the Z buffer/X-gal solution at 30 °C until blue colonies appeared or until background expression of the reporter gene was observed at 480 minutes (8 hours). The colour of the colonies was described as white (negative) (-) or blue (positive) (+, + +, or + + +) depending on the relative strength of the blue colour reaction. The results presented represent two repeats of the experiment.

5.7.2 Assay for a potential interaction between NSP1 and VP2

The yeast two-hybrid system was used to screen for a potential interaction between NSP1 and the viral structural protein VP2. VP2 is the inner-core structural protein, and is added to the pre-core complex at an early stage in the viral replication cycle. The yeast host strain SFY526 was transformed with experimental plasmids expressing fusions of NSP1 and VP2 with both the GAL4 DNA-binding and activation domains (Chapter Four) in all possible combinations and with the appropriate controls, and a β-galactosidase filter assay was used to screen for potential interactions. The efficiency of the double plasmid co-transformation was found to be approximately 10^3 cfu/μg DNA.

The results of the β-galactosidase filter assay for the controls and experimental transformations are shown (Table 5.8). All the control transformations gave the expected results. After 240 minutes incubation a faint blue colour was observed in colonies transformed with both experimental hybrid constructs expressing NSP1 and VP2 as GAL4 fusion proteins. However, this was matched by colonies transformed with the experimental constructs alone or together with the two-hybrid vector, and was probably due to a low level leaky expression of the reporter gene, and thus a false positive result. The results of a liquid (ONPG) β-galactosidase assay confirmed that an interaction could not be detected between NSP1 and VP2. It was not possible to calculate β-galactosidase units as the OD_{420} readings obtained in the assay were too low to be analysed ($OD_{420} < 0.02$) (data not shown). Thus, a protein-protein interaction was not detected between full length NSP1 and VP2 in the yeast two-hybrid system.

The SFY526 yeast reporter strain was transformed with plasmids pGBT9-gene Δ5 and pGAD424-gene 2, which express GAL4 fusion proteins with truncated NSP1 and VP2 respectively. A β-galactosidase assay was performed and it was observed that colonies transformed with both the experimental constructs remained white, indicating that an interaction between NSP1 and VP2 did not occur (Table 5.9). In conclusion, protein-protein interactions between VP2 and both full-length and truncated NSP1 were not detected in the two-hybrid system.

DNA-binding domain hybrid plasmid	Activation domain hybrid plasmid	Selection on SD medium	Result of β-galactosidase filter assay	Time elapsed in β-galactosidase filter assay (minutes)
pCL1	-	-Leu	+ + +	30
pGBT9	pGAD424	-Leu, -Trp	+/-	240
pVA3	pTD1	-Leu, -Trp	+ +	30
pLAM5'	pTD1	-Leu, -Trp	-	420
pGBT9-N	pGAD424-P	-Leu, -Trp	+ + +	30
pGBT9-gene 2	-	-Trp	+/-	240
-	pGAD424-gene 2	-Leu	-	420
pGBT9-gene 2	pGAD424	-Leu, -Trp	+/-	240
pGBT9	pGAD424-gene 2	-Leu, -Trp	+/-	240
pGBT9-gene 5	pGAD424	-Leu, -Trp	+/-	240
pGBT9	pGAD424-gene 5	-Leu, -Trp	+/-	240
pGBT9-gene 2	pGAD424-gene 5	-Leu, -Trp	+/-	240
pGBT9-gene 5	pGAD424-gene 2	-Leu, -Trp	+/-	240

Table 5.8 Two-hybrid assay screen for an interaction between NSP1 and VP2

The results of a yeast two-hybrid assay screen for a potential interaction between NSP1 and VP2 are shown. Transformation of SFY526 with the hybrid plasmids indicated in the table was performed by the lithium acetate/heat shock method as described (Section 3.5.1 and 3.5.2). The transformed yeast were plated on SD selection media (Section 3.1.10) lacking the amino acids leucine (-Leu) and/or tryptophan (-Trp). All the control reactions detailed previously (Table 5.2) were performed in conjunction with the experimental reactions and gave the expected results. The β-galactosidase filter assay was performed using plates containing the freshly transformed colonies (Section 3.5.3), and the filters were incubated in the Z buffer/X-gal solution at 30 °C until blue colonies appeared or until background expression of the reporter gene was observed at 420 minutes (7 hours). The colour of the colonies was described as white (negative) (-) or blue (positive) (+, + +, or + + +) depending on the relative strength of the blue colour reaction. A faint blue colour, which appeared after several hours incubation and was thought to be background was also described (+/-). The results presented represent three repeats of the experiment.

DNA-binding domain hybrid plasmid	Activation domain hybrid plasmid	Selection on SD medium	Result in β-galactosidase filter assay	Time elapsed in β-galactosidase filter assay (minutes)
pCL1	-	-Leu	+ + +	30
pGBT9	pGAD424	-Leu, -Trp	-	480
pVA3	pTD1	-Leu, -Trp	+ +	60
pLAM5'	pTD1	-Leu, -Trp	-	480
pGBT9-N	pGAD424-P	-Leu, -Trp	+ + +	30
pGBT9-gene Δ5	-	-Trp	-	480
-	pGAD424-gene 2	-Leu	-	480
pGBT9-gene Δ5	pGAD424-gene 2	-Leu, -Trp	-	480

Table 5.9 Two-hybrid assay for a potential interaction between truncated NSP1 and VP2

The results of a yeast two-hybrid assay to detect a potential interaction between a truncated mutant of NSP1, encoded by gene Δ5, and VP2 are shown. Gene Δ5 encodes a protein consisting of the amino terminal third of the full-length NSP1 protein. Transformation of SFY526 with the hybrid plasmids indicated in the table was performed by the lithium acetate/heat shock method as described (Section 3.5.1 and 3.5.2). The transformed yeast were plated on SD selection media (Section 3.1.10) lacking the amino acids leucine (-Leu) and/or tryptophan (-Trp). All the control reactions detailed previously (Table 5.2) were performed in conjunction with the experimental reactions and gave the expected results. The β-galactosidase filter assay was performed using plates containing the freshly transformed colonies (Section 3.5.3), and the filters were incubated in the Z buffer/X-gal solution at 30 °C until blue colonies appeared or until background expression of the reporter gene was observed at 480 minutes (8 hours). The colour of the colonies was described as white (negative) (-) or blue (positive) (+, + +, or + + +) depending on the relative strength of the blue colour reaction. The results presented represent three repeats of the experiment.

5.7.3 Assay for a potential interaction between NSP1 and VP3

The yeast two-hybrid system was also used to screen for a potential protein-protein interaction between NSP1 and the viral structural protein VP3. VP3 is found together with NSP1 in the pre-core RI at an early stage in the viral replication cycle. The yeast reporter strain SFY526 was transformed with experimental constructs encoding fusions of NSP1 and VP3 with both the GAL4 DNA-binding and activation domains (Chapter Four) in all possible combinations and with the appropriate controls, and a β-galactosidase filter assay was used to screen for potential interactions. The efficiency of the double plasmid co-transformation was found to be approximately 10^3 cfu/μg DNA.

The results of the β-galactosidase filter assay for the controls and experimental transformations are shown (Table 5.10). All the control transformations gave the expected results. After 240 minutes incubation a faint blue colour was observed in colonies co-transformed with both the experimental hybrid constructs expressing GAL4 fusion proteins of NSP1 and VP3. However, this was matched in colonies transformed with the experimental constructs either alone or together with the other two-hybrid vector (e.g. pGBT9-gene 3 and pGAD424). This was considered to be a false positive result and was probably due to a low level leaky expression of the reporter gene. The results of a liquid (ONPG) β-galactosidase assay confirmed that an interaction could not be detected between NSP1 and VP3. It was not possible to calculate β-galactosidase units as the OD_{420} readings obtained in the assay were too low to be analysed ($OD_{420} < 0.02$) (data not shown). Thus, a protein-protein interaction was not detected between full length NSP1 and VP3 in the yeast two-hybrid system.

The SFY526 yeast reporter strain was transformed with plasmids pGBT9-gene Δ5 and pGAD424-gene 3, which express GAL4 fusion proteins with truncated NSP1 and VP3 respectively. A β-galactosidase assay was performed and it was observed that colonies transformed with both the experimental constructs remained white, indicating that an interaction between NSP1 and VP3 did not occur (Table 5.11). In conclusion, protein-protein interactions between VP3 and both full-length and truncated NSP1 were not detected in the two-hybrid system.

DNA-binding domain hybrid plasmid	Activation domain hybrid plasmid	Selection on SD medium	Result of β-galactosidase filter assay	Time elapsed in β-galactosidase filter assay (minutes)
pCL1	-	-Leu	+ + +	30
pGBT9	pGAD424	-Leu, -Trp	+/-	240
pVA3	pTD1	-Leu, -Trp	+ +	60
pLAM5'	pTD1	-Leu, -Trp	-	380
pGBT9-N	pGAD424-P	-Leu, -Trp	+ + +	30
pGBT9-gene 3	-	-Trp	-	380
-	pGAD424-gene 3	-Leu	-	380
pGBT9-gene 5	-	-Trp	-	380
-	pGAD424-gene 5	-Leu	-	380
pGBT9-gene 3	pGAD424	-Leu, -Trp	+/-	240
pGBT9	pGAD424-gene 3	-Leu, -Trp	+/-	240
pGBT9-gene 5	pGAD424	-Leu, -Trp	+/-	240
pGBT9	pGAD424-gene 5	-Leu, -Trp	+/-	240
pGBT9-gene 3	pGAD424-gene 5	-Leu, -Trp	+/-	240
pGBT9-gene 5	pGAD424-gene 3	-Leu, -Trp	+/-	240

Table 5.10 Two-hybrid assay for a potential interaction between NSP1 and VP3

The results of a yeast two-hybrid assay to detect a potential interaction between NSP1 and VP3 are shown. Transformation of SFY526 with the hybrid plasmids indicated in the table was performed by the lithium acetate/heat shock method as described (Section 3.5.1 and 3.5.2). The transformed yeast were plated on SD selection media (Section 3.1.10) lacking the amino acids leucine (-Leu) and/or tryptophan (-Trp). All the control reactions detailed previously (Table 5.2) were performed in conjunction with the experimental reactions and gave the expected results. The β-galactosidase filter assay was performed using plates containing the freshly transformed colonies (Section 3.5.3), and the filters were incubated in the Z buffer/X-gal solution at 30 °C until blue colonies appeared or until background expression of the reporter gene was observed at 380 minutes (6.33 hours). The colour of the colonies was described as white (negative) (-) or blue (positive) (+, + +, or + + +) depending on the relative strength of the blue colour reaction. A faint blue colour, which appeared after several hours incubation and was thought to be background was also described (+/-). The results presented represent three repeats of the experiment.

DNA-binding domain hybrid plasmid	Activation domain hybrid plasmid	Selection on SD medium	Result in β-galactosidase filter assay	Time elapsed in β-galactosidase filter assay (minutes)
pCL1	-	-Leu	+ + +	30
pGBT9	pGAD424	-Leu, -Trp	-	480
pVA3	pTD1	-Leu, -Trp	+ +	60
pLAM5'	pTD1	-Leu, -Trp	-	480
pGBT9-N	pGAD424-P	-Leu, -Trp	+ + +	30
pGBT9-gene Δ5	-	-Trp	-	480
-	pGAD424-gene 3	-Leu	-	480
pGBT9-gene Δ5	pGAD424-gene 3	-Leu, -Trp	-	480

Table 5.11 Two-hybrid assay for a potential interaction between truncated NSP1 and VP3

The results of a yeast two-hybrid assay to detect a potential interaction between a truncated mutant of NSP1, encoded by gene Δ5, and VP3 are shown. Gene Δ5 encodes a protein consisting of the amino terminal third of the full-length NSP1 protein. Transformation of SFY526 with the hybrid plasmids indicated in the table was performed by the lithium acetate/heat shock method as described (Section 3.5.1 and 3.5.2). The transformed yeast were plated on SD selection media (Section 3.1.10) lacking the amino acids leucine (-Leu) and/or tryptophan (-Trp). All the control reactions detailed previously (Table 5.2) were performed in conjunction with the experimental reactions and gave the expected results. The β-galactosidase filter assay was performed using plates containing the freshly transformed colonies (Section 3.5.3), and the filters were incubated in the Z buffer/X-gal solution at 30 °C until blue colonies appeared or until background expression of the reporter gene was observed at 480 minutes (8 hours). The colour of the colonies was described as white (negative) (-) or blue (positive) (+, + +, or + + +) depending on the relative strength of the blue colour reaction. The results presented represent three repeats of the experiment.

5.7.4 Conclusions

In this chapter qualitative data from β-galactosidase filter assays generated in several yeast two-hybrid experiments has been presented. The aim was to determine if NSP1 interacted with any of the structural proteins found with it in early replication complexes. However, protein-protein interactions could not be detected between NSP1 and the rotavirus structural proteins VP1, VP2 and VP3 in this assay.

There are two obvious conclusions which can be drawn from this result. Firstly, it is possible that NSP1 does not interact with the structural proteins found in the early replication complexes. The second possible conclusion is that although protein-protein interactions might occur between NSP1 and one or all of these proteins, these interactions could not detected by this assay. The reasons to support this suggestion will be discussed subsequently (Section 5.8.1).

The yeast strain SFY526 was used throughout for the two-hybrid assays. The use of the second available strain HF7c was considered and preliminary control experiments were performed. However, as this strain has a weaker promoter than SFY526, it was considered that the use of HF7c would be unlikely to reveal an interaction that was not detected in strain SFY526.

5.8 Discussion

5.8.1 Discussion

The yeast two-hybrid system was employed to determine if direct protein-protein interactions occurred between NSP1 and itself, and with other proteins present in viral complexes formed at early times in the infected cell. Dimerisation of a second viral non-structural protein, NSP3, was also studied.

Two-hybrid assays to investigate potential interactions between NSP1 and the viral proteins VP1, VP2, VP3 and NSP3, all yielded negative results in β-galactosidase filter assays. These results suggested either that direct protein-protein interactions do not occur between NSP1 and these proteins, or that although interactions might occur they cannot be detected under the conditions of this assay. The hypothesis that NSP1 might form a dimer was also studied, however a negative result was obtained in the β-galactosidase assay. Thus, NSP1 does not form a dimer under the conditions of the yeast two-hybrid system.

A negative result in the two-hybrid system is not strong evidence against a specific interaction, as there are several possible explanations for why a protein-protein interaction might not be detected. For example, the protein-protein interactions may be too weak to be detected by the assay, or the conditions of the assay might not be favourable. As the assay was performed in yeast and not in a mammalian cell it is unlikely to represent the exact conditions that would be found in the mammalian cell. Although, the dimerisation of NSP3 was clearly shown with the yeast two-hybrid system, other protein interactions which do occur may not be detectable. In this case, it is possible that a two-hybrid assay in a mammalian cell system may give a different result.

A further consideration is that the proteins must be able to fold and exist stably in the yeast cell and to retain activity as fusion proteins for protein-protein interactions to occur. The fusion proteins could not be detected with polyclonal antiserum on a western blot, probably due to the low expression from the two-hybrid plasmids. Specific monoclonal antibodies against the GAL4 domain proteins do not detect fusion proteins expressed from the two-hybrid vectors pGBT9 and pGAD424 for this reason. Although it was not possible to ascertain the level of expression of the fusion proteins in the yeast cell, it does not necessarily mean that they were not expressed. Other researchers have proven protein-protein interactions using fusion proteins which were only expressed at extremely low levels (Tsui and Schubach, 1994), or when expression could not be detected by western blotting (Slack,1998).

In this two-hybrid assay the rotavirus proteins were expressed as carboxy-terminal extensions of the GAL4 domains (Section 4.2.1). It has been suggested that in some cases this might result in a protein-protein interaction site at the amino terminus of the protein of interest becoming occluded (Fields and Sternglanz, 1994). The fusion of the GAL4 domain might also interfere with the appropriate folding of the protein such that protein-protein interactions are prevented. This could be a possible explanation for the failure to detect protein-protein interactions in this study. The amino-terminal regions of some of the proteins studied may have functional significance, which could possibly have been affected by the fusion to the GAL4 domains. The proposed functional region in the amino-terminus of NSP1 has been noted previously (Section 1.6.2), and is reflected in the viability of the truncated mutant containing only the amino terminus of the protein (Section 5.2). Also, by analogy with the bluetongue virus system, there may be a requirement for a flexible

and free amino-terminus of VP2 that is probably functionally important (Gouet *et al.*, 1999).

Although the yeast two-hybrid assay did not detect direct protein-protein interactions between NSP1 and itself, or the other protein components of the pre-core RI, this does not mean that protein-protein interactions do not occur between these proteins. Failure in the identification of protein-protein interactions in the yeast two-hybrid system, which can be demonstrated in other systems, has been reported previously (Black *et al.*, 1998) (Van Aelst *et al.*, 1993).

5.8.2 NSP3 forms dimers and activates transcription when fused to the GAL4 DNA-binding domain alone

It has been shown previously that NSP3 forms a dimer in infected cell (Mattion *et al.*, 1992), and this was confirmed in a yeast two-hybrid assay. The strength of the self-interaction of NSP3 was quantified using a β-galactosidase assay and the level of enzyme activity was found to be 37 β-galactosidase units. This result suggested that in this assay the self-interaction of NSP3 was approximately half as strong as the interaction between p53 and SV40 large T-antigen, a well-characterised, relatively strong interaction (Li and Fields, 1993). Recently, results have been published which quantify the dimerisation of NSP3 in the YM strain of porcine rotavirus in the yeast two-hybrid system (González *et al.*, 1998). A similar strong blue phenotype was detected in the β-galactosidase filter assay, however the level of β-galactosidase activity recorded was considerably lower (1.31 β-galactosidase units) than the value stated here. The reason for this difference is unknown, although it was noted that all the recorded values of β-galactosidase units were lower than those obtained in this work. The researchers similarly found that NSP3 activated transcription when fused to the GAL4 DNA-binding domain in the absence of a fusion counterpart in the GAL4 activation domain.

When the yeast strains were transformed with plasmid pGBT9-gene 9 encoding a fusion of the GAL4 DNA-binding domain with NSP3, activation of the reporter gene was observed. This result suggested that NSP3 may have some intrinsic transcriptional activation properties, which can complement the DNA-binding activity of the GAL4 domain to activate the reporter gene. NSP3 is an acidic protein with a predicted net negative charge at pH 7.0 of -2.5 (Mattion *et al.*, 1992). The secondary

structure is predicted to be predominantly alpha-helical in nature. A short acidic region, consisting of nine glutamic acid or aspartic acid residues over a stretch of 19 amino acids (aa), has also been described. This acidic region is adjacent to a conserved basic region at the amino terminus of the protein which may be the location of the RNA-binding domain reported as being present in NSP3 (Patton, 1995). At the carboxy terminus of the protein is the conserved region which has been implicated in dimerisation (Mattion *et al.*, 1992). Proteins with transcriptional activation properties often contain highly acidic activating sequences. Ma and Ptashne (1987) identified novel acidic activating sequences which varied in length from 12-81 aa and showed no obvious sequence homology when compared with activating regions of GAL4 or GCN4 or among themselves. The novel acidic activators were identified by fusion of the sequence to the GAL4 DNA-binding domain and assaying for a functional GAL4 transcriptional activator. The fusion of NSP3 to the GAL4 DNA-binding domain, as described above, identified NSP3 as having transcriptional activation properties in an identical manner. It is possible that the acidic region of NSP3, between aa 150-169, may be responsible for the activation of transcription of the reporter gene which was observed.

5.8.3 Future work

This study has produced several constructs (Table 4.1) which will be valuable in future studies of rotavirus proteins. In particular, the availability of plasmids expressing rotavirus proteins VP1, VP2, and VP3, suggests further experiments with the yeast two-hybrid assay, which could potentially generate interesting data on the interactions between the enzymes, VP1 and VP3, in the transcriptional complex. In addition, interactions of the components of the transcriptional complex with the core protein VP2 could be studied. Investigation of these interactions would allow parallels to be drawn with recent structural studies (Prasad *et al.*, 1996) (Lawton *et al.*, 1997b), and the suggestion that VP2 may have a role during transcription and viral morphogenesis as a scaffold for the proper assembly of the viral RNA, and VP1 and VP3 in the viral core (Labbe *et al.*, 1994) (Zeng *et al.*, 1998). The interacting domains of these proteins could then be mapped.

Dimerisation of full-length NSP3 was demonstrated, although the interacting site was not mapped. Further experiments with these constructs, which are clearly

functional, could include mapping of the dimerisation domain and an investigation of potential interactions between NSP3 and the structural proteins VP1, VP2 and VP3. Alternatively, the NSP3 constructs could be used to screen a cDNA expression library for interactions with cellular proteins. Indeed, it has been suggested previously that NSP3 might have an association with the cell cytoskeleton (Mattion *et al.*, 1992).

In this study the rotavirus proteins were expressed as carboxy-terminal extensions of the GAL4 domains, which possibly could have resulted in a protein-protein interaction site at the amino terminus of the protein becoming occluded. The use of the alternative LexA system, which uses amino-terminal fusions to LexA of the protein of interest instead of carboxy-terminal fusion (Beranger *et al.*, 1997), would allow the detection of interactions which require a 'free' amino-terminus of the protein.

Results Chapter 3

Analysis of rotavirus protein-protein interactions

by radio-immunoprecipitation

6.1 Aims

The aim of the work described in this chapter was to investigate potential direct protein-protein interactions between NSP1 and viral structural proteins present in early replication complexes by means of co-immunoprecipitation analysis. An *in vitro* approach, using viral proteins translated in a rabbit reticulocyte system, was chosen as a complement to the *in vivo* analysis used in the yeast two-hybrid system.

6.2 Introduction

Protein-protein interactions are intrinsic to many viral processes within the infected cell. An ability to identify these interactions is integral to dissection of the virus replication cycle and understanding of the interactions between virus and host cell at the molecular level. Co-immunoprecipitation is the classical method for investigating protein-protein interactions. The use of a rabbit reticulocyte system to produce translated proteins allows the examination of individual proteins and the direct interactions between them. This method of co-immunoprecipitation, in contrast to the use of infected cell lysates where proteins may be interacting indirectly as part of a complex, means that direct protein-protein interactions can be unambiguously examined. This method of examining viral protein-protein interactions was successfully used by Shepard *et al.* (1996) in their study of the interactions between the reovirus capsid proteins σ3 and μ1, where they defined the amino-terminal zinc-binding motif of σ3 as the potential interacting domain by the *in vitro* expression of σ3 deletion mutants which failed to co-immunoprecipitate with μ1 (Shepard *et al.*, 1996).

Co-immunoprecipitation was chosen as a method of studying rotavirus protein-protein interactions as an *in vitro* complement to the genetic method of the yeast two-hybrid system. NSP1 has been shown to be present in early replication complexes with the viral structural proteins VP1 and VP3, and the non-structural protein NSP3 (Gallegos and Patton, 1989) in a complex that has been termed the pre-core replication intermediate (RI). VP2 is added to the pre-core RI to form the core RI. The function of NSP1 in these complexes is unknown but it is almost certain to involve the interaction of NSP1 with other components of the complex. It has been suggested that the pre-core RI assembles on the cytoskeleton by the interaction of

VP1 and VP3 with NSP1/NSP3-mRNA complexes (Patton, 1995), therefore interactions between these proteins must be a prerequisite for formation of the pre-core RI. It is for this reason that the structural proteins VP1, VP2 and VP3 were chosen for expression *in vitro* and used in co-immunoprecipitation experiments with NSP1.

6.3 Production of Antiserum

6.3.1 Recombinant vaccinia virus VR5

The decision to develop radio-immunoprecipitation as a method of studying protein-protein interactions necessitated the production of a monospecific antiserum against NSP1. A recombinant vaccinia virus, VR5, expressing the gene 5 protein product NSP1 from the UKtc strain of bovine rotavirus, which was produced in the Rotavirus laboratory at the University of Warwick by S. Stagg, was chosen as the source of rotavirus antigen. Expression of NSP1 by the vaccinia recombinant VR5 was confirmed by positive fluorescence in indirect immunofluorescence assays carried out on VR5-infected cells and stained with polyclonal anti-bovine rotavirus serum (Heath *et al.*, 1997).

It has been shown that immunisation of animals with recombinant vaccinia viruses can successfully produce monospecific antisera that recognise native proteins by immunoprecipitation, immunofluorescence and western blotting (Tine *et al.*, 1993) (Vafai and Yang, 1991). Also, the use of a recombinant virus for immunisation should allow a large quantity of the antigen to be easily grown and purified. Immunisation of a rabbit was expected to give a large quantity of specific antiserum that could be used for the intended experimental methods. The antiserum from the rabbit could be expected to be of a more consistent quality than from several batches of mice, and the use of a single, larger animal was also considered to be an easier approach.

6.3.2 Growth and purification of VR5

The strategy for the production of the antigenic material was to grow stocks of high titre VR5 and purify it by centrifugation through sucrose gradients. HeLa cells were chosen to grow the virus as they are known to consistently give high yields of vaccinia virus (Ausubel *et al.*, 1996). Briefly, HeLa cells were infected with VR5 at a

low multiplicity of infection (m.o.i.) and incubated until complete cytopathic effect (cpe) was observed. The virus was harvested and, as vaccinia virus is known to be extremely cell associated, careful freeze-thawing and sonication were performed to ensure adequate release of the virus. The virus was concentrated by low speed centrifugation before purification through a 20-40 % sucrose gradient (McCrae, 1975). Following centrifugation a band of virus was visible in the middle of the gradient and this was collected and the bands pooled. The virus stock was then further purified using a second sucrose gradient and concentrated in a small volume. A plaque assay was performed prior to use to ensure a sufficiently high titre of the virus. Highly purified virus stocks of 10^7-10^8 pfu/ml were obtained by this method and used for inoculation procedures.

6.3.3 Inoculation procedure

Rotaviruses are an extremely common infection of young animals and consequently the rabbit used for inoculation was obtained from a supplier who guaranteed that the animal was free from rotavirus infection and thus carried no anti-rotavirus antibodies. Prior to inoculation a sample of serum was taken and tested at dilutions between 10^{-2} and 10^{-3} by immunofluorescence though, as expected, no rotavirus antibodies were detected in the pre-immune serum (Figure 6.1, panel E). The inoculations were performed as described previously (Section 3.7.1). The serum was separated as described (Section 3.7.2) and was tested for the presence of the desired antibodies by immunofluorescence and immunoprecipitation analysis.

6.3.4 Analysis of the antiserum by immunofluorescence

The pre-immune and hyper-immune sera obtained from each bleed were tested for the presence of anti-VR5 and anti-rotavirus antibodies using an immunofluorescence assay. VR5-infected cells were used to test for the presence of anti-VR5 antibodies. The pre-immune serum did not react with the VR5-infected cells (Figure 6.1, panel A) as expected. All the hyper-immune sera were tested (data not shown for all bleeds) and each hyper-immune serum reacted strongly with the VR5-infected cells. Figure 6.1 (panel B) shows a typical fluorescence photograph obtained when the cells were stained with hyper-immune serum (bleed 2 weeks post

Figure 6.1 Immunofluorescence assay analysis of hyper-immune serum raised against VR5

BS-C-1 cells grown on coverslips were infected with VR5 at a low m.o.i. ($2x10^{-3}$), incubated until plaques were visible (approximately 24 hours) then fixed. A 10^{-2} dilution of pre-immune serum (Panel A) and a 10^{-2} dilution of hyper-immune serum from a bleed 2 weeks post boost I (Section 3.7.1) (Panel B) were added to separate coverslips and incubated at 37 °C for 1 hour. The coverslips were washed and incubated with a 10^{-2} dilution of FITC conjugate goat anti-rabbit Immunoglobulin as described (Section 3.7.3).

BS-C-1 cells grown on coverslips were infected with UKtc rotavirus (m.o.i. = $1x10^{-1}$), incubated for 16 hours and fixed. The cells were incubated with a 10^{-2} dilution of polyclonal anti-UKtc serum (Panel C), hyper-immune serum from a bleed 2 weeks post boost III (Section 3.7.1) (Panel D), and pre-immune serum (Panel E) for 1 hour at 37 °C, followed by a similar incubation with a 10^{-2} dilution of FITC conjugate goat anti-rabbit Immunoglobulin as described (Section 3.7.3). The cells were examined by UV microscopy and photographed.

Figure 6.1

A. VR5-infected cells
pre-immune serum

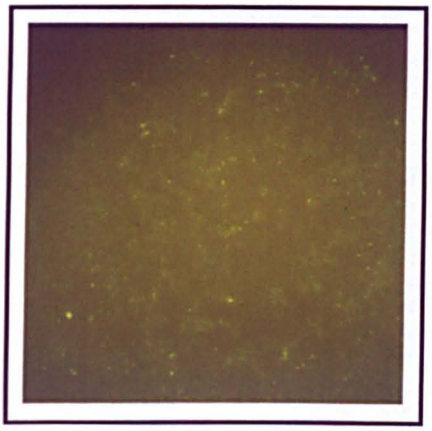

B. VR5-infected cells
hyper-immune serum

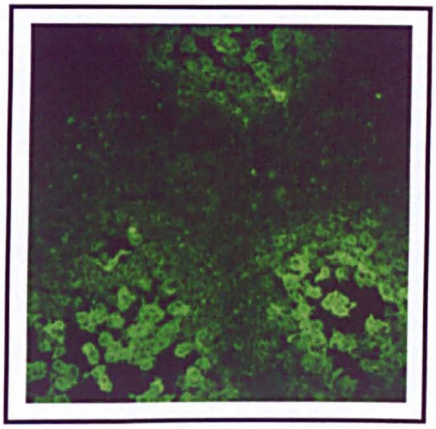

C. UKtc-infected cell
anti-UKtc serum

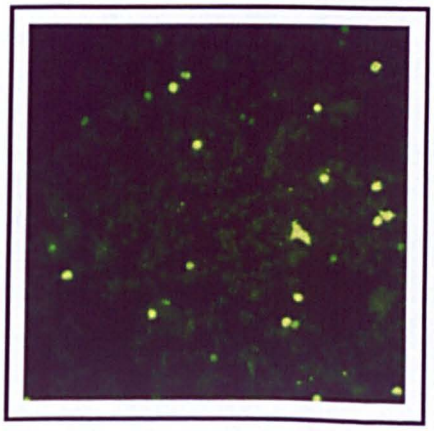

D. UKtc-infected cells
hyper-immune serum

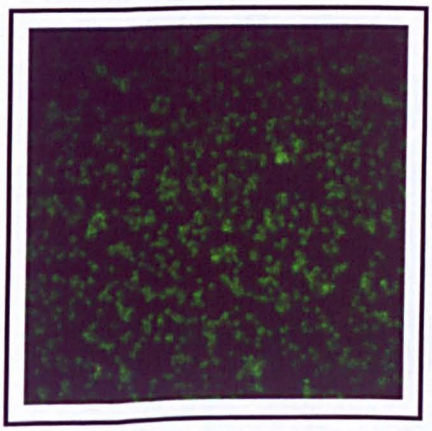

E. UKtc-infected cells
pre-immune serum

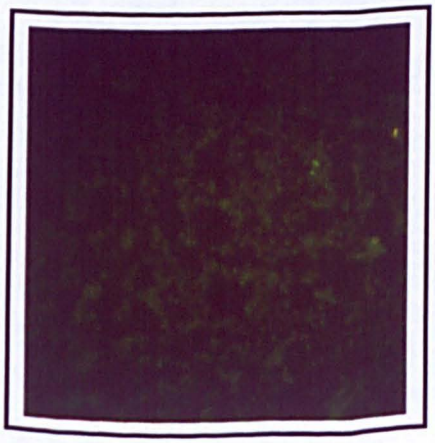

boost I). These results indicated that anti-vaccinia (VR5) antibodies had been generated and were present in the serum.

A similar assay was performed with UKtc rotavirus-infected cells to determine if anti-NSP1 antibodies had been generated. On analysis, it could be seen that the pre-immune serum did not react with the UKtc rotavirus-infected cells (Figure 6.1, panel E), while a positive control of polyclonal anti-rotavirus serum showed a strong fluorescence when examined by UV microscopy (Figure 6.1, panel C). However, all samples of hyper-immune sera (data shown for bleed 2 weeks post boost III but not for all bleeds tested) failed to react with the infected cells (Figure 6.1, panel D). Therefore, although anti-vaccinia antibodies were generated, indicating that VR5 was an efficient immunogen, the serum did not contain high enough levels of anti-NSP1 antibodies to be detectable by this assay.

6.3.5 Analysis of the antiserum by radio-immunoprecipitation

Hyper-immune sera obtained from each bleed were analysed by radio-immunoprecipitation to determine if NSP1 could be specifically precipitated by antibodies in the sera. The experiment was performed with *in vitro* translated NSP1 and also with infected cell lysates. Hyper-immune sera from all bleeds were tested in immunoprecipitation reactions with *in vitro* translated NSP1 and the results are shown in Figure 6.2. The positive control immunoprecipitation reaction, which used a specific anti-NSP1 antiserum known to precipitate NSP1 (lane 1), produced a broad band at approximately 50 kDa which corresponds to NSP1. The smaller bands below are incomplete translation products of NSP1. The pre-immune serum (lane 2) did not precipitate NSP1 as expected. Several different hyper-immune sera, including those from bleeds taken after booster inoculations were given, were tested and all sera failed to precipitate visible amounts of NSP1 (lanes 3-7). The fluorograph shown (Figure 6.2) represents a 4-week exposure of the gel. Although faint bands can be seen in lanes 3-7 they are only marginally above background and are only visible on an overexposed fluorograph.

A potential explanation for the failure of the sera to precipitate NSP1 was the possibility of antigenic differences between the recombinant vaccinia virus expressed protein and the *in vitro* translated protein, such that hyper-immune serum raised against the vaccinia expressed protein may fail to recognise the *in vitro* translated

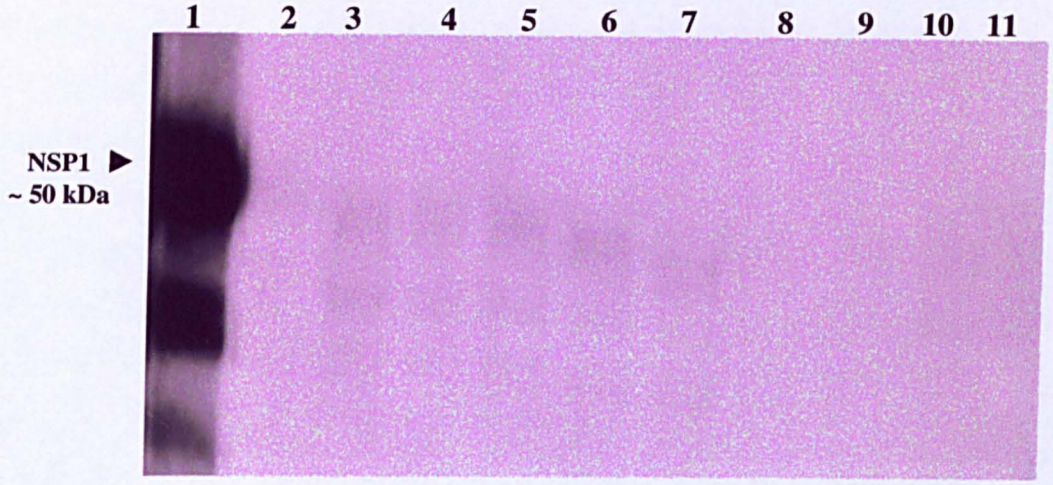

Figure 6.2 Immunoprecipitation of *in vitro* translated NSP1 with hyper-immune serum from a rabbit infected with VR5

^{35}S-methionine-labelled NSP1 protein was produced by *in vitro* coupled transcription-translation (Section 3.6.1). Equal aliquots of the translation reactions were incubated with 5 µl of antisera overnight at 4 °C (Section 3.6.4), precipitated with protein A-Sepharose and washed with a series of buffers. The precipitates were loaded onto a 5-11 % gradient polyacrylamide gel (Section 3.6.5) and analysed by dry gel fluorography after a four week exposure of the gel (Section 3.6.6). A known specific anti-NSP1 antiserum was used as the positive control (lane 1). Pre-immune serum from the rabbit was used as a negative control (lane 2). Lanes 3-11 represent immunoprecipitation reactions with hyper-immune sera from a rabbit infected with a vaccinia recombinant virus expressing NSP1 (VR5) at the following times post inoculation: 2 weeks (lane 3); 7 weeks (lane 4); 2 weeks post boost I (lane 5); 4 weeks post boost I (lane 6); 2 weeks post boost II (lane 7); 4 weeks post boost II (lane 8); 6 weeks post boost II (lane 9); 2 weeks post boost III (lane 10); 4 weeks post boost III (lane 11).

protein. For example, if antibodies were raised against a conformational epitope displayed in the vaccinia expressed protein *in vivo*, which was not present in the *in vitro* expressed protein due to a difference in protein folding, then NSP1 would not be precipitated by the serum. Indeed, proteins expressed in reticulocyte systems sometimes have different properties and structure to the native protein (Ausubel *et al.*, 1996). A second possible explanation may have been that the antigen-antibody interaction was of relatively low affinity and therefore may have been disrupted by the stringent conditions used for immunoprecipitation leading to a negative result.

To investigate these possibilities, immunoprecipitation experiments were performed to determine if the hyper-immune sera could precipitate NSP1 from infected cell lysates (Figure 6.3). A specific anti-NSP1 serum known to precipitate NSP1 was used as the positive control (lane 2) and a band corresponding to NSP1 can be seen on the fluorograph. The pre-immune serum was tested (lane 3) and did not precipitate NSP1. Hyper-immune sera from three different bleeds were tested in the experiment shown, but in others (data not shown) all samples of hyper-immune sera collected were tested. None of the hyper-immune sera tested precipitated NSP1 from the infected cell lysates. However, the results show that there was precipitation of other viral proteins, in particular VP2 and VP6, by the hyper-immune serum. These proteins were also non-specifically precipitated by the pre-immune serum. VP6, which is the sub-group specific antigen (Greenberg *et al.*, 1983) and a major structural protein within the virus (Prasad *et al.*, 1988), is considered to be a particularly "sticky" protein (M. A. McCrae, pers. comm.), hence non-specific interactions may occur between antibodies in the serum and epitopes on VP6.

All hyper-immune sera were tested by immunoprecipitation in two separate assays for antibodies against NSP1. *In vitro* translated NSP1 was not precipitated by the hyper-immune sera, and in addition, NSP1 was not precipitated from lysates made from cells infected with the UKtc strain of bovine rotavirus. These results indicated that no specific antibodies were produced by the inoculation procedure which could precipitate NSP1 in immunoprecipitation reactions.

6.3.6 Anti-NSP1 serum

The specific anti-NSP1 serum used as a positive control in the preceding experiment (Section 6.3.5) was generously donated by Dr Jean Cohen at the Institut

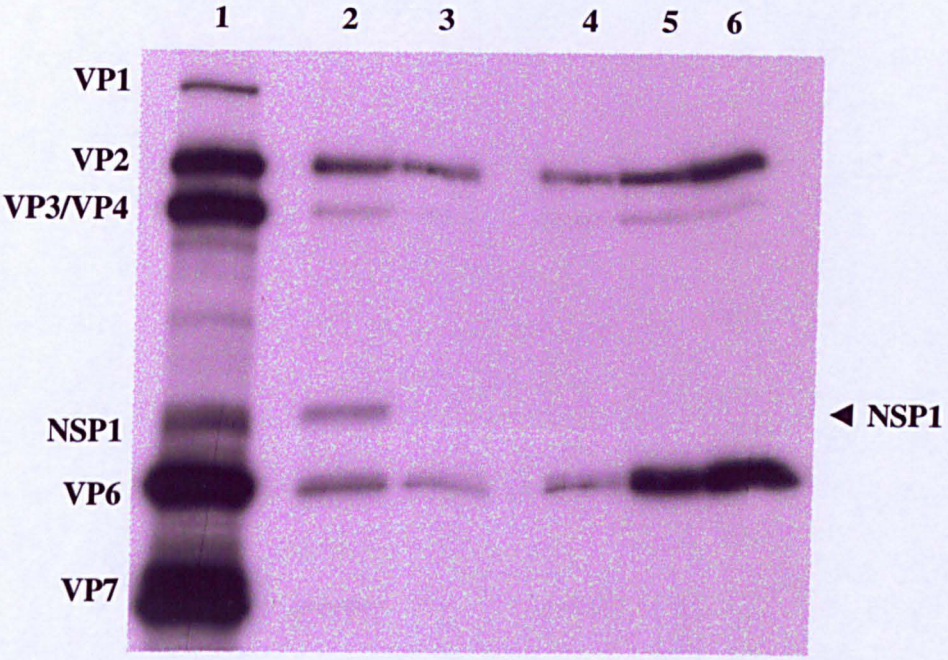

Figure 6.3 Immunoprecipitation of UKtc rotavirus-infected cell lysates with hyper-immune sera from a rabbit infected with VR5

Hyper-immune sera from a rabbit infected with a vaccinia recombinant virus expressing NSP1 (VR5) was analysed by immunoprecipitation for specific antibodies to NSP1. UKtc rotavirus-infected BS-C-1 cell lysates were labelled with ^{35}S-methionine (Section 3.6.3) and equal aliquots were incubated with 5 µl of antisera (Section 3.6.4). The lysates were precipitated with protein A-Sepharose and loaded onto a 5-11 % gradient SDS-polyacrylamide gel (Section 3.6.5) and analysed by dry gel fluorography after a one week exposure of the gel (Section 3.6.6). An aliquot of the infected cell lysate was run on the gel (lane 1) to show the characteristic pattern of rotavirus protein expression. Viral proteins are labelled on the left. The positive control for the immunoprecipitation reaction was a known specific anti-NSP1 serum (lane 2). Pre-immune serum from the rabbit was used as the negative control (lane 3). Lanes 4-6 represent immunoprecipitation with hyper-immune sera from bleeds 2 weeks post inoculation (lane 4), 2 weeks post boost I (lane 5), and 2 weeks post boost III (lane 6). The position of NSP1 is indicated by an arrow.

National de la Recherché Agronomique, Jouy-en-Josas, France. A monoclonal antibody against NSP1 was also obtained from Dr Cohen, however it did not precipitate NSP1 when used in radio-immunoprecipitation experiments (data not shown).

The anti-NSP1 serum was raised in New Zealand white rabbits which were inoculated with a crude lysate of *Spodoptera frugiperda* cells infected with a recombinant baculovirus containing gene 5 (Brottier *et al.*, 1992). Inoculation with protein purified by preparative PAGE or FPLC failed to give reacting sera. The serum was tested for the presence of antibodies by immunoprecipitation and western blotting and the specificity was confirmed by immunoprecipitation of *in vitro* translated NSP1 protein. The serum was shown to specifically precipitate NSP1 from infected cell lysates, while the pre-immune serum did not. Also, the anti-NSP1 serum did not react with a lysate of mock-infected cells. The researchers noted that VP2 and VP6 were also precipitated by the anti-NSP1 serum, suggesting that either these proteins were associated with NSP1 in some way or that the rabbit had been in contact with rotavirus during the immunisation period (Brottier *et al.*, 1992).

In addition to the analysis performed by Cohen's group, the anti-NSP1 serum was tested for its specificity in an immunofluorescence assay before use in this project. UKtc rotavirus-infected cells fixed onto coverslips were stained with anti-NSP1 serum and patches of fluorescent cells were observed (Figure 6.4, panels A and C). It was estimated that 15-20 % of the cells in each field of view were fluorescent. The same cells were then restained with polyclonal anti-rotavirus serum at the same dilution and examined. Again approximately 15-20 % of the cells were fluorescent - a figure which must represent the distribution of rotavirus infected cells (Figure 6.4, panels B and D). The fact that a similar proportion of cells were seen to fluoresce with each antibody suggested that only infected cells were stained in each case. It therefore appeared that the anti-NSP1 serum was specific to rotavirus-infected cells and did not cross-react with proteins in uninfected cells. The difference in the intensity of the fluorescence apparent in Figure 6.4 could reflect the fact that NSP1 is a minor protein in the infected cell.

A. Anti-NSP1 serum

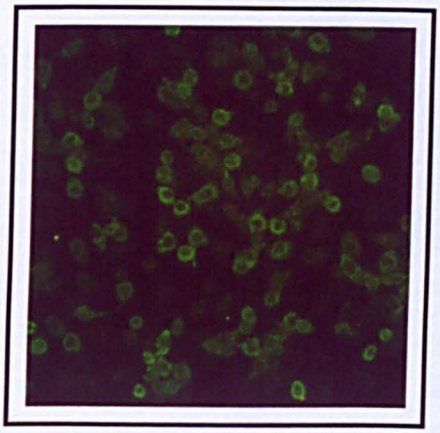

B. Anti-UKtc serum

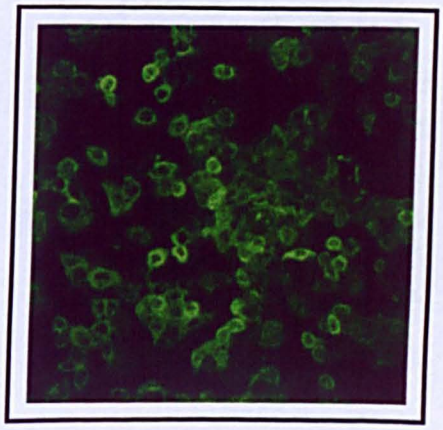

C. Anti-NSP1 serum

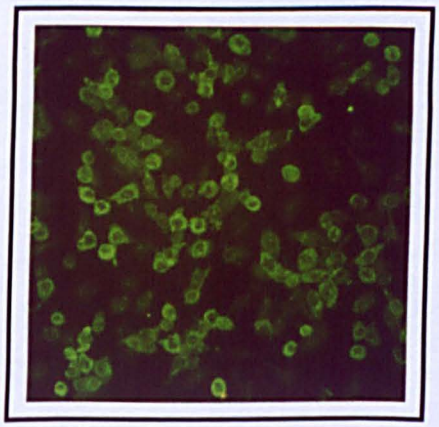

D. Anti-UKtc serum

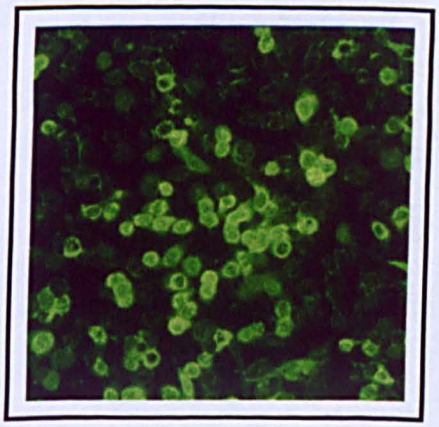

Figure 6.4 Immunofluorescence photographs of UKtc-infected BS-C-1 cells stained with anti-NSP1 serum or anti-UKtc serum

BS-C-1 cells infected with UKtc rotavirus (m.o.i. = 0.2) and fixed onto coverslips were incubated with a 10^{-3} dilution of anti-NSP1 serum (Panels A and C) for 1 hour at 37 °C, followed by a similar incubation with a 10^{-2} dilution of FITC conjugate goat anti-rabbit Immunoglobulin (Section 3.7.3). The cells were examined by UV microscopy and photographed. The cells were washed and then incubated with a 10^{-3} dilution of polyclonal anti-UKtc serum, followed by a 10^{-2} dilution of FITC conjugate goat anti-rabbit Immunoglobulin as before (Panels B and D).

6.3.7 Summary

Inoculation of a rabbit with a recombinant vaccinia virus expressing NSP1 (VR5) failed to generate anti-NSP1 antibodies. The serum did not immunoprecipitate NSP1 either from infected cell lysates or from a reaction containing *in vitro* translated NSP1. The serum reacted with VR5-infected cells but not with rotavirus-infected cells in an immunofluorescence assay, suggesting that anti-vaccinia, but not anti-rotavirus, antibodies were generated. This failure to produce a hyper-immune serum could be a result of the low antigenicity of NSP1. Also, it should be noted that other researchers have had difficulties in the production of an antiserum against this protein (Brottier *et al.*, 1992). As a result, the limited quantity of the anti-NSP1 serum obtained from Dr Cohen was used for all the immunoprecipitation experiments described here.

6.4 Construction of plasmids for *in vitro* expression of rotavirus proteins

6.4.1 Cloning strategy

The linked T7 transcription-translation system enables *in vitro* synthesis of proteins from DNA templates containing T7 promoters upstream of coding sequences. It was decided that this system would be a convenient one in which to produce proteins that could be used to test for co-precipitation of viral proteins with NSP1. A consequence of this was the need to produce plasmids containing rotavirus genes under control of the T7 promoter.

A plasmid containing UKtc rotavirus gene 5 coupled to the T7 promoter (G5T7-TA1) had already been constructed by Dr Xu Li in the Rotavirus laboratory. Gene 5 was cloned directly into the pCR^{TM}II vector (Invitrogen) by TA cloning and the gene was flanked by *Eco*R I sites and under control of the T7 promoter.

6.4.2 Cloning rotavirus genes 1, 2 and 3 into pTAg

PCR products of rotavirus genes 1,2 and 3 had previously been cloned directly into the TA vector pTAg as part of a sub-cloning procedure (Section 4.4). This vector contains the T7 promoter immediately adjacent to an MCS into which PCR products can be directly ligated by TA cloning (Figure 4.10). Therefore, these plasmids could be used for *in vitro* transcription-translation.

The orientation of the rotavirus genes in relation to the T7 promoter was confirmed by restriction enzyme digest analysis of mini-prep DNA (Figure 6.5). Clones of T7-pTAg-gene1 were digested with *Eco*R I and produced fragments of 5600 bp, 900 bp and 600 bp which indicated that all the clones analysed were in the correct orientation in relation to the T7 promoter. Clones of T7-pTAg-gene2 were digested with *Hind* III and *Mlu* I. Digests with *Hind* III produced fragments of 5300 bp, 800 bp and 340 bp. Digests with *Mlu* I produced fragments of 5800 bp and 700 bp. Thus, all clones of T7-pTAg-gene2 analysed were in the correct orientation with respect to the T7 promoter. Clones of T7-pTAg-gene3 were digested with *Eco*R I and produced fragments of 4400 bp, 1800 bp and 200 bp, again indicating that they were correctly orientated in relation to the T7 promoter.

Prior to using these plasmids for *in vitro* transcription-translation, additional cloning steps were performed to remove an ATG codon present in the 5' sequence of pTAg between the T7 promoter and the ATG start codon of the inserted rotavirus gene. This additional ATG codon could have led either to initiation of out-of-frame translation, or the addition of extra amino acids to the amino terminus of the translated protein, both of which were clearly undesirable. Removal of this upstream ATG was achieved by cutting the plasmids on either side of the codon at unique restriction sites, blunt ending the DNA with T4 DNA polymerase and ligating the free ends to recreate the plasmid. For example, the extra ATG in pTAg-gene3 was removed by cutting with *Kpn* I and *Mlu* I to excise the unwanted sequence, and then religating to create plasmid T7-pTAg-gene3 (Figure 6.6). The procedure resulted in the concomitant loss of a *Pst* I site, thus restriction enzyme digestion analysis with *Pst* I was used to identify the new clone. Digestion of the new plasmid with *Pst* I resulted in linearisation when previously the insert had been released. Sequence analysis revealed that the extra ATG site had been removed, but several additional nucleotides had also been removed in the process. However, this did not affect the T7 promoter or the ATG initiation codon of gene 3, and the gene 3 sequence was found to be intact.

Figure 6.5 Restriction enzyme digestion analysis of clones T7-pTAg-Gene1, T7-pTAg-Gene2 and T7-pTAg-Gene3

A. Restriction enzyme digestion analysis of new clones

Plasmid DNA from clones produced from the ligation of rotavirus genes 1, 2 and 3 into pTAg (3816 bp) was prepared by mini-prep (Section 3.4.13). Restriction enzyme digests (Section 3.4.6) were performed to determine the correct orientation of the gene in relation to the T7 promoter in pTAg and the results analysed by gel electrophoresis on a 1 % agarose gel (Section 3.4.3). Bands smaller than 500 bp are too faint to be visualized on this photograph. The individual clones of each plasmid construct are identified at the top of the gel. Lanes marked L were loaded with 1 Kb DNA ladder. Sizes of the markers are given in base pairs.

B. Schematic diagrams to show the restriction enzyme sites in each clone

T7-pTAg-Gene1 digested with *Eco*R I produces fragments of 5600 bp, 900 bp and 600 bp when in the correct orientation (Panel A, Gene 1 lanes). T7-pTAg-Gene2 digested with *Hind* III produces fragments of 5300 bp, 800 bp and 340 bp when in the correct orientation (Panel A, Gene 2 lanes, *Hind* III). T7-pTAg-Gene2 digested with *Mlu* I produces fragments of 5800 bp and 700 bp (Panel A, Gene 2 lanes, *Mlu* I). T7-pTAg-Gene3 digested with *Eco*R I produces fragments of 4400 bp, 1800 bp and 200 bp when in the correct orientation (Panel A, Gene 3 lanes).

Figure 6.5

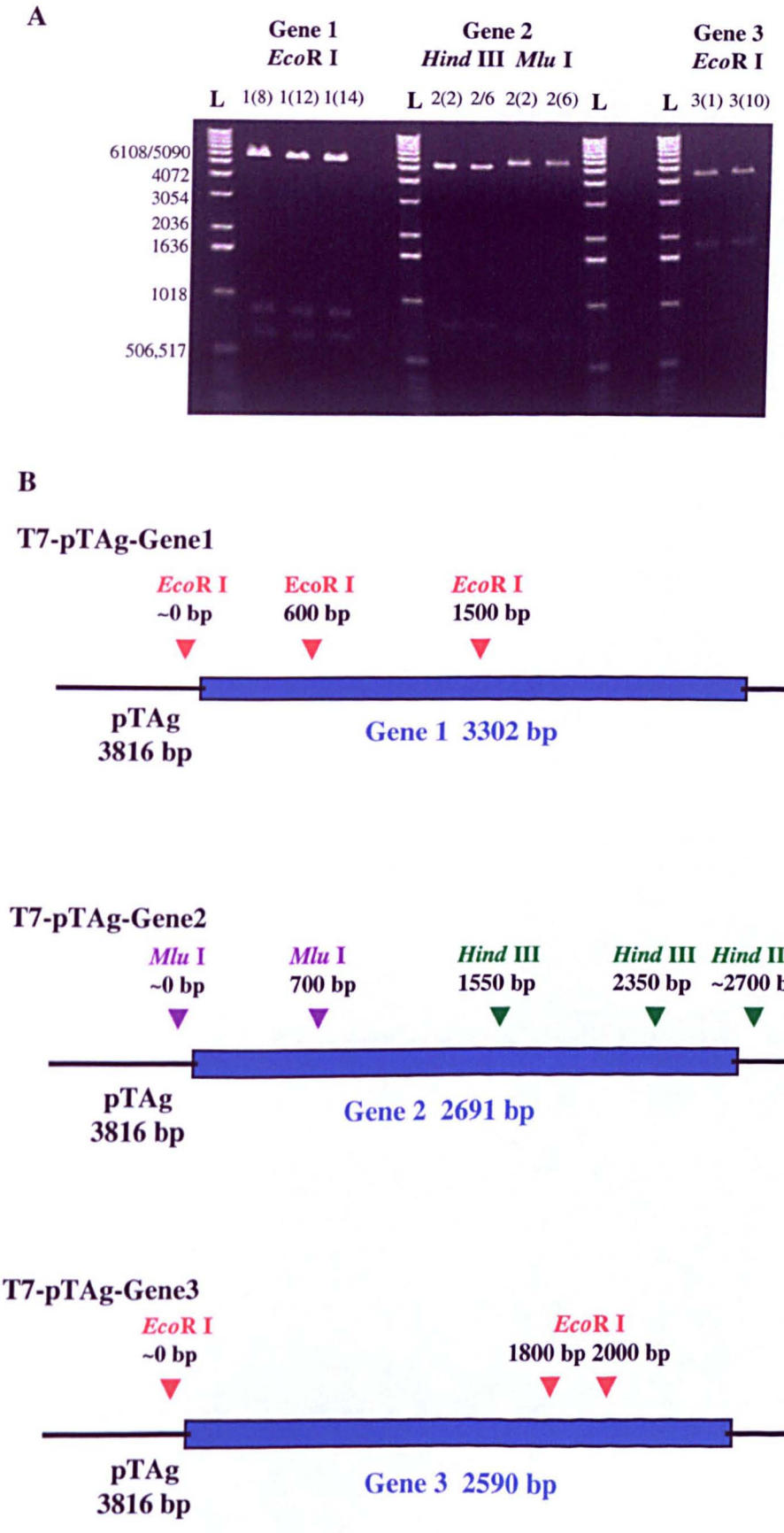
A
Gene 1
EcoR I
Gene 2
Hind III Mlu I
Gene 3
EcoR I
L 1(8) 1(12) 1(14) L 2(2) 2/6 2(2) 2(6) L L 3(1) 3(10)
6108/5090
4072
3054
2036
1636
1018
506,517
B
T7-pTAg-Gene1
EcoR I
~0 bp
EcoR I
600 bp
EcoR I
1500 bp
pTAg
3816 bp
Gene 1 3302 bp
T7-pTAg-Gene2
Mlu I
~0 bp
Mlu I
700 bp
Hind III
1550 bp
Hind III
2350 bp
Hind III
~2700 bp
pTAg
3816 bp
Gene 2 2691 bp
T7-pTAg-Gene3
EcoR I
~0 bp
EcoR I
1800 bp 2000 bp
pTAg
3816 bp
Gene 3 2590 bp

Figure 6.6 Analysis of the removal of sequence containing an additional ATG start site upstream of the 5' end of gene 3 in clone pTAg-Gene 3

A. Restriction enzyme digestion analysis

Clone pTAG-gene 3 was digested with restriction enzymes *Kpn* I and *Mlu* I (Section 3.4.6) which cut either side of the sequence containing the unwanted ATG start site in the pTAg MCS. The 5' and 3' end overhangs which were created, were blunt ended with T4 DNA polymerase and the Klenow fragment (Section 3.4.8). The blunt ends of the plasmid were then religated (Section 3.5.10). Plasmid DNA was amplified and purified by mini-prep (Section 3.4.13) and the new plasmid, T7-pTAg-gene3, was identified by restriction enzyme digestion (Section 3.4.6). The products of the digests were analysed by electrophoresis on a 1.0 % TAE agarose gel (Section 3.4.3). Lanes marked G3 contain the old plasmid pTAg-gene 3 digested with the enzymes indicated. Lanes marked G3* contain the new plasmid T7-pTAg-gene 3 digested with the enzymes indicated. Digestion of both pTAg-gene 3 and T7-pTAg-gene 3 plasmids with *Bam*H I released the insert, resulting in bands at 3816 bp and 2590 bp. Digestion with *Pst* I linearised the new plasmid T7-pTAg-gene 3 (6406 bp) but released the gene 3 insert in the old plasmid pTAg-gene 3 (3816 and 2590 bp), due to the loss of a *Pst* I site during the procedure. Lanes marked L were loaded with 1 Kb DNA ladder. The sizes of the markers are given in base pairs.

B. Sequence analysis

The 5' end of gene 3 in plasmid pTAg-gene 3 was sequenced (Section 3.4.18) with primer pTAg SEQ 5' (Table 3.3). Analysis of the sequence revealed that an extra ATG site was present in the MCS of pTAg between the T7 promoter and the ATG start site in gene 3, as shown in the figure. Plasmid pTAg-gene 3 was cut with *Kpn* I and *Mlu* I to excise the region containing the extra ATG site and thus create plasmid T7-pTAg-gene 3. The new plasmid T7-pTAg-gene 3 was sequenced as before. The restriction enzyme sites are shown in red. The *Pst* I site which was removed during this procedure is shown in yellow. The initiation codon for gene 3 is underlined in blue.

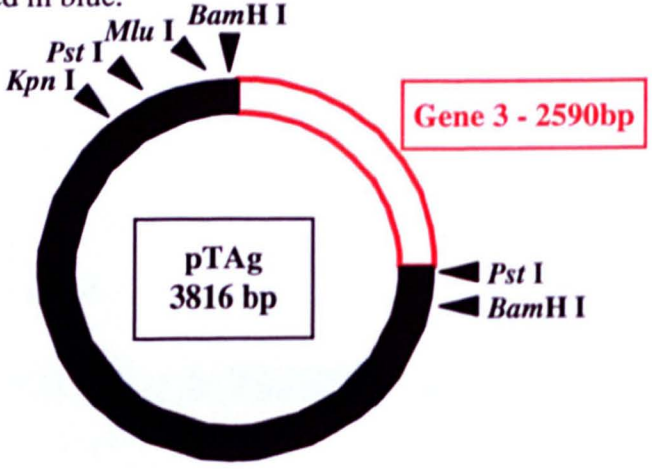

Figure 6.6

A

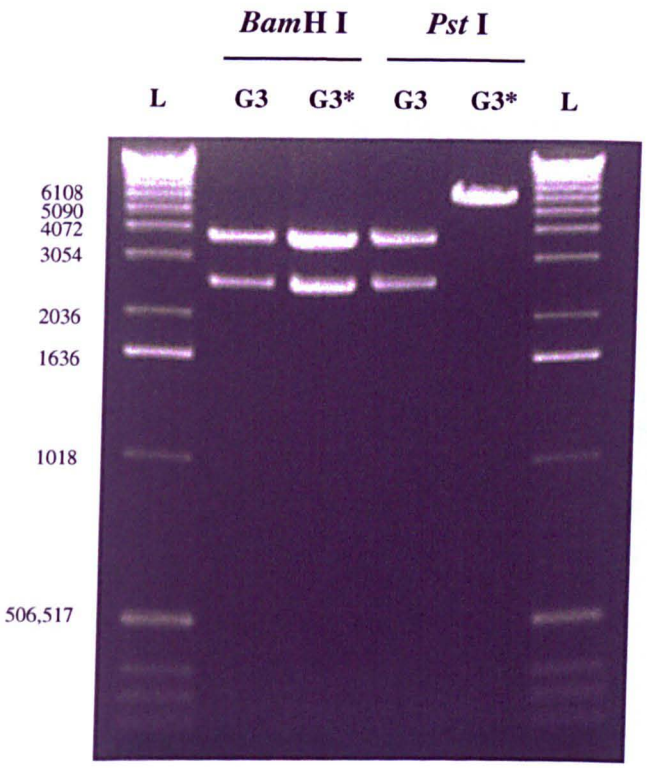

B

pTAg-Gene 3 (G3)

Kpn I *Mlu* I

TCGGTACCACGCATGCTGCAGACGCGTTACGTATCGGATCCAGAATTC

GTGATTATCCGGATG *Pst* I

T7-pTAg-Gene 3 (G3*)

TCGTATCGGATCCAGAATTCGTGATTATCCGGATG

6.5 Expression of NSP1 in vitro

6.5.1 In vitro coupled transcription-translation of Gene 5

A coupled T7 transcription-translation system (Section 3.6.1), based on transcription with T7 RNA polymerase followed by translation in an optimised rabbit reticulocyte lysate, was used to produce viral proteins for use in immunoprecipitation experiments. Optimisation of the *in vitro* coupled transcription-translation reaction was performed to ensure sufficient levels of full-length NSP1 and only minimum incomplete translation products were produced. It was desirable that only a single, full-length protein was produced as this leads to cleaner immunoprecipitation reactions, the results of which are less open to misinterpretation. Therefore optimisation of the production of NSP1 was performed initially.

The two variables which were tested in the coupled transcription-translation system were the concentration of plasmid G5T7-TA1, which contained gene 5 under control of the T7 promoter, and the quantity of the label ^{35}S-methionine which was added to the reaction. Increasing the concentration of plasmid DNA in the reaction was thought to increase the quantity of the translation product. The incorporation of the ^{35}S-methionine label depends upon the efficiency of translation and the number of methionine residues in the protein. The amount of label used was optimised so that the translation product could be easily visualised by autoradiography. A positive control plasmid, the *E. coli* β-galactosidase gene cloned into a pCITE vector, was translated to ensure efficiency of the reactions and a strong band at approximately 118 kDa, which corresponds to *E. coli* β-galactosidase, could be seen (Figure 6.7). A number of smaller bands which probably correspond to incomplete translation products were also seen. A blank reaction containing no plasmid DNA was performed to ensure there was no contamination of the reaction components with DNA from extraneous sources. As expected no protein was produced in this reaction (data not shown), indicating that the reaction components were not contaminated. Two different concentrations of G5T7-TA1 were compared for their translation efficiency [0.5 μg (lane 2); 1 μg (lane 3)]. In each case a protein band of approximately 53 kDa, which corresponds to NSP1, and only minimal incomplete translation products were seen. By inspection it appears that the quantity of protein in these NSP1 bands (lanes 2-3) are approximately equal. A translation reaction containing twice as much ^{35}S-methionine as the previous reaction (20 μCi) but the same quantity of plasmid DNA

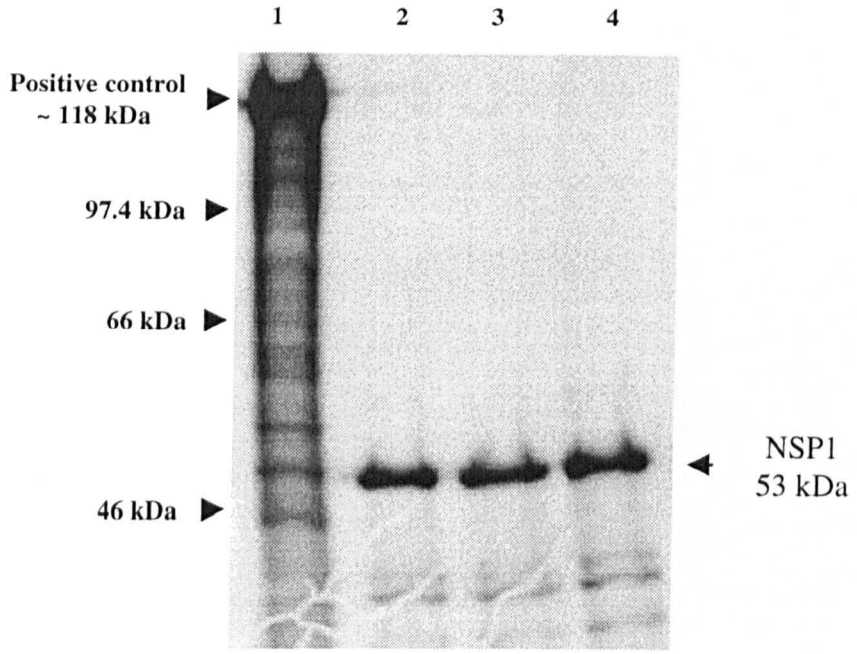

Figure 6.7 Optimization of expression of NSP1 from plasmid G5T7-TA1 in an *in vitro* coupled transcription-translation system

G5T7-TA1 was purified by phenol extraction (Section 3.4.4) and ethanol precipitation (Section 3.4.5) and used to programme *in vitro* coupled transcription-translation reactions (Section 3.6.1) for expression of NSP1. A positive control plasmid, the *E. coli* β-galactosidase gene cloned into a pCITE vector, was also translated. The products of the translation reactions were analysed on a 7.5 % polyacrylamide gel (Section 3.6.5) and visualized by dry gel fluorography after a three hour exposure of the gel (Section 3.6.6). Translation of the positive control plasmid produced a band at approximately 118 kDa (lane 1). The translation product of G5T7-TA1 is NSP1 (53 kDa) which is indicated on the figure. Lane 2 shows NSP1 (53 kDa) translated from 0.5 μg of G5T7-TA1 plasmid. Lane 3 shows NSP1 translated from 1.0 μg of G5T7-TA1 plasmid. Lane 4 shows NSP1 translated from 1.0 μg of G5T7-TA1 plasmid with double the concentration of ^{35}S-methionine (20 μCi). The sizes (in kDa) of the markers are indicated on the left of the gel.

(1.0 μg) produced more labelled protein, however more incomplete translation products were also seen (lane 4). After consideration of these results, 10 μCi of ^{35}S-methionine and 1 μg of G5T7-TA1 plasmid DNA was used in future *in vitro* coupled transcription-translation reactions to produce NSP1 protein for immunoprecipitation experiments.

6.5.2 Titration of anti-NSP1 serum.

A titration series was performed with the anti-NSP1 serum to determine the optimum dilution for effective precipitation of NSP1 from the *in vitro* translation reaction, and also the minimum amount of serum which could be used for the immunoprecipitation reactions. The objective was to reduce precipitation of incomplete translation products of NSP1 so that only the full length protein was visible on the gel. This would result in cleaner, easier to interpret immunoprecipitation reactions. Titration of polyclonal antiserum to determine the minimum amount required to precipitate the antigen often helps to lower the non-specific background. Therefore, it was thought that the use of a low concentration of anti-NSP1 serum may reduce any non-specific precipitation of other proteins. This experiment examined the immunoprecipitation of NSP1 only, although it was thought that determination of the minimum serum concentration required at this stage may reduce non-specific precipitation of other proteins in future co-precipitation experiments.

A serial two-fold dilution of the antiserum was made and immunoprecipitation reactions were performed with equal aliquots of NSP1 (Figure 6.8). All the serum dilutions precipitated visible amounts of NSP1, although the highest dilution (1/16) gave a considerably fainter protein band. A 1/8 dilution of the serum was chosen as the working dilution as this precipitated a quantity of NSP1 which was clearly visible on a gel after a short exposure and fewer incomplete translation products than lower dilutions.

Figure 6.8

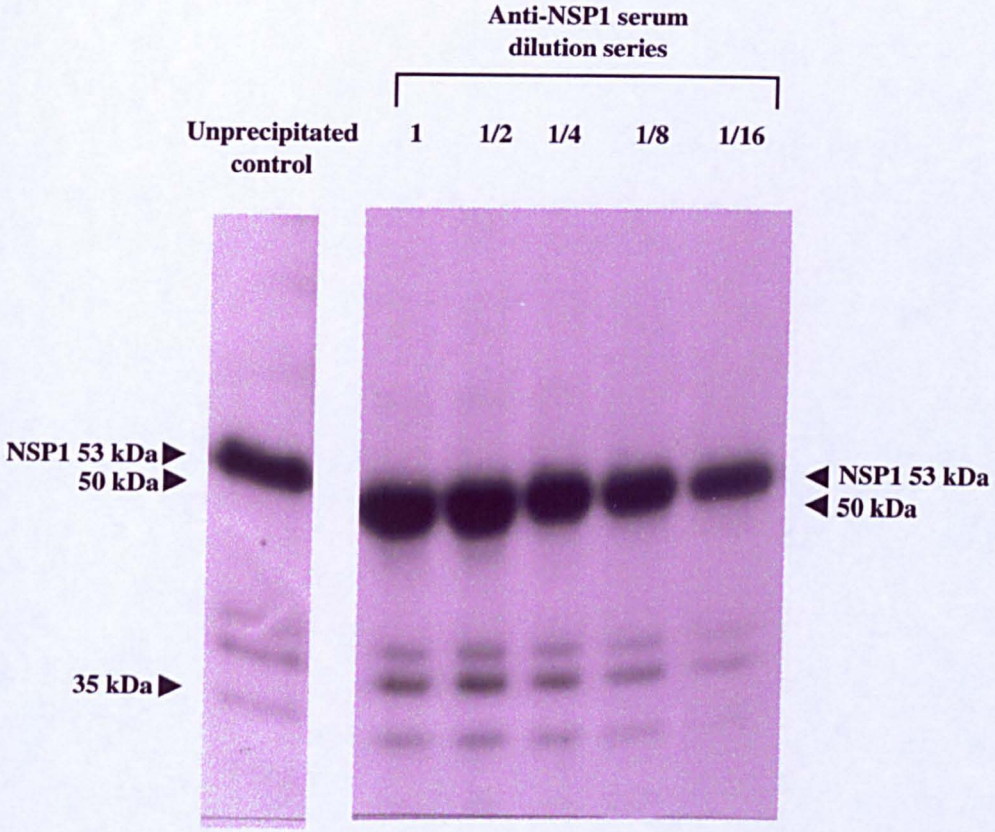

Figure 6.8 Titration of anti-NSP1 serum against *in vitro* translated NSP1

An *in vitro* coupled transcription-translation system (Section 3.6.1) was used to produce NSP1 protein. A serial two-fold dilution of specific anti-NSP1 serum was made and reactions were prepared containing equal aliquots of NSP1 protein (5 µl) with each dilution. The reactions were incubated overnight at 4 °C then precipitated with protein A-Sepharose (Section 3.6.4). The reactions were analysed on a 7.5 % polyacrylamide gel (Section 3.6.5) and the results visualised by dry gel fluorography after a 3 day exposure of the gel to X-ray film (Section 3.6.6). The dilution of antiserum used in the reaction is indicated at the top of the appropriate lane. A protein band at 53 kDa, corresponding to NSP1, was seen for each reaction. The unprecipitated control was 3 µl of the *in vitro* translate reaction run on the same gel. The positions of the size markers (in kDa) are indicated.

6.6 Co-Immunoprecipitation studies with NSP1 and structural proteins of the virus core

6.6.1 Co-Immunoprecipitation of NSP1 and VP2

An initial study was performed to determine if *in vitro* synthesised VP2 was co-immunoprecipitated with NSP1. NSP1 and VP2 were produced both in separate and co-translation reactions in the *in vitro* system (Section 3.6.1). Four separate immunoprecipitation reactions were prepared: (i) NSP1 only; (ii) VP2 only; (iii) NSP1 and VP2 translated separately then mixed together; (iv) NSP1 and VP2 co-translated. The reactions were incubated with anti-NSP1 serum before precipitation with protein A-Sepharose (Section 3.6.4). This experiment showed co-precipitation of VP2 with NSP1, however significant amounts of VP2 were also precipitated by the anti-NSP1 serum when VP2 was present alone (Figure 6.9, lanes 13-16).

As a result of the initial study described previously, further experiments were designed to analyse the observed co-precipitation of VP2 with NSP1. Although VP2 was shown to be co-precipitated with NSP1, it was also precipitated by the serum when NSP1 was not present. VP2 may have been precipitated by specific antibodies in the serum. Alternatively, background precipitation of VP2 caused by the protein sticking to the protein A-Sepharose or forming a particulate structure which spins down with the Sepharose, may have been the cause of the precipitation. Therefore, in addition to immunoprecipitation reactions with the anti-NSP1 serum, reactions were performed with no serum to determine if VP2 was precipitating as a result of a non-specific reaction with the protein A-Sepharose. A reaction with pre-immune serum was performed, and a polyclonal anti-rotavirus serum was also tested for precipitation of either protein. The experimental design was altered slightly in that the number of washes containing 2 % detergents and 1 M NaCl were increased in an attempt to improve the efficiency of removal of non-specifically bound proteins.

The results of the immunoprecipitation reactions containing NSP1 and VP2 with no serum (Figure 6.9, lanes 1-4) clearly showed that none of the proteins were precipitated. However, on a longer exposure of this gel (approximately four times longer) a faint band corresponding to VP2 could be seen in the immunoprecipitation reaction containing a mixture of NSP1 and VP2 (lane 4). This suggested that a small quantity of the VP2 protein was associated with the protein A-Sepharose. The results of the immunoprecipitation reactions with the polyclonal anti-rotavirus serum (Figure

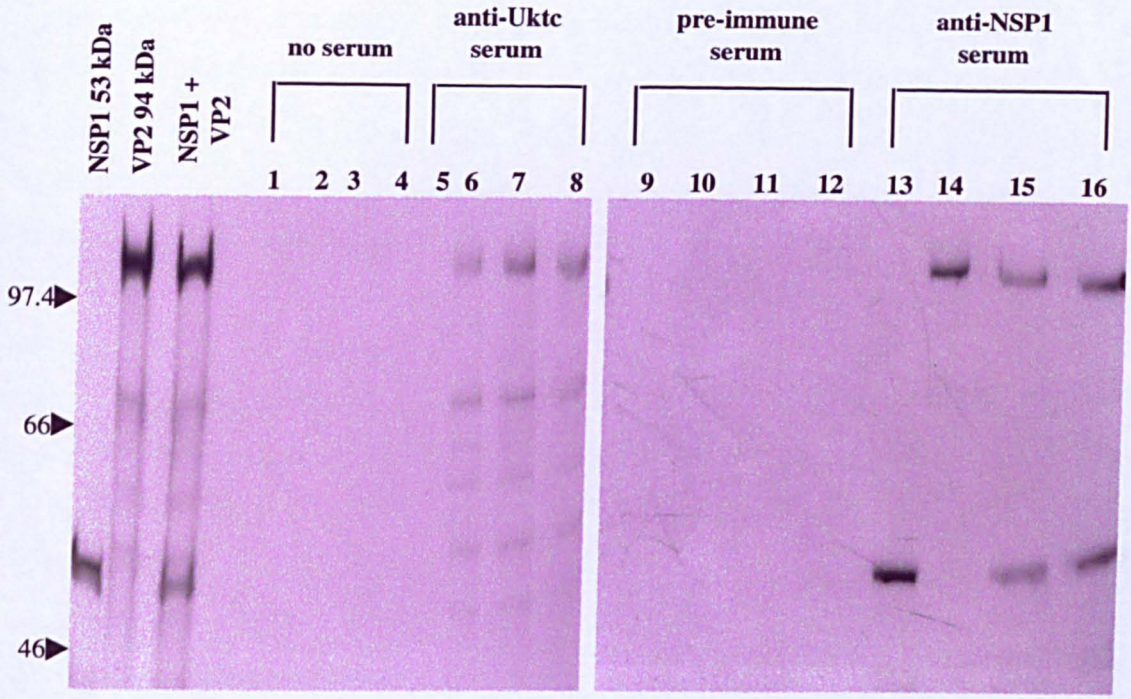

Figure 6.9 Co-immunoprecipitation of VP2 and NSP1

NSP1 and VP2 were translated in an *in vitro* coupled transcription-translation system (Section 3.6.1). Immunoprecipitation reactions with different sera, as indicated below, were performed as described (Section 3.6.4). The reactions were analysed on 7.5 % polyacrylamide gels (Section 3.6.5), and the results visualized by dry gel fluorography after a 24 hour exposure of the gel (Section 3.6.6). The unprecipitated *in vitro* translated proteins are shown on the far left of the gel, and the size of each protein is indicated above. Lanes 1-4 represent immunoprecipitation reactions of NSP1 (lane 1), VP2 (lane 2), NSP1 + VP2 cotranslated (lane 3) and NSP1 + VP2 mixed (lane 4) with no serum. Lanes 5-8 represent immunoprecipitation reactions with polyclonal anti-rotavirus serum (sample order as previously). Lanes 9-12 represent immunoprecipitation reactions with pre-immune serum (sample order as previously). Lanes 13-16 represent immunoprecipitation reactions with anti-NSP1 serum (sample order as previously). The sizes of the markers (in kDa) are indicated on the left of the gel.

6.9, lanes 5-8) showed that when the proteins were present individually VP2 (lane 6), but not NSP1 (lane 5), was precipitated by this serum. In the immunoprecipitation reaction containing both NSP1 and VP2 (Figure 6.9, lanes 7-8), a band corresponding to VP2 was observed, however there was no co-precipitation of NSP1 with VP2. Faint bands can be seen at approximately 50 kDa, however these are thought to be incomplete translation products of VP2. This result suggested that NSP1 does not bind to VP2 as it was not co-precipitated with VP2 using the anti-rotavirus serum. Immunoprecipitation of NSP1 and VP2 with pre-immune serum (Figure 6.9, lanes 9-12) failed to precipitate either protein. It should be noted that since the pre-immune serum taken from the same rabbit as the anti-NSP1 serum was not obtained, the pre-immune serum used in this case was from a rabbit used to raise antisera against rotavirus proteins at the University of Warwick. The results of immunoprecipitation reactions with the anti-NSP1 serum confirmed the initial observations (Figure 6.9, lanes 13-16). In a reaction containing both NSP1 and VP2 (lanes 15-16), VP2 co-precipitated with NSP1. However, when NSP1 was not added to the reaction (lane 14), VP2 was still precipitated by the anti-NSP1 serum.

It was observed that immunoprecipitation reactions with specific anti-NSP1 serum resulted in co-precipitation of VP2 with NSP1. However, the result of the negative control reaction showed that VP2 was precipitated by the anti-NSP1 serum when NSP1 was not present. This could suggest that the co-precipitation of VP2 with NSP1 was not a true co-precipitation resulting from an interaction between the two proteins, but was actually entirely non-specific precipitation of VP2. The possibility also exists however that an interaction between NSP1 and VP2 might be masked by the significant non-specific precipitation of VP2. Although VP2 was not precipitated by the pre-immune serum, a small quantity was precipitated by the protein A-Sepharose. This suggested a degree of non-specific precipitation of VP2 with the protein A-Sepharose. VP2, but not NSP1, was precipitated by the anti-rotavirus serum. Co-precipitation of NSP1 with VP2 was not observed in the reaction with anti-rotavirus serum, suggesting there may not be a direct interaction between the two proteins *in vitro*.

VP2 appeared to be specifically precipitated by the anti-NSP1 serum. VP2 has been shown to be precipitated from cell lysates by the anti-NSP1 serum as mentioned previously (Brottier *et al.*, 1992). It was suggested that the rabbit used to raise this serum may have become infected with rotavirus during serum production, however as

VP2 is the inner core protein it seems unlikely that antibodies specific to VP2 would have been raised as a result. Hence an alternative suggestion in this case is that *in vitro* expressed VP2 shares a common epitope with NSP1, resulting in precipitation of VP2 by the anti-NSP1 serum.

6.6.2 VP2 may share a common epitope with NSP1

To test the proposal that *in vitro* expressed VP2 shares a common epitope with NSP1 which causes it to be precipitated by the anti-NSP1 serum, a number of truncated VP2 proteins were produced and analysed by immunoprecipitation. The failure of the serum to precipitate a shorter protein might indicate the loss of the proposed common epitope, which could then be mapped to a particular region of the protein.

Truncated VP2 proteins were generated by digesting the T7-pTAg-gene2 plasmid used in the coupled transcription-translation reactions with various restriction enzymes prior to addition to the reaction. The T7-pTAg-gene2 plasmid was first linearised with *Sal* I which cuts in pTAg immediately adjacent to the 3' end of gene 2. A number of different restriction enzyme sites in gene 2 were chosen as the second cutting site with the following considerations. The sites were chosen, as far as possible, at approximately equal intervals of 300 bp from the 3' end. It was noted that only the full length VP2 protein was precipitated by the anti-NSP1 serum (Figure 6.9), while the incomplete translation products were not precipitated. Hence, this suggested that the common epitope must lie towards the carboxy terminus of the protein and was the rationale for incrementally removing this region of the protein. The second consideration was that the chosen enzymes must be single cutters in T7-pTAg-gene2. It was also necessary that digestion with the enzyme produced either a 5' overhang or a blunt end, as 3' overhangs can cause aberrant transcription from the non-coding strand by T7 RNA polymerase (Schenborn and Mierendorf, 1985). The combination of enzymes and the position in gene 2 at which they cut is shown in Figure 6.10. The lack of suitable restriction sites, by the criteria defined above, between 885 bp and 1886 bp, meant that the middle third of the protein could not be dissected as closely as desired.

DNA was cut sequentially with *Sal* I and a second enzyme as indicated (Figure 6.10), gel purified and used to programme *in vitro* transcription-translation

Figure 6.10

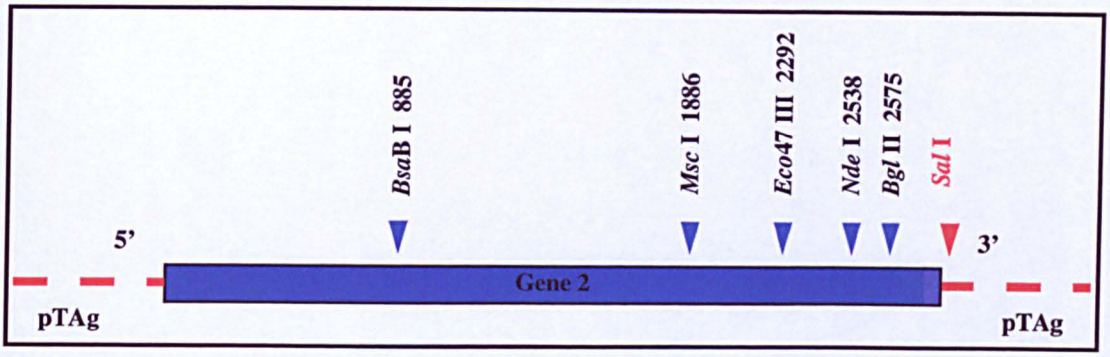

Enzymes	Position of second restriction enzyme site in Gene2	Predicted size of truncated VP2 (kDa)
Sal I	-	94
Sal I + *Bgl* II	2575	90
Sal I + *Nde* I	2538	89
Sal I + *Eco*47 III	2292	80
Sal I + *Msc* I	1886	66
Sal I + *Bsa*B I	885	31

Figure 6.10 Scheme employed to produce truncated VP2 proteins by restriction enzyme digestion of T7-pTAg-Gene2

Truncated VP2 proteins were produced by digesting the T7-pTAg-gene2 plasmid with various restriction enzymes. *Sal* I, which cuts in pTAg at the 3' end of gene 2, was used to linearise the plasmid. Restriction enzymes which cut at different points in gene 2 were then used to incrementally remove the 3' terminus of the gene. The positions at which the restriction enzymes cut in gene 2 are indicated in the figure. Translation of the digested plasmids in the *in vitro* system resulted in the production of a series of truncated proteins with different fragments of the carboxy terminus of VP2 removed. The predicted sizes of the truncated proteins are indicated in the table.

reactions. Translation products were examined by polyacrylamide electrophoresis and the rate of incorporation of the radiolabel was examined by TCA precipitation assay (Section 3.6.2). Protein translated from the linearised plasmid (*Sal* I only) could not be visualised on a gel, and appeared to be inefficiently translated. However, the remaining truncated proteins were clearly visible on a gel, although they were translated with different efficiencies. The protein bands for the truncated VP2 proteins of 89 kDa, 66 kDa, and 31 kDa were of approximately equal strength. Each truncated VP2 protein was added to an immunoprecipitation reaction with anti-NSP1 serum and the results analysed (Figure 6.11). The first three lanes on the left side of the gel show NSP1 and full-length VP2 precipitated with the anti-NSP1 serum and as this is a long exposure these lanes are very over-exposed. The immunoprecipitation of NSP1 and VP2 by the anti-NSP1 serum confirmed the result described previously (Section 6.6.1). The results of the immunoprecipitation reactions with the truncated VP2 proteins from 90 kDa to 31 kDa are shown. Protein bands of the expected sizes can clearly be seen in lanes 90 kDa to 66 kDa (the 94 kDa protein was not expressed sufficiently to visualise on a gel). However, no protein band was visible in lane 31 kDa although it is known that this protein was efficiently expressed. This suggested that the 31 kDa VP2 protein had lost the epitope recognised by the anti-NSP1 serum, thus placing the proposed common epitope between 31 kDa and 66 kDa in the middle third region of the protein. As mentioned previously, a lack of suitable restriction sites in this region denied the possibility of more accurate location of this epitope. The production of a truncated VP2 protein, representing the amino-terminal third of the protein, resulted in the loss of immunoprecipitation by the anti-NSP1 serum, implying that a proposed epitope for the serum in VP2 had been removed. This epitope has been mapped to the middle third region of the protein. Alternatively, the truncation of the protein might have disrupted the overall conformation such that a conformational epitope was no longer recognised by the anti-NSP1 serum.

6.6.3 Co-Immunoprecipitation of VP1 with NSP1

The coupled transcription-translation system, programmed with T7-pTAg-gene1, was used to produce VP1 *in vitro*. Analysis of the translation products by polyacrylamide gel electrophoresis revealed a band believed to correspond to VP1, which has a predicted molecular weight of 125 kDa (Figure 6.12, lane 2). A second

Figure 6.11

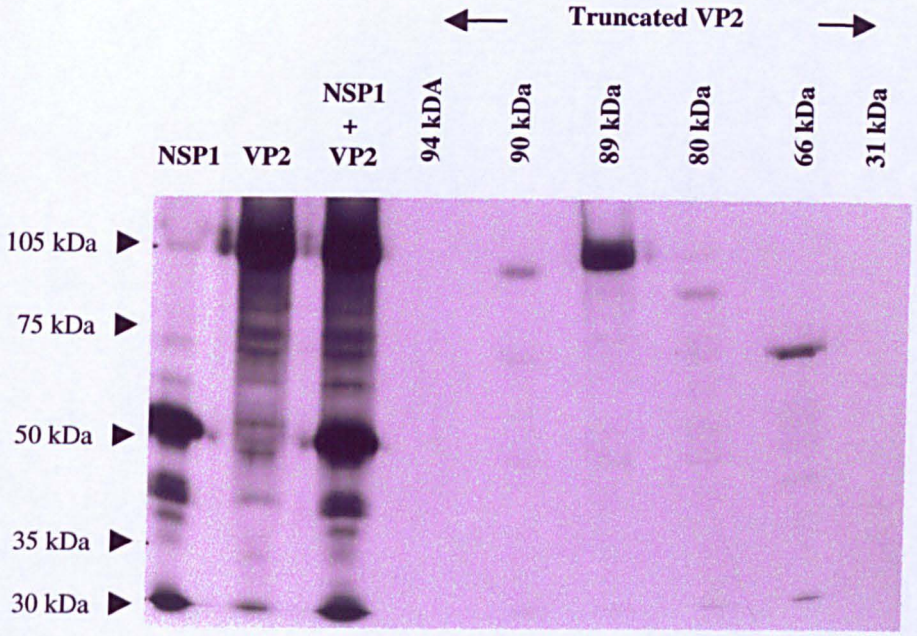

Figure 6.11 Location of an epitope in VP2 for anti-NSP1 serum by immunoprecipitation of *in vitro* expressed truncated VP2 proteins

Plasmid T7-pTAg-gene2 was specifically digested with a combination of restriction enzymes to give different sized fragments of gene 2 (Figure 6.10). Truncated VP2 proteins were expressed in an *in vitro* coupled transcription-translation system (Section 3.6.1) programmed with the specifically digested T7-pTAg-gene2 plasmids. Aliquots of the truncated VP2 protein reactions were incubated overnight at 4 °C with a 1/8 dilution of anti-NSP1 serum and precipitated with protein A-Sepharose (Section 3.6.4). The immunoprecipitation reactions were loaded onto a 7.5 % polyacrylamide gel (Section 3.6.5), and the results analysed by dry gel fluorography after a 4 week exposure of the gel (Section 3.6.6). Immunoprecipitation reactions of NSP1, VP2, and co-translated NSP1 and VP2 are shown (lanes 1-3). The results of immunoprecipitation reactions with the truncated VP2 proteins are also shown (lanes 4-9). The sizes of the truncated VP2 proteins are indicated at the the top of the gel. The 94 kDa protein (lane 4) was not expressed. The sizes of the markers (in kDa) are indicated on the left of the gel.

Figure 6.12

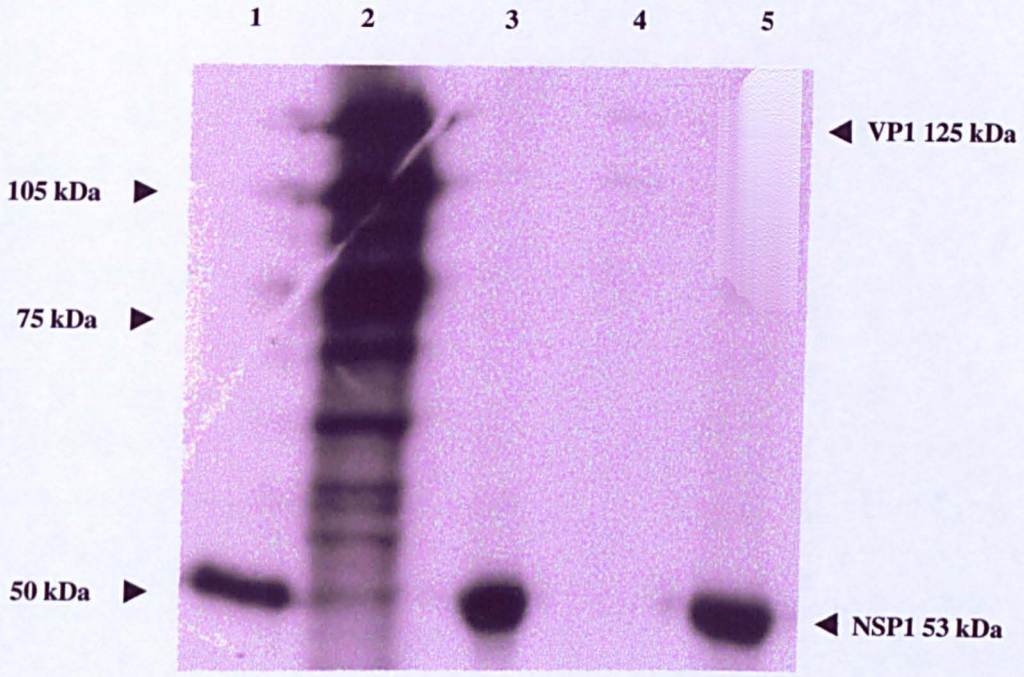

Figure 6.12 Co-immunoprecipitation of NSP1 and VP1 with anti-NSP1 serum

Plasmids G5T7-TA1 and T7-pTAg-Gene1 were used to programme *in vitro* coupled transcription-translation reactions to express NSP1 and VP1 respectively (Section 3.6.1). Approximately equal quantities of NSP1 and VP1 (judged by visualisation on a fluorograph) were incubated overnight at 4 °C with a 1/8 dilution of anti-NSP1 serum and precipitated with protein A-Sepharose (Section 3.6.4). The immunoprecipitation reactions were loaded onto a 7.5 % polyacrylamide gel (Section 3.6.5) and the results analysed by dry gel fluorography after a three day exposure of the gel (Section 3.6.6). Aliquots of the translation reactions of NSP1 (lane 1) and VP1 (lane 2) before immunoprecipitation were analysed on the gel. The position and size of each protein is indicated on the right of the gel. NSP1 (lane 3) and VP1 (lane 4) were each incubated alone with the anti-NSP1 serum. An immunoprecipitation reaction containing VP1 mixed with NSP1 was incubated with the anti-NSP1 serum (lane 5). The sizes of the markers (in kDa) are indicated on the left of the gel.

distinct band at approximately 105 kDa was also observed which could be a premature termination product of VP1. Several smaller bands, also believed to be incomplete translation products, were present.

Co-immunoprecipitation studies were performed with *in vitro* translated VP1 and NSP1. A mixture of *in vitro* translated NSP1 and VP1 was immunoprecipitated with anti-NSP1 serum. Immunoprecipitation reactions with the separate proteins were performed as controls. The results showed that NSP1 alone was strongly precipitated by the serum as expected (Figure 6.12, lane 3). However, VP1 alone was also weakly precipitated (lane 4). When the two proteins were mixed together and immunoprecipitated, both VP1 and NSP1 protein bands were observed. The VP1 band was several times stronger in this case, indicating a possible co-precipitation of VP1 with NSP1.

In the previous experiment VP1 appeared to co-precipitate with NSP1, however non-specific precipitation of VP1 was also observed. To try and eliminate this non-specific binding and thus show a true co-precipitation, the experimental protocol was modified to include an incubation with pre-immune serum prior to incubation with the anti-NSP1 serum. The incubation with the pre-immune serum was intended to act as a clearing step to remove any non-specific binding activity. Translation reactions of NSP1 and VP1, both separately and mixed together as before, were precipitated with pre-immune serum then centrifuged in a microfuge and the supernatant retained. The supernatants from these reactions were then incubated with anti-NSP1 serum. The result of the immunoprecipitation of NSP1 and VP1 mixed together is shown (Figure 6.13, lane 5). A faint VP1 band and a stronger NSP1 band were observed, however the faint VP1 band was matched by a similar faint band in the negative control (VP1 lane 4). This suggested that the incubation with the pre-immune serum removed most of the non-specific binding activity. A true co-precipitation of VP1 with NSP1 was probably not observed when the *in vitro* translated proteins were mixed and immunoprecipitated with anti-NSP1 serum.

6.6.4 Co-Immunoprecipitation of VP3 with NSP1

VP3 was translated *in vitro* in a coupled transcription-translation system programmed with plasmid T7-pTAg-Gene3. To ensure efficiency of expression of VP3, two different concentrations of the plasmid T7-pTAg-Gene3 (1 μg and 2 μg)

Figure 6.13

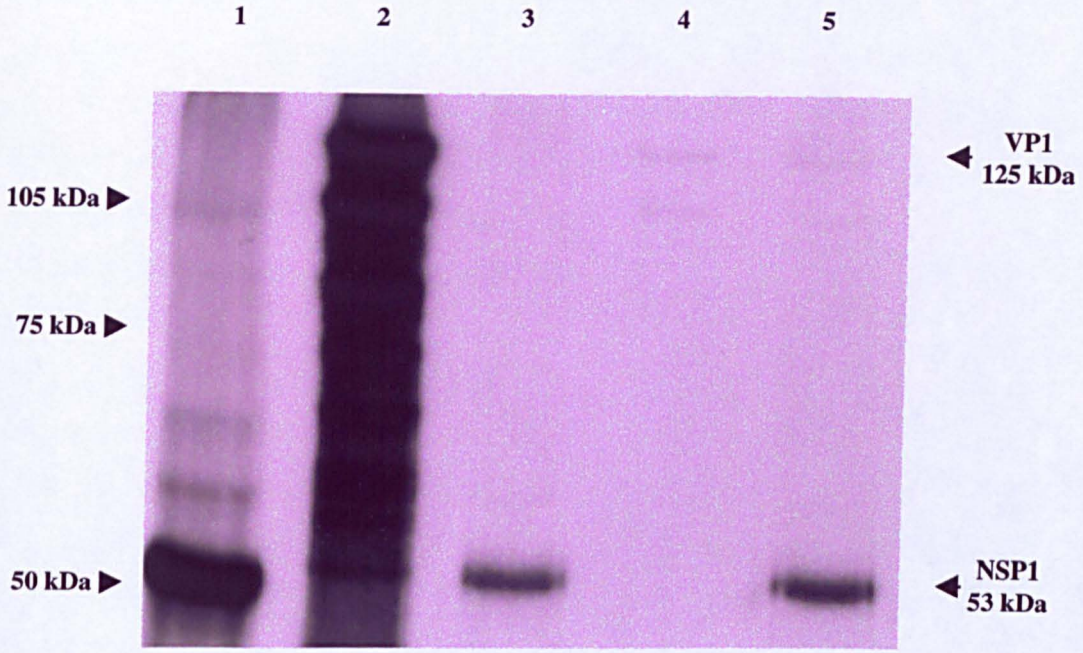

Figure 6.13 Co-immunoprecipitation of NSP1 and VP1 with pre-immune and anti-NSP1 serum

Plasmids G5T7-TA1 and T7-pTAg-Gene1 were used to programme *in vitro* coupled transcription-translation reactions to express NSP1 and VP1 respectively (Section 3.6.1). Approximately equal quantities of NSP1 and VP1 (judged by visualisation on a fluorograph) were incubated with pre-immune serum for 2 hours at 4 °C, precipitated with protein A-Sepharose (Section 3.6.4), then centrifuged in a microfuge for 1 min. and the supernatants retained. The supernatants from these reactions were then incubated overnight at 4 °C with a 1/8 dilution of anti-NSP1 serum and precipitated with protein A-Sepharose. The immunoprecipitation reactions were loaded onto a 7.5 % polyacrylamide gel (Section 3.6.5) and the results analysed by dry gel fluorography after a two-week exposure of the gel (Section 3.6.6). Aliquots of the translation reactions of NSP1 (lane 1) and VP1 (lane 2) before immunoprecipitation were analysed on the gel. Lane 2 is over-exposed. The position and size of each protein is indicated on the right of the gel. NSP1 (lane 3) and VP1 (lane 4) were each incubated separately with pre-immune serum followed by anti-NSP1 serum. A immunoprecipitation reaction containing VP1 mixed with NSP1 was also incubated with pre-immune serum followed by anti-NSP1 serum (lane 5). The sizes of the markers (in kDa) are indicated on the left of the gel.

were translated and compared (Figure 6.14). Significantly more VP3 was obtained when the reaction was primed with 2 μg of plasmid (lane 2) compared to a reaction initiated with only 1 μg of plasmid (lane 1). Several smaller bands, corresponding to incomplete translation products of VP3, were also observed. When VP3 and NSP1 were co-translated (lane 4), one of the incomplete translation products of VP3 was seen to migrate at a similar position to NSP1, making it difficult to determine the efficiency of translation of NSP1 when co-translated with VP3. Although NSP1 was efficiently translated alone (lane 3), it appeared to be much reduced when VP3 was also translated in the same reaction (lane 4).

Immunoprecipitation reactions containing NSP1, VP3, and NSP1 mixed with VP3, were performed with anti-NSP1 serum. An initial analysis of translated VP3 compared to NSP1 gave an approximate ratio of the proteins in the translation reactions of 2:1 (NSP1:VP3) (Figure 6.14 lanes 2 and 3) and this was used to determine approximately equal aliquots of the proteins to be mixed for the immunoprecipitation reactions. When NSP1 and VP3 were mixed together and immunoprecipitated with anti-NSP1 serum, VP3 was co-precipitated with NSP1 (Figure 6.15, lane 6). However, VP3 was also precipitated by the serum in the absence of NSP1 (negative control, lane 5), suggesting that the proposed co-precipitation must, in part, be composed of non-specific precipitation of VP3. The non-specific precipitation of VP3 might also mask a true co-precipitation of VP3 with NSP1.

Further immunoprecipitation experiments were designed to determine the exact nature of the proposed co-precipitation of VP3 with NSP1. Immunoprecipitation with pre-immune serum was carried out to see if there was binding by non-specific antibodies in the serum. An immunoprecipitation reaction with no serum was also performed to test for non-specific binding to the protein A-Sepharose. Polyclonal anti-rotavirus serum was tested to see if it would precipitate either protein. Finally, as a clearing step to remove any non-specific binding activity, an incubation with pre-immune serum was carried out, prior to precipitation with the anti-NSP1 serum. In this last reaction, after incubation with pre-immune serum the reaction was centrifuged and the supernatant, containing any proteins not bound by the pre-immune serum, was removed and incubated in a second reaction with anti-NSP1 serum. The results of these immunoprecipitation reactions are shown in Figure 6.16. VP3 was precipitated by the pre-immune serum, suggesting that it is recognised by specific

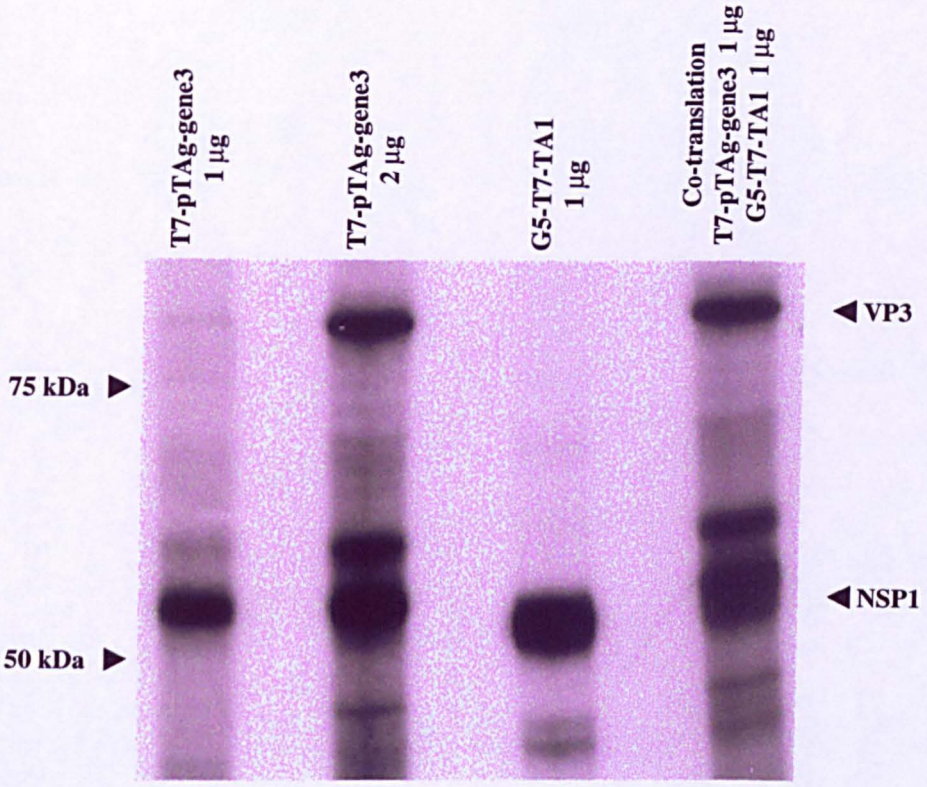

Figure 6.14 Co-expression of VP3 and NSP1 in an *in vitro* coupled transcription-translation system

Plasmids G5T7-TA1 and T7-pTAg-Gene3 were used to programme *in vitro* coupled transcription-translation reactions to express NSP1 and VP3 respectively (Section 3.6.1). The products of the translation reactions were loaded onto a 7.5 % polyacrylamide gel (Section 3.6.5) and the results analysed by dry gel fluorography after a 20 hour exposure of the gel to x-ray film (Section 3.6.6). Two different concentrations of the plasmid T7-pTAg-gene3 (1 µg and 2 µg) were tested. A reaction containing both plasmids G5T7-TA1 and T7-pTAg-Gene3 was analysed for co-translation efficiency of NSP1 and VP3. The plasmid and quantity of DNA used is indicated at the top of the corresponding lane. The positions of the protein bands corresponding to NSP1 and VP3 are indicated on the right of the gel. The sizes of the markers (in kDa) are indicated on the left of the gel.

Figure 6.15

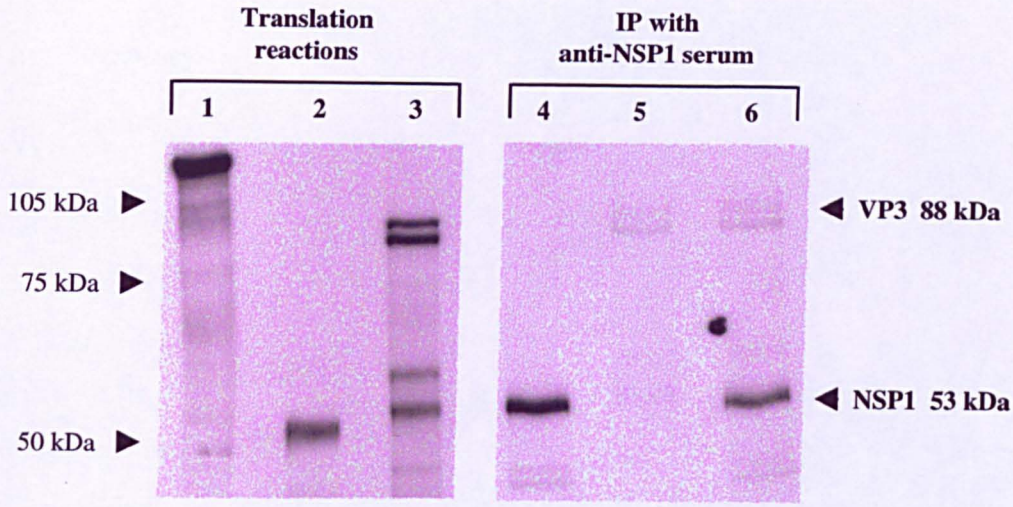

Figure 6.15 Co-Immunoprecipitation of *in vitro* translated NSP1 and VP3 with anti-NSP1 serum

Plasmids G5T7-TA1 and T7-pTAg-Gene3 were used to programme *in vitro* coupled transcription-translation reactions to express NSP1 and VP3 respectively (Section 3.6.1). A positive control plasmid, the *E. coli* β-galactosidase gene cloned into a pCITE vector, was also translated. Approximately equal quantities of NSP1 and VP3 (judged by visualisation on a fluorograph) were incubated overnight at 4 °C with a 1/8 dilution of anti-NSP1 serum and precipitated with protein A-Sepharose (Section 3.6.4). The immunoprecipitation reactions were loaded onto a 7.5 % polyacrylamide gel (Section 3.6.5) and the results analysed by dry gel fluorography after a one day exposure (lanes 1-3) and a one week exposure (lanes 4-6) of the gel (Section 3.6.6). The positive control translation reaction was analysed on the gel and a protein band at approximately 118 kDa was observed (lane 1). Aliquots of the translation reactions of NSP1 (lane 2) and VP3 (lane 3) before immunoprecipitation were analysed on the gel. The position and size of each protein band is indicated on the right of the gel. NSP1 (lane 4) and VP3 (lane 5) were each incubated alone with the anti-NSP1 serum. An immunoprecipitation reaction containing VP3 mixed with NSP1 was incubated with the anti-NSP1 serum (lane 6). The sizes of the markers (in kDa) are indicated on the left of the gel.

Figure 6.16

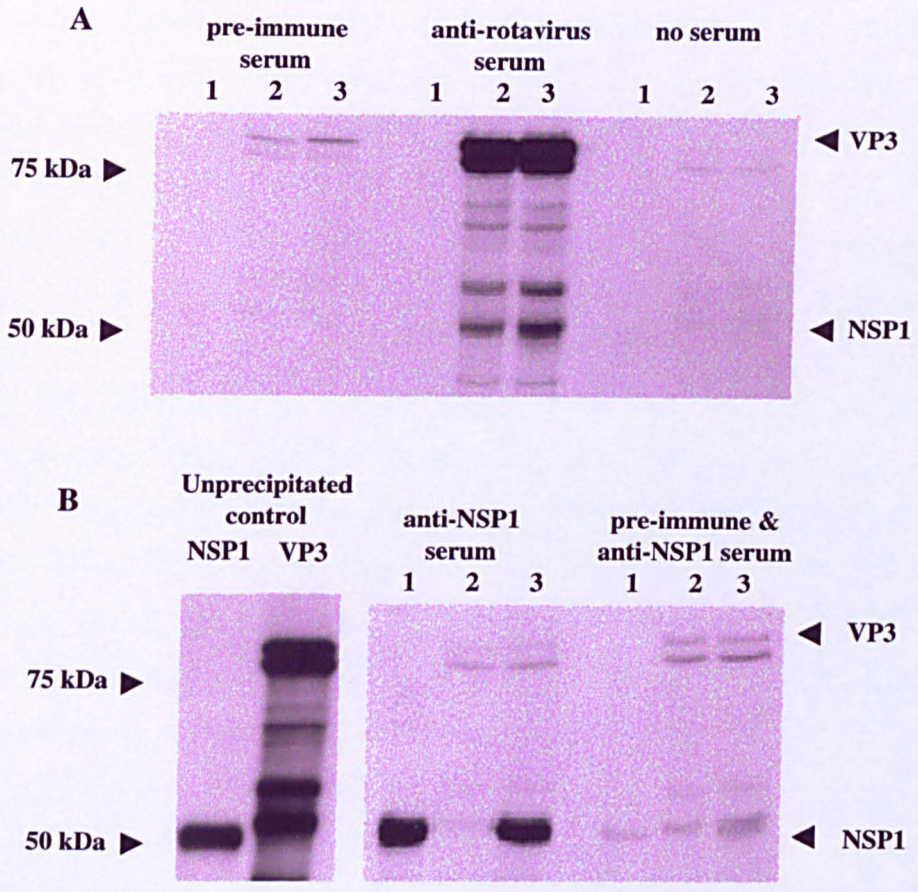

Figure 6.16 Immunoprecipitation of NSP1 and VP3 with pre-immune serum, anti-NSP1 serum, anti-rotavirus serum and protein A-Sepharose only

Plasmids G5T7-TA1 and T7-pTAg-Gene3 were used to programme *in vitro* coupled transcription-translation reactions to express NSP1 and VP3 respectively (Section 3.6.1). Reactions containing approximately equal quantities of NSP1 and VP3 (judged by visualisation on a fluorograph) were incubated overnight at 4 °C with different sera and precipitated with protein A-Sepharose (Section 3.6.4). The immunoprecipitation reactions were loaded onto a 7.5 % polyacrylamide gel (Section 3.6.5) and the results analysed by dry gel fluorography after 17 days exposure of the gel (Section 3.6.6). NSP1 (lane 1), VP3 (lane 2) and NSP1 mixed with VP3 (lane 3) were immunoprecipitated with different sera as indicated on the figure. Panel A shows the results when the reactions were incubated with pre-immune serum, anti-rotavirus serum and without serum. Panel B shows the results with anti-NSP1 serum and with pre-immune serum followed by anti-NSP1 serum. The unprecipitated control was aliquots of the *in vitro* translation reactions of NSP1 (2 µl) and VP3 (4 µl) run on the same gel (4 days exposure). The positions of NSP1 and VP3 on the gel are indicated. The sizes of the markers (in kDa) are shown on the left of the gel.

antibodies in the serum. NSP1 was not precipitated by this serum. When only protein A-Sepharose was present and no serum had been added to the reaction, VP3 was precipitated very slightly so that faint bands were visible. Again, NSP1 was not precipitated in this reaction. This precipitation of VP3 could represent either non-specific binding of the protein by formation of non-covalent bonds with the protein A-Sepharose beads, or possibly an aggregation of the protein that results in a complex which is recovered by centrifugation. In either case, these results suggest that a proportion of the VP3 which is precipitated is due to non-specific background precipitation.

VP3 was precipitated by the polyclonal anti-rotavirus serum however, as described previously NSP1 was not precipitated by this serum (Section 6.6.1). Although VP3 was precipitated from the mixture of NSP1 and VP3 by the polyclonal anti-rotavirus serum, there was no obvious co-precipitation of NSP1 with VP3. As noted before, an incomplete translation product of VP3 migrated at a similar position as NSP1 on the gel (~50 kDa), therefore if NSP1 had been weakly co-precipitated with VP3 it would have been difficult to distinguish it from the VP3 band. Indeed it could be argued that the relevant band at 50 kDa is stronger in the co-precipitation reaction (lane 3) than in the reaction containing VP3 alone (lane 2), a difference which may be accounted for by the presence of NSP1. However, as this evidence was not very convincing, it was concluded that NSP1 was not co-precipitated with VP3 by the anti-rotavirus serum.

The results of the immunoprecipitations in which a clearing reaction with pre-immune serum was performed prior to the incubation with anti-NSP1 serum suggested that an approximately equal quantity of VP3 was co-precipitated with NSP1. However, a similar protein band was seen when VP3 was present alone. These results (Figure 6.16) suggest that the observed co-precipitation of VP3 with NSP1 was probably due to an interaction of VP3 with either non-specific antibodies in the serum or with the protein A-Sepharose complex. However it is also possible that an interaction between VP3 and NSP1 was masked by the non-specific precipitation of VP3.

6.6.5 Co-Immunoprecipitation of VP3 with NSP1 can be blocked with ovalbumin

As indicated above, the results of immunoprecipitation reactions with a mixture of NSP1 and VP3 were ambiguous due to a high background of VP3 precipitation. In an attempt to reduce this non-specific precipitation, a quantity of ovalbumin was added to the reaction mixture to act as a blocking reagent. A BioRad protein assay (Section 3.6.2) was used to determine the protein concentrations of the reactions containing *in vitro* translated NSP1 and VP3. Approximately five times this concentration of ovalbumin was added prior to immunoprecipitation of NSP1 and VP3 with anti-NSP1 serum. The addition of ovalbumin resulted in an overall reduction of the amount of protein precipitated (Figure 6.17, lanes 4-6), when compared to the precipitation reactions without this addition (Figure 6.17, lanes 1-3). The reduction in VP3 was such that the bands were barely visible, even on a two week exposure of the gel. The blocking of non-specific interactions with the serum or the protein A-Sepharose by the addition of ovalbumin resulted in the virtual disappearance of the co-precipitation of VP3 with NSP1, lending further support to the conclusion that the apparent co-precipitation of VP3 was merely due to a non-specific interaction.

6.6.6 Summary

The co-immunoprecipitation experiments initially suggested that the viral core proteins VP1, VP2 and VP3, could be individually co-precipitated with NSP1. However, in each case it was also noted that the negative control reactions (VP1/VP2/VP3 without NSP1) showed precipitation of the core proteins to varying degrees. VP2 was strongly precipitated by the anti-NSP1 serum, leading to the conclusion that *in vitro* translated VP2 may share a common epitope with NSP1 and thus be specifically precipitated by the serum. To this end, a series of truncated VP2 proteins were produced and the proposed common epitope was mapped to the middle third of VP2 between 31-66 kDa. The truncation of the protein could also reflect the disuption of an appropriate conformation rather than the loss of a specific amino acid sequence. Treatment of cell lysates by boiling with β-mercaptoethanol prior to immunoprecipitation with anti-NSP1 serum resulted in a decrease in the precipitation of VP2, which could reflect the disruption of a conformational epitope recognised by

Figure 6.17

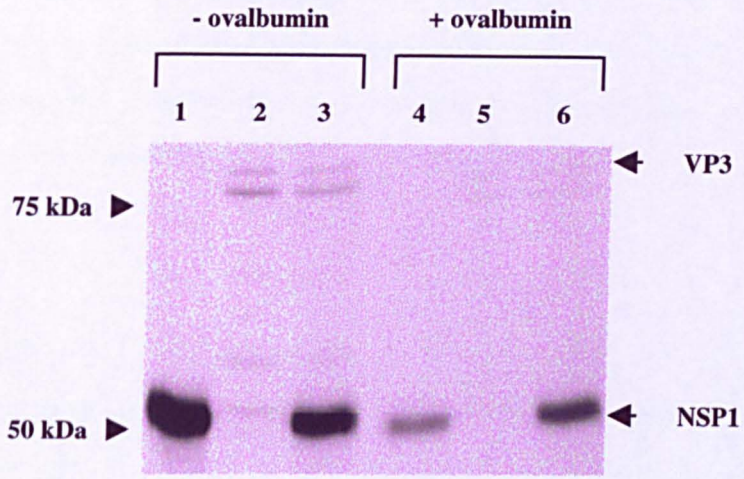

Figure 6.17 Co-precipitation of VP3 with NSP1 is blocked by the addition of ovalbumin

Plasmids G5T7-TA1 and T7-pTAg-Gene3 were used to programme *in vitro* coupled transcription-translation reactions to express NSP1 and VP3 respectively (Section 3.6.1). Reactions containing approximately equal quantities of NSP1 and VP3 (judged by visualisation on a fluorograph) were incubated overnight at 4 °C with a 1/8 dilution of anti-NSP1 serum and precipitated with protein A-Sepharose (Section 3.6.4). The immunoprecipitation reactions were loaded on a 7.5 % polyacrylamide gel (Section 3.6.5), and the results analysed by dry gel fluorography after a two week exposure of the gel (Section 3.6.6). Immunoprecipitation reactions were prepared containing NSP1 alone (lane 1); VP3 alone (lane 2); approximately equal quantities of NSP1 and VP3 mixed (lane 3). Reactions were also prepared containing approximately five times the *in vitro* translated protein volume of ovalbumin added prior to immunoprecipitation of NSP1 alone (lane 4); VP3 alone (lane 5); approximately equal quantities of NSP1 and VP3 mixed (lane 6). The position of each protein band is indicated on the right of the gel. The sizes of the markers (in kDa) are indicated on the left of the gel.

the serum (Section 7.3.4). When a pre-clearing step using pre-immune serum was introduced, prior to the precipitation of the mixture of NSP1 and VP1, the co-precipitation of VP1 with NSP1 almost disappeared, suggesting that there was no specific protein-protein interaction between them. VP3 was observed to precipitate with pre-immune serum and with protein A-Sepharose only, suggesting that the precipitation of VP3 was due to non-specific binding. Supporting this conclusion was the fact that the addition of ovalbumin as a blocking agent prevented the co-precipitation. The use of polyclonal anti-rotavirus serum resulted in the precipitation of each viral pre-core protein but no corresponding co-precipitation of NSP1, suggesting a lack of a true interaction between the two.

6.7 Discussion

Complexes formed early in the rotavirus replication cycle have been shown to contain NSP1 and several viral structural proteins and it has been suggested that protein-protein interactions might occur between them. Co-immunoprecipitation experiments with *in vitro* translated proteins did not demonstrate direct protein-protein interactions between NSP1 and the structural proteins found in virus core complexes. Co-precipitation of the core proteins with NSP1 was observed, however the high background meant that the validity of the co-precipitations was not substantiated. However, as it is still possible that specific co-precipitations were masked by the non-specific interactions, the existence of specific interactions between NSP1 and the core proteins cannot be completely dismissed. Reactions with a polyclonal anti-rotavirus serum precipitated the core proteins but NSP1 was not co-precipitated with them. This serum was raised against a preparation of the UKtc strain of bovine rotavirus and not the individual core proteins, so reciprocal immunoprecipitation reactions with sera specific for each core protein are required to confirm these results. The following conclusions can be drawn from the results of the experiments described in this chapter. Although NSP1 is found in early replication complexes with the core proteins it may not form direct protein-protein interactions with them. Alternatively, potential interactions with NSP1 were not identified due to the non-specific binding of the core proteins. It is also possible that the protein-protein interactions were not stable under the conditions of this assay.

An alternative explanation for the apparent failure of the proteins to interact *in vitro* could be due to a lack of viral mRNA in the reaction mixture. The pre-core RI complex described by Patton contains viral mRNA in addition to NSP1 and the viral structural proteins VP1 and VP3 (Patton, 1995). These proteins have been shown to have some degree of RNA-binding activity and consequently a scenario where the proteins interact indirectly with each other by means of their interactions with RNA can be envisaged. Another consideration is the possibility that a prior interaction with a third protein may be necessary before two given proteins can interact, for example to produce the correct confirmation or expose a hidden binding site. It is also sometimes the case that protein interactions which are observed *in vivo* cannot be recreated in an *in vitro* system (Black *et al.*, 1998). These results suggested that the use of infected cell lysates in co-immunoprecipitation experiments with anti-NSP1 serum might be a more effective way of investigating NSP1 protein-protein interactions.

In the assessment of the co-precipitation results, some consideration should also be given to the experimental design. In addition to co-translation of viral proteins, the proteins were also translated separately then mixed on ice for protein binding to occur. It is possible that optimum conditions for protein binding to occur in the mixture of proteins were not achieved and perhaps a longer incubation at an optimum temperature should have been investigated.

An experiment to be included in future work is immunoprecipitation with specific antisera against the other core proteins to determine if NSP1 is co-precipitated. That is the reciprocal of the experiments described in the present study. The feasibility of such experiments would clearly depend on the availability of specific antisera to these proteins which is not currently available in the Rotavirus laboratory.

A significant hindrance to the progression of this project was the failure to produce a specific antiserum against NSP1, although several attempts were made. Viruses are known to be highly immunogenic, and the use of recombinant vaccinia virus to produce specific antiserum has been documented (Section 6.3.1). The rabbit was primed with the antigen and given booster inoculations, including an inoculation at a higher dose, however this failed to produce a specific antiserum against NSP1. As discussed previously (Section 6.3.7), other researchers have had difficulty in producing an antiserum to this protein due to its low antigenicity. Perhaps a different

approach, such as the use of an alternative animal species (e.g. mice) or a method to increase the antigenicity of NSP1 in order to produce a serum response could be investigated in future. The production of a specific antiserum is essential to allow work on NSP1 to continue.

In this study it was shown that in addition to NSP1, *in vitro* translated VP2 was precipitated by the anti-NSP1 serum. Adsorption of the serum to remove the cross-reacting antibodies was not performed due to the difficulty in preparing suitable rotavirus-infected cell extracts to adsorb the serum against. Also, only a small volume of serum was available for the immunoprecipitation experiments. In an effort to reduce the background, the serum was titrated to determine the highest dilution that would still precipitate a sufficient quantity of NSP1 from a reaction mixture.

An epitope in VP2, recognised by the anti-NSP1 serum, was mapped to the middle third of the protein in the region lying between 31 kDa and 66 kDa from the amino terminus. The remarkable strength of the precipitation of VP2 by this serum perhaps suggests that this epitope has some functional significance in the virus replication cycle. For example, it might reflect the interaction of NSP1 and VP2 with the same site on mRNA or another protein during replication and assembly of the virus particle.

An experiment was designed to give further support to the location of the common epitope, whereby the middle third of the protein could be excised from the protein so only the terminal thirds were translated. Immunoprecipitation with the anti-NSP1 serum could then be performed to determine if the epitope had been removed. This experiment would help to confirm the existence of the proposed epitope recognised by the anti-NSP1 serum. The manipulative steps required to allow in frame translation of the two sections of the protein were however fairly complex, and this experiment was not deemed to have a sufficiently high priority to be done within the time frame of this study. The epitope in VP2 recognised by the anti-NSP1 serum could not be mapped more closely than the middle third of the protein due to the lack of suitable restriction sites in this region. Other researchers have successfully generated truncated proteins directly from PCR amplified cDNA copies in a vaccinia T7 system (P.P.C. Mertens, pers. comm.). It is thought that this method could also be applied in a linked T7 transcription-translation system, such as the one described in this study (Section 6.5.1). The cDNA copies are produced using a PCR primer with a built in T7 promoter and appropriate start site, while the second primer is designed to

give a product of a given length such that the desired truncated protein will be expressed. This approach would circumvent the problem of limited, appropriate restriction sites, and should be considered if this study was to be extended.

Results Chapter 4

Co-Immunoprecipitation studies

using rotavirus-infected cells

7.1 Aims

The aim of the work described in this chapter was to examine the protein composition of viral complexes containing NSP1 found in the rotavirus-infected cell by co-immunoprecipitation studies carried out on lysates made from cells infected with the UKtc strain of bovine rotavirus.

7.2 Introduction

7.2.1 NSP1 is found in early replication complexes

Studies to determine the composition of the rotavirus replicase complex have led to the characterisation of three distinct replication intermediates (RIs) (Gallegos and Patton, 1989). The protein composition of these RIs was elucidated by electrophoresis on polyacrylamide gels. The smallest intermediate, the pre-core RI, contained the structural proteins VP1 and VP3 and the non-structural proteins NSP1 (NS53), NSP2 (NS35), NSP3 (NS34) and NSP5 (VP9), although subsequently only NSP1 and NSP3 were considered to be truly present in the complex (Patton, 1995). The second intermediate, the core RI, contained VP1, VP2, VP3, NSP2, NSP3 and NSP5. The third and largest intermediate, the single-shelled RI, contained VP1, VP2, VP3, VP6, NSP2, NSP3 and NSP5, although the presence of the non-structural proteins NSP2 and NSP5 in the core and single-shelled RIs was equivocal. Pulse-chase analysis suggested that the core RI was formed by the addition of VP2 to a precursor such as the pre-core RI. The single-shelled particle was then formed by the subsequent addition of VP6 to the core RI. It was concluded in these early studies that NSP1 was not usually found in the single-shelled RI. However, the limitations of the experimental methods used made it impossible to confirm the absolute composition of the RIs, as there was potential for contamination with proteins from different fractions, from transcriptase particles or single-shelled virions.

All of the proteins which are associated with the RIs, with the exception of VP6, have RNA-binding activity, suggesting an important role for them in the replication process. NSP1 has been shown to bind to the 5'-end of rotavirus mRNAs (Hua *et al.*, 1994), while NSP3 has been shown to bind to the 3' end of rotavirus mRNA (Poncet *et al.*, 1993). VP1 and VP3 also bind viral mRNA and their binding sites probably overlap those of NSP3 and NSP1 respectively. Thus, it has been

suggested that the pre-core RI may be formed by the interaction of VP1 and VP3 with the NSP1/NSP3-mRNA complex (Patton, 1995). VP2, which has non-specific RNA-binding activity, then interacts with the pre-core RI to form the core RI.

On the basis of this work, a pathway for genome replication and virus assembly, with the corresponding protein interactions, was proposed (Patton, 1995). Briefly, it suggested that NSP1 and NSP3 form a complex with mRNA assembling on the cytoskeleton. The pre-core RI is then formed by the interaction of VP1 and VP3 with this complex, although it is not known what interactions occur at this stage. Movement of the complex to the viroplasm is accompanied by the loss of NSP1 and NSP3 and the sequential addition of VP2, to form the core RI, and subsequently VP6 to form the single-shelled RI. The precise stage at which the non-structural proteins are lost from the complex has not been defined. Clearly, protein-protein and protein-RNA interactions must occur with the proteins of the pre-core RI complex, and also with the proteins added to form subsequent RIs.

In a more recent investigation, immunoprecipitation from RF rotavirus-infected cell lysates was used to examine the structure of the rotavirus replicase complex (Aponte *et al.*, 1996). Antisera specific for different rotavirus proteins were used to immunoprecipitate complexes from infected cells which were then tested for replicase activity. The only complex shown to have replicase activity in the solid-phase assay developed was that precipitated with an anti-NSP2 monoclonal antibody (mAb), suggesting that the presence of NSP2 is essential for replicase activity. The protein composition of the complexes precipitated with the antisera were examined. The complex precipitated with the anti-NSP2 mAb was found to be different to the replicase complexes described by Patton (Helmberger-Jones and Patton, 1986; Patton and Gallegos, 1988) in that only VP1, VP2, VP6 and NSP2 were precipitated, and NSP1, NSP3 and NSP5 were not present. However, the complex containing NSP2 could not be reciprocally precipitated with anti-VP6 and anti-VP2 mAbs. Immunoprecipitation with two separate anti-VP6 mAbs gave rise to two kinds of complex with different protein compositions - one containing only VP2 and VP6, and the second containing VP3, NSP1, NSP2 and NSP3 in addition to VP2 and VP6.

Clearly there are still many details in the process of rotavirus replication/assembly which remain obscure, although detailed examination of replication complexes will help to dissect the sequence of events which occur in the

cell. Co-immunoprecipitation from rotavirus-infected cell lysates represents one approach for examining the protein composition of these complexes.

7.2.2 Co-Immunoprecipitation can be used to study viral complexes

Co-immunoprecipitation has been used as a method of studying viral complexes formed during the replication cycle of a number of RNA viruses, including those with segmented genomes. In the influenza system, eight single-stranded RNA segments of negative polarity encode ten proteins, only one of which, NS1, is a non-structural protein. Studies with NS1-specific serum have shown that the components of the RNA polymerase complex, subunits PB1, PB2 and PA, and the nucleoprotein (NP), were co-immunoprecipitated with NS1 (Marión *et al.*, 1997). These results were confirmed by western blot analysis using specific serum against NP and the RNA polymerase complex subunits. Dot blot hybridisation experiments using NP-specific riboprobes showed that viral mRNA and virion RNA were also co-immunoprecipitated by the anti-NS1 serum. However, the co-immunoprecipitates were not sensitive to treatment with RNase. These results led to the hypothesis that NS1 may be involved in a transcription-replication complex in influenza virus-infected cells, although it could not be determined whether this association involved direct protein-protein interactions or was mediated by RNA binding. Clearly, this approach can be used successfully to gain information about the association of specific proteins into viral complexes within the infected cell.

7.2.3 Co-Immunoprecipitation with anti-NSP1 serum from UKtc rotavirus-infected cell lysates

Immunoprecipitation analysis of rotavirus-infected cell lysates with specific antiserum allows characterisation of the type of complex in which NSP1 is found in the infected cell and identification of the constituent proteins. In contrast to the other methods utilised in this study, which focus on examining direct protein-protein interactions between NSP1 and selected viral proteins, immunoprecipitation from cell lysates allows investigation of the nature of NSP1-containing complexes found in the infected cell. It also allows analysis of complexes which may not be held together primarily by direct protein-protein interactions but indirectly, possibly by

RNA-protein interactions, or which require an interaction with additional factors (RNA or protein) to expose a binding site.

UKtc rotavirus-infected cell lysates were produced as described for use in immunoprecipitation experiments (Section 3.6.3). Lysates were prepared at 7 hours post-infection (p.i.) in most experiments. Studies on the kinetics of protein synthesis in rotavirus-infected cells have shown that by 4 hours p.i. cellular polypeptide synthesis is strongly inhibited and replaced by viral protein synthesis (McCrae and Faulkner-Valle, 1981). Viral transcription and RNA replication have been shown to begin by 3 hours p.i. and gradually increase so that synthesis of plus-strand RNAs (transcription) is maximal at 9 to 12 hours p.i., while RNA replication reaches maximal levels at 6 to 9 hours p.i. (Stacy-Phipps and Patton, 1987). Thus, RNA replication peaks several hours earlier than transcription. It has also been shown that virions released from rotavirus-infected cells can be detected by 6 hours p.i. (Stacy-Phipps and Patton, 1987). Hence, harvesting cells at 7 hours p.i., when RNA replication is at maximum levels, ensures the presence of high levels of viral proteins and RIs in the infected cell. A high m.o.i. was used to ensure synchronous infection (McCrae and Faulkner-Valle, 1981), such that detectable levels of viral protein would be present in the cell lysates.

7.3 Co-Immunoprecipitation of proteins from UKtc rotavirus-infected cell lysates

7.3.1 Production of UKtc rotavirus-infected cell lysates

UKtc rotavirus-infected cell lysates were produced essentially as described previously (Section 3.6.3). BS-C-1 cells, derived from African green monkey kidney (Hopps *et al.*, 1963), and MA-104 cells, derived from Rhesus monkey kidney (Whitaker and Hayward, 1985), were used interchangeably as they have a similar epithelial morphology and both cell lines support growth of rotaviruses. A high m.o.i. was always used when infecting the cells. One methodological change adopted to increase the amount of radioactivity incorporated into samples was to extend the labelling period to 2 hours. This enabled easier detection of NSP1 which is only present at low levels in the infected cell (Johnson and McCrae, 1989). Figure 7.1 shows mock-infected and UKtc rotavirus-infected BS-C-1 cell lysates analysed by gel

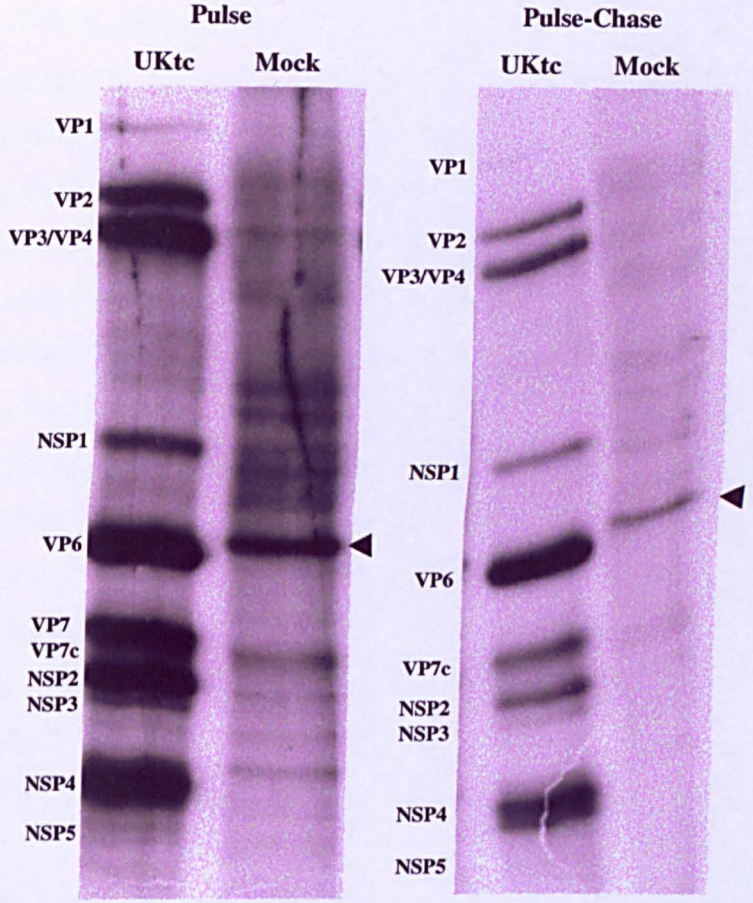

Figure 7.1 Production of ^{35}S-methionine labelled UKtc rotavirus-infected cell lysates and analysis of viral polypeptide synthesis

Confluent BS-C-1 cells were infected with a high m.o.i. of the UKtc strain of bovine rotavirus (m.o.i. = 20), or mock-infected, and incubated for 7 hours at 37 °C. The cells were pulsed with ^{35}S-methionine for 20 minutes, chased with 100X cold methionine for 2 hours and harvested (Section 3.6.3). Labelled samples (40 µl) were analysed on a 5-11 % gradient polyacrylamide gel (Section 3.6.5), and the results visualized by dry gel fluorography (24 hours exposure time) (Section 3.6.6). Pulse only and pulse-chase mock- and UKtc-infected cell lysates are shown. The identity of the viral polypeptides are indicated on the left of the lanes. VP indicates viral structural proteins. NSP indicates viral non-structural proteins. The arrow indicates the position of actin in the mock-infected cell lysates.

electrophoresis. Pulse-chase labelling of the cells was performed to allow analysis of the viral polypeptide synthesis. Comparison of the pulse-labelled mock and virus-infected cell lysates revealed that at 7 hours p.i. the host cell protein synthesis was significantly inhibited and replaced by rotavirus protein expression. With the exception of NSP5, which is only present at low levels, all the viral proteins are sufficiently labelled by this procedure to be visible on a polyacrylamide gel. The viral structural proteins VP3 and VP4 migrate at the same position and cannot be distinguished on this gel. The non-structural proteins NSP2 and NSP3 also migrate at a similar position, although separate protein bands can be detected in this case. Comparison of the pulse and the pulse-chase samples revealed that VP7 can be chased to the end product VP7c during the chase period. The unglycosylated precursor of VP7 is vpr7, which is only seen when glycosylation is blocked by the addition of tunicamycin (McCrae and Faulkner-Valle, 1981). VP7c, which is found in the virion, is the chase product of VP7, produced by an, as yet, undefined event. NSP4 is also glycosylated and is seen to have a slightly increased mobility by the end of the chase period. The identity of the polypeptide migrating at a similar position to VP6 in the mock-infected cell lysates is the cellular protein actin. Pulse-labelled UKtc rotavirus-infected cell lysates were used for subsequent immunoprecipitation experiments with specific antiserum against individual proteins.

7.3.2 Titration of monospecific polyclonal anti-NSP1 serum by immunoprecipitation of UKtc rotavirus-infected cell lysates

A monospecific polyclonal anti-NSP1 serum and an anti-NSP1 monoclonal antibody were available for immunoprecipitation of NSP1 from cell lysates (Section 6.3.6). Titration of the monospecific polyclonal anti-NSP1 serum was performed to determine the lowest concentration of serum that would precipitate NSP1 from infected cell lysates (Figure 7.2). This procedure was employed to try and minimise any background precipitation of other proteins from the cell lysates. The anti-NSP1 monoclonal antibody was also tested in an immunoprecipitation reaction with the infected cell lysates to determine whether it would precipitate NSP1 from the reaction.

A positive control reaction was performed using a 100,000Xg supernatant (S100 supernatant) of the cell lysate incubated with monospecific anti-VP7 serum which had been shown previously to precipitate VP7 from infected cell lysates

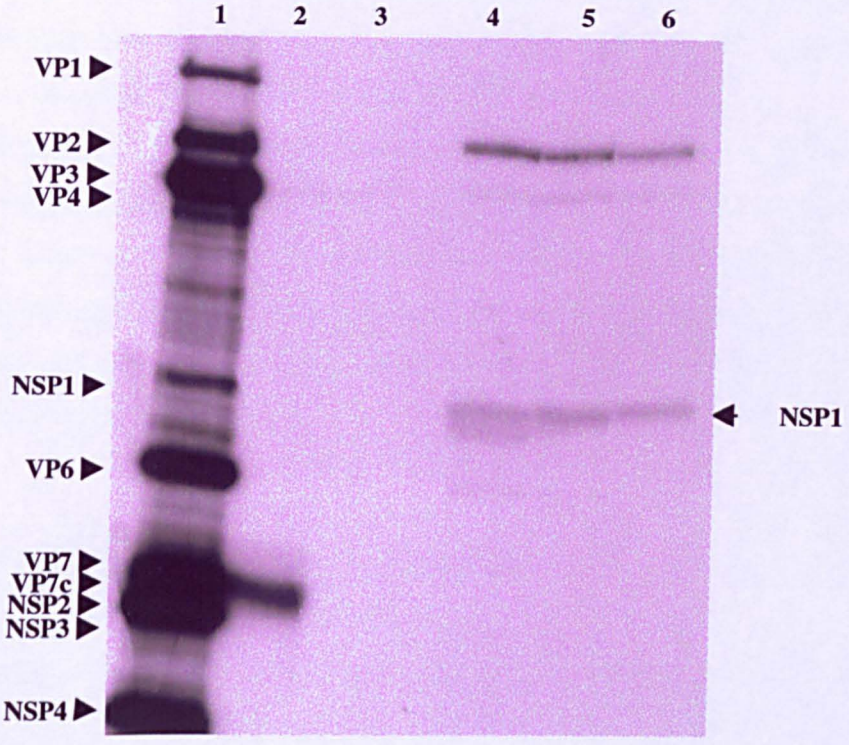

Figure 7.2 Titration of anti-NSP1 serum against UKtc rotavirus-infected MA104 cell lysates

UKtc rotavirus-infected MA104 cell lysates were prepared and centrifuged at 100,000Xg, as described previously (Section 3.6.3). 50 µl aliquots of the 100,000Xg supernatant were immunoprecipitated (Section 3.6.4) with increasing dilutions of anti-NSP1 serum. The immunoprecipitates were analyzed on a 5-11 % gradient polyacrylamide gel (Section 3.6.5), and the results visualized by dry gel fluorography (20 hours exposure time) (Section 3.6.6). The characteristic pattern of rotavirus protein expression is shown before immunoprecipitation (lane 1). Immunoprecipitation with monospecific anti-VP7 serum was used as a positive control (lane 2). Immunoprecipitation with pre-immune serum was used as a negative control (lane 3). Three dilutions of anti-NSP1 serum were tested - 1:20 (lane 4); 1:50 (lane 5); 1:100 (lane 6). The position of the bands corresponding to NSP1 are indicated. The identity of the viral polypeptides are indicated on the left of the lanes. VP indicates viral structural proteins. NSP indicates viral non-structural proteins.

(McCrae and McCorquodale, 1987). As expected, VP7 was precipitated from the cell lysate by this serum (Figure 7.2, lane 2). No proteins were precipitated by the pre-immune serum which was used as a negative control reaction (lane 3). Increasing dilutions of anti-NSP1 serum (1:20, 1:50 and 1:100) were tested for efficient precipitation of NSP1 from the cell lysates and NSP1 was clearly precipitated by all dilutions (lanes 4-6). Hence the highest dilution of 1:100 was used as the standard for immunoprecipitation reactions. The co-precipitation of viral protein VP2 with NSP1 in the reactions was noted, and this will be discussed in subsequent sections.

Two dilutions (1:10 and 1:100) of the anti-NSP1 monoclonal antibody were tested in immunoprecipitation reactions for precipitation of NSP1. The monoclonal antibody was found to precipitate NSP1 considerably less efficiently than the monospecific polyclonal serum and was too weak to be used in experimental reactions (data not shown). It was noted that VP2 was also weakly precipitated with NSP1 by this monoclonal antibody.

7.3.3 Immunoprecipitation of a viral protein complex from UKtc rotavirus-infected cells with anti-NSP1 serum

As discussed in previous chapters, direct protein-protein interactions between NSP1 and other viral proteins have not been shown. However, these results do not exclude the possibility that NSP1 is associated with other viral proteins in a complex in the infected cell, perhaps through an interaction with viral RNA. To investigate this possibility, NSP1 was immunoprecipitated from UKtc rotavirus-infected cells with anti-NSP1 serum and the co-precipitating viral proteins were examined by fluorography (Figure 7.3). The precipitated proteins were also detected by phosphoimaging, quantified using ImageQuant™ software and the data analysed using Excel™ software (Microsoft) (Appendix 2.1).

An immunoprecipitation reaction using anti-NSP1 serum was performed to examine the viral proteins which co-precipitated with NSP1. Immunoprecipitation of cell lysates which had been boiled with protein cracking buffer (4 % SDS; 10 % β-mercaptoethanol) prior to precipitation with anti-NSP1 serum was also carried out. Boiling the cell lysate in cracking buffer would disrupt any specific protein-protein or protein-RNA interactions, thus breaking up viral complexes which might be precipitated. Control reactions with pre-immune serum and no serum were performed

Figure 7.3

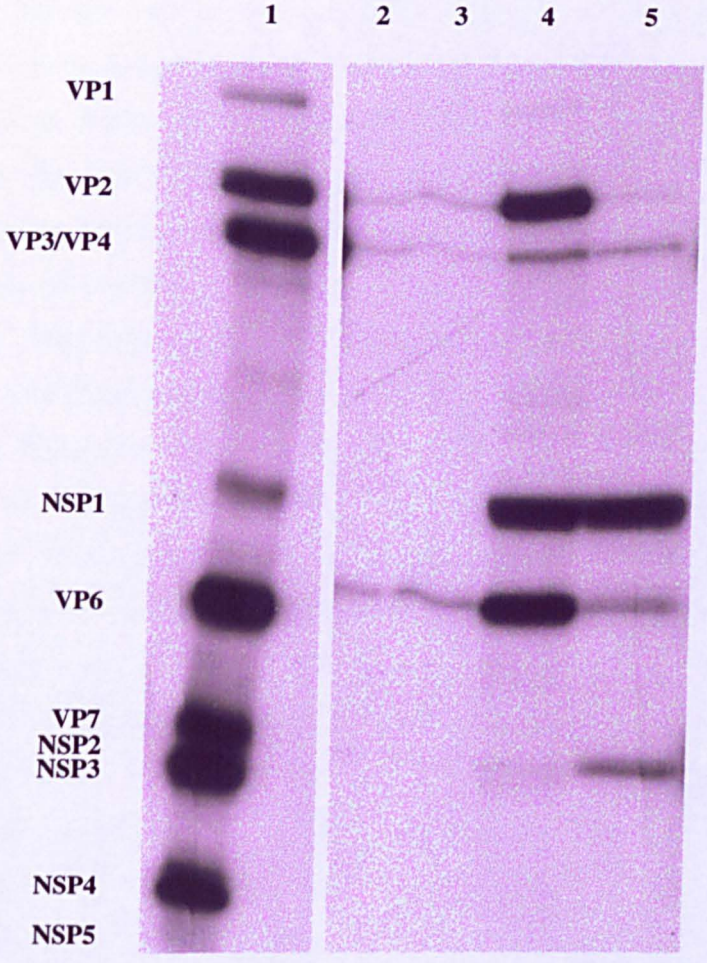

Figure 7.3 Immunoprecipitation of UKtc rotavirus-infected cell lysates with anti-NSP1 serum

Confluent MA104 cells were infected with a high m.o.i. of the UKtc strain of bovine rotavirus (m.o.i. = 20) and incubated for 7 hours at 37 °C. The cells were pulsed with ^{35}S-methionine for 2 hours and harvested (Section 3.6.3). The cell lysate was centrifuged for 1 min. in a microfuge prior to use. A 10 µl aliquot of the cell lysate was run on the gel to show the characteristic pattern of rotavirus protein expression before immunoprecipitation (lane 1). Immunoprecipitation reactions were performed with 10 µl aliquots of the cell lysate incubated with 1 µl 10 mg/ml ovalbumin/no serum (lane 2), pre-immune serum (lane 3) and anti-NSP1 serum (lane 4) (Section 3.6.4). A 10 µl aliquot of the cell lysate was boiled for 2 mins with cracking buffer (4 % SDS; 10 % β-mercaptoethanol) and diluted 10-fold with water prior to incubation with anti-NSP1 serum (lane 5). The immunoprecipitates were analyzed on a 5-11 % gradient polyacrylamide gel (Section 3.6.5), and the results visualized by dry gel fluorography (Section 3.6.6). Lane 1 represents a 24 hour exposure of the gel to x-ray film, while lanes 2-5 are a 5 day exposure. The identity of the viral polypeptides are indicated on the left of the lanes. VP indicates viral structural proteins. NSP indicates viral non-structural proteins.

so that the specificity of the reactions could be validated. In the control reaction lacking serum, an equivalent amount of a 10 mg/ml solution of ovalbumin was added to compensate for the lack of protein from the serum. The standard protein concentration of serum is known to be 10 mg/ml (M. A. McCrae, pers. comm.). The purpose of this no serum control was to determine if any viral proteins were precipitated by a non-specific reaction with the protein A-Sepharose or were carried over during the centrifugation stages of the reaction, although a pre-clearing spin was performed prior to the immunoprecipitation to minimise the latter.

Analysis of the immunoprecipitation reaction with anti-NSP1 serum showed a number of viral proteins co-precipitating with NSP1, including VP1, VP2, VP3/VP4, VP6 and NSP3 (Figure 7.3). As VP3 and VP4 migrate to a similar position on the gradient gel it was unclear which was precipitated, although VP3 was the most obvious candidate (Section 7.3.5). As NSP2 and NSP3 also migrate to a similar position the identity of the NSP3 band was also difficult to substantiate, although these protein bands are more easily distinguished than VP3 and VP4. Also, as NSP3 has previously been shown to be part of an early replication complex with NSP1 (Patton, 1995), it seems likely that this was the co-precipitating protein. It was particularly notable that neither VP7 or NSP4, both of which are present at significant levels in the infected cell, co-precipitated with NSP1 suggesting that the immunoprecipitation reaction was specific.

Analysis of the control reactions with no serum and with pre-immune serum showed small quantities of VP2, VP3/VP4 and VP6 were present. Similar quantities of each protein were precipitated from both reactions and therefore it did not seem likely that the proteins were being specifically precipitated by antibodies in the pre-immune serum. This in turn suggested that the proteins were pelleted with the protein A-Sepharose during the centrifugation stages of the immunoprecipitation reactions. Quantification of the proteins by phosphoimaging showed that in the case of VP2 and VP6 the amounts co-precipitated with NSP1 by the specific anti-NSP1 serum were approximately 10 times greater than those precipitated in the no serum and pre-immune controls. The amount of VP3/VP4 co-precipitated with NSP1 using the anti-NSP1 serum was approximately 5 times greater than that precipitated with the pre-immune control. NSP1 was not precipitated in either of the control reactions. It was therefore concluded that the proteins precipitated in the no serum and pre-immune controls represented non-specific background precipitation.

The results suggested that the co-precipitation of the viral proteins with NSP1 in the reaction with anti-NSP1 serum were specific, as the amounts of co-precipitating proteins were considerably greater than those seen in the controls. From these observations it can be postulated that VP1, VP2, VP3/VP4, VP6 and NSP3 form a complex with NSP1 which is specifically precipitated by the anti-NSP1 serum. The co-precipitation with NSP1 of the viral structural proteins that form the transcriptional complex, and both the core and inner capsid shells, led to the suggestion that an actual complex containing NSP1 was precipitated. This complex would be similar to the early replication complex suggested by Patton (1995), however with the notable addition of both VP2 and VP6.

7.3.4 Boiling the cell lysate prior to immunoprecipitation with anti-NSP1 serum changed the amounts of the proteins co-precipitating with NSP1

The cell lysate was boiled prior to immunoprecipitation in an attempt to disrupt specific protein-protein and protein-RNA interactions, thus breaking up viral complexes in the cell lysate. Comparison of the precipitated proteins with those in the unboiled reaction allowed speculation on the nature of complex which had been disrupted. A reaction was performed with cell lysates which had been boiled with protein cracking buffer (4 % SDS; 10 % β-mercaptoethanol) prior to immunoprecipitation with anti-NSP1 serum. This precipitation produced a distinctly different result to the unboiled sample (Figure 7.3). Although a similar quantity of NSP1 was precipitated, a significant decrease in the quantities of co-precipitating VP1, VP2 and VP6 was evident. These results suggested that VP1, VP2 and VP6 have disassociated from a complex with NSP1, due to the disruption of specific interactions. The quantity of VP3/VP4 appeared to remain the same. In contrast, the quantity of NSP3 was markedly increased after boiling by approximately 6 times by phosphoimager analysis. This increase could be explained in a number of ways. NSP3 appears to interact with denatured NSP1 that has disassociated from a complex (Lane 5), however when VP2 and VP6 are precipitated with NSP1 the amount of NSP3 is much reduced (Lane 4). This observation might suggest that NSP3 interacts with NSP1 alone, but is displaced from the complex after the addition of VP2 and VP6. Alternatively, it is possible that the boiling process revealed a specific epitope which allowed immunoprecipitation by the anti-NSP1 serum, resulting in precipitation of

greater quantities of the protein. Another possibility was an aggregation of the protein, formed as a result of the boiling process, was non-specifically precipitated with the protein A-Sepharose. Finally, it is possible that this protein band could represent the accumulation of breakdown products of other proteins which are non-specifically precipitated after the boiling process.

The process of boiling the cell lysate in protein cracking buffer would also serve to disrupt conformational epitopes in the proteins. The fact that a similar quantity of NSP1 was precipitated by the anti-NSP1 serum after boiling indicates that the site on NSP1 that reacts with this serum is not conformational. *In vitro* translated VP2 is also specifically precipitated by this serum (Section 6.6.2), hence the observation in this experiment that a reduced quantity of VP2 is precipitated after boiling might reflect the disruption of a conformational epitope in VP2 recognised by the anti-NSP1 serum.

7.3.5 Analysis of V8 protease digestion products of the VP3/VP4 band which co-immunoprecipitated with NSP1 from infected cell lysates

Several proteins were shown to co-immunoprecipitate with NSP1 from UKtc rotavirus-infected cell lysates (Figure 7.3), however not all of them were clearly identified. The band at approximately 90 kDa could have been either VP3 or VP4 as they both migrate to a similar position on the gel. The bands cannot be easily distinguished, even on a 5-11 % polyacrylamide gradient gel, which has been shown to give optimal separation of rotavirus proteins from infected cell lysates (M. A. McCrae, pers. comm.). Although the proteins were not easily distinguished on a gel, it was thought that the band at approximately 90 kDa was probably VP3. As VP3 is an inner core protein it is more likely to be found in a early replication complex with NSP1 than VP4 which is an outer capsid surface protein. However, it was desirable that this assumption was tested to rule out the slight possibility that VP4 was non-specifically precipitated by the serum.

To try and determine the identity of the protein in the VP3/VP4 band, an experiment was devised based on the method of McCrae and Joklik (1978) to differentiate the VP3 and VP4 bands. Digestion of proteins with the Type XVII-B protease from *Staphylococcus aureus* strain V8 (V8 protease) gives an unique pattern of peptide bands when resolved on an acrylamide gel. Comparison of the peptide

profile produced by digestion of an unknown protein with profiles of known proteins allows identification of the protein. The unknown 90 kDa protein band, found co-precipitating with NSP1 from infected cell lysates, was cut from the gel (Figure 7.4, Panel A). The protein was solubilised and incubated with 5 μg/ml or 50 μg/ml V8 protease and the resulting peptides were resolved on a polyacrylamide gel. To identify the co-precipitating protein, bands corresponding to VP3 and VP4 from infected cell lysates (Panel A) and *in vitro* translated VP3 (Panel B) were also excised from gels, digested with V8 protease and resolved on the gel with digests of the co-precipitating protein.

Comparison of the pattern of peptide bands produced by the unknown protein with known samples should enable identification of the co-precipitating protein. The *in vitro* translated VP3 protein was clearly digested by the V8 protease to produce a profile of peptide bands (Panel C). With 5 μg/ml of V8 protease peptide digestion products were seen, however there was still some full length protein remaining. However, with 50 μg/ml of V8 protease much less full length protein remained and there were many more peptide products, suggesting further digestion of the protein had occurred. The VP3/VP4 protein band was also successfully digested by the V8 protease. However, analysis of the gel by fluorography and phosphoimaging did not reveal a sufficiently clear image of the unknown sample which could be compared with the known pattern of peptides for VP3 and VP4. The results of this experiment remain inconclusive, as even an extremely long exposure of the gel to x-ray film (16 weeks; Figure 7.4) did not reveal a clear profile of peptide bands for the unknown sample. A possible explanation for this result is that the protein in the sample was insufficiently radiolabelled to permit analysis of the peptide digestion products. If the peptides contained very few methionine residues, visualization of the peptide profile would prove extremely difficult or even impossible. Therefore, the protein at approximately 90 kDa (VP3/VP4) that co-precipitated with NSP1 could not be unequivocally identified as either VP3 or VP4. It will be described henceforth as VP3/VP4, however as discussed previously, VP3 is considerably more likely to be contained in an early replication complex with NSP1 than VP4.

As VP3 is a GTP-binding protein, a GTP-binding assay can also be used to identify VP3 in a mixture of proteins (Zeng *et al.*, 1996). A similar assay could be used in this case to prove the presence of VP3 in the immunoprecipitates, however

Figure 7.4 Polyacrylamide gel analysis of the V8 protease digestion products of the VP3/VP4 band which co-precipitated with NSP1 from UKtc rotavirus-infected cell lysates

A. UKtc-infected cell lysates

Confluent BS-C-1 cells were infected with a high m.o.i. of the UKtc strain of bovine rotavirus (m.o.i. = 20) and incubated for 7 hours at 37 °C. The cells were pulsed with ^{35}S-methionine for 2 hours and harvested (Section 3.6.3). 10 µl of the cell lysate was run on the gel to show the pattern of bands before immunoprecipitation (lane 1). 50 µl aliquots of the cell lysate were immunoprecipitated (Section 3.6.4) with 1 µl of pre-immune (lane 2) or anti-NSP1 serum (lane 3). The immunoprecipitates were analysed on a 5-11 % gradient polyacrylamide gel (Section 3.6.5), and the results visualized by dry gel fluorography after a 19 hour exposure of the gel (Section 3.6.6). The bands corresponding to VP3 and VP4 in the cell lysate (lane 1) and the unknown VP3/VP4 band co-immunoprecipitating with NSP1 (lane 3) which were excised from the gel are indicated. The size of the protein markers (in kDa) are indicated on the left of the gel.

B. *In vitro* translated VP3

Plasmid T7-pTAg-gene3 was purified by phenol extraction (Section 3.4.4) and ethanol precipitation (Section 3.4.5) and used to programme an *in vitro* coupled transcription-translation reaction at concentrations of 1 µg or 2 µg of DNA for expression of VP3 (Section 3.6.1). The products of the translation reactions were analysed on a 7.5 % polyacrylamide gel (Section 3.6.5) and visualized by dry gel fluorography after a 18 hour exposure of the gel (Section 3.6.6). The positions of the translated VP3 bands which were excised from the gel are indicated by the arrow.

C. V8 protease digests

The protein bands which were excised from the gels [**(i)** *In vitro* translated VP3 (control reaction) (Panel B):**(ii)** Unknown, immunoprecipitated VP3/VP4 band (experimental reaction) (Panel A, lane 3):**(iii)** VP3/VP4 band from cell lysate (control reaction) (Panel A, lane 1)] were incubated with 5 µg/ml or 50 µg/ml of Type XVII-B protease from *Staphylococcus aureus* strain V8 for 30 minutes at 37°C according to the method of McCrae and Joklik (1978). The digestion products were analysed on a 5-11 % gradient polyacrylamide gel (Section 3.6.5), and the results visualized by dry gel fluorography after a 16 week exposure of the gel (Section 3.6.6). The enzyme concentrations used for each sample are indicated at the top of the gel. The position of the full length VP3 protein is indicated on the right of the gel. The size of the protein markers (in kDa) are indicated on the left of the gel.

Figure 7.4

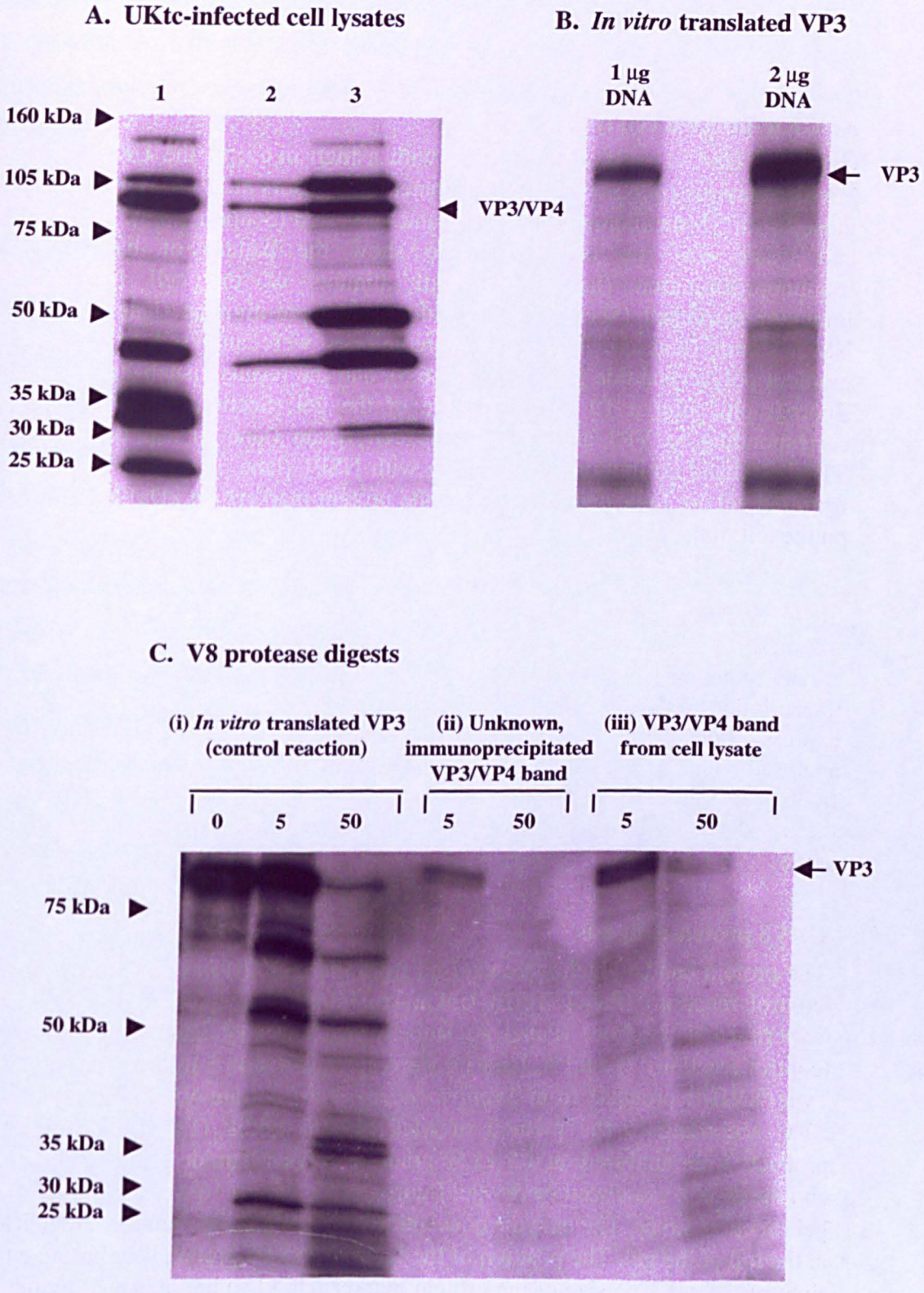
A. UKtc-infected cell lysates
1
2
3
160 kDa
105 kDa
75 kDa
50 kDa
35 kDa
30 kDa
25 kDa
VP3/VP4
B. In vitro translated VP3
1 µg DNA
2 µg DNA
VP3
C. V8 protease digests
(i) In vitro translated VP3 (control reaction)
(ii) Unknown, immunoprecipitated VP3/VP4 band
(iii) VP3/VP4 band from cell lysate
0
5
50
5
50
5
50
VP3
75 kDa
50 kDa
35 kDa
30 kDa
25 kDa

this assay would not rule out the possibility that VP4 was also precipitated. Another experiment which might distinguish between VP3 and VP4 is based on the fact that VP4 is cleaved by proteases to VP5* and VP8*. Mild trypsin treatment of the immunoprecipitates would change the migration of the unknown band if it was VP4, but would have no effect on VP3 (Fukuhara *et al.*, 1989). These experiments might be used in future immunoprecipitations to distinguish bands migrating at the position of VP3/VP4.

7.4 Analysis of viral complexes containing NSP1

7.4.1 Immunoprecipitation of viral complexes containing NSP1 from different cell fractions

The purpose of this experiment was to determine the nature of NSP1-containing viral complexes in different cellular fractions. The presence of NSP1 in a complex with other viral proteins suggests either that protein-protein interactions occur between NSP1 and these viral proteins or that they are interacting indirectly, possibly via RNA-protein interactions. To study this, rotavirus-infected cell lysates were fractionated by centrifugation. The cell lysate was first subjected to centrifugation at 10,000Xg to remove the cell nuclei and large protein complexes. The 10,000Xg supernatant was centrifuged at 30,000Xg, and the resulting supernatant was then centrifuged at 100,000Xg producing a supernatant fraction containing only soluble proteins. Equal fractions of the supernatant and pellet from each sample were saved for analysis. Co-immunoprecipitation analysis was performed using anti-NSP1 serum with each cell fraction and the precipitates analysed on a 5-11 % gradient polyacrylamide gel (Figure 7.5). Phosphoimager analysis was also used to quantify the immunoprecipitated proteins (Appendix 2.2). Analysis of the immunoprecipitations with anti-NSP1 serum from the unfractionated cell lysate (Figure 7.5, lane 3) confirmed the result discussed previously (Section 7.3.3) that several viral proteins co-precipitated with NSP1, including VP1, VP2, VP3/VP4, VP6 and a small quantity of NSP3. As before (Section 7.3.3), it was noted that small amounts of VP2, VP3/VP4 and VP6 were non-specifically precipitated from the unfractionated cell lysate in the pre-immune serum control reaction. Quantification of the relative amounts of each protein again showed that considerably greater amounts

Figure 7.5 Immunoprecipitation of viral protein complexes with anti-NSP1 serum from cell fractions created by centrifugation at 10,000Xg, 30,000Xg and 100,000Xg

Confluent MA104 cells were infected with a high m.o.i. of the UKtc strain of bovine rotavirus (m.o.i. = 20) and incubated for 7 hours at 37 °C. The cells were labelled with ^{35}S-methionine for 2 hours and harvested (Section 3.6.3). The cell lysate was fractionated by spinning at 10,000Xg (11,000 rpm) in a Beckman TL 100 ultracentrifuge using the TLS 55 rotor for 1 hour at 4 °C. The pellet was resuspended in an equivalent volume of 50 mM Tris.HCl pH 8.0 and samples of both the pellet and the supernatant were saved for analysis. The supernatant was then centrifuged at 30,000Xg (19,000 rpm) as before. The pellet was resuspended in an equivalent volume of 50 mM Tris.HCl pH 8.0 and samples of the pellet and the supernatant were saved. The supernatant was then centrifuged at 100,000Xg (34,000 rpm) as before. The pellet was resuspended in an equivalent volume of 50 mM Tris.HCl pH 8.0 and samples of the pellet and the supernatant were saved.

50 µl aliquots of the pellet and supernatant of each cell fraction and also an unfractionated sample of the cell lysate were immunoprecipitated (Section 3.6.4) with 1 µl of pre-immune or anti-NSP1 serum. The immunoprecipitates were analyzed on a 5-11 % gradient polyacrylamide gel (Section 3.6.5), and the results visualized by dry gel fluorography (Section 3.6.6). A sample of the unfractionated cell lysate (10 µl) was loaded on the gel to show the characteristic pattern of rotavirus protein expression before immunoprecipitation (lane 1). This lane represents a gel exposure time of 1 day. Immunoprecipitation of a sample of the unfractionated cell lysate with pre-immune serum (lane 2) and with anti-NSP1 serum (lane 3) was performed. Immunoprecipitation of the following cell fractions with anti-NSP1 serum was performed: 10,000Xg pellet (lane 4); 10,000Xg supernatant (lane 5); 30,000Xg pellet (lane 6); 30,000Xg supernatant (lane 7); 100,000Xg pellet (lane 8); 100,000Xg supernatant (lane 9). Lanes 2-9 represent a gel exposure time of 4 days. The identity of the viral polypeptides are indicated on the left of the lanes. VP indicates viral structural proteins. NSP indicates viral non-structural proteins.

Figure 7.5

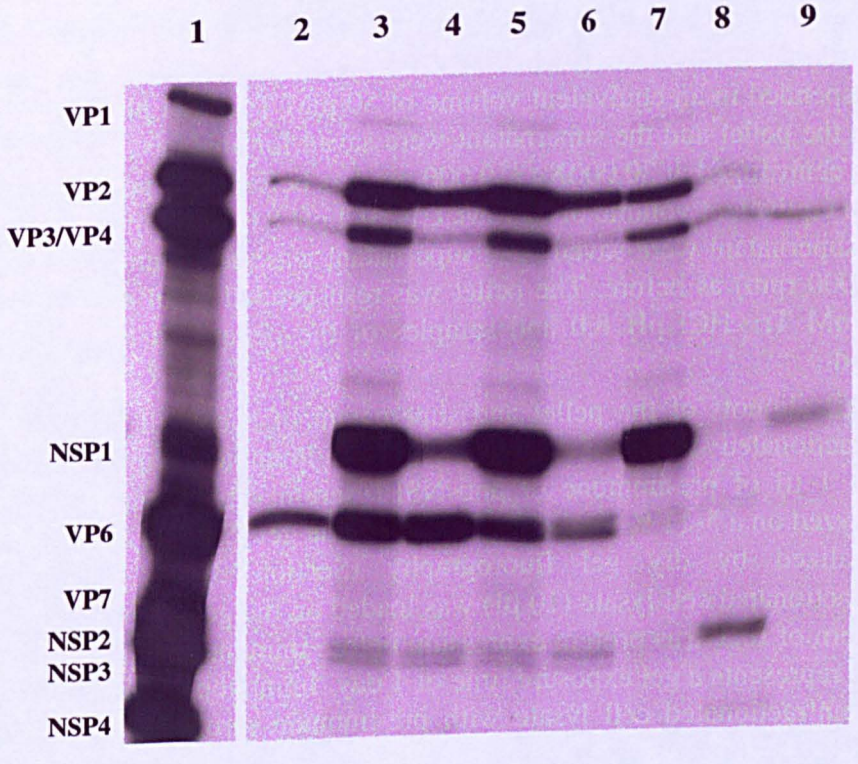

were specifically co-precipitated with the anti-NSP1 serum compared to the pre-immune serum control.

7.4.2 Analysis of the immunoprecipitated protein volumes in different cell fractions

The different quantities of each protein contained in the cell fractions were determined by phosphoimager analysis (Appendix 2.2). Visual inspection of the protein bands suggested that almost equivalent quantities of NSP1 were present in the unfractionated cell lysate and the 10,000Xg and 30,000Xg supernatants. Phosphoimager analysis confirmed that the approximate amount of NSP1 contained in the 10,000Xg supernatant sample was almost equal to the amount contained in the unfractionated cell lysate, while the 30,000Xg supernatant contained almost two thirds of this quantity. There was a loss of NSP1 to the pellet at each centrifugation stage, however a large proportion of NSP1 remained in the soluble fraction.

The approximate quantities of the proteins which co-precipitated with NSP1 in each cell fraction were also determined. A small amount of VP1 was found in the unfractionated cell lysate and in the soluble supernatant fraction after each centrifugation stage. Analysis of the VP2 bands showed that a proportion of the protein was pelleted during the 10,000Xg centrifugation stage, however a large amount still remained in the 10,000Xg supernatant. The 30,000Xg supernatant and pellet consisted of approximately equal proportions of protein, and the majority of the remaining soluble protein was pelleted by the 100,000Xg centrifugation step. Analysis of the bands corresponding to VP3/VP4 suggested that the majority of the protein remained in the soluble supernatant fraction until the 100,000Xg centrifugation stage, although there was a slight loss of protein to the pellet at each stage. NSP3 was found at low levels in each fraction with the notable exception of the 100,000Xg pellet where there was an increase in the quantity of NSP3 present. Given the disproportionate increase in NSP3 compared to the protein present in the 30,000Xg supernatant fraction, a possible explanation was that the band represented degraded protein. Analysis of the bands corresponding to VP6 showed that more than half of the total quantity of VP6 contained in the cell lysate was pelleted during the 10,000Xg centrifugation step. This suggested that a large proportion of VP6 is held in an insoluble complex in the cell. The equivalent orbivirus protein VP7(T13), which

shares structural conservation with VP6, sometimes forms large crystalline assemblies in infected cells that are pelleted rapidly on centrifugation of cell lysates (P.P.C. Mertens, pers. comm.). These structures are formed by protein-protein interactions similar to those found in the outer core layer, which is composed entirely of VP7(T13). By analogy with this system, it is possible that VP6 also forms similar macromolecular structures in the infected cell, and this would explain the pelleting of large quantities of VP6 during the first centrifugation stage.

It was apparent from the gel that there was a significant loss of proteins in the 100,000Xg cell fractions compared to the 30,000Xg supernatant fraction from which they were produced. Although there was a broad band of NSP1 in the 30,000Xg supernatant fraction, there was very little NSP1 protein in either the 100,000Xg supernatant or pellet fractions. The amount of VP2 present was also less than expected, although not to the same extent as NSP1. These observations made using fluorographs were confirmed by phosphoimager analysis of the appropriate bands. There are several possible explanations for the decrease in the amounts of these proteins including the possibility that a proportion of NSP1 was degraded during the 100,000Xg centrifugation stage or that it was not efficiently resuspended from the compact pellet produced during high speed centrifugation, and thus less protein was available for immunoprecipitation. If a smaller amount of NSP1 was precipitated, then this would obviously result in less co-immunoprecipitation of other proteins.

7.4.3 NSP1 may be a component of a viral protein complex with VP6

The immunoprecipitation experiments described above showed different amounts of viral proteins co-precipitating with NSP1 from the cell fractions. These results suggested that NSP1 may be a component of a number of different viral complexes in the infected cell. Immunoprecipitation of NSP1 from the unfractionated cell lysate resulted in co-precipitation of VP1, VP2, VP3/VP4, VP6 and NSP3. When the cell lysate was subjected to centrifugation at 10,000Xg, a complex containing NSP1, VP2 and VP6 with small amounts of VP3/VP4 and NSP3 was seen in the pellet fraction. It is proposed that this represents a novel NSP1-containing complex. An anti-VP6 monoclonal antibody also co-precipitated NSP1 with VP6 from these fractions (Figure 7.8). Immunoprecipitation of the soluble supernatant fraction with anti-NSP1 serum resulted in the co-precipitation of VP1, VP3/VP4 and small amounts

of VP2 and NSP3 with NSP1. It is proposed that this represents a second NSP1-containing complex which does not contain VP6. This latter complex is similar to the pre-core RI described by Patton (Patton, 1995).

The majority of precipitated NSP1 was present in the soluble protein fraction. Hence, only a small proportion of the total amount of NSP1 must be contained in the complex with VP6. Quantitative analysis of the protein bands revealed that only about 10 % of the total NSP1 contained in the unfractionated cell lysate was present in the 10,000Xg pellet fraction which probably represents the proportion contained in a complex with VP6 (Appendix 2.2).

7.5 NSP1 may be held in the viral complex by an interaction with RNA

7.5.1 Co-immunoprecipitation of viral proteins with NSP1 might be due to binding to RNA

The results described above have demonstrated that several viral proteins co-immunoprecipitate with NSP1 and it is proposed that these proteins form a complex in the infected cell. However, it did not prove possible to detect direct protein-protein interactions between NSP1 and the co-precipitating proteins using a yeast two-hybrid assay. Since these proteins have all been shown to have RNA-binding activity, it could be argued that co-immunoprecipitation of the proteins with NSP1 might be due to binding to RNA. To address this question, an experiment was designed such that the cell lysate was treated with RNAase prior to immunoprecipitation with anti-NSP1 serum. If NSP1 was held in the complex by binding to RNA then successful degradation of the RNA would result in a decrease in the co-immunoprecipitation of the proteins contained in the complex with NSP1. However, if RNA was not involved in the formation of the complex then treatment with the RNA-degrading agent would have no effect on the quantity of proteins which were immunoprecipitated. Micrococcal nuclease was used as it is known to efficiently degrade RNA. Cell lysate samples were incubated with micrococcal nuclease for varying lengths of time at room temperature. It was not known how the RNA might be packaged with the protein complex, so a longer incubation time might be required if it was protected from nuclease attack. The nuclease-treated samples were then immunoprecipitated with anti-NSP1 serum to determine whether the degradation of

RNA made a difference to the protein complex which was co-immunoprecipitated with NSP1.

7.5.2 Micrococcal nuclease efficiently destroys RNA in the cell lysate

A problem was anticipated with the potential results of this experiment if no change was observed in the proteins immunoprecipitated by the anti-NSP1 serum after treatment with the micrococcal nuclease. If this was the case, then a valid conclusion could not be drawn as it would be unclear whether the micrococcal nuclease actually had an effect. To address this problem, a control experiment was designed to run in conjunction with the immunoprecipitation reactions to demonstrate the activity of the micrococcal nuclease. To perform the control experiment, the labelled infected cell lysate was divided into two aliquots, one of which was incubated with micrococcal nuclease for 90 minutes and a second which was not. The nuclease was then destroyed by treatment with proteinase K and a phenol/chloroform extraction was performed with both samples to remove protein from the cell extract. The RNA in the samples was then extracted by ethanol precipitation. An aliquot was removed at this point to confirm that the labelled viral proteins had been removed from the cell extracts (data not shown). The extracted samples were then added to a rabbit reticulocyte lysate translation system so that any RNA present would be translated to protein. The translation reactions were immunoprecipitated with serum raised against a preparation of the UKtc strain of bovine rotavirus and analysed on a polyacrylamide gel. The sample which was not treated with nuclease contained viral RNA which was translated to protein. The sample was divided and immunoprecipitated with pre-immune serum (Figure 7.6, lane 8) and anti-UKtc serum (Figure 7.6, lane 9) to show that viral proteins were present. If the nuclease treatment was effective, then the RNA in the nuclease-treated sample would be destroyed and hence no viral proteins would be produced for immunoprecipitation. Immunoprecipitation of the nuclease-treated sample with pre-immune serum (Figure 7.6, lane 10) and anti-UKtc serum (Figure 7.6, lane 11) showed that no viral proteins were present in the extract. Thus, this control experiment demonstrated that the nuclease-treatment successfully degraded viral mRNA in the cell extract.

Figure 7.6 Immunoprecipitation with anti-NSP1 serum of UKtc rotavirus-infected cell lysates pre-treated with micrococcal nuclease for varying lengths of time

Confluent MA104 cells were infected with a high m.o.i. of the UKtc strain of bovine rotavirus (m.o.i. = 20) and incubated for 7 hours at 37 °C. The cells were labelled with ^{35}S-methionine for 2 hours and harvested (Section 3.6.3). 10 µl aliquots of the cell lysate were treated with micrococcal nuclease by adding 2.5 µl of 100 mM $CaCl_2$ and 2.5 µl of 1 mg/ml micrococcal nuclease. An equivalent volume of 50 mM Tris.HCl pH 8.0 was added to the untreated samples in place of the nuclease. The samples were incubated at room temperature for 10, 30, 60 or 90 mins. The experimental samples were then immunoprecipitated with 1 µl of pre-immune serum, anti-NSP1 serum or anti-UKtc serum (Section 3.6.4).

The control samples were treated with 100 µg/ml proteinase K in buffer (1 % SDS: 0.1 M Tris.HCl pH 7.5: 12.5 mM EDTA: 0.15 M NaCl) to destroy the nuclease, and the RNA was extracted with phenol-chloroform (Section 3.4.4) and ethanol precipitation (Section 3.4.5) and resuspended in 10 µl of RNAse-free H_2O. The RNA samples were translated in a rabbit reticulocyte lysate system (Section 3.6.1.2) and the resulting proteins immunoprecipitated with pre-immune or anti-UKtc serum (Section 3.6.4). The immunoprecipitates were analyzed on a 5-11 % gradient polyacrylamide gel (Section 3.6.5), and the results visualized by dry gel fluorography (Section 3.6.6).

Untreated cell lysates were immunoprecipitated with pre-immune serum (lane 1) and anti-NSP1 serum (lane 2). 10 µl aliquots of the cell lysate were treated with micrococcal nuclease for 10 minutes (lane 3), 30 minutes (lane 4), 60 minutes (lane 5) and 90 minutes (lane 6) then immunoprecipitated with anti-NSP1 serum. An untreated aliquot was also incubated at room temperature for 90 minutes before immunoprecipitation with anti-NSP1 serum (lane 7). As a control for the micrococcal nuclease activity, RNA was extracted and translated from two untreated aliquots and the samples immunoprecipitated with pre-immune serum (lane 8) and anti-UKtc serum (lane 9). RNA was also extracted from aliquots treated with micrococcal nuclease for 90 minutes. The samples were translated and immunoprecipitated with pre-immune serum (lane 10) and anti-UKtc serum (lane 11). A sample of the unprecipitated cell lysate was not run on this gel. However, a 10 µl sample from the same stock of cell lysate that was used in this experiment is shown on a previous gel (Figure 7.5, lane 1). This figure represents a gel exposure time of 1 week. The identity of the viral polypeptides are indicated on the left of the lanes. VP indicates viral structural proteins. NSP indicates viral non-structural proteins.

Figure 7.6

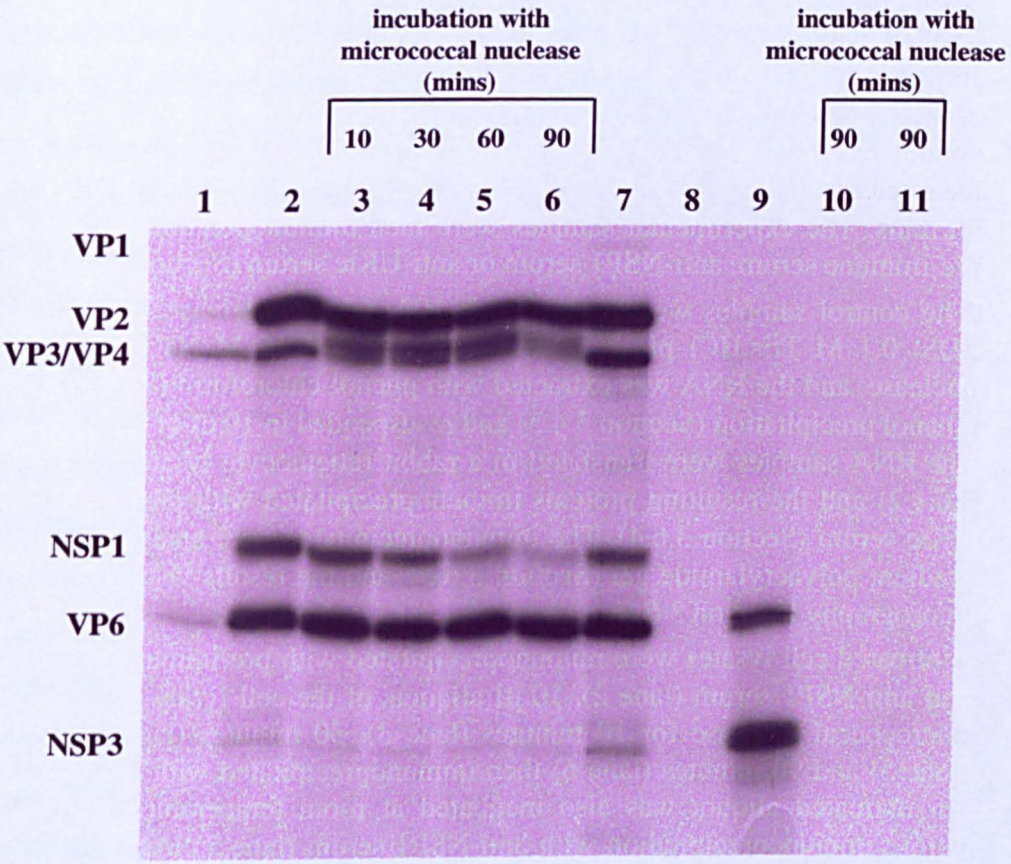
incubation with micrococcal nuclease (mins)
10
30
60
90
incubation with micrococcal nuclease (mins)
90
90
1
2
3
4
5
6
7
8
9
10
11
VP1
VP2
VP3/VP4
NSP1
VP6
NSP3

7.5.3 Immunoprecipitation with anti-NSP1 serum of micrococcal nuclease treated cell lysates

Micrococcal nuclease-treated rotavirus-infected cell lysates were immunoprecipitated with anti-NSP1 serum as described (Section 7.5.3) and the results were analysed on a 5-11 % gradient polyacrylamide gel by fluorography of the dried gel (Figure 7.6). Phosphoimager analysis of the gel was used to provide estimates of the protein content of the immunoprecipitated protein bands (Appendix 2.3). Immunoprecipitation of the untreated lysate with anti-NSP1 serum (lane 2) showed the complex described previously (Section 7.3.3) which consists of VP2, VP3/VP4, VP6 and small quantities of VP1 and NSP3 co-immunoprecipitating with NSP1. On examination of the immunoprecipitates from the nuclease-treated samples, a considerable reduction in the quantity of NSP1 and VP3/VP4 could be seen as the incubation time increased (lanes 3-6). The quantity of NSP3 also appeared to be less in the nuclease-treated samples. However, VP2 and VP6 appeared to be constant throughout the time course. A sample of untreated lysate was incubated at room temperature for 90 minutes to determine whether any protein degradation was occurring due to inherent proteases in the cell lysate. If considerable degradation of the viral proteins occurred it might obscure the result of the nuclease-treated samples. By fluorographic examination of the gel it appeared that visible levels of protein degradation did not occur in the cell lysate during the incubation period (lane 7). Quantification of the protein bands by phosphoimager analysis showed that the amount of VP6 did not decrease throughout the time course treatment with micrococcal nuclease (Appendix 2.3). However, similar analysis of VP2, VP3/VP4 and NSP1 showed a decrease in the amount of protein immunoprecipitated from cell lysates treated with micrococcal nuclease over time. The quantity of NSP3 which co-precipitated was not sufficient for phosphoimager analysis.

The protein bands resulting from the immunoprecipitation from cell lysates treated with micrococcal nuclease for 10 minutes were analysed and the approximate amounts of protein were determined by phosphoimager analysis (Appendix 2.3). The amount of NSP1 precipitated by the anti-NSP1 serum did not decrease after 10 minutes incubation with nuclease. However, the quantities of VP2 and VP3/VP4 which were co-precipitated were reduced to approximately 70 % of those present in the initial reaction (no nuclease). If NSP1, VP2 and VP3/VP4 were held together in the complex by RNA-protein interactions, then degradation of the RNA would result

in a decrease in the quantities of these proteins held in the complex, and thus a corresponding decrease in the co-precipitation of VP2 and VP3/VP4 with NSP1. This result suggested that the nuclease was active in degrading RNA within the first 10 minutes of the reaction, and the decrease in co-precipitation of VP2 and VP3/VP4 with NSP1 which was observed could be due to degradation of RNA holding the proteins together in the complex.

In the reactions incubated with nuclease for between 30 and 90 minutes there was a reduction in the quantity of NSP1 which was immunoprecipitated by the anti-NSP1 serum. There was also a decrease in the quantities of VP2 and VP3/VP4, however the change was slower than in the 10 minute reaction and could be due to the fact that less NSP1 was immunoprecipitated. The decrease in immunoprecipitation of NSP1 could be due to the degradation of the complex, resulting in the release of NSP1 which might be inefficiently precipitated when free in the lysate compared to when it is held in a large complex. A slight decrease in the quantity of NSP1 was also noted in the reaction which was incubated without nuclease for 90 minutes, perhaps indicating that NSP1 was subject to low level degradation by ubiquitous proteases in the lysate. The latter might therefore also account for the decrease in immunoprecipitation of NSP1 over time.

Quantification of the VP6 protein bands by phosphoimager analysis showed that the amount of VP6 did not decrease throughout the time course treatment with micrococcal nuclease. As VP6 does not appear to have RNA-binding activity it is unlikely to be held in the complex by RNA-protein interactions, as suggested for the other components, and thus would not be expected to be affected by treatment with nuclease. VP6 is the inner capsid protein and the most abundant protein in the virus. As it is such an abundant protein it seems likely that there would be a high ratio of molecules of VP6 to NSP1 in the complex. If the proportion of VP6 in the complex was considerably higher than the proportion of NSP1, a small decrease in NSP1 might not necessarily produce a noticeable decrease in the quantity of VP6 precipitated.

7.6 Analysis of NSP1 production and complex formation during the early stages of virus infection

7.6.1 Time course analysis of NSP1 complex formation *in vivo*

To examine the formation of NSP1-containing complexes in the early stages of rotavirus infection, pulse-chase labelled infected cell lysates were harvested at various times p.i. and immunoprecipitated with anti-NSP1 serum. It was thought that immunoprecipitation of NSP1 at different time points and analysis of the co-precipitating proteins might offer some insight into the protein components of the complex, how it was formed and how it changed over time. Immunoprecipitation of the samples after a two hour chase with cold methionine would show whether the co-precipitating proteins had changed during that time period.

Cells were pulse-labelled for 30 minutes with ^{35}S-methionine at 1, 3, 5 and 7 hours p.i. with the UKtc strain of bovine rotavirus. Following the pulse-labelling, one sample of cells was harvested immediately (pulse sample) and a second sample was chased for 2 hours with unlabelled methionine (pulse-chase sample). In the experiments described earlier in this chapter, rotavirus-infected cells were pulse-labelled at 7 hours p.i. and harvested without a chase period. The alternative labelling regimes described in this section were designed to show which proteins co-precipitated with NSP1 during the earlier stages of infection and whether the NSP1-containing complex was maintained in the cell during the chase period.

Polyacrylamide gel analysis of immunoprecipitates made from pulse-labelled samples revealed that NSP1 was not detected in the cell until 3 hours p.i. (Figure 7.7). This indicated that in the very early stages of infection either no NSP1 or only undetectable amounts of the protein were present. However, by 3 hours p.i. it can be clearly seen that NSP1 was precipitated from both the pulse and pulse-chase samples. Analysis of the protein bands using phosphoimaging revealed that approximately the same amounts of NSP1 were precipitated from both the pulse and the pulse-chase samples (Appendix 2.4.1). Small quantities of other viral proteins, including VP1, VP2, VP3/VP4, VP6 and a protein thought to be NSP3, co-precipitated with NSP1. Approximately equal quantities of each co-precipitating protein were found in both the pulse and the pulse-chase samples (Appendix 2.4.1). No proteins were precipitated by the pre-immune serum suggesting that the co-precipitation of these proteins with NSP1 was due to a specific interaction between them.

Figure 7.7 Immunoprecipitation of UKtc rotavirus-infected cell lysates pulse-chase labelled with ^{35}S-methionine at regular time intervals

MA104 cells were grown to confluence then incubated in methionine-free media overnight. The cells were infected with a high m.o.i. of the UKtc strain of bovine rotavirus (m.o.i. = 20) and incubated for varying lengths of time at 37 °C (Section 3.6.3). The cells were pulse-labelled, in duplicate, with ^{35}S-methionine for 30 minutes at 1, 3, 5, or 7 hours post-infection. After the pulse-labelling period, one well of cells was harvested and the second was chased with media containing 100X unlabelled methionine for 2 hours before harvesting. 50 µl of each sample was immunoprecipitated with 1 µl of pre-immune serum or 1 µl anti-NSP1 serum (Section 3.6.4). The immunoprecipitates were analyzed on a 5-11 % gradient polyacrylamide gel (Section 3.6.5), and the results visualized by dry gel fluorography (Section 3.6.6).

The times of pulse-labelling at 1, 3, 5 and 7 hours post-infection are indicated on the figure. There are four reactions for each incubation time showing the immunoprecipitation of the pulse (P) and pulse-chase (C) samples with both pre-immune and anti-NSP1 serum. This figure represents a gel exposure time of 3 weeks. The identity of the viral polypeptides are indicated on the left of the lanes. VP indicates viral structural proteins. NSP indicates viral non-structural proteins.

Figure 7.7

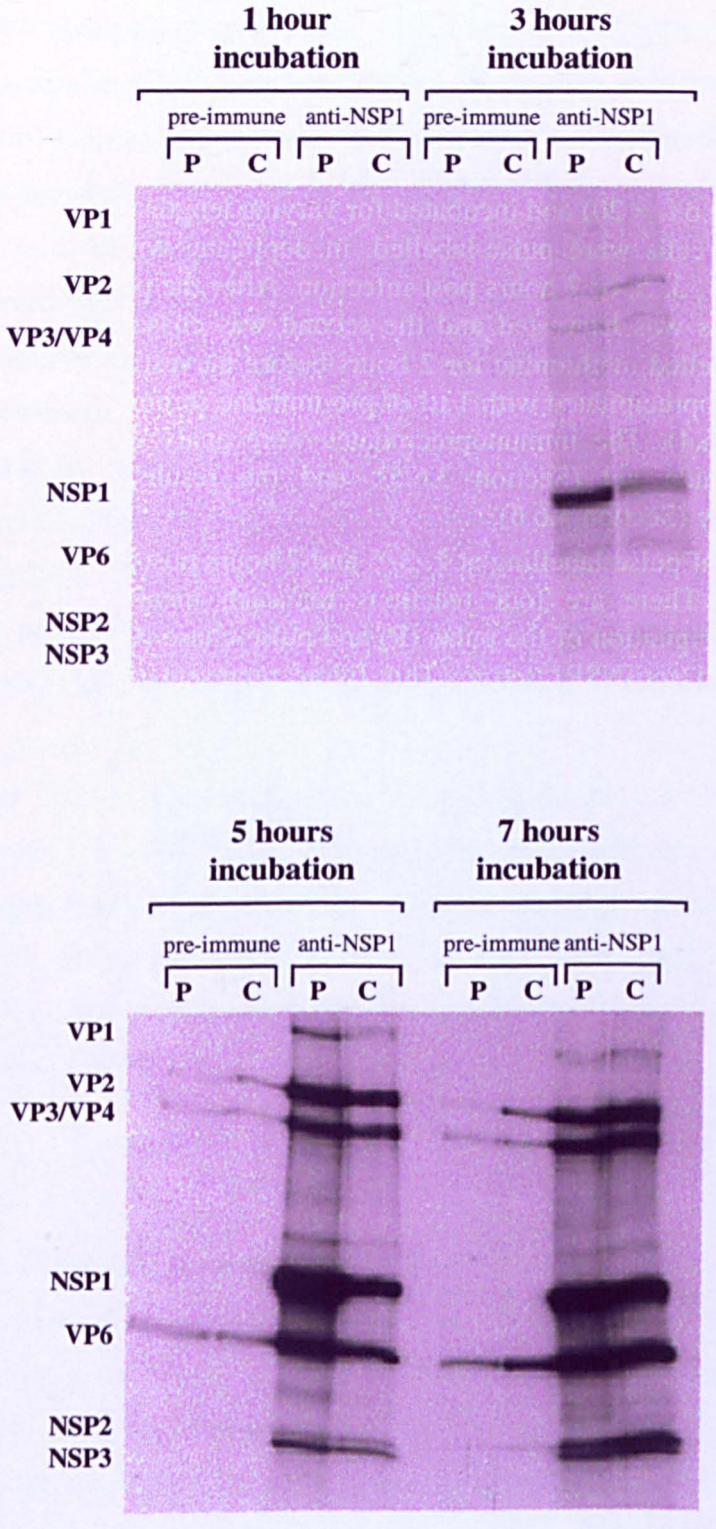
1 hour incubation
3 hours incubation
pre-immune
anti-NSP1
pre-immune
anti-NSP1
P
C
P
C
P
C
P
C
VP1
VP2
VP3/VP4
NSP1
VP6
NSP2
NSP3
5 hours incubation
7 hours incubation
pre-immune
anti-NSP1
pre-immune
anti-NSP1
P
C
P
C
P
C
P
C
VP1
VP2
VP3/VP4
NSP1
VP6
NSP2
NSP3

At 5 hours p.i. several proteins, VP1, VP2, VP3/VP4, VP6 and NSP3, were again co-precipitated with NSP1 from both the pulse and pulse-chase samples. Phosphoimager analysis of the protein bands showed there was a sharp increase in the amount of NSP1 precipitated at 5 hours p.i. compared to 3 hours p.i. (Appendix 2.4.1). This increase in NSP1 was matched by an increase in the co-precipitating proteins. In addition, considerably more NSP1 was precipitated from the pulse sample compared to the pulse-chase sample at this time point. This observation was also true for the viral proteins co-precipitating with NSP1. This suggested that NSP1 may be contained in a transient complex with these proteins which is rapidly turned over such that only small quantities remain to be precipitated from the pulse-chase sample after the 2 hour chase period.

At 7 hours p.i., the viral proteins were again co-precipitated with NSP1. At this stage, similar quantities of each protein were precipitated from both the pulse and pulse-chase samples. These results suggested that by this time point the co-precipitating proteins were found associated in a complex with NSP1 which was either stable during the 2 hour chase period, or was present at a constant level in the infected cell.

At 5 and 7 hours p.i. small quantities of proteins were precipitated by the pre-immune serum. Using phosphoimager analysis, the amounts precipitated by the pre-immune serum were compared to that co-precipitated by the anti-NSP1 serum (Appendix 2.4.3). In all cases the amounts co-precipitated with NSP1 by the anti-NSP1 serum were considerably higher, suggesting they were specifically co-precipitated with NSP1.

7.6.2 Summary

Analysis of the data produced from the immunoprecipitation of a time course of pulse-chase labelled samples by examination of the gel and phosphoimager quantification of the protein bands allowed speculation about the nature of a complex formed with NSP1. Several viral proteins consistently and specifically co-precipitated with NSP1 over the time course and it is suggested that NSP1 forms a complex with these proteins. The proteins were first detected at 3 hours p.i.. By 7 hours p.i. similar amounts of each protein were precipitated from the pulse and pulse-chase samples, indicating either that the NSP1-containing complex was stable during the chase period

or that it was now at a constant level in the cell. This was in contrast to the situation at 5 hours p.i. when the quantity of each protein in the pulse sample greatly exceeded the quantity precipitated from the pulse-chase sample, which could be due to high levels of a transient NSP1-containing complex at this time. The length of the time course was chosen with the consideration that RNA replication is maximal at 6-9 hours, and virions can be detected by 6 hours p.i. (McCrae and Faulkner-Valle, 1981) (Stacy-Phipps and Patton, 1987). However, future experiments might include an extension of the time course in order to determine how the complex changes after 7 hours p.i.. Shorter intervals between the pulse times may also reveal additional information about the nature of the NSP1-containing complex.

7.7 Analysis of NSP1 complex by co-immunoprecipitation studies with anti-VP6 monoclonal antibody

7.7.1 Co-immunoprecipitation of NSP1 with VP6

Previous work in this chapter has described a novel NSP1-containing complex in UKtc rotavirus-infected cell lysates. This complex contained VP1, VP2, VP3/VP4, VP6, and NSP3 in addition to NSP1. The presence of the viral structural proteins associated with the double-layered virus particle led to the suggestion that a novel NSP1-containing complex or particle had been precipitated. As VP6 has not previously been found in an NSP1-containing complex, an experiment was designed to determine whether NSP1 would co-precipitate with VP6 using a specific anti-VP6 antibody. An anti-VP6 monoclonal antibody (mAb) was obtained and it was confirmed that it could immunoprecipitate VP6 from UKtc rotavirus-infected cell lysates (data not shown).

Earlier immunoprecipitation experiments using anti-NSP1 serum and carried out on cell fractions (Figure 7.5) showed that more than half of the total amount of VP6 co-precipitating with NSP1 was found in the 10,000Xg centrifugation stage pellet sample. Most of the remaining VP6 protein was found in the 30,000Xg centrifugation stage pellet sample. Therefore, the 10,000Xg supernatant and pellet and the 30,000Xg pellet fractions were chosen for analysis in the present experiment using the anti-VP6 mAb. A sample of the unfractionated cell lysate was also analysed by immunoprecipitation with the anti-VP6 monoclonal antibody. VP6 was precipitated

from the unfractionated cell lysate and also from each of the cell fractions analysed (Figure 7.8). The pre-immune serum precipitated a small quantity of VP6 from the unfractionated sample equivalent to 1.5 % of the total protein precipitated by the specific anti-VP6 antibody (as determined by phosphoimager analysis), and this was considered to be a negligible quantity (Appendix 2.5.1). The amount of VP6 precipitated from the 10,000Xg pellet fraction was over a third of the total precipitated from the cell lysate, and of the remaining VP6 protein in the fraction, almost a half was then precipitated from the 30,000Xg pellet fraction. Clearly, although much VP6 was pelleted by low speed centrifugation, a significant amount remained in the supernatant fractions.

The proteins co-precipitating with VP6 were examined. Small quantities of NSP1 were found co-precipitating with VP6. Although the bands were faint on the fluorograph of the gel, they were detectable by phosphoimager analysis (Appendix 2.5.1). NSP3 was also co-precipitated with VP6, although a high background in this region of the gel meant the bands were harder to detect. Higher levels of NSP1 and NSP3 were precipitated from the unfractionated cell lysate compared to the samples fractionated by centrifugation. Only very low levels of NSP1 and NSP3 were non-specifically precipitated by the pre-immune serum. VP2 and VP3/VP4 were co-precipitated with VP6 from all fractions, however they were also precipitated by the pre-immune serum which brings into question the specificity of their co-precipitation with VP6. Visible levels of VP1 were not detected on the gel fluorograph.

7.7.2 NSP1 complex contains only a small proportion of total VP6 in the cell

Co-immunoprecipitation experiments with the available anti-VP6 mAb resulted in precipitation of small quantities of NSP1 together with the complex proteins described previously. VP6 is an abundant structural protein while NSP1 is only expressed at very low levels. Phosphoimager analysis showed that the percentage of VP6 contained in the NSP1 complex was only about 4 % of the total VP6 in the cell lysate (Appendix 2.5.2). Hence, the proportion of molecules of VP6 contained in a complex with NSP1 appears to be very low.

The bands thought to be NSP1 co-precipitated with VP6 were quite faint on the fluorograph. Prior isolation of the NSP1-containing complex with specific anti-

Figure 7.8 Immunoprecipitation of UKtc rotavirus-infected cell lysates with anti-VP6 monoclonal antibody

Confluent MA104 cells were infected with a high m.o.i. of the UKtc strain of bovine rotavirus (m.o.i. = 20) and incubated for 7 hours at 37 °C. The cells were labelled with ^{35}S-methionine for 2 hours and harvested (Section 3.6.3). The cell lysate was fractionated by centrifugation at 10,000Xg (11,000 rpm) in a Beckman TL 100 ultracentrifuge using the TLS 55 rotor for 1 hour at 4 °C. The pellet was resuspended in an equivalent volume of 50 mM Tris.HCl pH 8.0 and samples of both the pellet and the supernatant were saved for analysis. The supernatant was then centrifuged at 30,000Xg (19,000 rpm), the pellet was resuspended and samples saved as before. 50 µl aliquots of the pellet and supernatant of each cell fraction and also an unfractionated sample of the cell lysate were immunoprecipitated (Section 3.6.4) with 10 µl of pre-immune serum or anti-VP6 monoclonal antibody. The immunoprecipitates were analyzed on a 5-11 % gradient polyacrylamide gel (Section 3.6.5), and the results visualized by dry gel fluorography (Section 3.6.6).

A sample of the unfractionated cell lysate (2 µl) was loaded on the gel to show the characteristic pattern of rotavirus protein expression before immunoprecipitation (cell lysate). This lane represents a gel exposure time of 6 days. Immunoprecipitation of a sample of the unfractionated cell lysate with pre-immune serum (lane 1) and with the anti-VP6 monoclonal antibody (lane 2) was performed. Immunoprecipitation of the following cell fractions with the anti-VP6 monoclonal antibody was performed: 10,000Xg pellet (lane 3); 30,000Xg pellet (lane 4); 10,000Xg supernatant (lane 5). Lanes 1-5 represent a gel exposure time of 15 days. The identity of the viral polypeptides are indicated on the left of the lanes. VP indicates viral structural proteins. NSP indicates viral non-structural proteins.

Figure 7.8

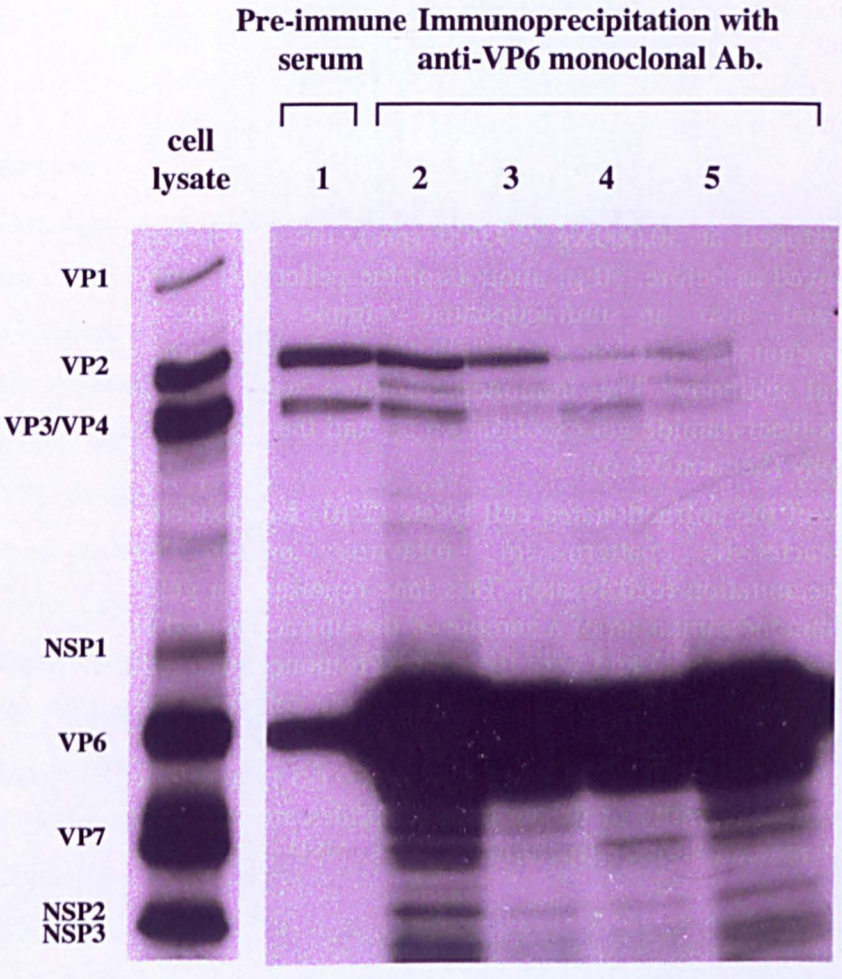
Pre-immune serum
Immunoprecipitation with anti-VP6 monoclonal Ab.
cell lysate
1
2
3
4
5
VP1
VP2
VP3/VP4
NSP1
VP6
VP7
NSP2
NSP3

NSP1 antibody, followed by selection with anti-VP6 antibody should allow a clearer resolution of the components of the complex. However, following the selection of the NSP1-containing complex by immunoprecipitation with anti-NSP1 serum, it would then be necessary to dissociate the complex and antibody in a procedure that might cause disruption to the complex such that it was no longer recognised by the anti-VP6 serum. Caution should therefore be exercised in the design and evaluation of such an experiment.

7.8 Discussion

This chapter describes initial studies on a previously unrecognised complex containing NSP1 that was immunoprecipitated with anti-NSP1 serum from rotavirus-infected cells. Viral proteins VP1, VP2, VP3/VP4, VP6 and NSP3 were specifically co-immunoprecipitated with NSP1 from infected cell lysates, and it was postulated that these proteins formed a novel complex in the infected cell. In addition, an anti-VP6 monoclonal antibody reciprocally precipitated small amounts of NSP1. The presence of VP2 and VP6, which are the major structural proteins of the double-layered virus particle, suggested that a complex or particle had been precipitated. Further experiments to examine various aspects of the formation of this complex were performed. Immunoprecipitation with anti-NSP1 serum of fractions created by centrifugation of cell lysates showed this complex co-precipitated with NSP1 mainly from the pellet of the low speed centrifugation sample. Phosphoimager analysis showed that only a small proportion of NSP1 was contained in the complex with VP6. The VP6 found in the complex only represented a small proportion of total protein in the cell lysate. Therefore, it seems probable that this complex is only found in small amounts in the infected cell.

Direct protein-protein interactions were not demonstrated between NSP1 and other proteins in this complex using a yeast two-hybrid assay, consequently it was proposed that NSP1 may be held in the complex indirectly via an interaction with viral mRNA. Treatment of the cell lysate with micrococcal nuclease resulted in a decrease in the quantity of VP2, VP3/VP4 and NSP3 co-immunoprecipitating with NSP1. This was particularly notable in the first 10 minutes of the incubation time when there was a considerable decrease in the amount of VP2 and VP3/VP4 co-precipitating with NSP1 compared to the quantity which co-precipitated with a

similar amount of NSP1 before nuclease treatment. This result supports the hypothesis that some interactions in the NSP1-containing complex might be mediated by RNA-binding. VP6 does not have RNA-binding activity and no visible decrease was observed in the quantity of VP6 which co-precipitated with NSP1 on the addition of nuclease. VP6 must interact with the complex in a different manner, perhaps by protein-protein interactions with other members of the complex, and indeed there is evidence to suggest that VP6 interacts with VP2 in the formation of the double-layered virus particle (Zeng *et al.*, 1994) (Estes, 1996).

At present the function of this novel complex is unknown. It may be similar to the RIs which have been described previously (Gallegos and Patton, 1989), however in contrast with those complexes, NSP1 appeared to be retained in the complex until after the addition of VP6. It seems to be present at low levels in the infected cell. Hence, it is possible that it is a transient assembly complex formed during the replication process, which is rapidly turned over so that only small amounts are present in the infected cell at any one time. Future work should include an attempt to precipitate the complex with antisera raised against the other protein components and these experiments would help to confirm the composition of the complex.

Discussion

8.1 Discussion

Rotavirus encodes six non-structural proteins whose functions in the virus infectious cycle have not as yet been well characterised. The non-structural proteins would be expected to play a role in the viral replication cycle, in association with the viral RNA and those structural proteins that operate in an enzymatic capacity in the cycle. In order to elucidate the details of the replication process, it is essential to characterise the nature of the interactions that occur between the protein constituents of replication complexes. The non-structural protein NSP1 has been shown to be a component of a complex formed with several viral structural proteins at early times in the replication cycle (Gallegos and Patton, 1989). The primary aim of this project was to determine whether protein-protein interactions occurred between NSP1 and the other components of the early replication complex in an attempt to elucidate the role of NSP1 in the viral replication cycle.

NSP1 is unusual among the non-structural proteins in that it shows an extremely high level of divergence in its primary sequence. Despite this, the predicted secondary structure of the protein appears to be conserved, suggesting there is a selective pressure to maintain the overall structure of the protein to facilitate a function in the virus infectious cycle. A highly conserved, cysteine-rich region at the amino-terminus of the protein is proposed to be a functional domain and may contain a zinc finger motif (Mitchell and Both, 1990a). The protein has also been shown to have non-specific ssRNA-binding activity (Brottier *et al.*, 1992). Early attempts to define complexes associated with the rotavirus replication cycle identified three replication intermediates (RIs) in the infected cell (Gallegos and Patton, 1989). NSP1 was found to be associated with the earliest complex, the pre-core RI, suggesting a role for the protein in the early stages of the replication cycle. The core RI is formed by the subsequent addition of VP2 to the pre-core RI. The intermolecular interactions between the components of these complexes were not defined. Clearly, in order to fully understand the virus replication cycle and the function of individual proteins within it, the protein-protein interactions that occur between the constituents of these complexes must be determined.

To investigate potential protein-protein interactions between NSP1 and the other protein components of the RIs, two different systems were employed. The yeast two-hybrid system is now established as a practical assay for quickly detecting

protein-protein interactions *in vivo*, and this system was chosen as the primary tool to investigate NSP1 protein interactions. A second approach, based on an *in vitro* radio-immunoprecipitation assay, was developed to confirm results obtained with the two-hybrid system. The protein-protein interactions occurring in the RIs were expected to be of a transient nature and this view was influential in the choice of the yeast two-hybrid system, as it is known to be a sensitive assay for detection of weak or transient interactions.

A cloning strategy was devised to construct plasmids expressing fusions of the GAL4 DNA-binding and activation domains with the rotavirus proteins NSP1, NSP3, VP1, VP2, and VP3. The reading frame was maintained during the cloning procedure such that GAL4 domain fusion proteins would be produced. These plasmids were co-transformed into a reporter yeast strain to test for protein-protein interactions. The reporter gene used was *lacZ*, and consequently the detection of β-galactosidase indicated that the two proteins being studied were interacting. All proteins were tested in both the GAL4 DNA-binding and activation domains. This was because previous work has shown that this system can be subject to directionality, with the orientation of the proteins determining whether or not an interaction is detected (Estojak *et al.*, 1995). No self-interaction of NSP1 with itself was detected and it also did not show any interaction with the other non-structural protein, NSP3, tested. In addition, no interactions were demonstrated between NSP1 and the viral structural proteins VP1, VP2 and VP3.

There are a number of possible explanations as to why interactions between the rotavirus proteins were not demonstrated in the yeast two-hybrid assay. First, it is conceivable that NSP1 does not form direct protein-protein interactions with the other protein components of the RIs but interacts with them indirectly. The implications of this possibility will be discussed later. A second explanation is that authentic protein-protein interactions exist but could not be detected under the conditions of this assay. There are a number of examples in the literature where proteins shown to interact with each other in other assays have failed to give a positive result in the yeast two-hybrid system. For example, use of the GAL4 domain two-hybrid vectors to characterise interactions among non-structural proteins of poliovirus failed to detect all the interactions which were shown with an *in vitro* system (Cuconati *et al.*, 1998). Similarly, a study of the nucleocapsid proteins of rinderpest virus failed to show a

self-association of the N protein in the GAL4 domain yeast two-hybrid system, despite the fact that the protein has been shown to self-assemble when expressed in *E. coli* (Shaji and Shalia, 1999). Clearly, genuine protein-protein interactions cannot always be detected in the two-hybrid system, and there are several explanations for this. First, if the interactions occur only weakly in yeast they may not be detected by the assay. Reporter systems used in two-hybrid assays have been shown to be subject to a threshold corresponding to the minimum affinity of the protein interaction required to score as positive in the assay (Estojak *et al.*, 1995). Although the *lacZ* reporter system is known to be sensitive for some interactions, very weak interactions may still fall below the minimum threshold required for detection. Secondly, as the assay was performed in yeast and not in a mammalian cell, it is unlikely to represent the exact conditions that would be found in the mammalian cell. Although the yeast system should produce proteins more similar to their native state than that obtained in a bacterial system there are still modifications, such as proteins containing disulphide bonds, which cannot always be properly expressed in a nuclear-based system such as the two-hybrid system (Fields and Sternglanz, 1994). Thirdly, an interaction would not be detected if the fusion protein was not localised to the nucleus, although the possibility of this is unlikely for proteins that do not contain strong localisation signals for other compartments of the cell or for the plasma membrane. Further, it is possible that the fusion of the GAL4 domains to the viral proteins may mean that the protein is misfolded or unstable. A point that must be taken into consideration is that the expression of the fusion proteins was not detectable by western blot. This was probably due to the low expression from the two-hybrid vectors pGBT9 and pGAD424, as even specific monoclonal antibodies (mAb) against the GAL4 domains cannot detect fusion proteins expressed from these vectors by western blot analysis. The small possibility that fusion proteins were not stably expressed in the yeast cell cannot however be completely dismissed. Finally, in some cases the attached GAL4 domain can occlude the protein interaction site. The proteins of interest are expressed as carboxy-terminal extensions of the GAL4 domains, and the attached activation domain can sometimes block accessibility to the amino-terminus of the protein (Fields and Sternglanz, 1994). Hence, the orientation of the proteins - whether they are fused to the GAL4 DNA-binding or activation domains - can be an important factor in the success of the assay.

It is perhaps surprising that protein-protein interactions were not detected between NSP1 and the viral proteins with which it is associated in the pre-core RI, as the protein components of the RIs would probably be expected to interact. A possible explanation is that an additional component, such as viral mRNA, is needed to bridge the interactions between the proteins. As all the protein components of the pre-core RI, including NSP1, have mRNA-binding activity, it is a distinct possibility that protein interactions might be mediated by mRNA. If NSP1 interacted with mRNA in the early replication complexes, rather than forming protein-protein interactions, then this would explain the negative results from the two-hybrid assays. Alternatively, interactions between the proteins may only occur when they are assembled in the RI, due to the presence of new interaction domains in the proteins exposed by the complex formation. A similar scenario has been proposed for the association of influenza NS1 protein with the transcription-replication complex in influenza-infected cells, since direct protein interactions were not shown between NS1 and the polymerase subunits in a two-hybrid assay (Marión *et al.*, 1997). The yeast two-hybrid assay would not detect protein-protein interactions of this nature as viral RNA cannot be added to the system.

While this work was in progress, the report by González *et al.* (1998) appeared which presented data to suggest that NSP1 interacted with the viral non-structural proteins NSP2, NSP3, NSP5 and NSP6, which are found associated at different times with the RIs. Using the GAL4 yeast two-hybrid system, NSP1 was shown to interact with each protein, albeit at a low level. Interactions were only observed when NSP1 was fused to the GAL4 DNA-binding domain, and this fusion protein also activated transcription at a low level in the absence of a GAL4 activation domain fusion counterpart. Immunoprecipitation analysis demonstrated co-immunoprecipitation of NSP1 with each non-structural protein using specific sera, but reciprocal precipitation of the proteins with NSP1 by anti-NSP1 serum was not observed.

In contrast to the results presented by González *et al.* (1998), an interaction between NSP1 and NSP3 was not observed using the yeast two-hybrid system in the present study. The reason for this discrepancy is unknown, but it has been noted that experiments performed with the same or similar plasmids, but different cell preparations, may not necessarily produce the same levels of interaction signal (Cuconati *et al.*, 1998). Since the interactions observed by González *et al.* (1998)

were not much higher than background, it is conceivable that contradictory results might be obtained under slightly different conditions in a heterologous system. Although the sequence of NSP1 from the YM strain of porcine rotavirus used in the study by González *et al.* (1998) has not been published, on the basis of previous sequence comparisons it would be expected to show a high level of divergence with the sequence of NSP1 from the UKtc strain of bovine rotavirus used in this study. This expected variance in the two proteins may underlie the differences observed between the work of González *et al.* (1998) and the present study.

A self-interaction of NSP3 was demonstrated in the yeast two-hybrid assay, which confirmed, *in vivo*, earlier reports that NSP3 formed multimers in infected cells (Mattion *et al.*, 1992). This correlated with recent two-hybrid data, although the strengths of the interactions were found to be different (González *et al.*, 1998) (Poncet *et al.*, 1997). Recently, the dimerisation domain of NSP3 has been mapped between amino acids 150 and 206 - a region of the protein predicted to form a coiled coil structure - using a yeast two-hybrid assay (Piron *et al.*, 1999).

Future experiments to examine NSP1 protein-protein interactions should include the use of a mammalian two-hybrid system, which may provide a more suitable environment in which to examine viral protein-protein interactions. Alternatively, the use of a different yeast two-hybrid system, such as the original LexA system or the amino-terminal fusion LexA system (Section 5.8.3), might be attempted. The use of high expression GAL4 two-hybrid vectors might also yield a different result. If protein-protein interactions were demonstrated in the two-hybrid system, then deletion analysis of the proteins could be used to define the regions of the proteins involved in the interaction. In addition, the two-hybrid system could be used to screen a cellular protein library for proteins interacting with NSP1, as it has been suggested previously that NSP1 might interact with a cellular protein (Hua *et al.*, 1994) (Xu *et al.*, 1994). It would also be interesting to determine if any of the other non-structural proteins, such as NSP3, associate with cellular proteins.

Simultaneously with the yeast two-hybrid assays, co-immunoprecipitation experiments were performed with *in vitro* translated viral proteins in an attempt to support the results obtained *in vivo*. To investigate whether VP1, VP2, or VP3 were specifically co-precipitated with NSP1, mixtures of *in vitro* translated proteins were immunoprecipitated with anti-NSP1 serum. Although VP1, VP2, and VP3 were

observed separately co-precipitating with NSP1, control experiments suggested that non-specific precipitations also occurred. The existence of specific protein-protein interactions was not clearly demonstrated, although it is possible that the non-specific precipitations obscured the identification of genuine co-precipitations of the core proteins with NSP1. These results suggested similar conclusions to the yeast two-hybrid assays, in that either protein-protein interactions do not occur or that existing interactions cannot be detected under the conditions of the assay. As indicated earlier this may be due either to a requirement for an intermediary such as viral mRNA or the prior assembly of the proteins into a complex.

Further experiments should include reciprocal immunoprecipitation of protein mixtures with specific serum against VP1, VP2 and VP3. If a new anti-NSP1 serum was available, then co-immunoprecipitation experiments with this serum might be attempted. The availability of an anti-NSP1 serum that did not also specifically precipitate VP2 could be used to confirm the co-immunoprecipitation of VP2 with NSP1. The immunoprecipitation of an *in vitro* translate of total denatured genomic RNA with the anti-NSP1 serum might reveal some interactions between NSP1 and other viral proteins. If the proteins required viral mRNA before they could interact, the study of protein-protein interactions *in vitro* would be complicated by the necessity of adding viral RNA to the protein binding mixture. This could perhaps be achieved by adding a translation inhibitor, such as emetine, to the *in vitro* translated proteins prior to adding viral mRNA for the binding reaction, followed by immunoprecipitation analysis. It would be imperative that the binding conditions were carefully optimised to allow association of the proteins with the viral mRNA, and the achievement of the ideal conditions would clearly be an important factor in the success of the experiment.

The results discussed thus far suggested that the use of infected cell lysates for co-immunoprecipitation experiments might be a more effective way of investigating NSP1 protein-protein interactions. Immunoprecipitation of rotavirus-infected cell lysates with anti-NSP1 serum co-precipitated viral proteins VP1, VP2, VP3/VP4, VP6 and NSP3, suggesting that NSP1 formed a complex with these proteins in the infected cell. Due to the presence of the structural proteins VP2 and VP6, which are associated with the double-layered virus particle, it was suggested that a novel NSP1-containing complex or particle had been precipitated. This complex might be an intermediary in the morphogenesis pathway. Because previous work did not demonstrate direct

protein-protein interactions between NSP1 and these proteins, it was proposed that viral RNA was an essential component of the complex, and immunoprecipitation of nuclease-treated cell lysates suggested that this was indeed the case. The fact that negative results were obtained in protein-protein interaction assays with NSP1 perhaps indicates that it only interacts with mRNA in the complex, hence suggesting that these negative results might be valid. As VP6 has not been shown to have RNA-binding activity, it was proposed that VP6 might interact with another protein, such as VP2, in the complex.

This newly recognised complex was notably different to the RIs described by Gallegos and Patton (1989). In contrast to their data, which demonstrated that NSP1 was not found in the single-shelled RI, in this study NSP1 was found in a complex with VP6. The appearance of NSP1 in a complex with VP6 is not without precedent, as a complex containing NSP1 has been precipitated from RF rotavirus-infected cells using an anti-VP6 mAb (Aponte *et al.*, 1996). This result was confirmed in the present study with a mAb against VP6. The mAb against VP6 precipitated small amounts of NSP1 and the associated complex proteins. Only a relatively small fraction of the total NSP1 and VP6 present in infected cells were found in the complex, and thus it was suggested that this newly recognised complex might be a transient complex with a high turnover rate. In the assembling virus particle NSP1 might be lost as the VP6 layer is added. Further experiments to elucidate the function of this complex would initially require reciprocal immunoprecipitation of NSP1 and the associated complex proteins with specific sera against each protein to confirm the association of each protein with the complex. Immunofluorescence studies could also be performed to assess whether NSP1 co-localised with any of these proteins, and VP6 in particular. Isolation of this complex by gradient fractionation would confirm that the co-immunoprecipitation of VP6 and the associated proteins with NSP1 actually represents a novel NSP1-containing complex or particle. Immunoprecipitation of cross-linked UKtc rotavirus-infected cells could be performed to determine whether viral RNA is associated with the NSP1-containing complex. UKtc rotavirus-infected cells, maintained in the presence of actinomycin D to inhibit cellular transcription and [^{3}H]uridine to label viral RNA products, would be treated with UV light to promote the formation of RNA-protein cross-links, and then immunoprecipitated with specific anti-NSP1 serum to precipitate the complex. Polyacrylamide gel analysis of the immunoprecipitates would determine which

proteins were associated with the labelled viral RNA. Specific digestion with RNases prior to immunoprecipitation would reveal the nature of the RNA associated with the viral protein complex. If the complex could be purified then it would be interesting to determine if it is a functional intermediate in the viral replication cycle by investigating whether it has replicase activity. This could be assayed by dsRNA labelling *in vitro* by the addition of radioactive substrates for RNA synthesis.

A function for NSP1 in regulating translation versus replication of viral mRNA has been proposed (Patton, 1995). If NSP1 bound to the 5'-end of mRNA, it would protect the 5'-end of the mRNA template during replication and prevent translation by blocking attachment of ribosomes. In this manner NSP1 would play a role in the regulation of RNA replication, which indeed is thought to be regulated by factors other than simply the level of mRNAs in the infected cell (Estes, 1996). There is some doubt however as to whether NSP1 has specific RNA-binding activity (Section 1.6.4). Nevertheless, if NSP1 blocked translation by binding mRNA and then remained associated with the replicase complex until completion of dsRNA replication, which occurs concomitantly with the addition of VP6 to the core particle, this would give rise to an intermediate assembly complex similar in composition to the complex described in this study. Although VP3 was proposed to replace NSP1 in binding to the 5'-end of mRNA in the pre-core RI (Patton, 1995), previous research has identified replicase particles containing NSP1 but not VP3 (Helmberger-Jones and Patton, 1986). The binding of VP3 to the 5'-end of ssRNA is more likely to be related to its demonstrated activity as a guanylyltransferase in transcriptase particles. Recent structural data on the *Reoviridae* has indicated that proteins cannot be imported or exported from the core once the inner core protein shell (VP2 in rotavirus) has been completed (Section 1.3.2). The non-structural proteins associated with the pre-core RI must lose all direct contact with the inner core proteins following the assembly of the transcriptase complex (VP1 and VP3), and the addition of the VP2 layer. In this case, NSP3 must be displaced from the 3'-end of mRNA, probably by the RNA polymerase VP1 as previously suggested (Patton, 1995), prior to completion of the VP2 layer. The internal location of VP3 as part of the transcriptase complex within the subcore suggests that it does not displace NSP1, which remains bound to the 5'-end of mRNA. Replication of the dsRNA genome occurs by synthesis of the minus strand on the mRNA template starting at the 3'-end. If replication proceeds by the gradual passage of the mRNA into the subcore through pores at the 5-fold axes, then NSP1 might not

be displaced from the 5'-end until the completion of replication. In this model NSP1 would remain bound to the 5'-end of mRNA as it is reeled into the transcription complex for replication, and would only be displaced as the final stretch of mRNA disappeared into the subcore of the virus particle. As replication and morphogenesis are concomitant processes, addition of the VP6 layer would occur during replication and before NSP1 dissociates from the 5'-end of mRNA and is lost from the particle. It has also been demonstrated that NSP1 interacts with NSP2 and NSP5, both of which are found associated with the core and VP6 RIs in the viroplasm (Gonzalez *et al.*, 1998). This lends further support to the theory that NSP1 remains associated with the assembling virus particle until the final stages of replication and after VP6 is added to the core particle. Such a role for NSP1 in regulating replication might explain why viruses carrying mutant NSP1 are viable, since replication would still proceed, albeit not at an optimal level.

One of the most puzzling questions in the replication of the segmented dsRNA viruses is the mechanism by which the genome is packaged. Unlike the negative-stranded RNA viruses, these viruses do not contain a nucleoprotein that packages the genome, hence the details of the process are still in debate. It has been proposed that NSP1, perhaps in association with NSP3, might have a function in the selective assortment of the genome (Brottier *et al.*, 1992), since both proteins bind ssRNA and are found in early replication complexes. However, the non-specific RNA-binding activity of NSP1 does not immediately suggest a mechanism for selective packaging of viral mRNAs. The mechanism of viral mRNA assortment in the closely related reovirus has not yet been elucidated, although the non-structural proteins σNS and μNS of reovirus have been implicated (Section 2.1.2). Alternatively, NSP1 may play a role in transporting the viral mRNA to the viroplasm for replication, possibly in association with a cytoskeletal element since NSP1 is known to be associated with the cytoskeleton. NSP1 would then be displaced from the ensuing replication complex at some point during replication and morphogenesis of the virus particle.

The availability of a gene rescue system for dsRNA viruses would generate a resurgence in the field of rotavirus research. A reverse genetics system would allow structure-function studies of viral genes and their corresponding protein products in the context of the infectious virus. For example, studies could be made of the effect of

non-structural protein mutants on replication and transcription. The characterisation of *trans*-acting elements and domains in specific viral proteins necessary for replication and packaging of viral RNA segments could be attempted. *Cis*-acting packaging signals in viral mRNA might also be identified. Clearly, the development of such a system would considerably enhance the prospect of providing answers to the major questions still remaining in the replication cycles of these viruses.

Bibliography

9.1 Bibliography

Acs, G., Klett, H., Schonberg, M., Christman, J., Levin, D. H. and Silverstein, J. C. (1971). Mechanism of reovirus double-stranded RNA synthesis in vivo and in vitro. *J. Virol.* **8**, 684-689.

Afrikanova, I., Fabbretti, E., Miozzo, M. C. and Burrone, O. R. (1998). Rotavirus NSP5 phosphorylation is up-regulated by interaction with NSP2. *J. Gen. Virol.* **79**, 2679-2686.

Altenburg, B. C., Graham, D. Y. and Estes, M. K. (1980). Ultrastructural study of rotavirus replication in cultured cells. *J. Gen. Virol.* **46**, 75-85.

Anderson, N. and Doane, F. W. (1966). An electron microscope study of reovirus type 2 in L cells. *J. Path. Bact.* **92**, 433-439.

Andrew, M. E., Boyle, D. B., Coupar, B. E. H., Whitfeld, P. L., Both, G. W. and Bellamy, A. R. (1987). Vaccinia virus recombinants expressing the SA11 rotavirus VP7 glycoprotein gene induce serotype specific neutralising antibodies. *J. Virol.* **61**, 1054-1060.

Andrew, M. E., Boyle, D. B., Whitfeld, P. L., Lockett, L. J., Anthony, I. D., Bellamy, A. R. and Both, G. W. (1990). The immunogenicity of VP7, a rotavirus antigen resident in the endoplasmic reticulum, is enhanced by cell surface expression. *J. Virol.* **64**, 4776-4783.

Antczak, J. B. and Joklik, W. K. (1992). Reovirus genome segment assortment into progeny genomes studied by the use of monoclonal antibodies directed against reovirus proteins. *Virology* **187**, 760-776.

Aponte, C., Poncet, D. and Cohen, J. (1996). Recovery and characterization of a replicase complex in rotavirus-infected cells by using a monoclonal antibody against NSP2. *J. Virol.* **70**, 985-991.

Au, K.-S., Chan, W.-K. and Estes, M. K. (1989). Receptor activity of rotavirus nonstructural glycoprotein NS28. *J. Virol.* **63**, 4553-4562.

Au, K.-S., Mattion, N. M. and Estes, M. K. (1993). A subviral particle binding domain on the rotavirus nonstructural glycoprotein NS28. *Virology* **194**, 665-673.

Ausubel, F. M., Brent, R., Kingston, R. E., Moore, D. O., Seidman, J. G., Smith, J. A. and Struhl, K. (1996). Current protocols in molecular biology. Chichester: John Wiley & Sons, Inc.

Ball, J. M., Tian, P., Zeng, C. Q.-Y., Morris, A. P. and Estes, M. K. (1996). Age-dependent diarrhea induced by a rotaviral nonstructural glcoprotein. *Science* **272**, 101-104.

Banerjee, A. K. and Shatkin, A. J. (1970). Transcription *in vitro* by reovirus-associated ribonucleic acid dependent polymerase. *J. Virol.* **6**, 1-11.

Barry, R. D., Ives, D. R. and Cruikshank, J. G. (1962). Participation of deoxyribonucleic acid in the multiplication of influenza virus. *Nature* **194**, 1139-1140.

Bartel, P. L., Chien, C. T., Sternglanz, R. and Fields, S. (1993). Using the two-hybrid system to detect protein-protein interactions. In *Cellular interactions in development : A practical approach,* pp 153-179. Edited by D. A. Hartley, Oxford: Oxford University Press.

Bartlett, N. M., Gillies, S. C., Bullivant, S., and Bellamy, A. R. (1974). Electron microscopy study of reovirus reaction cores. *J. Virol.* **14**, 315-326.

Bastardo, J. W. and Holmes, I. H. (1980). Attachment of SA-11 rotavirus to erythrocyte receptors. *Infect. Immun.* **29**, 1134-1140.

Beards, G. M., Desselberger, U. and Flewett, T. H. (1989). Temporal and geographical distributions of human rotavirus serotypes, 1983 to 1988. *J. Clin. Microbiol.* **27**, 2827-2833.

Beranger, F., Aresta, S., de Gunzburg, J. and Camonis, J. (1997). Getting more from the two-hybrid system: N-terminal fusions to LexA are efficient and sensitive baits for two-hybrid studies. *Nucleic Acid Res.* **25**, 2035-2036.

Berg, J. M. (1990). Zinc fingers and other metal-binding domains. *J. Biol. Chem.* **265**, 6513-6516.

Bern, C., Martines, J., de Zoysa, I. and Glass, R. I. (1992). The magnitude of the global problem of diarrhoeal disease: a ten year update. *Bull. WHO.* **70**, 705-714.

Bican, P., Cohen, J., Charpilienne, A. and Scherrer, R. (1982). Purification and characterisation of bovine rotavirus cores. *J. Virol.* **43**, 1113-1117.

Bishop, R. F., Barnes, G. L., Cipriani, E. and Lund, J. S. (1983). Clinical immunity after neonatal rotavirus infection: a prospective longitudinal study in young children. *N. Engl. J. Med.* **309**, 72-76.

Bishop, R. F., Davidson, G. P., Holmes, I. H. and Ruck, B. J. (1973). Virus particles in epithelial cells of duodenal mucosa from children with viral gastroenteritis. *Lancet* **2**, 1281-1283.

Bishop, R. F., Davidson, G. P., Holmes, I. H. and Ruck, B. J. (1974). Detection of a new virus by electron microscopy of fecal extracts from children with acute gastroenteritis. *Lancet* **1**, 149-151.

Black, E. P., Moussatche, N. and Condit, R. C. (1998). Characterization of the interactions among vaccinia virus transcription factors G2R, A18R, and H5R. *Virology* **245**, 313-322.

Blackhall, J., Fuentes, A., Hansen, K. and Magnusson, G. (1997). Serine protein kinase activity associated with rotavirus phosphoprotein NSP5. *J. Virol.* **71**, 138-144.

Blackhall, J., Munoz, M., Fuentes, A. and Magnusson, G. (1998). Analysis of rotavirus nonstructural protein NSP5 phosphorylation. *J. Virol.* **72**, 6398-6405.

Bodkin, D. K. and Fields, B. N. (1989). Growth of reovirus in intestinal tissue: role of the L2 and S1 genes. *J. Virol.* **63**, 1188-1193.

Borsa, J., Sargent, M. D., Lievaart, P.A. and Copps, T. P. (1981). Reovirus: evidence for a second step in the intracellular uncoating and transcriptase activation process. *Virology* **111**, 191-200.

Both, G. W., Lockett, L. J., Janardhana, V., Edwards, S. J., Bellamy, A. R., Graham, F. L., Prevec, L. and Andrew, M. E. (1993). Protective immunity to rotavirus-induced diarrhoea is passively transferred to newborn mice from naive dams vaccinated with a single dose of a recombinant adenovirus expressing rotavirus VP7sc. *Virology* **193**, 940-950.

Bouloy, M., Plotch, S. J. and Krug, R. M. (1978). Globin mRNAs are primers for the transcription of influenza viral RNA *in vitro*. *Proc. Natl. Acad. Sci. USA* **75**, 4886-4890.

Boyle, J. F. and Holmes, K. V. (1986). RNA-binding proteins of bovine rotavirus. *J. Virol.* **58**, 561-568.

Brent, R. and Ptashne, M. (1985). A eukaryotic transcriptional activator bearing the DNA specificity of a prokaryotic repressor. *Cell* **43**, 729-736.

Bridger, J. C., Dhaliwal, W., Adamson, M. J. V. and Howard, C. R. (1998). Determinants of rotavirus host range restriction - A heterologous bovine NSP1 gene does not affect replication kinetics in the pig. *Virology* **245**, 47-52.

Bridger, J. C., Pedley, S. and McCrae, M. A. (1986). Group C rotaviruses in humans. *J. Clin. Microbiol.* **23**, 760-763.

Brookes, S. M., Hyatt, A. D., and Eaton, B. T. (1993). Characterization of virus inclusion bodies in bluetongue virus-infected cells. *J. Gen. Virol.* **74**, 525-530.

Broome, R. L., Vo, P. T., Ward, R. L., Clark, H. F. and Greenberg, H. B. (1993). Murine rotavirus genes encoding outer capsid proteins VP4 and VP7 are not major determinants of host range restriction and virulence. *J. Virol.* **67**, 2448-2455.

Brottier, P., Nandi, P., Bremont, M. and Cohen, J. (1992). Bovine rotavirus segment 5 protein expressed in the baculovirus system interacts with zinc and RNA. *J. Gen. Virol.* **73**, 1931-1938.

Browne, J. G. and Jochim, M. M. (1967). Cytopathologic changes and development of inclusion bodies in cultured cells infected with bluetongue virus. *Am. J. Vet. Res.* **28**, 1091-1105.

Butcher, S. J., Dokland, T., Ojala, D. M., Namford, D. H., and Fuller, S. D. (1997). Intermediates in the assembly pathway of the double-stranded RNA virus ϕ6. *EMBO J.* **16**, 4477-4487.

Calvert, J. G., Nagy, E., Soler, M. and Dobos, P. (1991). Characterization of the VPg-dsRNA linkage of infectious pancreatic necrosis virus. *J. Gen. Virol.* **2**, 2563-2567.

Chan, W. K., Au, K. S. and Estes, M. K. (1988). Topography of the simian rotavirus non-structural glcoprotein (NS28) in the endoplasmic reticulum membrane. *Virology* **164**, 435-442.

Chen, C. M., Hung, T., Bridger, J. C. and McCrae, M. A. (1985). Chinese adult rotavirus is a group B rotavirus. *Lancet* **2**, 1123-1124.

Chen, D. Y., Luongo, C. L., Nibert, M. L. and Patton, J. T. (1999). Rotavirus open cores catalyze 5'-capping and methylation of exogenous RNA: Evidence that VP3 is a methyltransferase. *Virology* **265**, 120-130.

Chen, D. and Patton, J. T. (1998). Rotavirus RNA replication requires a single-stranded 3'end for efficient minus-strand synthesis. *J. Virol.* **72**, 7387-7396.

Chen, D., Zeng, C. Q.-Y., Wentz, M. J., Gorziglia, M., Estes, M. K. and Ramig, R. F. (1994). Template-dependent , *in vitro* replication of rotavirus RNA. *J. Virol.* **68**, 7030-7039.

Chen, G., Fan, R., Guox, X. and Hung, T. (1988). Group C rotavirus found in sporadic diarrhoea in China. *J. Exp. Virol.* **2**, 1-3.

Chen, S. C., Fynan, E. F., L., R. H., Lu, S., Greenberg, H. B., Santoro, J. C. and Herrmann, J. F. (1997). Protective immunity induced by rotavirus DNA vaccines. *Vaccine* **15**, 899-902.

Cheng, R. H., Caston, J. R., Wang, G-J., Gu, F., Smith, T. J., Baker, T. S., Bozarth, R. F., Trus, B. L., Cheng, N., Wickner, R. B., and Steven, A. C. (1994). Fungal virus capsids, cytoplasmic compartments for the replication of double-stranded RNA, formed as icosahedral shells of asymmetric gag dimers. *J. Mol. Biol.* **244**, 255-258.

Chien, C. T., Bartel, P. L., Sternglanz, R. and Fields, S. (1991). The two-hybrid system: A method to identify and clone genes for proteins that interact with a protein of interest. *Proc. Natl. Acad. Sci. USA* **88**, 9578-9582.

Ciarlet, M. and Estes, M. K. (1999). Human and most animal rotavirus strains do not require the presence of sialic acid on the cell surface for efficient infectivity. *J. Gen. Virol.* **80**, 943-948.

Clark, S. M., Roth, J. R., Clark, M. L., Barnett, B. B. and Spendlove, R. S. (1981). Trypsin enhancement of rotavirus infectivity: mechanism of enhancement. *J. Virol.* **39**, 816-822.

Clark, S. M., Spendlove, R. S. and Barnett, B. B. (1980). Role of two particle types in bovine rotavirus morphogenesis. *J. Virol.* **34**, 272-276.

Clarke, I. M. and McCrae, M. A. (1983). The molecular biology of rotaviruses. VI. RNA species-specific terminal conservation in rotaviruses. *J. Gen. Virol.* **64**, 1877-1884.

Cleveland, D. W., Zarbl, H. and Millward, S. (1986). Reovirus guanylyltransferase is L2 gene product lambda 2. *J. Virol.* **60**, 307-311.

Cohen, J. (1977). Ribonucleic acid polymerase activity associated with purified calf rotavirus. *J. Gen. Virol.* **36**, 395-402.

Cohen, J., Charpilienne, A., Chilmonczyk, S. and Estes, M. K. (1989). Nucleotide sequence of bovine rotavirus gene 1 and expression of the gene product in baculovirus. *Virology* **171**, 131-140.

Cong, P. and Shuman, S. (1993). Covalent catalysis in nucleotidyl transfer. A KTDG motif essential for enzyme-GMP complex formation by mRNA capping enzyme is conserved at the active sites of RNA and DNA ligases. *J. Biol. Chem.* **268**, 7256-7260.

Connor, M. E., Zarley, C. D., Hu, B., Parsons, S., D., D., Greiner, S., Smith, R., Jiang, B., Corsaro, B., Barniak, V., Madore, H. P., Crawford, S. and Estes, M. K. (1996). Virus-like particles as a rotavirus subunit vaccine. *J. Infect. Dis.* **174**, 88-92.

Coulson, B. S., Londrigan, S. L. and Lee, D. J. (1997). Rotavirus contains integrin ligand sequences and a distintegrin-like domain that are implicated in virus entry into cells. *Proc. Natl. Acad, Sci. USA* **94**, 5389-5394.

Crawford, S. E., Labbe, M., Cohen, J., Burroughs, M. H., Zhou, Y. and Estes, M. K. (1994). Characterisation of virus-like particles produced by the expression of rotavirus capsid proteins in insect cells. *J. Virol.* **68**, 5945-5952.

Cuconati, A., Xiang, W., Lahser, F., Pfister, T. and Wimmer, E. (1998). A protein linkage map of the P2 nonstructural proteins of poliovirus. *J. Virol.* **72**, 1297-1307.

Dalton, S. and Treisman, R. (1992). Characterization of SAP-1, a protein recruited by serum response factor to the c-fos serum response element. *Cell* **68**, 597-612.

Dang, C. V., Barrett, J., Villa-Garcia, M., Resar, L. M. S., Kato, G. and Fearon, E. R. (1991). Intracellular leucine zipper interactions suggest c-myc hetero-oligomerisation. *Mol. and Cell. Biol.* **11**, 954-962.

Davidson, G. P., Townley, R. R. W., Bishop, R. F., Holmes, I. H. and Ruck, B. J. (1975). Importance of a new virus in acute sporadic enteritis in children. *Lancet* **I**, 242-245.

DeHaas, F., Paatero, A. O., Mindich, L., Bamford, D. H. and Fuller, S. D. (1999). A symmetry mismatch at the site of RNA packaging in the polymerase complex of dsRNA bacteriophage ϕ6. *J. Mol. Biol.* **294**, 357-372.

Denisova, E., Dowling, W., LaMonica, R., Shaw, R., Scarlata, S., Ruggeri, F. and Mackow, E. R. (1999). Rotavirus capsid protein VP5* permeabilizes membranes. *J. Virol.* **73**, 3147-3153.

Desselberger, U. and McCrae, M. A. (1994). The rotavirus genome. In *Rotaviruses*, pp. 31-66. Edited by R. F. Ramig. Berlin: Springer-Verlag.

Dobos, P. (1995). Protein primed RNA synthesis *in vitro* by the virion associated RNA polymerase of infectious pancreatic necrosis virus. *Virology* **208**, 19-25.

Dormitzer, P. R. and Greenberg, H. B. (1992). Calcium chelation induces a conformational change in recombinant herpes simplex virus-I-expressed rotavirus VP7. *Virology* **189**, 828-832.

Dryden, K. A., Farsetta, D. L., Wang, G., Keegan, J. M., Fields, B. N., Baker, T. S. and Nibert, M. L. (1998). Internal structures containing transcriptase-related proteins in top component particles of mammalian orthoreovirus. *Virology* **245**, 33-46.

Dryden, K. A., Wang, G., Yeager, M., Nibert, M. L., Coombs, K. M., Furlong, D. B., Fields, B. N. and Baker, T. S. (1993). Early steps in reovirus infection are associated with dramatic changes in supramolecular structure and protein conformation: analysis of virions and subviral particles by cryoelectron microscopy and image reconstruction. *J. Cell Biol.* **122**, 1023-1041.

Dunn, S. J., Cross, T. L. and Greenberg, H. B. (1994). Comparison of the rotavirus nonstructural protein NSP1 (NS53) from different species by sequence analysis and northern blot hybridization. *Virology* **203**, 178-183.

Dyall-Smith, M. L., Azad, A. A. and Holmes, I. H. (1983). Gene mapping of rotavirus double-stranded RNA segments by northern blot hybridization: application to segments 7, 8 and 9. *J. Virol.* **46**, 317-320.

Eaton, B. T., Hyatt, A. D. and Brookes, S. M. (1990). The replication of bluetongue virus. *Curr. Topics Microbiol. Immunol.* **162**, 89-118.

Ehrenfeld, E., ed. (1993). Translational regulation. *Semin. Virology* **4**, 1-268.

Eley, S. M., Gardner, R., Molyneux, D. H. and Moore, N. F. (1987). A reovirus from the bedbug, Cimex lectularius. *J. Gen. Virol.* **68**, 195-198.

Enami, M., Sharma, G., Benham, C. and Palese, P. (1991). An influenza virus containing 9 different RNA segments. *Virology* **185**, 291-298.

Ericson, B. L., Graham, D. Y., Mason, B. B. and Estes, M. K. (1982). Identification, synthesis, and modifications of simian rotavirus SA11 polypeptides in infected cells. *J. Virol.* **42**, 825-839.

Ericson, B. L., Graham, D. Y., Mason, B. B., Hanssen, H. H. and Estes, M. K. (1983). Two types of glycoprotein precursors are produced by the simian rotavirus SA11. *Virology* **127**, 320-332.

Estes, M. K. (1996). Rotaviruses and their replication. In *Fields Virology*, 3rd edn, pp. 1625-1655. Edited by B. N. Fields, D. M. Knipe, P. M. Howley, *et al.*. Philadelphia: Lippincott-Raven Publishers.

Estes, M. K., Crawford, S. E., Penaranda, M. E., *et al.* (1987). Synthesis and immunogenicity of the rotavirus major capsid antigen using a baculovirus expression system. *J. Virol.* **61**, 1488-1494.

Estes, M. K., Graham, D. Y., Smith, E. M. and Gerba, C. P. (1979). Rotavirus stability and inactivation. *J. Gen. Virol.* **43**, 403-409.

Estes, M. K., Palmer, E. L. and Obijeski, J. F. (1983). Rotaviruses: a review. *Curr. Topics Microbiol. Immunol.* **105**, 123-184.

Estojak, J., Brent, R. and Golemis, E. A. (1995). Correlation of two-hybrid affinity data with in vitro measurements. *Mol. and Cell. Biol.* **15**, 5820-5829.

Fabbretti, E., Afrikanova, I., Vascotto, F. and Burrone, O. R. (1999). Two non-structural rotavirus proteins, NSP2 and NSP5, form viroplasm-like structures in vivo. *J. Gen. Virol.* **80**, 333-339.

Fearon, E. R., Finkel, T., Gillison, M. L., Kennedy, S. P., Casella, J. F., Tomaselli, G. F., Morrow, J. S. and Dang, C. V. (1992). Karyoplasmic interaction selection strategy: A general strategy to detect protein-protein interactions in mammalian cells. *Proc. Natl. Acad. Sci. USA* **89**, 7958-7962.

Fields, S. and Song, O.-K. (1989). A novel genetic system to detect protein-protein interactions. *Nature* **340**, 245-246.

Fields, S. and Sternglanz, R. (1994). The two-hybrid system: an assay for protein-protein interactions. *Trends Genet.* **10**, 286-292.

Flewett, T. H., Bryden, A. S. and Davies, H. (1973). Virus particles in gastroenteritis. *Lancet* **2**, 1497.

Flewett, T. H., Bryden, A. S., Davies, H., Woode, G. N., Bridger, J. C. and Derrick, J. M. (1974). Relationship between virus from acute gastroenteritis of children and newborn calves. *Lancet* **2**, 61-63.

Frankel, A. D., Bredt, D. S. and Pabo, C. O. (1988). Tat protein from human immunodeficiency virus forms a metal-linked dimer. *Science* **240**, 70-73.

Fukudome, K., Yoshie, O. and Konno, T. (1989). Comparison of human, simian, and bovine rotaviuses for requirement of sialic acid in hemagglutination and cell adsorption. *Virology* **172**, 196-205.

Fukuhara, N., Nishikawa, K., Gorziglia, M. and Kapikian, A. Z. (1989). Nucleotide sequence of gene segment 1 of a porcine rotavirus strain. *Virology* **173**, 743-749.

Fukuhara, N., Yoshie, O., Kitaoka, S. and Konno, T. (1988). Role of VP3 in human rotavirus internalization after target cell attachment via VP7. *J. Virol.* **62**, 2209-2218.

Furuichi, Y., Morgan, M. A., Muthukrishnan, S. and Shatkin, A. J. (1975). Reovirus messenger RNA contains a methylated, blocked 5' terminal structure: m7GpppGmC. *Proc. Natl. Acad. Sci. USA* **72**, 362-366.

Furuichi, Y., Muthukrishnan, S., Tomasz, J. and Shatkin, A. J. (1976). Mechanism of formation of reovirus mRNA 5'-terminal blocked and methylated sequence M^7GpppG^mpC. *J. Biol. Chem.* **251**, 5043-5053.

Gallegos, C. O. and Patton, J. T. (1989). Characterization of Rotavirus Replication Intermediates: A Model for the Assembly of Single-Shelled Particles. *Virology* **172**, 616-627.

Gillian, A. L. and Nibert, M. L. (1998). Amino terminus of reovirus nonstructural protein σNS is important for ssRNA binding and nucleoprotein complex formation. *Virology* **240**, 1-11.

Glass, R. I., Gentsch, J. and Smith, J. C. (1994). Rotavirus vaccines: success by reassortment? *Science* **265**, 1389-1391.

Glass, R. I., Lang, D. R., Ivanoff, B. N. and Compans, R. W. (1996). Introduction: Rotavirus - from basic research to a vaccine. *J. Infect. Dis.* **174 (S1)**, S1-S2.

Glass, R. I., Lew, J. F., Gangarosa, R. E., Lebaron, C. W. and Ho, M. S. (1991). Estimates of the morbidity and mortality from diarrhoeal diseases in American children. *J. Paediatr.* **118**, S27-S33.

Gomatos, P. J., Prakash, O. and Stamatos, N. M. (1981). Small reovirus particles composed solely of sigma NS with specificity for binding different nucleic acids. *J. Virol.* **39**, 115-124.

Gomatos, P. J., Tamm, I., Dales, S. and Franklin, R. M. (1962). Reovirus type 3: physical characteristics and interactions with L cells. *Virology* **17**, 441-454.

Gombold, J. L., Estes, M. K. and Ramig, R. F. (1985). Assignment of simian rotavirus SA11 temperature-sensitive mutant groups B and E to genome segments. *Virology* **143**, 309-320.

Gombold, J. L. and Ramig, R. F. (1986). Analysis of reassortment of genome segments in mice mixedly infected with rotavirus SA11 and RRV. *J. Virol.* **57**, 110-116.

Gombold, J. L. and Ramig, R. F. (1987). Assignment of simian rotavirus SA11 temperature-sensitive mutant groups A, C, F, and G to genome segments. *Virology* **161**, 463-473.

Gomez-Puertas, P., Mena, I., Castillo, M., Vivo, A., Perez-Pastrana, E. and Portela, A. (1999). Efficient formation of influenza virus-like particles: dependence on the expression of viral proteins. *J. Gen. Virol.* **80**, 1635-1645.

González, R. A., Torres-Vega, M. A., López, S. and Arias, C. F. (1998). In vivo interactions among rotavirus nonstructural proteins. *Arch. Virol.* **143**, 981-996.

Gorziglia, M., Nishikawa, K. and Fukuhara, N. (1989). Evidence of duplication and deletion in super short segment 11 of rabbit rotavirus Alabama strain. *Virology* **170**, 587-590.

Gottlieb, P., Qiao, X., Strassman, J., Frilander, M. and Mindich, L. (1994). Identification of the packaging regions within the genomic RNA segments of bacteriophage ϕ6. *Virology* **200**, 42-47.

Gouet, P., Diprose, J. M., Grimes, J. M., Malby, R., Burroughs, J. N., Zientara, S., Stuart, D. I. and Mertens, P. P. C. (1999). The highly ordered double-stranded RNA genome of bluetongue virus revealed by crystallography. *Cell* **97**, 481-490.

Green, K. Y., Midthun, K., Gorziglia, M., Hoshino, Y., Kapikian, A. Z., Chanock, R. M. and Flores, J. (1987). Comparison of the amino acid sequences of the major neutralization protein of four human rotavirus serotypes. *Virology* **161**, 153-159.

Greenberg, H. B., Kalica, A. R., Wyatt, R. W., Jones, R. W., Kapikian, A. Z. and Chanock, R. M. (1981). Rescue of non-cultivable human rotavirus by gene reassortant during mixed infection with ts mutants of a cultivable bovine rotavirus. *Proc. Natl. Acad. Sci. USA* **78**, 420-424.

Greenberg, H. B., McAuliffe, V., Valdesuso, J., Wyatt, R., Flores, J., Kalica, A., Hoshino, Y. and Singh, N. H. (1983). Serological analysis of the subgroup protein of rotavirus, using monoclonal antibodies. *Infect. Immun.* **39**, 91-99.

Greenberg, H. B., Valdesuso, J., VanWyke, K., Midthun, K., Walsh, M., McAuliffe, V., Wyatt, R. G., Kalica, A. R., Flores, J. and Hoshino, Y. (1983). Production and preliminary characterisation of monoclonal antibodies directed at two surface proteins of rhesus rotavirus. *J. Virol.* **47**, 267-275.

Grimes, J. M., Burroughs, J. N., Gouet, P., Diprose, J. M., Malby, R., Zientras, S., Mertens, P. P. C. and Stuart, D. I. (1998). The atomic structure of the bluetongue virus core. *Nature* **395**, 470-478.

Grimes, J. M., Jakana, J., Ghosh, M., Basak, A. K., Roy, P., Chiu, W., Stuart, D. I. and Prasad, B. V. V. (1997). An atomic model of the outer layer of the bluetongue virus core derived from X-ray crystallography and electron cryomicroscopy. *Structure* **5**, 885-893.

Grunstein, M. and Hogness, D. S. (1975). Colony hybridization: A method for the isolation of cloned DNAs that contain a specific gene. *Proc. Natl. Acad. Sci. USA* **72**, 3961-3965.

Guerrant, R. L., Hughes, J. M., Lima, N. L. and Crane, J. (1990). Diarrhoea in developed and developing countries: magnitude, special settings, and etiologies. *Rev. Infect. Dis.* **12**, S41-S50.

Heath, R. R., Stagg, S., Xu, F. and McCrae, M. A. (1997). Mapping of the target antigens of the rotavirus-specific cytotoxic T cell response. *J. Gen. Virol.* **78**, 1065-1075.

Helmberger-Jones, M. and Patton, J. T. (1986). Characterization of subviral particles in cells infected with simian rotavirus SA11. *Virology* **155**, 655-665.

Herrmann, J. E., Chen, S. C., Fynan, E. F., Santoro, J. C., Greenberg, H. B., Wang, S. and Robinson, H. L. (1996). Protection against rotavirus infection by DNA vaccination. *J. Infect. Dis.* **174**, 93-97.

Hewish, M. J., Takada, Y. and Coulson, B. S. (2000). Integrins $\alpha 2\beta 1$ and $\alpha 4\beta 1$ can mediate SA11 rotavirus attachment and entry into cells. *J. Virol.* **74**, 228-236.

Hill, C. L., Booth, T. F., Prasad, B. V. V., Grimes, J. M., Mertens, P. P. C., Sutton, G. C., and Stuart, D. I. (1999). The structure of a cypovirus and the functional organisation of dsRNA viruses. *Nature Struct. Biol.* **6**, 565-568.

Ho, M.-S., Glass, R. I., Pinsky, P. F. and Anderson, L. J. (1988). Rotavirus as a cause of diarrhoeal morbidity and mortality in the United States. *J. Infect. Dis.* **158**, 1112-1116.

Hopps, H. E., *et al.* (1963). Biologic characteristics of the continuous kidney cell line derived from the African green monkey. *J. Immunol.* **91**, 416-424.

Hoshino, Y., Gorziglia, M., Valdesuso, J., Askaa, J., Glass, R. I. and Kapikian, A. Z. (1987). An equine rotavirus (FI-14 strain) which bears both subgroup I and subgroup II specificities on its VP6. *Virology* **157**, 488-496.

Hoshino, Y. and Kapikian, A. Z. (1994). Rotavirus antigens. In *Rotaviruses*, pp. 179-227. Edited by F. R. Ramig. Berlin: Springer-Verlag.

Hoshino, Y. and Kapikian, A. Z. (1996). Classification of rotavirus VP4 and VP7 serotypes. *Arch. Virol.* **S12**, 99-111.

Hoshino, Y., Saif, L. J., Kang, S.-Y., Sereno, M. M., Chen, W.-K. and Kapikian, A. Z. (1995). Identification of group A rotavirus genes associated with virulence of a porcine rotavirus and host range restriction of a human rotavirus in the gnotobiotic piglet model. *Virology* **209**, 274-280.

Hoshino, Y., Wyatt, R. G., Greenberg, H. B., Flores, J., Kapikian, A. Z. (1984). Serotypic similarity and diversity of rotaviruses of mammalian and avain origin as studied by plaque reduction neutralization. *J. Infect. Dis.* **149**, 694-702.

Hua, J., Chen, X. and Patton, J. T. (1994). Deletion mapping of the rotavirus metalloprotein NS53 (NSP1): the conserved cysteine-rich region is essential for virus specific RNA-binding. *J. Virol.* **68**, 3990-4000.

Hua, J., Mansell, E. A. and Patton, J. T. (1993). Comparative analysis of the rotavirus NS53 gene: Conservation of basic and cysteine-rich regions in the protein and possible stem-loop structures in the RNA. *Virology* **196**, 372-378.

Hua, J. and Patton, J. T. (1994). The carboxyl-half of the rotavirus nonstructural protein NS53 (NSP1) is not required for virus replication. *Virology* **198**, 567-576.

Huang, T. S., Palese, P. and Krystal, M. (1990). Determination of influenza virus proteins required for genome replication. *J. Virol.* **64**, 5669-5673.

Huismans, H. and Joklik, W. K. (1976). Reovirus-coded polypeptides in infected cells: isolation of two native monomeric polypeptides with high affinity for single-stranded and double-stranded RNA, respectively. *Virology* **70**, 411-424.

Huismans, H., van Dijk, A. A. and Els, H. J. (1987). Uncoating of parental bluetongue virus to core and subcore particles in infected L cells. *Virology* **157**, 180-188.

Hundley, F., McIntyre, M., Clark, B., Beards, G., Wood, D., Chrystie, I. and Desselberger, U. (1987). Heterogeneity of genome rearrangements in rotaviruses isolated from a chronically infected immunodeficient child. *J. Virol.* **61**, 3365-3372.

Hung, T., Chen, G., Wang, C., *et al.* (1987). Seroepidemiology and molecular biology of the Chinese rotavirus. *Ciba. Found. Symp.* **128**, 49-62.

Hyatt, A. D. and Eaton, B. T. (1988). Ultrastructural distribution of the major capsid proteins within bluetongue virus and infected cells. *J. Gen. Virol.* **69**, 805-815.

Hyatt, A. D., Eaton, B. T. and Lunt, R. (1987). The grid-cell-culture-technique: the direct examination of virus-infected cells and progeny viruses. *J. Microsec.* **145**, 97-106.

Hyatt, A. D., Gould, A. R., Coupar, B. and Eaton, B. T. (1991). Localization of the non-structural protein NS3 in bluetongue virus-infected cells. *J. Gen. Virol.* **72**, 2263-2267.

Ijaz, M. K., Alkarmi, T. O., El-Mekki, A. W., Galadari, S. H. I., Dar, F. K. and Babiuk, L. A. (1995). Priming and induction of anti-rotavirus antibody response by synthetic peptides derived from VP7 and VP4. *Vaccine* **13**, 331-338.

Imai, M., Akatani, K., Ikegami, N. and Furuichi, Y. (1983). Capped and conserved terminal structures in human rotavirus genome double-stranded RNA segments. *J. Virol.* **47**, 125-136.

Institute of Medicine (1985). New vaccine development, establishing priorities, vol. 1. Washington DC: National Academic Press.

Iwabuchi, K., Li, B., Bartel, P. and Fields, S. (1993). Use of the two-hybrid system to identify the domain of p53 involved in oligomerization. *Oncogene* **8**, 1693-1696.

Johnson, M. A. and McCrae, M. A. (1989). Molecular Biology of Rotaviruses VIII. Quantitative analysis of regulation of gene expression during virus replication. *J. Virol.* **63**(5), 2048-2055.

Joklik, W. K. (1983). The reovirus particle. In *The Reoviridae*, pp. 9-78. Edited by W. K. Joklik. New York: Plenum Press.

Joklik, W. K. and Roner, M. R. (1995). What reassorts when reovirus genome segments reassort? *J. Biol. Chem.* **270**, 4181-4184.

Kabcenell, A. K. and Atkinson, P. H. (1985). Processing of the rough endoplasmic reticulum membrane glcoproteins of rotavirus SA11. *J. Cell Biol.* **101**, 1270-1280.

Kabcenell, A. K., Poruchynsky, M. S., Bellamy, A. R., Greenberg, H. B. and Atkinson, P. H. (1988). Two forms of VP7 are involved in assembly of SA11 rotavirus in endoplasmic reticulum. *J. Virol.* **62**, 2929-2941.

Kaijot, K. T., Shaw, R. D., Rubin, D. H. and Greenberg, H. B. (1988). Infectious rotavirus enters cells by direct cell membrane penetration, not by endocytosis. *J. Virol.* **62**, 1136-1144.

Kalica, A. R., Flores, J. and Greenberg, H. B. (1983). Identification of the rotaviral gene that codes for haemagglutinin and protease-enhanced plaque formation. *Virology* **125**, 194-205.

Kalica, A. R., Purcell, R. H., Sereno, M. M., Wyatt, R. G., Kim, H. W., Chanock, R. M. and Kapikian, A. Z. (1977). A microtiter solid phase radioimmunoassay for detection of the human reovirus-like agent in stools. *J. Immunol.* **118**, 1275-1279.

Kapikian, A. Z. and Chanock, R. M. (1996). Rotaviruses. In *Fields Virology*, 3rd edn, pp. 1657-1708. Edited by B. N. Fields, D. M. Knipe, P. M. Howley, *et al.*. Philadelphia: Lippincott-Raven Publishers.

Kapikian, A. Z., Cline, W. L., Kim, H. W., *et al.* (1976). Antigenic relationships among five reovirus-like (RVL) agents by complement fixation (CF) and development of a new substitute CF antigen for the human RVL agent of infantile gastroenteritis. *Proc. Soc. Exp. Biol. Med.* **152**, 535-539.

Kapikian, A. Z., Kim, H. W., Wyatt, R. G., *et al.* (1974). Reovirus-like agent in stools: association with infantile diarrhoea and development of serologic tests. *Science* **185**, 1049-1053.

Kapikian, A. Z., Wyatt, R. G., Dolin, R., Thornhill, T. S., Kalica, A. R. and Chanock, R. M. (1972). Visualization by immune electron microscopy of a 27 nm particle associated with acute infectious non-bacterial gastroenteritis. *J. Virol.* **10**, 1075-1081.

Kattoura, M. D., Chen, X. and Patton, J. T. (1994). The rotavirus RNA-binding protein NS35 (NSP2) forms 10S multimers and interacts with the viral RNA polymerase. *Virology* **202**, 803-813.

Kattoura, M. D., Clapp, L. L. and Patton, J. T. (1992). The rotavirus nonstructural protein, NS35, possesses RNA-binding activity *in vitro* and *in vivo*. *Virology* **191**, 698-708.

Keegan, L., Gill, G. and Ptashne, M. (1986). Separation of DNA binding from the transcription-activating function of a eukaryotic regulatory protein. *Science* **231**, 699-704.

Keljo, D. J. and Smith, A. K. (1988). Characterization of binding of simian rotavirus SA-11 to cultured epithelial cells. *J. Pediatr. Gastroenterol. Nutr.* **7**, 249-256.

Knipe, D. M. (1996). Virus-host cell interactions. In *Fields Virology*, 3rd edn, pp. 273-299. Edited by B. N. Fields, D. M. Knipe, P. M. Howley, *et al.*. Philadelphia: Lippincott-Raven Publishers.

Kohli, E., Pothier, P., Tosser, G., Cohen, J., Sandino, A. M. and Spenser, E. (1993). *In vitro* reconstitution of rotavirus transcriptional activity using viral cores and recombinant baculovirus expressed VP6. *Arch. Virol.* **133**, 451-458.

Kojima, K., Taniguchi, K. and Kobayashi, N. (1996). Species-specific and interspecies relatedness of the NSP1 sequences in human, porcine, bovine, feline, and equine rotavirus strains. *Arch. Virol.* **141**, 1-12.

Krug, R. M., Broni, B. and Bouloy, M. (1979). Are the 5' ends of influenza viral mRNAs synthesised *in vivo* donated by host mRNAs. *Cell* **18**, 329-334.

Kuchino, Y., Nishimura, S., Smith, R. E. and Furuichi, Y. (1982). Homologous terminal sequences in the double-stranded RNA genome segments of cytoplasmic polyhedrosis virus of silkworm. *J. Virol.* **44**, 538-543.

Kumar, A., Charpilienne, A. and Cohen, J. (1989). Nucleotide sequence of the gene encoding for the RNA binding protein (VP2) of RF bovine rotavirus. *Nucleic Acid Res.* **17**, 2126.

Labbe, M., Baudoux, P., Charpilienne, A., Poncet, D. and Cohen, J. (1994). Identification of the nucleic acid binding domain of the rotavirus VP2 protein. *J. Gen. Virol.* **75**, 3423-3430.

Labbe, M., Charpilienne, A., Crawford, S. E., Estes, M. K. and Cohen, J. (1991). Expression of rotavirus VP2 produces empty corelike particles. *J. Virol.* **65**, 2946-2952.

Lamb, R. A. and Krug, R. M. (1996). Orthomyxoviridae: The viruses and their replication. In *Fields Virology*, 3rd edn, pp. 1353-1395. Edited by B. N. Fields, D. M. Knipe, P. M. Howley, *et al.*. Philadelphia: Lippincott-Raven Publishers.

Laemmli, U. K. (1970). Cleavage of structural proteins during the assembly of the head of bacteriophage T4. *Nature* **227**, 680-685.

Lane, D. P. and Crawford, L. V. (1979). T antigen is bound to a host proteinin SV40 transformed cells. *Nature* **278**, 261-263.

Lawton, J. A., Estes, M. K., and Prasad, B. V. V. (1997a). Three-dimensional visualization of mRNA release from actively transcribing rotavirus particles. *Nature Struct. Biol.* **4**, 118-121.

Lawton, J. A., Zeng, C. Q.-Y., Mukherjee, S. K., Cohen, J., Estes, M. K. and Prasad, B. V. V. (1997b). Three-dimensional structural analysis of recombinant rotavirus-like particles with intact and amino-terminal-deleted VP2: Implications for the architecture of the VP2 capsid layer. *J. Virol.* **71**, 7353-7360.

Leanna, C. A. and Hannink, M. (1996). The reverse two-hybrid system: a genetic scheme for selection against specific protein/protein interactions. *Nucleic Acid Res.* **24**, 3341-3347.

Le Blois, H., French, T., Mertens, P.P., Burroughs, J. N. and Roy, P. (1992). The expressed VP4 protein of bluetongue virus binds GTP and is the candidate guanylyltransferase of the virus. *Virology* **189**, 757-761.

Lee, P. W. K., Hayes, E. C. and Joklik, W. K. (1981). Characterization of anti-reovirus immunoglobulins secreted by cloned hybridoma cell lines. *Virology* **108**, 134-146.

Li, B. and Fields, S. (1993). Identifiction of mutations in p53 that affect its binding to SV40 large T antigen by using the yeast two-hybrid system. *FASEB J.* **7**, 957-963.

Li, X. and Palese, P. (1994). Characterization of the polyadenylation signal of influenza RNA. *J. Virol.* **68**, 1245-1249.

Linzer, D. I. H. and Levine, A. J. (1979). Characterization of a 54 K dalton cellular SV40 tumor antigen present in SV40-transformed cells and uninfected embryonal carcinoma cells. *Cell* **17**, 43-52.

Liu, M. and Estes, M. K. (1989). Nucleotide sequence of the simian rotavirus SA11 genome segment 3. *Nucleic Acid Res.* **17**, 7991.

Liu, M., Mattion, N. M. and Estes, M. K. (1992). Rotavirus VP3 expressed in insect cells possesses guanylyltransferase activity. *Virology* **188**, 77-84.

Liu, M., Offit, P. A. and Estes, M. K. (1988). Identification of the simian SA11 genome segment 3 product. *Virology* **163**, 26-32.

Loeber, G., Parson, R. and Tegtmeyer, P. (1989). The zinc finger region of simian virus 40 large T antigen. *J. Virol.* **63**, 94-100.

Lopez, S., Arias, C. F., Bell, J. R., Strauss, J. H. and Espejo, R. T. (1985). Primary structure of the cleavage site associated with trypsin enhancement of rotavirus SA11 infectivity. *Virology* **144**, 11-19.

Lopez, S., Arias, C. F., Mendez, E. and Espejo, R. T. (1986). Conservation in rotaviruses of the protein region containing the two sites associated with trypsin enhancement of infectivity. *Virology* **154**, 224-227.

Loudon, P. T. and Roy, P. (1991). Assembly of five bluetongue virus proteins expressed by recombinant baculoviruses: inclusion of the largest protein VP1 in the core and virus-like particles. *Virology* **180**, 798-802.

Luban, J., Alin, K. B., Bossolt, K. L., Humaran, T. and Goff, S. (1992). Genetic assay for mulimerization of retroviral *gag* polyproteins. *J. Virol.* **66**, 5157-5160.

Ludert, J. E., Feng, N., Yu, J. H., Broome, R. L., Hoshino, Y. and Greenberg, H. B. (1996). Genetic mapping indicates that VP4 is the rotavirus cell attachment protein *in vitro* and *in vivo*. *J. Virol.* **70**, 487-493.

Ludert, J. E., Gil, F., Liprandi, F. and Esparza, J. (1986). The structure of the rotavirus inner capsid studied by electron microscopy of chemically disrupted particles. *J. Gen. Virol.* **67**, 1721-1725.

Ludert, J. E., Michelangeli, F., Gil, F., Liprandi, F. and Esparza, J. (1987). Penetration and uncoating of rotaviruses in cultured cells. *Intervirology* **27**, 95-101.

Ma, J. and Ptashne, M. (1987). A new class of yeast transcriptional activators. *Cell* **51**, 113-119.

Ma, J. and Ptashne, M. (1988). Converting a eukaryotic transcriptional inhibitor into an activator. *Cell* **55**, 443-446.

Maass, D. R. and Atkinson, P. H. (1990). Rotavirus proteins VP7, NS28, and VP4 form oligomeric structures. *J. Virol.* **64**, 2632-2641.

Mackow, E. R., Barnett, J. W., Chan, H. and Greenberg, H. B. (1989). The rhesus rotavirus outer capsid protein VP4 functions as a haemagglutinin and is antigenically conserved when expressed by a baculovirus recombinant. *J. Virol.* **63**, 1661-1668.

Mackow, E. R., Shaw, R. D., Matsui, S. M., Vo, P. T., Dang, M. N. and Greenberg, H. B. (1988). The rhesus rotavirus gene encoding protein VP3: location of amino acids involved in homologous and heterologous rotavirus neutralization and identification of a putative fusion region. *Proc. Natl. Acad. Sci. USA* **85**, 645-649.

Mackow, E. R., Vo, P. T., Broome, R., Bass, D. and Greenberg, H. B. (1990). Immunisation with baculovirus expressed VP4 protein passively protects against simian and murine rotavirus challenge. *J. Virol.* **64**, 1698-1703.

Mansell, E. A. and Patton, J. T. (1990). Rotavirus RNA replication: VP2, but not VP6, is necessary for viral replicase activity. *J. Virol.* **64**, 4988-4996.

Mao, Z. and Joklik, W. K. (1991). Isolation and enzymatic characterization of protein λ2, the reovirus guanylyltransferase. Virology 185, 377-386.

Marión, R. M., Zürcher, T., de la Luna, S. and Ortín, J. (1997). Influenza virus NS1 protein interacts with viral transcription-replication complexes *in vivo*. *J. Gen. Virol.* **78**, 2447-2451.

Martin, K. and Helenius, A. (1991). Nuclear transport of influenza virus roibonucleoproteins: the viral matrix protein (M_1) promotes export and inhibits import. *Cell* **67**, 117-130.

Mason, B. B., Graham, D. Y. and Estes, M. K. (1980). *In vitro* transcription and translation of simian rotavirus SA11 gene products. *J. Virol.* **33**, 1111-1121.

Matson, D. O. and Estes, M. K. (1990). Impact of rotavirus infection at a large paediatric hospital. *J. Infect. Dis.* **162**, 598-604.

Matsui, S. M., Mackow, E. R. and Greenberg, H. B. (1989). The molecular determinant of rotavirus neutralization and protection. *Advances Virus Res.* **36**, 181-214.

Matsui, S. M., Mackow, E. R., Matsuno, S., Paul, P. S. and Greenberg, H. B. (1990). Sequence analysis of gene 11 equivalents from "short" and "super short" strains of rotavirus. *J. Virol.* **64**, 120-124.

Matthews, R. E. F. (1979). The classification and nomenclature of viruses. *Intervirology II*, 133-135.

Mattion, N. M., Cohen, J., Aponte, C. and Estes, M. K. (1992). Characterization of an oligomerization domain and RNA-binding properties on rotavirus non-structural protein NS34. *Virology* **190**, 68-83.

Mattion, N. M., Cohen, J. and Estes, M. K. (1994). The rotavirus proteins. In *Viral infections of the gastrointestinal tract.* Edited by A. Z. Kapikian. New York: Marcel Dekker Inc.

Mattion, N. M., Mitchell, D. B., Both, G. W. and Estes, M. K. (1991). Expression of rotavirus proteins encoded by alternative open reading frames of genome segment 11. *Virology* **181**, 295-304.

McCormack, S. J., Thomas, D. C. and Samuel, C. E. (1992). Mechanism of interferon action: identification of a RNA binding domain within the N-terminal region of the human RNA-dependent P1/eIF-2a protein kinase. *Virology* **188**, 47-56.

McCrae, M. A. (1975). Preparation and characterisation of a subviral particle of vaccinia virus containing the DNA-dependent RNA polmerase activity. PhD thesis, University of Glasgow.

McCrae, M. A. and Faulkner-Valle, G. P. (1981). Molecular biology of rotaviruses I. Characterization of basic growth parameters and pattern of macromolecular synthesis. *J. Virol.* **39**(2), 490-496.

McCrae, M. A. and McCorquodale, J. G. (1982). The molecular biology of rotaviruses II. Identification of protein coding assignments of calf rotavirus genome RNA species. *Virology* **117**, 435-443.

McCrae, M. A. and McCorquodale, J. G. (1983). Molecular biology of rotaviruses. V. Terminal structure of viral RNA species. *Virology* **126**, 204-212.

McCrae, M. A. and McCorquodale, J. G. (1987). Expression of a major bovine rotavirus neutralisation antigen (VP7c) in *Escherichia coli. Gene* **55**, 9-18.

McGonigal, T. P., Turon, M. C., Komar-Hartnett, K., Kister, S. E. and Smith, R. E. (1992). Expression of the gene coding for the major outer capsid protein of SA-11 rotavirus in a baculovirus system. *Virus Research* **23**, 135-150.

McIntyre, M., Rosenbaum, V., Rappold, W., Desselberger, M., Wood, D. and Desselberger, U. (1987). Biophysical characterization of rotavirus particles containing rearranged genomes. *J. Gen. Virol.* **68**, 2961-2966.

McNulty, M. S. (1978). Rotaviruses. *J. Gen. Virol.* **40**, 1-18.

McNulty, M. S., Curran, W. L. and McFerran, J. B. (1976). The morphogenesis of a cytopathic bovine rotavirus in Madin-Darby bovine kidney cells. *J. Gen. Virol.* **33**, 503-508.

Mena, I., Jambrina, E., Albo, C., Perales, B., Ortin, J., Arrese, M., Vallejo, D. and Portela, A. (1999). Mutational analysis of influenza A virus nucleoprotein: identification of mutations that affect RNA replication. *J. Virol.* **73**, 1186-1194.

Mendez, E., Arias, C. F. and Lopez, S. (1994). Binding of sialic acids is not an essential step for the entry of animal rotaviruses to epithelial cells in culture. *J. Virol.* **67**, 5253-5259.

Mendez, E., Romero, P., Arias, C. F. and Lopez, S. (1998). Rotaviruses isolated from different species interact with a common cellular molecule during virus entry. American Society for Virology, 17th Annual Meeting, University of British Columbia, Vancouver, Canada.

Mertens, P., Grimes, J., Gouet, P., Diprose, J., Malby, R., Burroughs, N. and Stuart, D. (1999).Crystallographic studies show ordered double-stranded RNA in Bluetongue Virus. XIth International Congress of Virology, Sydney, Australia.

Mertens, P. P. C. and Sanger, D. V. (1985). Analysis of the terminal sequence of the genome segments of four orbiviruses. In *Bluetongue and related orbiviruses*, pp. 371-387. Edited by T. L. Barger and M. M. Yochim. New York: Alan R. Liss.

Meyer, J. C., Bergmann, C. C. and Bellamy, A. R. (1989). Interaction of rotavirus cores with the nonstructural glycoprotein NS28. *Virology* **171**, 98-107.

Middleton, P. J., Syzmanski, M. T., Abbot, G. D., Bortolussi, R. and Hamilton, J. R. (1974). Orbivirus acute gastroenteritis of infancy. *Lancet* **1**(1241-1244).

Mindich, L. (1999). Precise packaging of the three genomic segments of the double-stranded-RNA bacteriophage ϕ6. *Microbiol. Mol. Biol. Rev.* **63**, 149-152.

Mitchell, D. B. and Both, G. W. (1990a). Conservation of a potential metal binding motif despite extensive sequence diversity in the rotavirus nonstructural protein NS53. *Virology* **174**, 618-621.

Mitchell, D. B. and Both, G. W. (1990b). Completion of the genomic sequence of the simian rotavirus SA11: nucleotide sequences of segments 1, 2 and 3. *Virology* **177**, 324-331.

Monto, A. S., Koopman, J. S., Longini, I. M. and Issacson, R. E. (1983). The Tecumseh study. XII. Enteric agents in the community, 1976-1981. *J. Infect. Dis.* **148**, 284-291.

Mora, M., Partin, K., Bhatia, M., Partin, J. and Carter, C. (1987). Association of reovirus proteins with the structural matrix of infected cells. *Virology* **159**, 265-277.

Morgan, E. M. and Kingsbury, D. W. (1981). Reovirus enzymes that modify messenger RNA are inhibited by perturbation of the lambda proteins. *Virology* **113**, 565-572.

Morgan, E. M. and Zweerink, H. J. (1975). Characterization of transcriptase and replicase particles isolated from reovirus infected cells. *Virology* **68**, 455-466.

Moss, S. R. and Nuttall, P. A. (1994). Subcore- and core-like particles of Broadhaven virus (BRDV), a tick-bourne orbivirus, synthesized from baculovirus expressed VP2 and VP7, the major core proteins of BRDV. *Virus Res.* **32**, 401-407.

Murphy, F. A. (1985). Virus taxonomy. In *Fields Virology*, 1st edn., pp. 7-25. Edited by B. N. Fields, D. M. Knipe, R. M. Chanock, J. L. Melnick, B. Roizman and R. E. Shope. New York: Raven Press.

Murphy, F. A. (1996). Virus taxonomy. In *Fields Virology*, 3rd edn., pp. 15-57. Edited by B. N. Fields, D. M. Knipe, P. M. Howley, *et al.*. Philadelphia USA: Lippincott-Raven Publishers.

Nibert, M. L., Schiff, L. A. and Fields, B. N. (1996). Reoviruses and their replication. In *Fields Virology*, 3rd edn., pp. 1557-1596. Edited by B. N. Fields, D. M. Knipe, P. M. Howley, *et al.*. Philadelphia USA: Lippincott-Raven Publishers.

Offit, P. A. and Blavat, G. (1986). Identification of two rotavirus genes determining neutralising specificities. *J. Virol.* **57**, 376-378.

Offit, P. A., Blavat, G., Greenberg, H. B. and Clark, H. F. (1986). Molecular basis of rotavirus virulence: role of gene segment 4. *J. Virol.* **57**, 46-49.

Offit, P. A., Shaw, R. D. and Greenberg, H. B. (1986). Passive protection against rotavirus induced diarrhea by monoclonal antibodies to surface proteins VP3 and VP7. *J. Virol.* **58**, 700-703.

Palmer, E. L., Martin, M. L. and Murphy, F. A. (1977). Morphology and stability of infantile gastroenteritis virus: comparison with reovirus and bluetongue virus. *J. Gen. Virol.* **35**, 403-414.

Patton, J. T. (1986-1987). Synthesis of simian rotavirus SA11 double-stranded RNA in a cell-free system. *Virus Res.* **6**, 217-233.

Patton, J. T. (1995). Structure and function of the rotavirus RNA-binding proteins. *J. Gen. Virol.* **76**, 2633-2644.

Patton, J. T. (1996). Rotavirus VP1 alone specifically binds to the 3' end of viral mRNA, but the interaction is not sufficient to initiate minus-strand synthesis. *J. Virol.* **70**, 7940-7947.

Patton, J. T. and Chen, D. (1999). RNA-binding and capping activities of proteins in rotavirus open cores. *J. Virol.* **73**, 1382-1391.

Patton, J. T. and Gallegos, C. O. (1988). Structure and Protein Composition of the Rotavirus Replicase Particle. *Virology* **166**, 358-365.

Patton, J. T. and Gallegos, C. O. (1990). Rotavirus RNA replication: single-stranded RNA extends from the replicase particle. *J. Gen. Virol.* **71**, 1087-1094.

Patton, J. T., Jones, M. T., Kalbach, A. N., He, Y.-W. and Xiaobo, J. (1997). Rotavirus RNA polymerase requires the core shell protein to synthesis the double-stranded RNA genome. *J. Virol.* **71**, 9618-9626.

Patton, J. T., Salter-Cid, L., Kalbach, A., Mansell, E. A. and Kattoura, M. (1993). Nucleotide and amino acid sequence analysis of the rotavirus nonstructural RNA-binding protein NS35. *Virology* **192**, 438-446.

Payne, C. C. and Mertens, P. P. C. (1983). Cytoplasmic polyhedrosis viruses. In *The Reoviridae*, pp. 425-504. Edited by W. K. Joklik. New York: Plenum.

Petrie, B. L. (1983). Biological activity of rotavirus particles lacking glycoylated proteins. In *Double-stranded RNA viruses*, pp. 146-156. Edited by R. W. Compans and D. H. L. Bishop. New York: Elsevier.

Petrie, B. L., Estes, M. K. and Graham, D. Y. (1983). Effects of tunicamycin on rotavirus morphogenesis and infectivity. *J. Virol.* **46**, 270-274.

Petrie, B. L., Graham, D. Y., Hanssen, H. and Estes, M. K. (1982). Localization of rotavirus antigens in infected cells by ultrastructural immunocytochemistry. *J. Gen. Virol.* **63**, 457-467.

Petrie, B. L., Greenberg, H. B., Graham, D. Y. and Estes, M. K. (1984). Ultrastructural localization of rotavirus antigens using colloidal gold. *Virus Research* **1**, 133-152.

Phizicky, E. M. and Fields, S. (1995). Protein-protein interactions: Methods for detection and analysis. *Microbiol. Revs.* **59**, 94-123.

Piron, M., Delaunay, T., Grosclaude, J. and Poncet, D. (1999). Identification of the RNA-binding, dimerization, and eIF4GI-binding domains of rotavirus nonstructural protein NSP3. *J. Virol.* **73**, 5411-5421.

Piron, M., Vende, P., Cohen, J. and Poncet, D. (1998). Rotavirus RNA-binding protein NSP3 interacts with eIF4GI and evicts the poly(A) binding protein from eIF4F. *EMBO J.* **17**, 5811-5821.

Pizarro, J. L., Sandino, A. M., Pizarro, J. M., Fernandez, J. and Spencer, E. (1991). Characterization of rotavirus guanylyltransferase activity associated with polypeptide VP3. *J. Gen. Virol.* **72**, 325-332.

Poncet, D., Aponte, C. and Cohen, J. (1993). Rotavirus protein NSP3 (NS34) is bound to the 3' end consensus sequence of viral mRNAs in infected cells. *J. Virol.* **67**(6), 3159-3165.

Poncet, D., Aponte, C. and Cohen, J. (1996). Structure and function of rotavirus nonstructural protein NSP3. *Arch. Virol.* **S12**, 29-35.

Poncet, D., Laurent, S. and Cohen, J. (1994). Four nucleotides are the minimal requirement for RNA recognition by rotavirus non-structural protein NSP3. *EMBO J.* **13**, 4165-4173.

Poncet, D., Lindenbaum, P., L'Haridon, R. and Cohen, J. (1997). *In vivo* and *in vitro* phosphorylation of rotavirus NSP5 correlates with its localization in viroplasms. *J. Virol.* **71**, 34-41.

Poruchynsky, M. S., Maass, D. R. and Atkinson, P. H. (1991). Calcium depletion blocks the maturation of rotavirus by altering the oligomerization of virus-encoded proteins in the ER. *J. Cell Biol.* **114**, 651-661.

Prasad, B. V. V., Burns, J. W., Marietta, E., Estes, M. K. and Chiu, W. (1990). Localisation of VP4 neutralisation sites in rotavirus by three-dimensional cryoelectron microscopy. *Nature* **343**, 476-478.

Prasad, B. V. V. and Chiu, W. (1994). Structure of rotavirus. In *Rotaviruses*, pp. 9-29. Edited by R. F. Ramig. Berlin: Springer-Verlag.

Prasad, B. V. V., Rothnagel, R., Zeng, C. Q.-Y., Jakana, J., Lawton, J. A., Chiu, W. and Estes, M. K. (1996). Visualization of ordered genomic RNA and localization of transcriptional complexes in rotavirus. *Nature* **382**, 471-473.

Prasad, B. V. V., Wang, G. J., Clerx, J. P. M. and Chiu, W. (1988). Three-dimensional structure of rotavirus. *J. Mol. Biol.* **199**, 269-275.

Prasad, B. V. V., Yamaguchi, S. and Roy, P. (1997). Three-dimensional structure of single-shelled bluetongue virus. *J. Virol.* **66**, 2135-2142.

Quan, C. M. and Doane, F. W. (1983). Ultrastructural evidence for the cellular uptake of rotavirus by endocytosis. *Intervirology* **20**, 223-231.

Qiao, X., Qiao, J. and Mindich, L. (1997). Stoichiometric packaging of the three genomic segments of dsRNA bacteriophage ϕ6. *Proc. Natl. Acad. Sci. USA* **94**, 4074-4079.

Ramadevi, N., Burroughs, N. J., Mertens, P.P.C., Jones, I. M. and Roy, P. (1998). Capping and methylation of mRNA by purified recombinant VP4 protein of bluetongue virus. *Proc. Natl. Acad. Sci. USA* **95**, 13537-13542.

Ramig, R. F. and Petrie, B. L. (1984). Characterization of temperature-sensitive mutants of simian rotavirus SA11: protein synthesis and morphogenesis. *J. Virol.* **49**, 665-673.

Richardson, S. C., Mercer, L. E., Sonza, S. and Holmes, I. H. (1986). Intracellular localization of rotaviral proteins. *Arch. Virol.* **88**, 251-264.

Roseto, A., Escaig, J., Delain, G., Cohen, J. and Scherrer, R. (1979). Structure of rotaviruses as studied by the freeze-drying technique. *Virology* **98**, 471-475.

Rossi, F., Gallina, A. and Milanesi, G. (1996). NEF-CD4 physical interaction sensed with the yeast two-hybrid system. *Virology* **217**, 397-403.

Rott, R., Saber, S. and Scholtissek, C. (1965). Effect on myxovirus of mitomycin C, actinomycin D and pretreatment of the host cell with ultraviolet light. *Nature* **205**, 1187-1190.

Roy, P. (1989). Bluetongue virus genetics and genome structure. *Virus Research* **13**, 179-206.

Roy, P. (1996). Orbiviruses and their replication. In *Fields Virology*, 3rd edn., pp.1709-1734. Edited by B. N. Fields, D. M. Knipe, P. M. Howley, *et al.*. Philadelphia USA: Lippincott-Raven Publishers.

Roy, P., Fukusho, A., Ritter, D. G., Lyon, D. (1988). Evidence for genetic relationship between RNA and DNA viruses from the sequence homology of a putative polymerase gene bluetongue virus with that of vaccinia virus: conservation of RNA polymerase genes from diverse species. *Nuc. Acids. Res.* **16/24**, 11759-11767.

Ruggeri, F. M. and Greenberg, H. B. (1991). Antibodies to the trypsin cleavage peptide VP8* neutralize rotavirus by inhibiting binding of virions to target cells in culture. *J. Virol.* **65**, 2211-2219.

Ruiz, M. C., Abad, M. J., Charpilienne, A., Cohen, J. and Michelangeli, F. (1997). Cell lines susceptible to infection are permeabilized by cleaved and solubilized outer layer proteins of rotavirus. *J. Gen. Virol.* **78**, 2883-2893.

Sabara, M., Gilchrist, J. E., Hudson, G. R. and Babiuk, L. A. (1985). Preliminary characterisation of an epitope involved in neutralisation and cell attachment that is located on the major bovine rotavirus glcoprotein. *J. Virol.* **53**, 58-66.

Sandino, A. M., Fernandez, J., Pizzaro, M. V. and Spencer, E. (1994). Structure of rotavirus particle: interaction of the inner capsid protein VP6 with the core polypeptide VP3. *Biol. Res.* **27**, 39-48.

Sandino, A. M., Jashes, M., Faundez, G. and Spencer, E. (1986). Role of the inner protein capsid on *in vitro* human rotavirus transcription. *J. Virol.* **60**, 797-802.

Schenborn, E. T. and Mierendorf, R. C. (1985). A novel transcription property of SP6 and T7 RNA polymerases : dependence on template structure. *Nucleic Acid Res.* **13**, 6223-6236.

Schiff, L. A., Nibert, L. M., Man Sung, C. O., Brown, E. G. and Fields, B. N. (1988). Distinct binding sites for zinc and double-stranded RNA in the reovirus outer capsid protein σ3. *Mol. and Cell. Biol.* **8**, 273-283.

Shahrabadi, M. S., Babiuk, L. A. and Lee, P. W. (1987). Further analysis of the role of calcium in rotavirus morphogenesis. *Virology* **158**, 103-111.

Shahrabadi, M. S. and Lee, P. W. (1986). Bovine rotavirus maturation is a calcium-dependent process. *Virology* **152**, 298-307.

Shaji, D. and Shalia, M. S. (1999). Domains of rinderpest virus phosphoprotein involved in interaction with itself and the nucleocapsid protein. *Virology* **258**, 415-424.

Sharpe, A. H., Chen, L. B. and Fields, B. N. (1982). The interaction of mammalian reoviruses with the cytoskeleton of monkey kidney CV-1 cells. *Virology* **120**, 399-411.

Shatkin, A. J., and Kozak, M. (1983). Biochemical aspects of reovirus transcription and translation. In *The Reoviridae*, pp. 79-106. Edited by W. K. Joklik. New York: Plenum Press.

Shepard, D. A., Ehnstrom, J. G., Skinner, P. J. and Schiff, L. A. (1996). Mutations in the zinc-binding motif of the reovirus capsid protein σ3 eliminates its ability to associate with capsid protein μ1. *J. Virol.* **70**, 2065-2068.

Shuman, S. (1982). RNA capping by HeLa cell guanylyltransferase. Characterization of a covalent protein-guanylate intermediate. *J. Biol. Chem.* **257**, 7237-7245.

Shuman, S., Liu, Y. and Schwer, B. (1994). Covalent catalysis in nucleotidyl transfer reactions: essential motifs in Saccharomyces cerevisiae RNA capping enzyme are conserved in Schizosaccharomyces pombe and viral capping enzymes and among polynucleotide ligases. *Proc. Natl. Acad. Sci. USA* **91**, 12046-12050.

Shuman, S. and Schwer, B. (1995). RNA capping enzyme and DNA ligase: a superfamily of covalent nucleotide transferases. *Mol. Microbiol.* **17**, 405-410.

Silver, P. A., Keegan, L. P. and Ptashne, M. (1984). Amino terminus of the yeast GAL4 gene product is sufficient for nuclear localization. *Proc. Natl. Acad. Sci. USA* **81**, 5951-5955.

Slack, M. S. (1998). Functional analysis of the phosphoprotein of respiratory syncytial virus. PhD thesis, University of Warwick.

Slack, M. S. and Easton, A. J. (1998). Characterization of the interaction of the human respiratory syncytial virus phosphoprotein and nucleocapsid protein using the two-hybrid system. *Virus Research* **55**, 167-176.

Snyder, J. D. and Merson, M. H. (1982). The magnitude of the global problem of acute diarrhoeal disease: a review of active surveillance data. *Bull. WHO.* **60**, 605-613.

Spencer, E. and Arias, M. L. (1981). *In vitro* transcription catalyzed by heat-treated human rotavirus. *J. Virol.* **40**, 1-10.

Spencer, E. and Garcia, B. I. (1984). Effect of S-adenosylmethionine on human rotavirus RNA synthesis. *J. Virol.* **52**, 188-197.

Spendlove, R. S., McClain, M. E. and Lennette, E. H. (1970). Enhancement of reovirus infectivity by extracellular removal or alteration of the virus capsid by proteolytic enzymes. *J. Gen. Virol.* **8**, 83-93.

Stacy-Phipps, S. and Patton, J. T. (1987). Synthesis of plus- and minus-strand RNA in rotavirus-infected cells. *J. Virol.* **61**, 3479-3484.

Stamatos, N. M. and Gomatos, P. J. (1982). Binding to selected regions of reovirus mRNAs by a nonstructural reovirus protein. *Proc. Natl. Acad. Sci. USA* **79**, 3457-3461.

Starnes, M. C. and Joklik, W. K. (1993). Reovirus protein λ3 is a poly(C)-dependent poly(G) polymerase. *Virology* **193**, 356-366.

Stirzaker, S. C., Whitteld, P. L., Christie, D. L., Bellamy, A. R. and Both, G. W. (1987). Processing of rotavirus glycoprotein VP7: implications for the retention of the protein in the endoplasmic reticulum. *J. Cell Biol.* **105**, 2897-2903.

Streckert, H. J., Brussow, H. and H., W. (1988). A synthetic peptide corresponding to the cleavage region of VP4 from rotavirus SA11 induces neutralising antibodies. *J. Virol.* **62**, 4265-4269.

Sturzenbecker, L. J., Nibert, M., Furlong, D. and Fields, B. N. (1987). Intracellular digestion of reovirus particles requires a low pH and is an essential step in the viral infectious cycle. *J. Virol.* **61**, 2351-2361.

Suzuki, H., Kitaoka, S., Konno, T., Sato, T. and Ishida, N. (1985). Two modes of human rotavirus entry into MA 104 cells. *Arch. Virol.* **85**, 25-34.

Suzuki, H., Sato, T., Konno, T., Kitaoka, S., Ebina, T. and Ishida, N. (1984). Effect of tunicamycin on human rotavirus morphogenesis and infectivity. Brief Report. *Arch. Virol.* **81**, 363-369.

Svensson, L., Grahnquist, L., Peterson, C. A., Granndien, M., Stintzing, G. and Greenberg, H. B. (1988). Detection of human rotavirus which do not react with subgroup I and subgroup II specific monoclonal antibodies. *J. Clin. Microbiol.* **26**, 1238-1240.

Takacs, A. M. and Banerjee, A. K. (1995). Efficient interaction of the vesicular stomatitis virus P protein with the L protein or the N protein in cells expressing the recombinant proteins. *Virology* **208**, 821-826.

Takacs, A. M., Das, T. and Banerjee, A. K. (1993). Mapping of interacting domains between the nucleocapsid protein and the phosphoprotein of vesicular stomatitis virus by using a two-hybrid system. *Proc. Natl. Acad. Sci. USA* **90**, 10375-10379.

Tam, J. S., Szymanski, M. T., Middleton, P. J. and Petric, M. (1976). Studies on the particles of infantile gastroenteritis virus (orbivirus group). *Intervirology* **7**, 181-191.

Taniguchi, K., Kojima, K. and Urasawa, S. (1996). Nondefective rotavirus mutants with an NSP1 gene which has a deletion of 500 nucleotides, including a cysteine-rich zinc finger motif-encoding region (nucleotides 156 to 248), or which has a nonsense codon at nucleotides 153 to 155. *J. Virol.* **70**, 4125-4130.

Taniguchi, K., Okada, J., Kojima, K., Kobayashi, N., Wu, H., Kusuhara, Y., Maeno, Y. and Urasawa, S. (1999). Further studies on nondefective rotavirus mutants with an NSP1 gene encoding a truncated protein. XIth International Congress of Virology, Sydney, Australia.

Taylor, J. A., Meyer, J. C., Legge, M. A., *et al.*. (1992). Transient expression and mutational analysis of the rotavirus intracellular receptor: the C-terminal methionine residue is essential for ligand binding. *J. Virol.* **66**, 3566-3572.

Taylor, J. A., O'Brien, J. A., Lord, V. J., Meyer, J. C. and Bellamy, A. R. (1993). The RER-localised rotavirus intracellular receptor: a truncated purified soluble form is multivalent and binds virus particles. *Virology* **194**, 807-814.

Tian, P., Ball, J. M., Zeng, C. Q.-Y. and Estes, M. K. (1996). The rotavirus nonstructural glycoprotein NSP4 possesses membrane destabilization activity. *J. Virol.* **70**, 6973-6981.

Tian, P., Estes, M. K., Hu, Y. F., Ball, J. M., Zeng, C. Q.-Y. and Schilling, W. P. (1995). The rotavirus nonstructural glycoprotein NSP4 mobilizes Ca2+ from the endoplasmic reticulum. *J. Virol.* **69**, 5763-5772.

Tian, P., Hu, Y., Schilling, W. P., Lindsay, D. A., Eiden, J. and Estes, M. K. (1994). The nonstructural glycoprotein of rotavirus affects intracellular calcium levels. *J. Virol.* **68**, 251-257.

Tian, Y., Tarlow, O., Ballard, A., Desselberger, U. and McCrae, M. A. (1993). Genomic concatemerization/deletion in rotaviruses: a new mechanism for generating rapid genetic change of potential epidemiological importance. *J. Virol.* **67**(11), 6625-6632.

Tian, Y., Tarlow, O. and McCrae, M. A. (1990). Nucleotide-sequence of gene-2 of the UK tissue-culture adapted strain of bovine rotavirus. *Nucleic Acid Res.* **18**, 4015.

Tine, J. A., Conseil, V., Delplace, P., de Taisne, C., Camus, D. and Paoletti, E. (1993). Immunogenicity of the *Plasmodium falciparum* Serine Repeat Antigen (p126) expressed by vaccinia virus. *Infect. Immun.* **61**(9), 3933-3941.

Tsui, S. and Schubach, W. H. (1994). Epstein-Barr virus nuclear protein 2A forms oligomers in vitro and in vivo through a region required for B-cell transformation. *J. Virol.* **68**, 4287-2494.

Tyler, K., McPhee, D. and Fields, B. (1986). Distinct pathways of viral spread in the host determined by reovirus S1 gene segemnt. *Science* **233**, 770-774.

Ueda, S., Masuta, C. and Uyeda, I. (1997). Hypothesis on particle structure and assembly of rice dwarf phytoreovirus: interactions among multiple structural proteins. *J. Gen. Virol.* **78**, 3135-3140.

Ulmanen, I., Broni, B. A. and Krug, R. M. (1981). Role of two of the influenza virus core P proteins in recognising cap 1 structures (m^7GpppNm) on RNAs and in initiating viral transcription. *Proc. Natl. Acad. Sci. USA* **78**, 7355-7359.

Vafai, A. and Yang, W. (1991). Neutralizing antibodies induced by recombinant vaccinia virus expressing Varicella-Zoster virus gpIV. *J. Virol.* **65**(10), 5593-5596.

Valenzuela, S., Pizarro, J., Sandino, A. M., Vasquez, M., Fernandez, J., Hernandez, O., Patton, J. and Spencer, E. (1991). Photoaffinity labeling of rotavirus VP1 with 8-azido-ATP: identification of the viral RNA polymerase. *J. Virol.* **65**, 3964-3967.

Van Aelst, L., Barr, M., Marcus, S., Polverino, A. and Wigler, M. (1993). Complex formation between RAS and RAF and other protein kinases. *Proc. Natl. Acad. Sci. USA* **90**, 6213-6217.

Vesikari, T. (1999). Rotavirus vaccines: development and use for the prevention of diarrhoeal disease. *Annal. Med.* **31**, 79-85.

Vesikari, T., Isolauri, E. and D'Hondt, E. (1984). Protection of infants against rotavirus diarrhea by RIT 4237 attenuated bovine rotavirus strain vaccine. *Lancet* **1**, 977-981.

Vojtek, A. B., Hollenberg, S. M. and Cooper, J. A. (1993). Mammalian Ras interacts directly with the serine/threonine kinase Raf. *Cell* **74**, 527-534.

von Bonsdorff, C.-H. and Svensson, L. (1988). Human serogroup C rotavirus in Finland. *Scand. J. Infect. Dis.* **20**, 475-478.

Wang, P., Palese, P. and O'Neill, R. E. (1997). The NPI-1/NPI-3 (karyopherin α) binding site on the influenza A virus nucleoprotein NP is a nonconventional nuclear localization signal. *J. Virol.* **71**, 1850-1856.

Weclewicz, K., Kristensson, K. and Svensson, L. (1994). Rotavirus causes selective vimentin reorganization in monkey kidney CV-1 cells. *J. Gen. Virol.* **75**, 3267-3271.

Weiner, J. R., Bartlett, J. A. and Joklik, W. K. (1989). The sequences of reovirus serotype 3 genome segments M1 and M3 encoding the minor protein mu 2 and the major nonstructural protein mu NS, repectively. *Virology* **169**, 293-304.

Weiner, J. R. and Joklik, W. K. (1987). Comparison of the reovirus serotype 1, 2 and 3 S3 genome segments encoding the nonstructural protein σ NS. *Virology* **161**, 332-339.

Welch, A. B. and Thompson, T. L. (1973). Physicochemical characterization of a neonatal calf diarrhea virus. *Can. J. Compr. Med.* **37**, 295-301.

Wentz, M. J., Patton, J. T. and Ramig, R. F. (1996). The 3'-terminal consensus sequence of rotavirus mRNA is the minimal promoter of negative-strand RNA synthesis. *J. Virol.* **70**, 7833-7841.

Whitaker, A. M. and Hayward, C. J. (1985). The characterization of three monkey kidney cell lines. *Rev. Biol. Stand.* **60**, 125-131.

White, C. K. and Zweerink, H. J. (1976). Studies on the structure of reovirus cores: Selective removal of polypeptide λ2. *Virology* **70**, 171-180.

Whitteld, P. L., Tyndall, C., Stirzaker, S. C., Bellamy, A. R. and Both, G. W. (1987). Location of sequences within rotavirus SA11 glycoprotein VP7 which direct it to the endoplasmid reticulum. *Mol. Cell. Biol.* **7**, 2491-2497.

Wickner, R. B. (1996). Viruses of yeast, fungi and parasitic micro-organisms. In *Fields Virology*, 3rd edn., pp.557-585. Edited by B. N. Fields, D. M. Knipe, P. M. Howley, *et al.* Philadelphia: Lippincott-Raven Publishers.

Wolff, T., O'Neill, R. E. and Palese, P. (1996). Interaction cloning of NS1-I, a human protein that binds to the nonstructural NS1 proteins of influenza A and B viruses. *J. Virol.* **70**, 5363-5372.

Wu, A. Z. and Sun, Y. K. (1986). Isolation and reconstitution of the RNA replicase of the cytoplasmic polyhedrosis virus of silkworm, *Bombyx mori. Theoretical and Applied Genetics* **72**, 662-664.

Xu, C. W., Mendelsohn, A. and Brent, R. (1997). Cells that register logical relationships among proteins. *Proc. Natl. Acad. Sci. USA* **94**, 12473-12478.

Xu, L., Tian, Y., Tarlow, O., Harbour, D. and McCrae, M. A. (1994). Molecular Biology of Rotaviruses IX. Conservation and divergence in genome segment 5. *J. Gen. Virol.* **75**, 3413-3421.

Yazaki, K. and Miura, K.-I. (1980). Relation of the structure of cytoplasmic polyhedrosis virus and the synthesis of its messenger RNA. *Virology* **105**, 467-479.

Yazaki, K., Mizuno, A., Sano, T., Fujii, H. and Miura, K. (1986). A new method for extracting circular and supercoiled genome segments from cytoplasmic polyhedrosis virus. *J. Virol. Methods* **14**, 275-283.

Yeager, M., Dryden, K. A., Olson, N. H., Greenberg, H. B. and Baker, T. S. (1990). Three-dimensional structure of rhesus rotavirus by cryoelectron microscopy and image reconstruction. *J. Cell Biol.* **110**, 2133-2144.

Yolken, R. H., Willoughby, R., Wee, S. B., Miskuff, R. and Vonderfecht, S. (1987). Sialic acid glycoproteins inhibit *in vitro* and *in vivo* replication of rotaviruses. *J. Clin. Invest.* **79**, 148-154.

Zarbl, H. and Millward, S. (1983). The reovirus multiplication cycle. In *The Reoviridae*, pp. 107-196. Edited by W. K. Joklik. New York: Plenum Press.

Zeng, C. Q., Estes, M. K., Charpilienne, A. and Cohen, J. (1998). The N terminus of rotavirus VP2 is necessary for encapsidation of VP1 and VP3. *J. Virol.* **72**, 201-208.

Zeng, C. Q.-Y., Labbe, M., Cohen, J., Prasad, B. V. V., Chen, D., Ramig, R. F. and Estes, M. K. (1994). Characterization of rotavirus VP2 particles. *Virology* **201**, 55-65.

Zeng, C. Q.-Y., Wentz, M. J., Cohen, J., Estes, M. K. and Ramig, R. F. (1996). Characterization and replicase activity of double-layered and single-layered rotavirus-like particles expressed from baculovirus recombinants. *J. Virol.* **70**, 2736-2742.

Zhang, M. D., Zeng, C. Q.-Y., Dong, Y. J., Ball, J. M., Saif, L. J., Morris, A. P. and Estes, M. K. (1998). Mutations in rotavirus nonstructural glycoprotein NSP4 are associated with altered virus virulence. *J. Virol.* **72**, 3666-3672.

Zweerink, H. J. (1974). Multiple forms of ss-dsRNA polymerase activity in reovirus-infected cells. *Nature* **247**, 313-315.

Zweerink, H. J., Morgan, E. M. and Skyler, J. S. (1976). Reovirus morphogenesis: Characterization of subviral particles in infected cells. *Virology* **73**, 442-453.

Appendix

Apendix 1 - Results Chapter 2

Appendix 1.1 Calculation of β-galactosidase units

1 U β-galactosidase is defined as the amount which hydrolyses 1 μmole ONPG to o-nitrophenol and D-galactose per minute.

β-galactosidase units = $1000 \times OD_{420}/(t \times V \times OD_{600})$

t = elapsed time (in minutes) of incubation

V = 0.1 ml × concentration factor

OD_{600} = Abs at 600 nm of 1 ml of culture

Worked Example - Transformants carrying pGBT9-Gene 9

OD_{420}	t	V	OD_{600}	β-galactosidase units
0.049	212	0.5	0.769	0.60
0.054	212	0.5	0.769	0.66
0.048	212	0.5	0.769	0.59
0.115	1050	0.3	0.769	0.47
0.137	1050	0.3	0.769	0.56
0.129	1050	0.3	0.769	0.53

ΣX = Sum of β-galactosidase values = 3.41

Mean = $\Sigma X/N = 3.41/6 = 0.57$

Standard Deviation (s) = 0.07

Standard error of mean = $s/\sqrt{N} = 0.027$

Students t test

95 % confidence limits = $0.57 \pm t_{0.05} \times 0.027$, where t has five degrees of freedom

i.e. $0.57 \pm 2.571 \times 0.027$

0.57 ± 0.07 β-galactosidase units

Appendix 1.2 Equation for calculation of the co-transformation efficiency of two-hybrid plasmids into yeast

Co-Transformation efficiency (cfu/μg DNA)

$$\frac{\text{cfu x TV (μl)}}{\text{V x D x DNA}}$$

cfu = colony forming units on plate

TV = Total suspension volume (μl)

V = Volume of suspension plated (μl)

D = Dilution factor of suspension plated

DNA = Quantity of plasmid DNA used in transformation (μg) [in a co-transformation, this is the amount of limiting plasmid, i.e. the lesser of the two plasmids, not the sum of them (usually 1 μg)]

Appendix 2 - Results Chapter 4

Appendix 2.1 ImageQuant™ analysis of viral protein complex immunoprecipitated with anti-NSP1 serum from UKtc rotavirus-infected cell lysates (Figure 7.3)

The 5-11 % gradient polyacrylamide gel shown in Figure 7.3 was exposed to the phosphoimager for 8 days. The proteins in the viral complex (NSP1, VP6, VP2, VP3/VP4, VP1, NSP3) which were detected by phosphoimaging were quantified using ImageQuant™ software and the data analyzed using Excel™ software (Microsoft). The data presented are from the results of one experiment.

The amounts of the precipitated proteins are displayed in arbitrary units assigned by the ImageQuant™ software. As radioactivity detected was a measure of the number of ^{35}S-methionine residues in each protein and not the amount of protein, data were corrected for the methionine content of each protein.

The IP reactions are indicated on the x axis:
no serum = IP reaction with no serum/1 µl of 10 mg/ml ovalbumin
pre-immune = IP reaction with pre-immune serum
anti-NSP1 = IP reaction with anti-NSP1 serum
boiled = IP reaction with cell lysate sample boiled for 2 minutes with cracking buffer (4 % SDS; 10 % β-mercaptoethanol) and diluted 10-fold with water prior to incubation with anti-NSP1 serum.

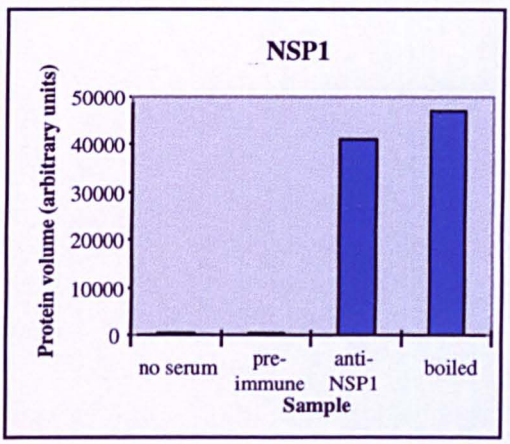
NSP1
Protein volume (arbitrary units)
50000
40000
30000
20000
10000
0
no serum
pre-immune
anti-NSP1
boiled
Sample

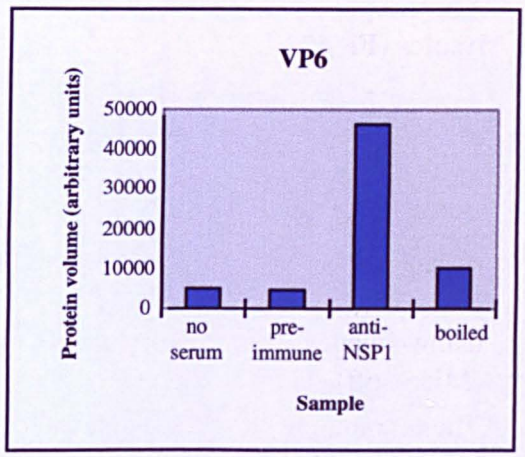
VP6
Protein volume (arbitrary units)
50000
40000
30000
20000
10000
0
no serum
pre-immune
anti-NSP1
boiled
Sample

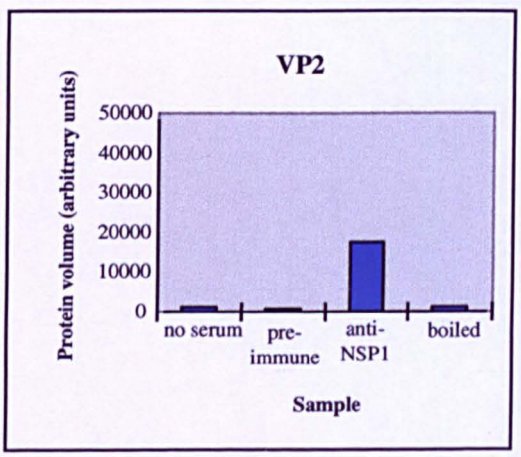
VP2
Protein volume (arbitrary units)
50000
40000
30000
20000
10000
0
no serum
pre-immune
anti-NSP1
boiled
Sample

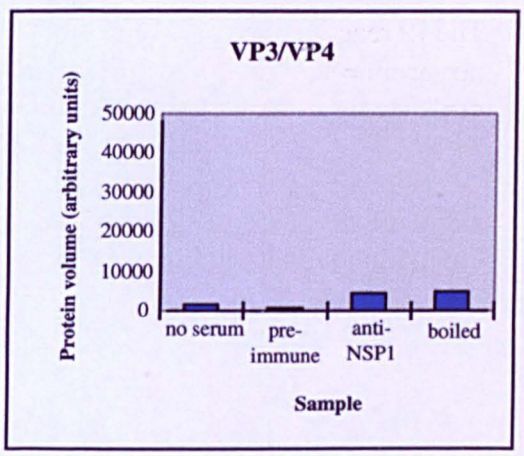
VP3/VP4
Protein volume (arbitrary units)
50000
40000
30000
20000
10000
0
no serum
pre-immune
anti-NSP1
boiled
Sample

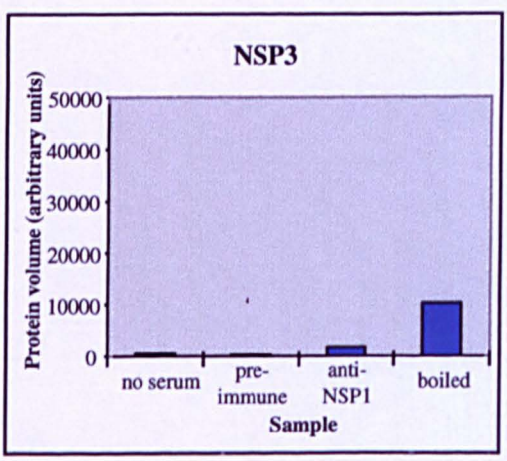
NSP3
Protein volume (arbitrary units)
50000
40000
30000
20000
10000
0
no serum
pre-immune
anti-NSP1
boiled
Sample

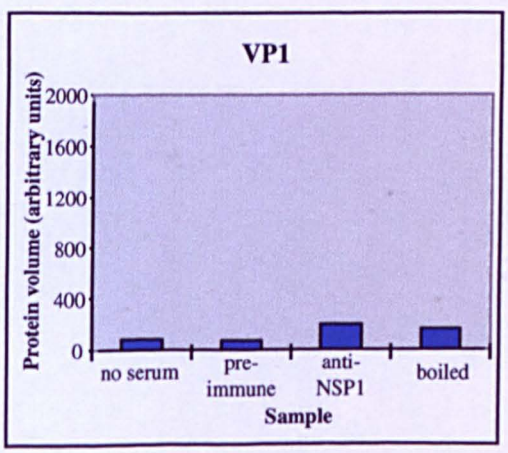
VP1
Protein volume (arbitrary units)
2000
1600
1200
800
400
0
no serum
pre-immune
anti-NSP1
boiled
Sample

Appendix 2.2 ImageQuant™ analysis of viral protein complexes immunoprecipitated with anti-NSP1 serum from cell fractions created by centrifugation at 10,000Xg, 30,000Xg and 100,000Xg (Figure 7.5)

The 5-11 % gradient polyacrylamide gel shown in Figure 7.5 was exposed to the phosphoimager for 8 days. The proteins in the viral complex (NSP1, VP6, VP2, VP3/VP4, VP1, NSP3) which were detected by phosphoimaging were quantified using ImageQuant™ software and the data anlysed using Excel™ software (Microsoft). The data presented are from the results of one experiment.

The amounts of the precipitated proteins are displayed in arbitrary units assigned by the ImageQuant™ software. As radioactivity detected was a measure of the number of ^{35}S-methionine residues in each protein and not the amount of protein, data were corrected for the methionine content of each protein.

IP reaction samples shown on the x axis of each graph are as follows:
(1) IP of cell lysate with pre-immune serum.
(2) IP of cell lysate with anti-NSP1 serum.
(3) IP of 10,000Xg cell lysate pellet with anti-NSP1 serum.
(4) IP of 10,000Xg cell lysate supernatant with anti-NSP1 serum.
(5) IP of 30,000Xg cell lysate pellet with anti-NSP1 serum.
(6) IP of 30,000Xg cell lysate supernatant with anti-NSP1 serum.
(7) IP of 100,000Xg cell lysate pellet with anti-NSP1 serum.
(8) IP of 100,000Xg cell lysate supernatant with anti-NSP1 serum.

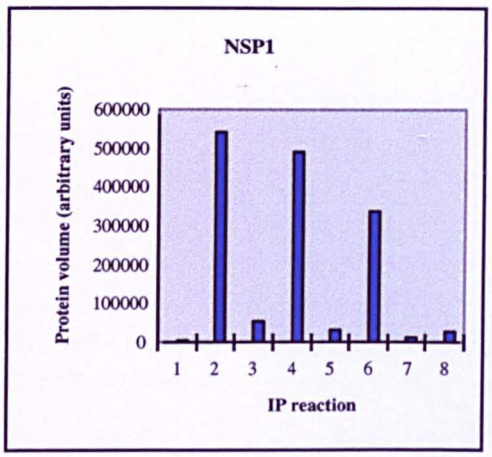
NSP1
Protein volume (arbitrary units)
600000
500000
400000
300000
200000
100000
0
1 2 3 4 5 6 7 8
IP reaction

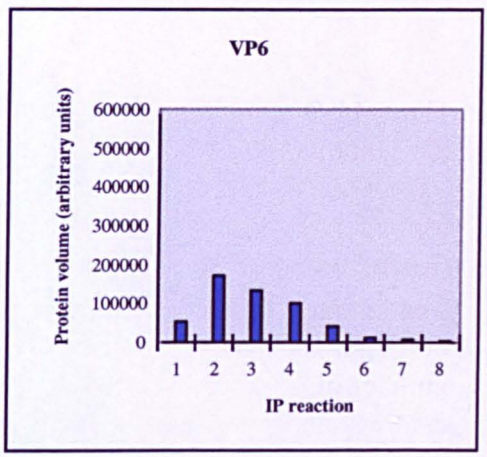
VP6
Protein volume (arbitrary units)
600000
500000
400000
300000
200000
100000
0
1 2 3 4 5 6 7 8
IP reaction

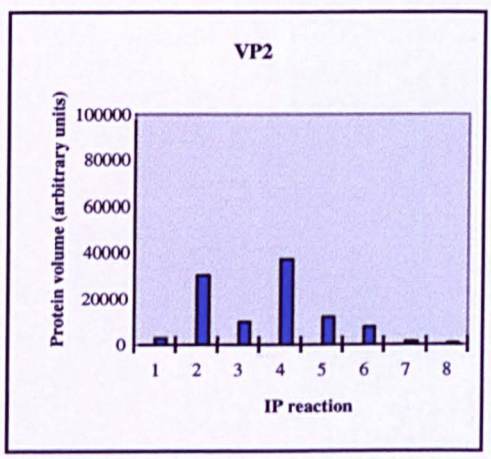
VP2
Protein volume (arbitrary units)
100000
80000
60000
40000
20000
0
1 2 3 4 5 6 7 8
IP reaction

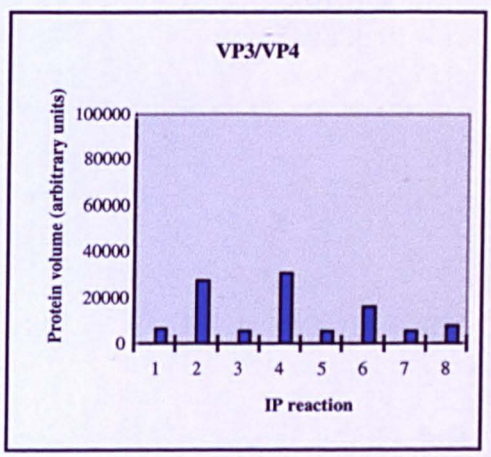
VP3/VP4
Protein volume (arbitrary units)
100000
80000
60000
40000
20000
0
1 2 3 4 5 6 7 8
IP reaction

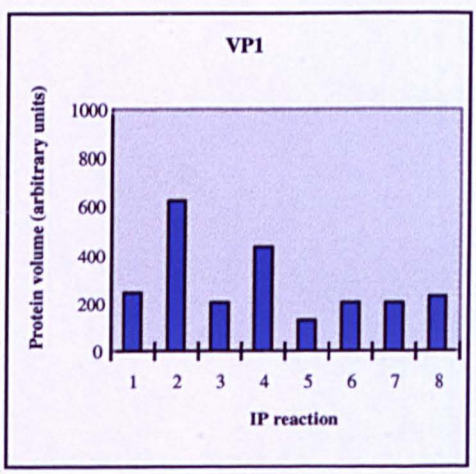
VP1
Protein volume (arbitrary units)
1000
800
600
400
200
0
1 2 3 4 5 6 7 8
IP reaction

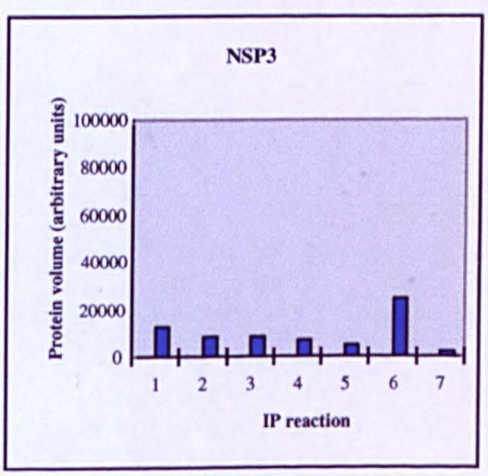
NSP3
Protein volume (arbitrary units)
100000
80000
60000
40000
20000
0
1 2 3 4 5 6 7
IP reaction

Appendix 2.3 ImageQuant™ analysis of viral proteins immunoprecipitated with anti-NSP1 serum from UKtc rotavirus-infected cell lysates pre-treated with micrococcal nuclease for varying lengths of time (Figure 7.6)

The 5-11 % gradient polyacrylamide gel shown in Figure 7.6 was exposed to the phosphoimager for 9 days. The proteins in the viral complex which were clearly visible on the phosphoimage (NSP1, VP6, VP2, VP3/VP4) were quantified using ImageQuant™ software and the data analysed using Excel™ software (Microsoft). The data presented are from the results of one experiment.

Graphs to show the changing amounts of each individual protein over the incubation time with micrococcal nuclease are shown. A graph comparing the changing amounts of each protein with increasing incubation time with micrococcal nuclease is also shown.

The incubation time (minutes) of each sample with 1 mg/ml micrococcal nuclease at room temperature is shown on the x axis of the graph for each protein.

The amounts of the precipitated proteins are displayed in arbitrary units assigned by the ImageQuant™ software. As radioactivity detected was a measure of the number of ^{35}S-methionine residues in each protein and not the amount of protein, data were corrected for the methionine content of each protein.

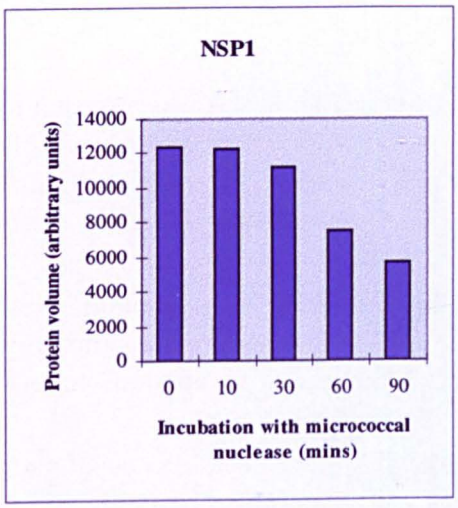
NSP1
Protein volume (arbitrary units)
14000
12000
10000
8000
6000
4000
2000
0
0
10
30
60
90
Incubation with micrococcal nuclease (mins)

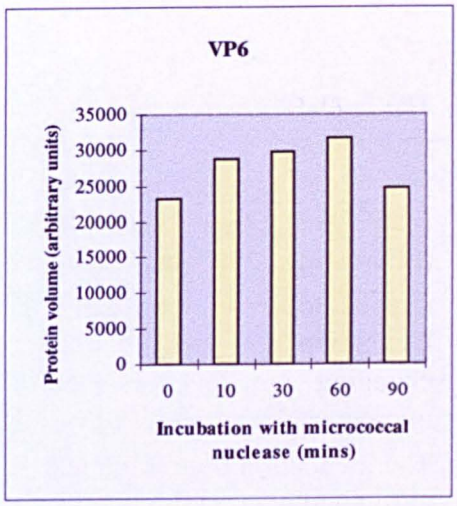
VP6
Protein volume (arbitrary units)
35000
30000
25000
20000
15000
10000
5000
0
0
10
30
60
90
Incubation with micrococcal nuclease (mins)

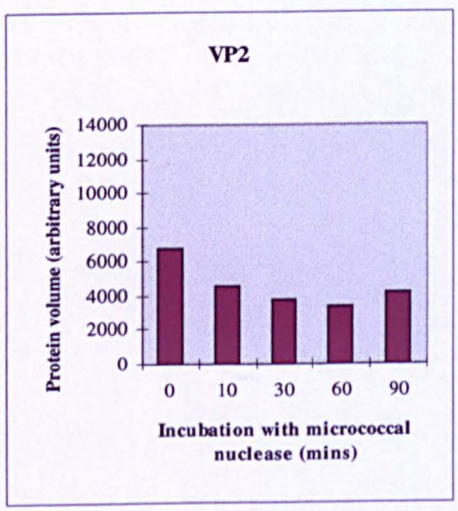
VP2
Protein volume (arbitrary units)
14000
12000
10000
8000
6000
4000
2000
0
0
10
30
60
90
Incubation with micrococcal nuclease (mins)

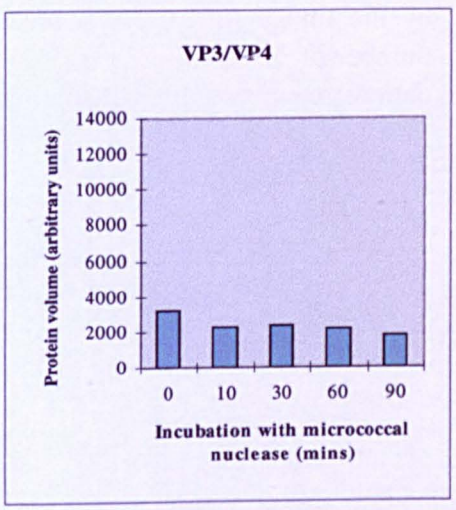
VP3/VP4
Protein volume (arbitrary units)
14000
12000
10000
8000
6000
4000
2000
0
0
10
30
60
90
Incubation with micrococcal nuclease (mins)

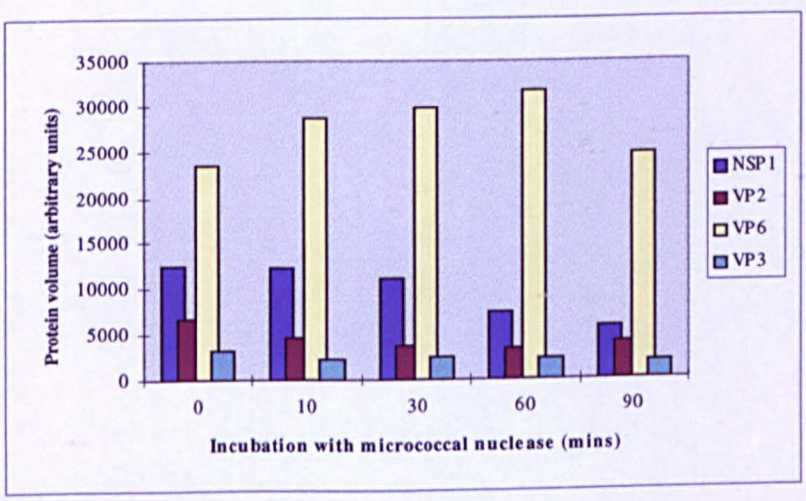
Protein volume (arbitrary units)
35000
30000
25000
20000
15000
10000
5000
0
0
10
30
60
90
Incubation with micrococcal nuclease (mins)
NSP1
VP2
VP6
VP3

Appendix 2.4.1 ImageQuant™ analysis of viral proteins immunoprecipitated with anti-NSP1 serum from UKtc rotavirus-infected cell lysates pulse-chase labelled with ^{35}S-methionine at regular time intervals (Figure 7.7)

The 5-11 % gradient polyacrylamide gel shown in Figure 7.7 was exposed to the phosphoimager for 16 days. The proteins in the viral complex (NSP1, VP6, VP1, VP2, VP3/VP4, NSP3) which were detected by phosphoimaging were quantified using ImageQuant™ software and the data analyzed using Excel™ software (Microsoft). The data presented are the volumes of each protein in the pulse-labelled (Pulse) and pulse-chase labelled (Chase) samples at each time point from one experiment.

The x axis indicates the time post-infection at which the cells were pulse-labelled. The cells were pulse-labelled with ^{35}S-methionine for 30 minutes at 1, 3, 5, or 7 hours post-infection. After the pulse-labelling period, one well of cells was harvested and the second was chased with media containing 100X unlabelled methionine for 2 hours before harvesting.

The amounts of the precipitated proteins are displayed in arbitrary units assigned by the ImageQuant™ software. As radioactivity detected was a measure of the number of ^{35}S-methionine residues in each protein and not the amount of protein, data were corrected for the methionine content of each protein.

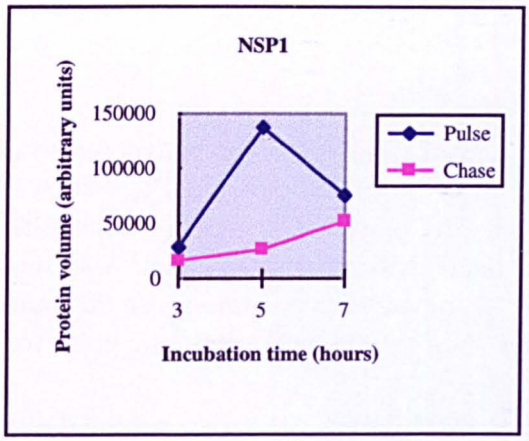
NSP1
Protein volume (arbitrary units)
150000
100000
50000
0
3
5
7
Incubation time (hours)
Pulse
Chase

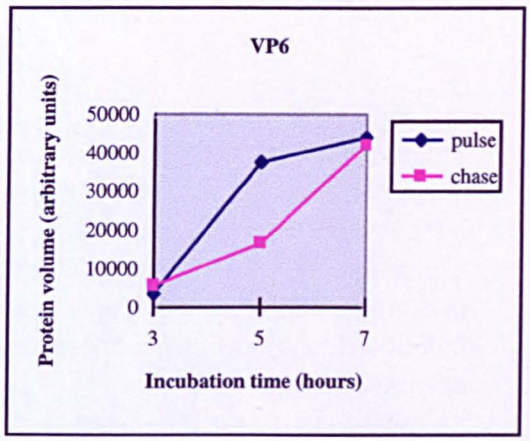
VP6
Protein volume (arbitrary units)
50000
40000
30000
20000
10000
0
3
5
7
Incubation time (hours)
pulse
chase

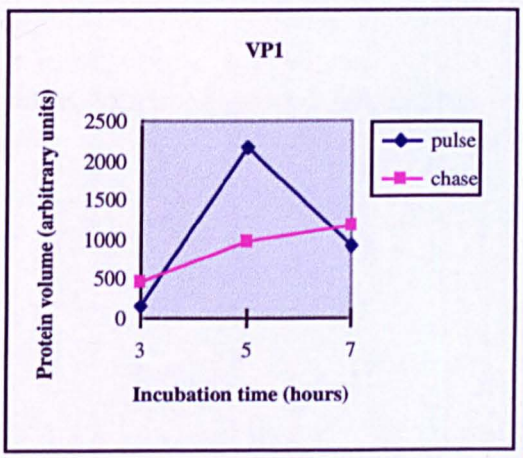
VP1
Protein volume (arbitrary units)
2500
2000
1500
1000
500
0
3
5
7
Incubation time (hours)
pulse
chase

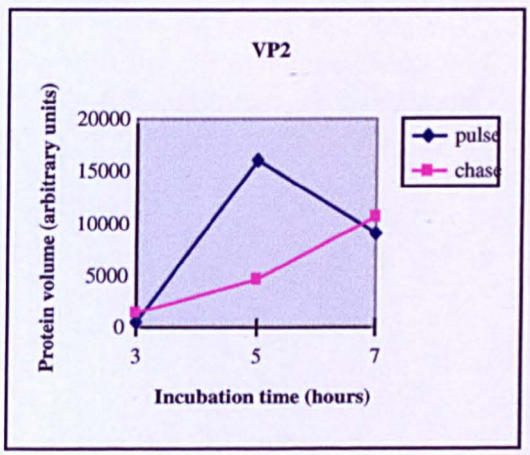
VP2
Protein volume (arbitrary units)
20000
15000
10000
5000
0
3
5
7
Incubation time (hours)
pulse
chase

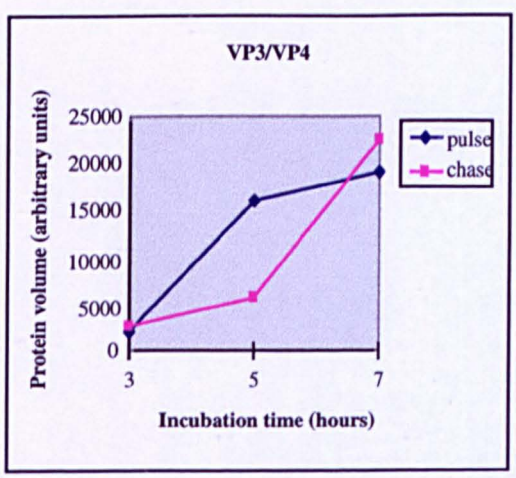
VP3/VP4
Protein volume (arbitrary units)
25000
20000
15000
10000
5000
0
3
5
7
Incubation time (hours)
pulse
chase

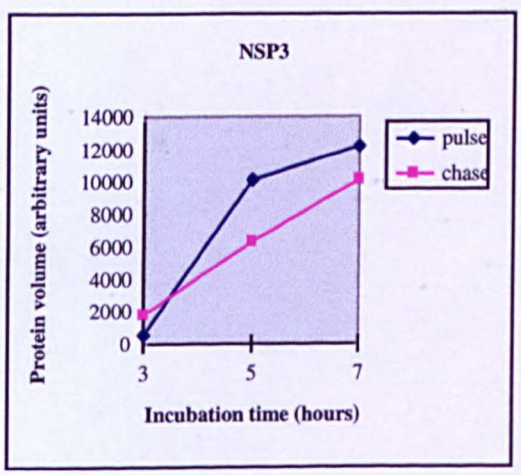
NSP3
Protein volume (arbitrary units)
14000
12000
10000
8000
6000
4000
2000
0
3
5
7
Incubation time (hours)
pulse
chase

Appendix 2.4.2 ImageQuant™ analysis of viral proteins immunoprecipitated with pre-immune and anti-NSP1 serum from UKtc rotavirus-infected cell lysates pulse-chase labelled with ^{35}S-methionine at regular time intervals (Figure 7.7)

The 5-11 % gradient polyacrylamide gel shown in Figure 7.7 was exposed to the phosphoimager for 16 days. The proteins in the viral complex (NSP1, VP6, VP1, VP2, VP3/VP4, NSP3) which were detected by phosphoimaging were quantified using ImageQuant™ software and the data analyzed using Excel™ software (Microsoft). The data presented are the amounts of each protein immunoprecipitated with either pre-immune or anti-NSP1 serum from pulse-labelled (Pulse) and pulse-chase labelled (Chase) samples at each time point from one experiment.

The x axis indicates the time post-infection at which the cells were pulse-labelled. The cells were pulse-labelled with ^{35}S-methionine for 30 minutes at 1, 3, 5, or 7 hours post-infection. After the pulse-labelling period, one well of cells was harvested and the second was chased with media containing 100X unlabelled methionine for 2 hours before harvesting.

The amounts of the precipitated proteins are displayed in arbitrary units assigned by the ImageQuant™ software. As radioactivity detected was a measure of the number of ^{35}S-methionine residues in each protein and not the amount of protein, data were corrected for the methionine content of each protein.

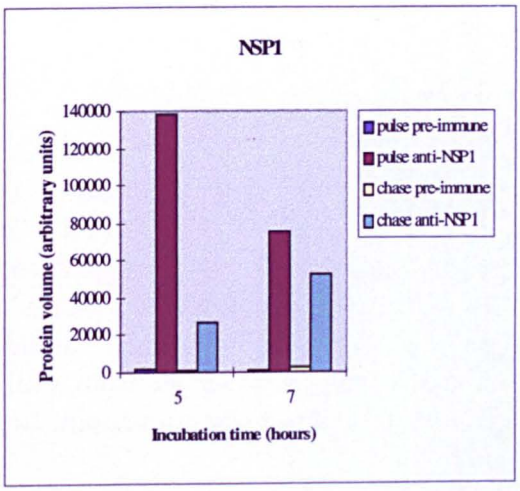
NSP1
Protein volume (arbitrary units)
140000
120000
100000
80000
60000
40000
20000
0
5
7
Incubation time (hours)
pulse pre-immune
pulse anti-NSP1
chase pre-immune
chase anti-NSP1

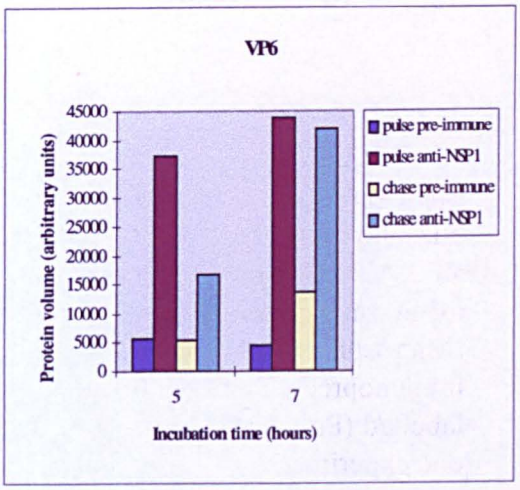
VP6
Protein volume (arbitrary units)
45000
40000
35000
30000
25000
20000
15000
10000
5000
0
5
7
Incubation time (hours)
pulse pre-immune
pulse anti-NSP1
chase pre-immune
chase anti-NSP1

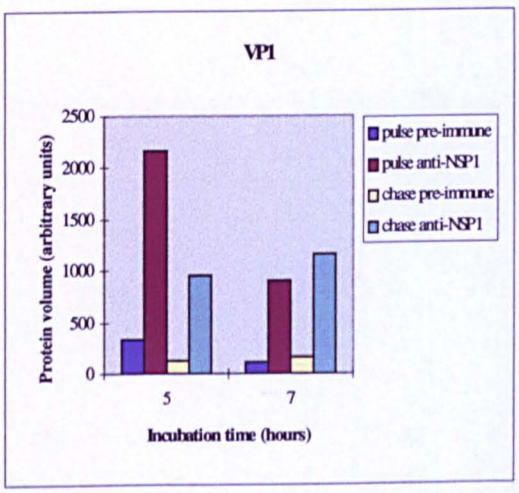
VP1
Protein volume (arbitrary units)
2500
2000
1500
1000
500
0
5
7
Incubation time (hours)
pulse pre-immune
pulse anti-NSP1
chase pre-immune
chase anti-NSP1

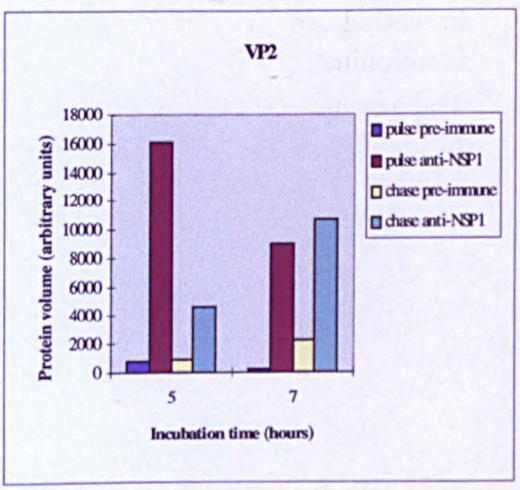
VP2
Protein volume (arbitrary units)
18000
16000
14000
12000
10000
8000
6000
4000
2000
0
5
7
Incubation time (hours)
pulse pre-immune
pulse anti-NSP1
chase pre-immune
chase anti-NSP1

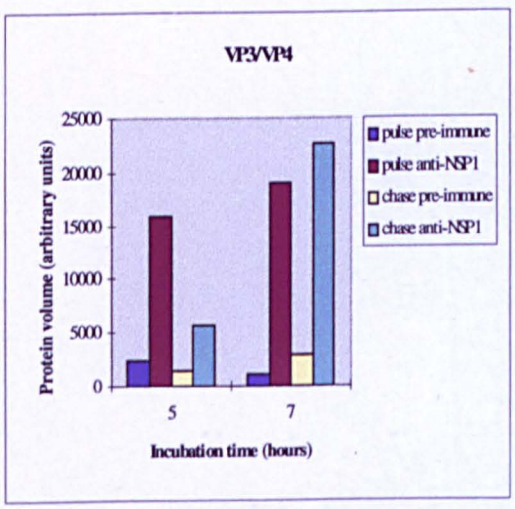
VP3/VP4
Protein volume (arbitrary units)
25000
20000
15000
10000
5000
0
5
7
Incubation time (hours)
pulse pre-immune
pulse anti-NSP1
chase pre-immune
chase anti-NSP1

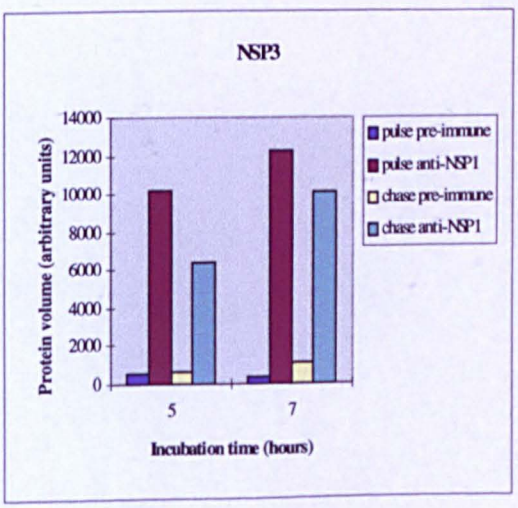
NSP3
Protein volume (arbitrary units)
14000
12000
10000
8000
6000
4000
2000
0
5
7
Incubation time (hours)
pulse pre-immune
pulse anti-NSP1
chase pre-immune
chase anti-NSP1

Appendix 2.5.1 ImageQuant™ analysis of viral proteins immunoprecipitated with anti-VP6 monoclonal antibody from UKtc rotavirus-infected cell lysates (Figure 7.8)

The 5-11 % gradient polyacrylamide gel shown in Figure 7.8 was exposed to the phosphoimager for 8 days. The viral proteins in the IP reactions (VP6, NSP1, VP2, VP3/VP4, NSP3) which were detected by phosphoimaging were quantified using ImageQuant™ software and the data analyzed using Excel™ software (Microsoft). The data presented are from the results of one experiment.

The amounts of the precipitated proteins are displayed in arbitrary units assigned by the ImageQuant™ software. As radioactivity detected was a measure of the number of ^{35}S-methionine residues in each protein and not the amount of protein, data were corrected for the methionine content of each protein.

The IP reactions are indicated on the x axis:
(1) IP of unfractionated cell lysate with pre-immune serum
(2) IP of unfractionated cell lysate with anti-VP6 monoclonal antibody
(3) IP of 10,000Xg cell lysate pellet with anti-VP6 monoclonal antibody
(4) IP of 30,000Xg cell lysate pellet with anti-VP6 monoclonal antibody
(5) IP of 10,000Xg cell lysate supernatant with anti-VP6 monoclonal antibody.

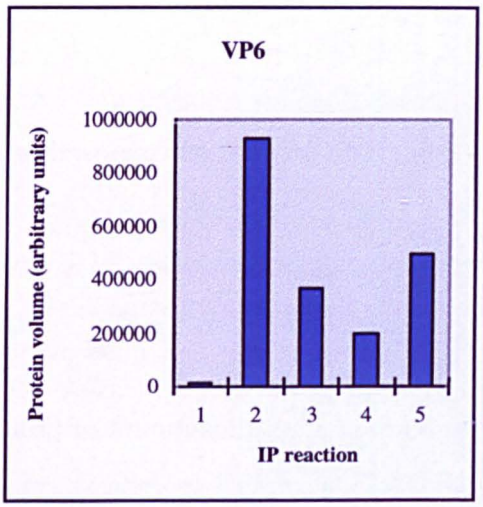
VP6
Protein volume (arbitrary units)
1000000
800000
600000
400000
200000
0
1
2
3
4
5
IP reaction

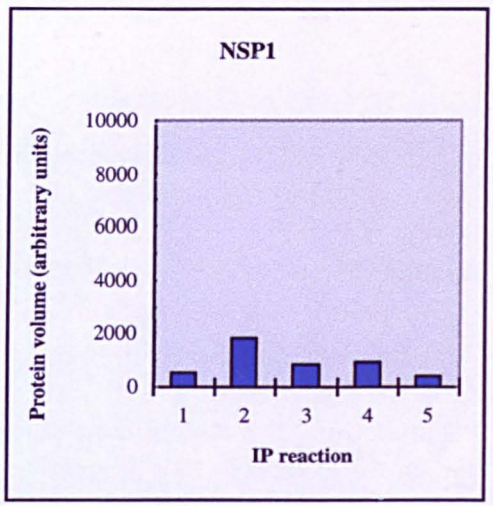
NSP1
Protein volume (arbitrary units)
10000
8000
6000
4000
2000
0
1
2
3
4
5
IP reaction

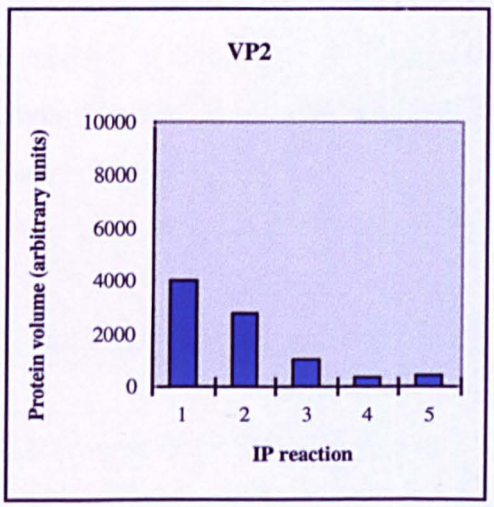
VP2
Protein volume (arbitrary units)
10000
8000
6000
4000
2000
0
1
2
3
4
5
IP reaction

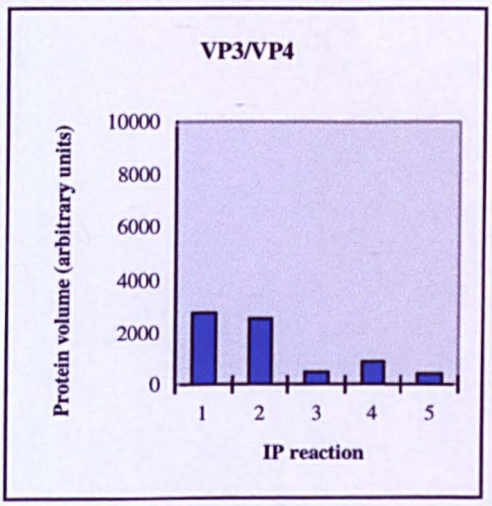
VP3/VP4
Protein volume (arbitrary units)
10000
8000
6000
4000
2000
0
1
2
3
4
5
IP reaction

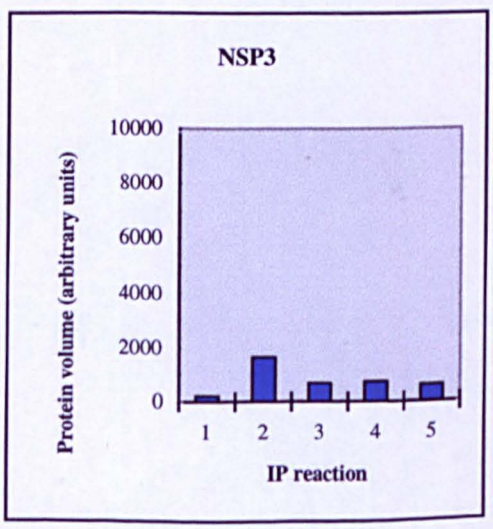
NSP3
Protein volume (arbitrary units)
10000
8000
6000
4000
2000
0
1
2
3
4
5
IP reaction

Appendix 2.5.2 Calculation of the proportion of total VP6 in the UKtc rotavirus-infected cell which is co-immunoprecipitated with NSP1

The 5-11 % gradient polyacrylamide gel shown in Figure 7.5 was exposed to the phosphoimager for 8 days. The protein bands corresponding to NSP1 and VP6 in both the cell lysate sample and the IP reaction with anti-NSP1 serum from cell lysates were quantified using ImageQuant™ software and the data analysed using Excel™ software (Microsoft).

The volumes of the protein bands are calculated in arbitrary units by the ImageQuant™ software. As radioactivity detected was a measure of the number of ^{35}S-methionine residues in each protein and not the amount of protein, data were corrected for the methionine content of each protein.

Calculation of efficiency of immunoprecipitation reaction with anti-NSP1 serum

Volume of NSP1 in cell lysates (10 µl) = 1.7×10^5

Volume (50 µl) = 8.3×10^5

Volume of NSP1 precipitated by anti-NSP1 serum = 5.4×10^5

Efficiency of IP reaction = $(5.4 \times 10^5)/(8.3 \times 10^5) \times 100$ = 65.4 %

Percentage of total VP6 in cell lysate which co-immunoprecipitated with NSP1

Volume of VP6 in cell lysate (10 µl) = 1.6×10^6

Volume (50 µl) = 7.9×10^6

Volume of VP6 co-immunoprecipitated with NSP1 by anti-NSP1 serum = 1.9×10^5

Percentage of total VP6 contained in complex with NSP1

= $(1.9 \times 10^5)/(7.9 \times 10^6) \times 100$ = 2.4 %

Percentage of total VP6 contained in complex with NSP1 (corrected for efficiency of IP reaction)

= 100/65.4 x 2.4 = 3.7 %